

**Lockheed Martin Corporation**  
**1195 Sarasota Center Boulevard**  
**Sarasota, Florida 34240**  
**Telephone 240-687-1813**



July 12, 2017

**VIA OVERNIGHT CARRIER**

Mr. James R. Carroll  
Program Administrator  
Land Restoration Program  
Land Management Administration  
Maryland Department of the Environment  
1800 Washington Road, Suite 625  
Baltimore, Maryland 21230

Re: Transmittal of the 2017 Groundwater-Flow and Solute-Transport Modeling Dump Road Area  
Martin State Airport, 701 Wilson Point Road, Middle River, Maryland

Dear Mr. Carroll:

For your review, please find enclosed two hard copies with CDs of the above-referenced document. This report describes the updated numerical groundwater-flow and solute-transport modeling conducted as part of the interim remedial action for the groundwater operable unit at the Dump Road Area site at Martin State Airport, in Baltimore County, Maryland. If possible, we respectfully request to receive MDE's comments by September 7, 2017.

If you have any questions or require any additional information please contact me by phone at 240-687-1813, or via e-mail at paul.e.calligan@lmco.com.

Sincerely,

A handwritten signature in black ink that reads "Paul E. Calligan".

Paul E. Calligan, P.G.  
Project Lead, Environmental Remediation  
Lockheed Martin Corporation

cc: (via email without enclosure)  
Anuradha Mohanty, MDE  
Christine Kline, Lockheed Martin  
Norm Varney, Lockheed Martin  
Michael Martin, Tetra Tech  
Peter Shilland, CDM Smith

cc: (via shipping courier; with enclosures)  
Mark Williams, Maryland Aviation Administration  
Al Pollard, Martin State Airport

cc: (via mail with CD enclosure)  
Jann Richardson, Lockheed Martin  
Pete Lekas, EA Environmental

---

# **2017 Groundwater-Flow and Solute-Transport Modeling Dump Road Area Martin State Airport 701 Wilson Point Road Middle River, Maryland**

Prepared for:

Lockheed Martin Corporation

Prepared by:

Tetra Tech, Inc.

July 2017



---

Michael Martin, P.G.  
Regional Manager



---

Chris Pike  
Project Manager

---

## TABLE OF CONTENTS

<u>Section</u>	<u>Page</u>
<b>ACRONYMS .....</b>	<b>v</b>
<b>1 INTRODUCTION .....</b>	<b>1-1</b>
1.1 SITE INFORMATION .....	1-2
1.2 MODELING OBJECTIVES .....	1-3
<b>2 CONCEPTUAL MODEL .....</b>	<b>2-1</b>
2.1 GEOLOGY .....	2-3
2.2 HYDROGEOLOGY .....	2-4
2.3 SURFACE WATER AND WETLANDS .....	2-5
2.4 WATER BUDGET .....	2-5
<b>3 NUMERICAL GROUNDWATER-FLOW-MODEL UPDATE .....</b>	<b>3-1</b>
3.1 CODE SELECTION .....	3-1
3.2 MODEL GRID AND LAYERING .....	3-1
3.3 BOUNDARY CONDITIONS .....	3-2
3.4 HYDRAULIC PROPERTIES .....	3-3
<b>4 NUMERICAL FLOW AND SOLUTE-TRANSPORT MODEL .....</b>	<b>4-1</b>
4.1 INTRODUCTION .....	4-1
4.1.1 Steady-State Flow .....	4-3
4.1.2 Simulation of Pumping Tests .....	4-4
4.1.3 Tidal Influence Simulation .....	4-5
4.1.4 Flow-Model Sensitivity Analysis .....	4-5
4.2 SOLUTE-TRANSPORT MODEL .....	4-6
4.2.1 Summary of Previous Transport Modeling .....	4-6
4.2.2 Revisions to Existing Transport Model .....	4-6
4.3 INITIALIZING MASS IN PLACE .....	4-8

---

## TABLE OF CONTENTS (continued)

<b><u>Section</u></b>	<b><u>Page</u></b>
<b>5 ANALYSIS OF PLANNED REMEDIAL ACTION.....</b>	<b>5-1</b>
5.1 PREDICTIVE-SIMULATION METHODOLOGY .....	5-1
5.2 PREDICTIVE-MODELING ANALYSES.....	5-2
5.2.1 Particle Tracking.....	5-2
5.2.2 Solute-Transport Modeling.....	5-2
<b>6 SUMMARY AND NEXT STEPS.....</b>	<b>6-1</b>
<b>7 REFERENCES.....</b>	<b>7-1</b>

### LIST OF FIGURES

*(Figures appear at the end of the document)*

- Figure 1 Site Location Map
- Figure 2 Distribution of TCE in Upper, Intermediate, and Lower Zones of Surficial Aquifer, 2013–2016
- Figure 3 Distribution of *cis*-1,2-DCE in Upper, Intermediate, and Lower Zones of Surficial Aquifer, 2013–2016
- Figure 4 Distribution of VC in Upper, Intermediate, and Lower Zones of Surficial Aquifer, 2013–2016
- Figure 5 Water Table Map Based on Groundwater Levels in the Upper Zone of Surficial Aquifer, March 2016
- Figure 6 Hydraulic Head Contours Based on Groundwater Levels in the Intermediate Zone of Surficial Aquifer, March 2016
- Figure 7 Hydraulic Head Contours Based on Groundwater Levels in the Lower Zone of Surficial Aquifer, March 2016
- Figure 8 Model Grid and Boundary Conditions
- Figure 9 Simulated Distribution of Groundwater Recharge and Evapotranspiration in the Calibrated Model
- Figure 10 Plot of Measured versus Simulated Groundwater Levels, March 2016
- Figure 11 Simulated Potentiometric Surface and Residuals in the Upper (Layer 2), Intermediate (Layer 9), and Lower (Layer 14) Zones of the Surficial Aquifer
- Figure 12 Simulated and Observed Hydraulic Head Changes at MW-48S, MW-48I, and MW-48D during Tidal Fluctuation April 5, 2015 to– April 7, 2015



---

## TABLE OF CONTENTS (continued)

### LIST OF FIGURES (continued) (*Figures appear at the end of the document*)

- Figure 13 Predicted Steady-State Capture Zone for Remedial-System Startup Pumping Rates in the Upper (Layers 1–7), Intermediate (Layers 8–11), and Lower (Layers 12–15) Zones of the Surficial Aquifer
- Figure 14 Vertical Cross-Sectional View of Simulated-Forward Particle-Tracking Results for Conditions during Remedial System Pumping
- Figure 15 Predicted TCE under “No Further Remedial Action” in the Upper (Layer 7), Intermediate (Layer 11), and Lower (Layer 14) Zones of the Surficial Aquifer after 5 Years
- Figure 16 Predicted VC under “No Further Remedial Action” in the Upper (Layer 7), Intermediate (Layer 11), and Lower (Layer 14) Zones of the Surficial Aquifer after Years
- Figure 17 Predicted TCE under Planned Pumping Conditions in the Upper (Layer 7), Intermediate (Layer 11), and Lower (Layer 14) Zones of the Surficial Aquifer after 5 Years
- Figure 18 Predicted VC under Planned Pumping Conditions in the Upper (Layer 7), Intermediate (Layer 11), and Lower (Layer 14) Zones of the Surficial Aquifer after 5 Years

### LIST OF TABLES (*Tables appear at the end of the document after the figures*)

- Table 1 Summary of Groundwater-Flow Model-Parameter Values
- Table 2 March 23, 2016 Measured Groundwater-Elevations and Vertical Hydraulic-Gradients versus Simulated Values in the Calibrated Groundwater-Flow Model
- Table 3 Summary Statistics for Steady-State-Flow Model-Simulation for March 2016 Conditions
- Table 4 Comparison of Simulated and Measured Drawdowns at the End of the Step-Drawdown Tests
- Table 5 Summary of Flow-Model Sensivity-Analysis
- Table 6 Summary of Solute-Transport Model-Parameter Values
- Table 7 Summary of Pumping Rates (gpm) of the Recovery Wells

### APPENDICES (*Appendices appear at the end of the document after the tables*)

#### APPENDIX A—TRANSIENT MODELING-ANALYSIS OF RECOVERY WELL VARIABLE-RATE PUMPING TESTS

---

This page intentionally left blank.

---

# ACRONYMS

3D	three dimensional
ASTM	ASTM International
bgs	below ground surface
<i>cis</i> -1,2-DCE	<i>cis</i> -1,2-dichloroethene
COC	chemical(s) of concern
cVOC	chlorinated volatile organic compound
DRA	Dump Road Area
FMC	Frog Mortar Creek
foc	fraction of organic carbon
ft	feet
gpm	gallon(s) per minute
GSP	Greater Strawberry Point
Handex	Handex Environmental Management
in/yr	inch(es) per year
IRA	interim remedial action
Kd	distribution coefficient
K <sub>h</sub>	horizontal hydraulic-conductivity
K <sub>z</sub>	vertical hydraulic-conductivity
Koc	soil-water partitioning coefficient
Lockheed Martin	Lockheed Martin Corporation
MAA	Maryland Aviation Administration
MES	Maryland Environmental Services
µg/L	microgram(s) per liter
MRC	Middle River Complex
MSA	Martin State Airport
msl	mean sea level
MVS	<i>Mining Visualization Software</i> <sup>™</sup>
NAVD88	North American Vertical Datum of 1988
PFM	passive flux-meter
R	retardation coefficient
RAO	remedial action objective
SP	Strawberry Point
TCE	trichloroethene

---

Tetra Tech	Tetra Tech, Inc.
TMR	telescopic-mesh refinement
USGS	United States Geological Survey
VAS	vertical aquifer-sampling
VC	vinyl chloride
VOC	volatile organic compound

---

## Section 1

# Introduction

On behalf of Lockheed Martin Corporation (Lockheed Martin), Tetra Tech, Inc. (Tetra Tech) has prepared this report describing the updated numerical groundwater-flow and solute-transport modeling conducted as part of the interim remedial action (IRA) for the groundwater operable unit<sup>1</sup> at the Dump Road Area (DRA) site at Martin State Airport (MSA) in Middle River, Maryland (see Figure 1). This modeling effort updates previous groundwater-flow modeling for the site (Tetra Tech, 2004; GeoTrans, 2011; Tetra Tech, 2014a) that used data collected since 2014, including data from the recent recovery-well step testing. The primary objective of the groundwater modeling is to help develop an effective remedial system design that hydraulically captures high-concentration zones of contaminants in groundwater at the Dump Road Area site. This modeling will also facilitate improved predictions of groundwater and plume response to planned remediation efforts.

Groundwater modeling described in this report was performed with knowledge gained from prior modeling efforts, and with data collected during current and ongoing site remediation. Recently collected hydrogeologic and groundwater-quality data include data from the drilling, installation, and hydraulic testing of new extraction wells, groundwater- and surface-water-quality sampling, and water level measurements. These data, including stratigraphic boring data, water levels, and contaminant concentrations, were used to update the flow model and to conduct predictive simulations using the numerical solute-transport model.

The engineering team uses the model iteratively to implement technically sound remediation approaches for meeting the primary remedial action objective (RAO) for groundwater: preventing migration of groundwater with contaminant concentrations greater than remedial action levels

<sup>1</sup> *Operable unit:* each of a number of separate activities (such as the removal of drums or contaminated soil) undertaken as part of a Superfund site cleanup.

---

toward Frog Mortar Creek (FMC). The planned remedial approach consists of creating a hydraulic barrier resulting from the pumping of 16 extraction wells aligned parallel to the Frog Mortar Creek shoreline. The primary contaminants driving the remedial action plan include three chlorinated volatile organic compounds (cVOCs)—trichloroethene (TCE) and its sequential degradation products: *cis*-1,2-dichloroethene (DCE) and vinyl chloride (VC). The primary area of concern is shown by mapping the groundwater concentrations of these three volatile organic compounds (VOCs), using results from groundwater sampling performed in 2012–2016. The plumes of these primary contaminants were used to guide the development of groundwater remediation scenarios tested via predictive simulations.

This report discusses modifications made to update the existing numerical model (Tetra Tech, 2011, 2014), including supplemental steady-state calibration based on March 2016 water-level data, confirmatory calibration checking via transient simulation of step-drawdown results for the newly installed extraction wells, and transient simulation of tidally influenced groundwater levels. The calibrated groundwater-flow model was applied to help select appropriate pumping rates that will prevent migration of contaminated groundwater toward Frog Mortar Creek. The model will be used as a decision-analysis tool, based on simulations using various extraction-well pumping rates, associated changes in hydraulic heads, and contaminant concentrations in the plume over time.

## **1.1 SITE INFORMATION**

Martin State Airport is at 701 Wilson Point Road in Middle River, Maryland. It is bounded by Frog Mortar Creek to the east and Stansbury Creek to the west (Figure 1). Both creeks are tidal tributaries of Chesapeake Bay and join the bay at the south side of the airport. The Dump Road Area is in the southeastern portion of Martin State Airport and is bounded by Frog Mortar Creek to the east and the airport runway to the west. This area has been under investigation since the 1990s, and Lockheed Martin Corporation (Lockheed Martin) has designated the site as the Dump Road Area (DRA) to distinguish it from other Martin State Airport areas under investigation (e.g., Frog Mortar Creek and Greater Strawberry Point [GSP]).

Recent investigations at Martin State Airport in 2013–2015 (Tetra Tech, 2013; 2014b; 2014c; 2015a–e) were completed after the previous groundwater model was developed, and include soil borings, groundwater sampling, and groundwater profiling by means of direct-push technology and vertical-aquifer sampling (VAS). In 2014 and 2015, Tetra Tech conducted a groundwater

---

characterization study on behalf of Lockheed Martin at Frog Mortar Creek and the Dump Road Area. That investigation further characterized the discharge of Dump Road Area groundwater to Frog Mortar Creek. As discussed in Tetra Tech (2015e), water-level data-loggers were deployed in and retrieved from the creek, and chemically analyzed seepage was measured based on data collected by passive flux-meters (PFMs) installed in the sediment of Frog Mortar Creek and laboratory analyses of the chemical data by the University of Florida. A comprehensive water-level measuring-event in March 2016 also included monitoring wells from both Dump Road Area and Greater Strawberry Point.

## **1.2 MODELING OBJECTIVES**

Primary objectives for this modeling effort were to: (1) improve the conceptualization of the hydrostratigraphy<sup>2</sup>, hydrogeology<sup>3</sup>, and contaminant sources in the Dump Road Area; (2) update and recalibrate the numerical groundwater-flow model to more accurately predict subsurface-flow pathways and interactions between groundwater and surface water; (3) implement solute-transport modeling to examine the fate and transport of identified chemicals of concern (COC) over time; and (4) help predict and evaluate remedial-action performance using the modeling tools in predictive-simulation mode. These modeling tools provide the engineering team with recommendations for optimizing remedial-system performance.

<sup>2</sup> *Hydrostratigraphy*: the structure of subsurface porous materials in reference to the flow of groundwater.

<sup>3</sup> *Hydrogeology*: a branch of geology concerned with the occurrence, use, and functions of surface water and groundwater.

---

## Section 2

# Conceptual Model

The conceptual model of a hydrogeologic system is a working description of its characteristics and dynamics; it consolidates site and regional hydrologic data into a set of assumptions and concepts that can be quantitatively evaluated (ASTM International [ASTM], 2008). The conceptual model is translated into a numerical representation to simulate groundwater flow characteristics, and includes simulation-based development, testing, and predictive evaluation of remediation performance. Data collected subsequent to the 2014 groundwater model (Tetra Tech, Inc., 2014b; 2014c; 2015a–e) were used to update the conceptual hydrologic and contaminant-transport model for the Dump Road Area (DRA) site at Martin State Airport (MSA). New soil boring, monitoring well, and recovery well data helped improve the definition of the stratigraphy<sup>4</sup> and groundwater quality of the surficial aquifer.

Three primary volatile organic compounds (VOCs) drive the groundwater remedial action at the DRA: trichloroethene (TCE), *cis*-1,2-dichloroethene (*cis*-1,2-DCE), and vinyl chloride (VC). Figures 2 through 4 (respectively) are based on the presentation of the geology in Section 2.1. Using groundwater-sampling results from 2013–2016, they show the distribution of these chemicals of concern (COC). The original historical sources of contamination at DRA are not fully known, but the vertical and horizontal extents of soil and groundwater contamination near the following possible sources of contamination (see Figures 2 through 4) have recently been investigated (Tetra Tech, 2013; 2014b; 2014c):

- Taxiway Tango Median Anomaly Area
- Drum Area
- two on-site ponds
- Petroleum Hydrocarbon Area

<sup>4</sup> *Stratigraphy*: area of geology that deals with the origin, composition, distribution, succession, and arrangement of geologic strata (i.e., layers).



---

Physical and chemical processes affecting the fate and transport of dissolved constituents in study-area groundwater include advection, hydrodynamic dispersion, molecular diffusion, adsorption, and degradation. These processes change the mass and distribution of dissolved constituents in groundwater. A brief discussion of these processes is provided here:

- **Advection** is the migration of dissolved COC in moving groundwater. Advection is typically the dominant factor for transport of dissolved COC. In addition, changes in groundwater flow patterns over time can also impart what can be labeled as “advective dispersion,” because contaminant plumes can appear to have dispersed laterally and/or vertically, whereas the dominant factor was actually a significant change in flow direction.
- **Hydrodynamic dispersion** is a physical process whereby dissolved constituents spread at the pore-scale level, leading to larger-scale macroscopic spreading both horizontally and vertically away from the center of the plume mass. As noted above, “advective dispersion” is often the dominant dispersive phenomenon at larger scales.
- **Molecular diffusion** is a physical process defined as the movement of molecules from an area of higher concentration to an area of lower concentration, and the rate of diffusion is typically dwarfed by advective and dispersive fluxes. However, molecular diffusion is often a significant factor in terms of pore-scale transfer of COC mass, as well as in certain low-permeability geologic formations with very slow advective movement and correspondingly slow dispersive-fluxes.
- **Adsorption** is a chemical process whereby dissolved chemicals react with the surfaces of solids. Several laboratory studies have shown that in equilibrium the mass of organic constituents adsorbed to soil is proportional to the amount of organic carbon in the soil (e.g., Karickhoff, 1985). Field studies indicate that adsorption is the primary reason organic-compound plumes migrate at a slower rate than groundwater; a retardation factor is applied to the model to account for the reduced migration rate.
- **Degradation** processes are biological and chemical mechanisms that decrease the mass of dissolved constituents. These processes include biodegradation effects, photolysis<sup>5</sup>, oxidation reduction, and hydrolysis<sup>6</sup>, and are generally grouped into either biologic or abiotic (chemical) degradation processes. Sequential degradation includes transformation of parent compounds (e.g., TCE) into degradation products (*cis*-1,2-DCE, VC, and ethene) via reductive dechlorination. During sequential degradation, daughter products may initially increase and then later decrease over time, depending on the degradation rates of the parent and daughter compounds.

<sup>5</sup> *Photolysis*: chemical decomposition by the action of radiant energy (such as light).

<sup>6</sup> *Hydrolysis*: a chemical reaction in which a chemical compound decomposes by reaction with water.

---

## 2.1 GEOLOGY

MSA is in the western shore of the Coastal Plain physiographic province. Regional studies (Andreasen, 2007; Andreasen et al., 2013; Vroblesky and Fleck, 1991; Fleck and Vroblesky, 1996; Chapelle, 1985) indicate that MSA lies on the Patapsco Formation. This formation consists of complex and interbedded mixtures of gray, brown, and red sand, silt, and clay originating from sediment deposition in a low coastal plain traversed by low-gradient meandering streams. The Patapsco aquifer in the Baltimore area has been divided into sand and clay facies<sup>7</sup>. The sand facies consists predominantly of medium to fine sand and has a horizontal hydraulic conductivity ranging from four to 125 feet per day (Andreasen et al., 2013). In the Baltimore area, the Patapsco aquifer coincides with the sand facies of the Patapsco Formation and is mostly unconfined. In the Middle River area, the Patapsco Formation outcrops within and west of the MSA.

The Patapsco aquifer is the aquifer of concern at the DRA. Storage coefficients for unconfined portions of the Patapsco aquifer have been estimated at 0.01 to 0.1 (dimensionless parameter). In the confined portions of the aquifer, transmissivity values range between 1,900–3,800 square feet per day, and storativity ranges between 0.000086–0.025 (dimensionless parameter), with an average of 0.00061 (Chapelle, 1985; Andreasen et al., 2013). Recharge to the Patapsco aquifer occurs primarily where the Patapsco Formation outcrops subparallel to the fall line (Vroblesky and Fleck, 1991).

Previous (MES, 1994; Tetra Tech, 1999; 2002a; 2002b; 2004) and recent (Tetra Tech, 2013; 2014b–c; AECOM, 2016) site-specific investigations at MSA indicate that the subsurface is characterized by interbedded zones of heterogeneous sand, silt, and clay deposits of the Patapsco Formation. Boring logs and cross-sections across MSA indicate relatively continuous layers of sand and gravel separated by discontinuous but locally significant lenses of silt and clay. These shallow permeable zones form the surficial aquifer. Both regional information (Andreasen, 2007; Andreasen et al., 2013; Fleck and Vroblesky, 1996; Chapelle, 1985) and recent deep borings at

<sup>7</sup> *Facies*: a part of a rock or group of rocks that differs from the whole formation (as in composition, age, or fossil content).

---

MSA (Tetra Tech, 2013; AECOM, 2016) indicate a thick clay unit approximately 120 feet (ft) below MSA, which is likely the top of the Arundel Formation.

## **2.2 HYDROGEOLOGY**

The hydrogeologic system beneath the DRA consists of relatively continuous zones of sand and gravel that provide the primary pathways for groundwater flow and contaminant transport. Water typically enters these units via natural infiltration of precipitation (recharge) through the shallow fill materials, or via overland flow of water on paved areas toward areas of lower topography. Infiltrated water then flows laterally to the northeast through permeable zones, and eventually discharges to Frog Mortar Creek (FMC). When remediation pumping is occurring, contaminated groundwater is captured and thus diverted from discharging to FMC.

The surficial aquifer beneath the site is divided into three hydraulically connected zones for study purposes: the upper, intermediate, and lower surficial aquifer. Figures 5 through 7 present maps of the March 2016 hydraulic heads in the upper, intermediate, and lower zones of the surficial aquifer. Although mounding is present in the upper zone near Pond 1, groundwater flow is primarily to the east toward FMC. The surficial aquifer, which is part of the Patapsco Formation, is underlain at approximately -75 feet (ft) mean sea level (msl) by a relatively thick clay unit that acts as a basal confining unit.

Both Frog Mortar Creek and Stansbury Creek are affected by tidal fluctuations, and have average amplitudes of approximately 1.2 feet and a tidal range of about 2.4 feet. Transducer data from the upper-aquifer zone indicate that tidal fluctuation amplitudes decrease to less than 0.1 foot within a few hundred feet from Frog Mortar Creek. This damping effect is due to the relatively high storage coefficient (i.e., “specific yield”), given the unconfined conditions in the upper-aquifer zone. Tidal fluctuations likely diminish less rapidly with distance from the creeks in the intermediate and deep surficial-aquifer zones, because these zones are fully saturated and are under artesian pressure in semiconfined or confined conditions.

---

## 2.3 SURFACE WATER AND WETLANDS

MSA is bounded by Frog Mortar Creek to the east and Stansbury Creek to the west. Stansbury Creek is northwest of Dark Head Creek. These estuarine<sup>8</sup> creeks discharge south of the airport to Middle River, which discharges into Chesapeake Bay to the east. Seneca Creek, southeast of FMC and the airport, also flows easterly into Chesapeake Bay. Two local freshwater ponds, referred to as Pond 1 and Pond 2, and a wetland area are also in the area of concern.

The 2012 field program investigated the hydrologic relationship between the two on-site ponds (Ponds 1 and 2) and the groundwater system, and included installation and monitoring of stilling wells in both ponds and installation of new monitoring wells adjacent to the ponds (Tetra Tech, 2013). Hydrographs for late October to late November 2012 reveal an approximately four-foot head-differential between the water level in Pond 1 (approximately seven feet above msl) North American Vertical Datum 1988 [NAVD 88]) and the adjacent shallow zone well (MW-43S, approximately three feet msl NAVD 88). A similar water level was recorded in Pond 2, but the water level at the adjacent shallow zone well (MW-44S) was only a few tenths of a foot lower. These limited data suggest that Pond 1, an area where substantial sediment contamination has been detected (Tetra Tech, 2013), is hydraulically isolated from the adjacent aquifer, whereas Pond 2 is not. Pond 1, a former disposal pit constructed in the 1950s, is clay-lined and has no outlet, whereas Pond 2 surface water flows to Frog Mortar Creek.

## 2.4 WATER BUDGET

Groundwater flow at the site is generated almost exclusively by recharge (i.e., precipitation infiltration, and infiltration of redirected storm runoff and snowmelt). The conceptual groundwater model therefore focuses on identifying and characterizing the processes affecting recharge. The conceptual and numerical modeling includes the assumption that a single parameter (called “net effective recharge”) could be defined that incorporates all of the recharge processes involved. In

<sup>8</sup> *Estuarine*: a partially enclosed coastal body of brackish water with one or more rivers or streams flowing into it, and with a free connection to the open sea.

---

highly vegetated areas, an evapotranspiration<sup>9</sup> rate was applied to represent the observed lower water table in such areas.

MSA topography ranges from approximately 42 ft in the upland area to near sea level near Frog Mortar Creek. Topography is relatively flat over most of the site, but slopes steeply near FMC. The nature of the ground surface (much of which is paved or covered by buildings) creates significant potential for precipitation runoff. Runoff from buildings and from some or all of the paved areas is captured and conveyed through a storm sewer system. In the area of interest, additional overland flow drains into locally perched<sup>10</sup> ponds or FMC. Therefore, the net effective recharge is expected to be lower at MSA than in open areas that do not have runoff controls.

Recharge rates are influenced by areal variations in topography, surficial geology, and the presence or absence of paved surfaces. Precipitation in the MSA area is approximately 44 inches per year. Recharge occurs primarily in late winter and early spring, when precipitation is relatively high and evapotranspiration is minimal; at the nearby Graces Quarters site, recharge rates are estimated at 0–9 inches per year (Tenbus and Fleck, 2001). Recharge to the groundwater system in site locations where the ground surface is not covered by buildings or pavement is expected to be at the high end of this range, due to high soil permeability. Outside the DRA, the groundwater mounding in two localized areas of Greater Strawberry Point (GSP) is likely the result of recharge from leaks in subsurface pipes.

<sup>9</sup> *Evapotranspiration*: the process of transferring moisture from the earth to the atmosphere by evaporation and by transpiration from plants.

<sup>10</sup> *Perched*: an accumulation of groundwater above a water table in an unsaturated zone. The groundwater is usually trapped above a soil layer that is impermeable and forms a lens of saturated material in the unsaturated zone.

---

## Section 3

# Numerical Groundwater-Flow-Model Update

Developing a numerical groundwater-flow model entails transforming the conceptual model into a mathematical form. Fundamental components of the numerical groundwater-flow modeling process prior to model calibration include: (1) selection of an appropriate mathematical model and solution basis, or code; (2) development of a three-dimensional-model grid; (3) assignment of representative initial and boundary conditions for calibration and predictive-simulation purposes; and (4) characterization of hydraulic and geochemical properties (ASTM, 1996).

### 3.1 CODE SELECTION

The groundwater-flow model described herein was developed using *MODFLOW 2000*, a well documented, widely used and accepted code developed and frequently updated by the United States Geological Survey (USGS) (McDonald and Harbaugh, 1988; Harbaugh et al., 2000a–b). The contaminant-mass fate and transport modeling used the well known and widely used finite-difference code *RT3D* (Clement, 1997). *RT3D* uses *MODFLOW 2000* to simulate the flow field, providing the basis for representing (in *RT3D*) the advective transport of dissolved constituents. *RT3D* also directly accounts for other significant transport mechanisms, including hydrodynamic dispersion, diffusion, sorption<sup>11</sup>, and sequential biodegradation.

### 3.2 MODEL GRID AND LAYERING

The model grid shown on Figure 8 is oriented approximately 45 degrees off true north, so that the columns are aligned parallel from northeast (NE) to southwest (SW), and the rows are parallel from northwest (NW) to southeast (SE). The model domain includes the Middle River Complex (MRC),

<sup>11</sup> *Sorption*: a physical and chemical process by which one substance becomes attached to another.

---

which is approximately one mile northwest of Martin State Airport (MSA). Given the distance between the MRC and MSA, different models are used to simulate local plume fate and transport characteristics at each site. At MSA, the model grid spacing varies from 6.25 feet in the area of interest to 115 feet at the outer regions of the model domain.

The site-specific model uses 19 layers to represent the groundwater system beneath Martin State Airport (MSA). The base layer of the model is approximately 120 feet below ground surface (bgs), which is where deep borings at MSA have encountered thick clay. This clay is likely the top of the Arundel-clay confining unit, which is represented in the model as a no-flow boundary. Table 1 summarizes model layering information.

### **3.3 BOUNDARY CONDITIONS**

Model boundaries are mathematical statements specifying the groundwater level (head), groundwater flux, or head-dependent flux at the boundaries of the model domain. Beginning with the top layer, this section discusses the boundary conditions specified for each layer in the numerical groundwater-flow model. The boundary conditions simulated in Layer 1 include net effective recharge, localized pipeline leakage, enhanced evapotranspiration, river leakage, and zero flux (no flow), as shown on Figure 8. The primary source of water to the model is from precipitation-derived recharge. Uniform recharge rates simulated in the model are 7.5 inches per year for unpaved areas and four inches per year for paved areas (Figure 9). Localized groundwater mounding in two areas of Greater Strawberry Point (GSP) is simulated as additional net effective recharge, and the model used a local calibrated value of 394 inches per year for simulating leakage from subsurface pipes.

The historically low water levels in monitoring wells MW-16S and MW-17S indicate that these wells are in an area of possibly high evapotranspiration. A calibrated evapotranspiration rate of 21.9 inches per year was applied to account for heavy vegetation (Figure 9) near these wells.

The principal surface water drainages, which include FMC, Stansbury Creek, Dark Head Creek, Galloway Creek, and Seneca Creek, are simulated using river boundary-condition cells. A no-flow boundary corresponding to prevailing groundwater-flow paths was placed along the northeastern and southeastern edges of the model. A no-flow boundary corresponding to the approximate position of a groundwater divide was also assigned along the northwestern edge of the model.

---

The high water level in well MW-44S suggests that Pond 2 may affect groundwater levels, so Pond 2 was added to the existing groundwater-flow model using the *MODFLOW* river package. In this representation, Pond 2 has fixed water levels to simulate the approximate steady-state conditions detected during water-level measurements. The conductance of the pond bottom was estimated based on site-specific information, and was updated during model calibration. Inverse parameter estimation was performed using the parameter estimation software *PEST* (Watermark Numerical Computing, 2004) to improve the model calibration based on available hydraulic head data and surface water elevations. The calibrated flow-model produced an estimated flux from Pond 2 of 3650 cubic feet (ft<sup>3</sup>)/day.

Except for recharge and evapotranspiration, the boundary conditions for Layers 2 and 3 are similar to those of Layer 1, in that they include river leakage and zero-flux conditions. Recharge and evapotranspiration are applied only to Layer 1. Head conditions and areal extent of the river cells in Layers 2 and 3 are identical to the Layer 1 specifications. Similarly, the no-flow boundary specifications for model Layers 2 and 3 are the same as the specifications for model Layer 1. The same boundary-condition settings are used for Layers 4 through 19. In each of these layers, the entire perimeter of the model is designated as a no-flow boundary. The bottom of Layer 19 is also designated as a no-flow boundary.

### **3.4 HYDRAULIC PROPERTIES**

Both hydraulic conductivity (horizontal and vertical) and storage coefficients were used during the transient model-simulations of pumping tests and tidal fluctuations. The specific yield was specified in the upper zone to simulate water table (unconfined) conditions. For simulation of confined conditions, storativity was specified in the intermediate and lower zones. In the steady-state simulations, changes in storage were not simulated; thus, storage coefficients were needed only in the transient simulations. Various information sources were used to characterize hydraulic properties at the site, including: (1) hydraulic tests in a limited number of wells at the site, (2) analyses of tidally influenced water levels from select monitoring wells equipped with recorders, (3) calibration results from prior site-specific modeling (Tetra Tech 2004; GeoTrans, 2011; Tetra Tech, 2014a) for Lockheed Martin Corporation (Lockheed Martin), and (4) site-specific geologic information from boring logs.

Initial hydraulic-conductivity values in the model were assigned using calibrated values from the previous groundwater-flow model (Tetra Tech, 2014a). These initial values are consistent with



---

observed hydraulic conductivity values determined by slug and pumping tests (Tetra Tech, 2004; GeoTrans, 2011). Boring-log data from the site, in combination with published grain-size-based hydraulic-conductivity ranges, were also used to help assign hydraulic conductivity parameters in the model.

Hydraulic testing results used to improve modeling accuracy include data from multi-rate pumping tests and short-term slug testing. AECOM (2016) conducted variable-rate pumping tests on each of the 13 recovery wells; these test results were used to estimate local horizontal and vertical hydraulic conductivities, and confined and unconfined storage coefficients near the recovery wells. Initial values for the model were modified as appropriate during model calibration to match data from the new recovery well tests, as described in the next section.

Tidal data were also analyzed to refine hydraulic conductivity and storativity values estimated during initial calibration testing. Analysis of water level response to surface water tidal fluctuations in the lower zone of the surficial aquifer that were measured in 2010 indicated a hydraulic conductivity value of 100 feet per day for the lower zone of the surficial aquifer (GeoTrans, 2011). Additional tidal data measured in 2015 were also examined using the groundwater-flow model. Supplemental numerical-model simulations were performed to confirm that the model simulates tidal influences in an adequately accurate manner.

# Numerical Flow- and Solute-Transport Modeling

## 4.1 INTRODUCTION

Calibration of a groundwater-flow model entails adjusting hydraulic parameters, initial conditions, and boundary conditions within reasonable ranges so that simulated hydraulic heads, flow rates, or other calibration targets match measured values (ASTM, 1996). The existing groundwater-flow model for the Dump Road Area (DRA) was updated and recalibrated using data collected since 2014. For Martin State Airport (MSA), the updated flow-model calibration simulated the following measured conditions:

- transient responses for 13 recovery-well variable-rate pumping tests in the upper, intermediate, and lower zones of the surficial aquifer
- transient responses to tidal water-level changes in the lower zone of the surficial aquifer
- approximate steady-state conditions throughout all three vertical zones of the surficial aquifer, based on March 23, 2016 water-level measurements

Calibration was conducted by initial steady-state calibration testing, followed by transient simulations for local area adjustments and model-domain-wide adjustments. Steady-state conditions were re-simulated for final fine-tuning and consistency checking. In some cases, the transient and steady-state simulation sequence was re-run to ensure full consistency and sufficient accuracy. Although steady-state simulations are described before reporting transient-calibration efforts, the calibration was iterative between the different types of runs.

The quality of the steady-state calibration was assessed and quantified through statistical analysis of residuals (ASTM Standard D5981-96 [2008]; Anderson and Woessner, 1992). Residuals are the difference between the measured and simulated water levels in each well. Flow calibration-criteria are based on:

- 
- a mean residual-value near zero
  - an absolute-mean residual less than or equal to 10% of the observed range in water level elevations
  - a standard deviation less than or equal to 20% of the observed range in water-level elevations
  - a random spatial distribution of the positive and negative residuals

Plots of observed versus predicted water levels were used to examine the spread of points around the ideal line of a perfect calibration. Horizontal and vertical flow directions in the model were examined for consistency, with directions inferred from contour maps drawn using field data, and from monitoring well clusters in which vertical-head differences were measured.

Calibration of a groundwater-flow model to a single set of field measurements, assumed to represent steady-state conditions, does not provide the foundation for obtaining a unique solution. To reduce the problem of “non-uniqueness,” the model should be tested against a different set of boundary conditions or stresses, labeled “verification” (ASTM, 1996). Calibrating to transient conditions caused by groundwater flows (typically, extraction well pumping) can reduce the non-uniqueness of the model. Therefore, the groundwater-flow-model calibration focused on simulations of groundwater flow in the surficial aquifer during the 13 recovery-well variable-rate pumping tests.

The objective of the transient calibration is to examine the model’s ability to match both observed responses over time and final drawdowns at the end of each test. Responses observed in well clusters help estimate vertical and horizontal hydraulic-conductivity values in the surficial aquifer. This simulation has dual advantages: (1) verification of the model by calibrating to stresses associated with a second hydrologic scenario, and (2) testing the model’s ability to simulate transient hydraulic-responses by comparing simulated outcomes to carefully measured stresses associated with pumping, thereby reducing its non-uniqueness. Another important calibration scenario is a simulation of hydraulic properties in the upper, intermediate, and lower surficial-aquifer zones. Tidal response data were used to test and adjust the model, using what could be labeled a “naturally conducted” pumping test (i.e., the “pumping” action of the tidal waters in the estuaries surrounding the MSA peninsula).

---

#### 4.1.1 Steady-State Flow

The steady-state-flow model results presented in this section represent the final flow model, based on the large number of adjustments made during calibration of the flow model. Steady-state calibration targets were chosen using groundwater levels measured at MSA on March 23, 2016. Hydraulic conductivities of different materials were modified to improve simulation of hydraulic test data during calibration. The calibrated values of the horizontal conductivity of the permeable sand zones were in agreement with ranges given in Andreasen et al. (2013) for the Patapsco aquifer. Recharge and evapotranspiration rates were also adjusted slightly during model calibration.

Table 1 displays the final distribution of hydraulic conductivity by model layer. Calibrated values for horizontal hydraulic conductivity in the upper, intermediate, and lower zones are consistent with available field data from slug tests, pumping tests, and tidal data. In general, vertical hydraulic conductivity is estimated at one tenth of the horizontal hydraulic conductivity.

Figure 9 shows the zones of calibrated recharge and evapotranspiration rates in the model domain. Calibrated net effective recharge rates are estimated at 7.5 inches per year (in/yr) in the unpaved areas and 4.0 inches per year in paved areas. The observed water table mounding at GSP and utility maps led to the inclusion of a local area of higher recharge (394 in/yr) in the model to represent recharge from probable leaks in subsurface water lines. The historically low water levels in MW-16S and MW-17S at DRA indicate that these two wells are in an area of possibly high evapotranspiration. The calibrated enhanced evapotranspiration rate is 21.9 inches per year for the localized situation near MW-16S and 17S.

Simulated and observed (March 2016) groundwater levels for 149 wells are in Table 2. Table 3 presents a statistical summary of model residuals (i.e., simulated minus observed head) for the 149 water-level targets. The mean residual (-0.03 feet) is near zero, indicating that positive and negative residuals cancel out. In addition, the absolute mean residual is 0.54 feet, a value more than one order of magnitude (10 times) less than the difference between the minimum and maximum water level targets (11.95 feet). The standard deviation is also relatively small (0.79 ft), and only 6.6% of the observed range. Model calibration is thereby accepted, because the metrics have been achieved.

---

Measured and simulated water levels are plotted relative to one another in Figure 10. The linear trend in this plot, with its limited spread around the best-fit line, together with the favorable residual statistics, indicate that the model adequately represents water levels at MSA. Figure 11 shows simulated steady-state potentiometric surfaces and residuals in the upper zone (model Layer 2), intermediate zone (Layer 9), and lower zone (Layer 14). These plots indicate that simulated groundwater flow at MSA is predominantly to the east toward Frog Mortar Creek. This simulated flow direction is consistent with data observed in March 2016 (see Figures 5 through 7) and with each zone's historical potentiometric surface maps (Tetra Tech, Inc. [Tetra Tech], 2002a 2002b; 2004; 2014a).

In general, residuals are relatively low in each layer, and statistical measures meet the calibration criteria. As shown in Figure 11, simulated downward gradients in the upland areas and upward gradients near Frog Mortar Creek (FMC) are consistent with field data (Table 2). Furthermore, calibrated values for hydraulic conductivity are consistent with estimated field values for MSA, based on aquifer-test-data analyses. The flow model also agrees with observed prevailing groundwater flow directions, providing additional evidence of an adequately accurate calibration.

#### **4.1.2 Simulation of Pumping Tests**

AECOM (2016) conducted 13 variable-rate pumping tests in the newly installed extraction wells, with transient drawdown measurements of each extraction well and of nearby observation wells. During transient model-calibration, refinements to the model grid and hydraulic conductivity values were made to improve the match to the drawdown data obtained from each pumping test. Table 4 compares simulated and measured drawdowns measured at the wells monitored for each pumping test. Plots of simulated and observed drawdown for each test are in Appendix A.

These analyses show that the model adequately simulates pumping effects, and therefore satisfies the objectives established for transient calibration. The model's transient response exhibited a good match to the drawdown data for both the pumping wells and most of the observation wells. The difference in simulated and observed response in a few observation wells might be attributed to local, small-scale heterogeneity not represented in the model. Given the match of the model to data in and near the recovery wells, these results indicate that the flow model cannot only predict new hydraulic stresses in the surficial aquifer within the tested area, but can also be applied to examine hydraulic capture, plume transport, and contaminant of concern (COC)-mass reduction during the planned remedial action.

---

### **4.1.3 Tidal Influence Simulation**

A transient simulation of tidal responses in selected site monitoring wells was performed after calibrating the groundwater-flow model to steady-state conditions. The simulation period was divided into 48 stress periods, with each stress period representing a 1.5-hour period. The transient river-stage measurements from the FMC gage at Parkside Marina were averaged over 1.5-hour intervals.

Hydraulic conductivity values and the storage coefficient for the lower-aquifer zone were adjusted slightly to match water-level fluctuations. Figure 12 shows simulated versus observed hydraulic-head changes at MW-48S, MW-48I, and MW-48D during the tidal fluctuation between April 5–7, 2015. These plots show that model results closely match field data. The model’s ability to match transient tidal variations in each zone of the surficial aquifer in the area of concern provides additional confidence in using the groundwater-flow model to evaluate and optimize remedial performance.

### **4.1.4 Flow-Model Sensitivity Analysis**

A sensitivity analysis was performed to evaluate how changes in selected model parameters affect the model. One parameter at a time was varied while all other parameters were held constant. The tested model parameters were varied by 50% of the calibrated values. Results of the sensitivity analysis are in Table 5. These results were analyzed to identify parameters that cause the greatest sensitivity when changed, and to confirm that the final calibrated values fall within the range of expected values, according to the ranges set during formulation of the conceptual model.

Model results are most sensitive to changes in unpaved-area recharge, mounding recharge rate, and horizontal hydraulic conductivity values in the surficial aquifer (especially in the lower zone of the surficial aquifer). This is expected, because recharge in the unpaved-area is the source of all groundwater flow in the model. In addition, all local groundwater flow occurs within the surficial aquifer, and horizontal hydraulic conductivity is the primary property describing the flow field. Hydraulic conductivity can be adjusted in direct linear proportion to adjustments in the prevailing recharge rate when conducting steady-state simulations; this is the “non-uniqueness” concern cited above that is addressed by calibrating the model to transient conditions.

Calibrated values for these parameters are consistent with values in the study area, as identified during the conceptual-model formulation stage. No significant improvement in model calibration

---

would be achieved by adjusting these parameters at this time. Thus, changes to the model are not warranted, and the model is accepted for predictive use, according to the objectives set forth at the beginning of modeling and the model-calibration criteria established during numerical-model development. Additional water-level-recorder data, including tidal influences, will be collected before and during recovery well startup. These data will be used to refine the model and more fully examine hydraulic capture under observed pumping conditions of the groundwater-recovery well system.

## **4.2 SOLUTE-TRANSPORT MODEL**

### **4.2.1 Summary of Previous Transport Modeling**

Initial transport modeling (Tetra Tech, 2004) included calibration of a groundwater-flow and solute-transport model to available data for DRA. Additional transport model simulations were performed in 2012 using the 2004 model (Tetra Tech, 2004) to estimate trichloroethene (TCE) concentrations over time for the groundwater remedial design. Using a new flow model (Tetra Tech, 2014a) and a companion transport-model, contaminant fate and transport were simulated under alternative remediation scenarios by initializing the distribution of TCE in model layers 1-6 (upper zone), 7-10 (intermediate zone), and 11 (deep zone). The simulations assume that no source(s) remain in place. Simulations using the *RT3D* simulation code (Clement, 1997) were conducted to visualize plume concentrations over time.

### **4.2.2 Revisions to Existing Transport Model**

Building on the previous modeling, the recent groundwater-flow model simulations used a refined site-wide flow model with 19 layers, consisting of a grid-spacing ranging from 6.25–115 feet. To improve the simulation accuracy of the model's advective-transport-velocity field, the groundwater-flow model was calibrated to new data collected in 2015 and 2016 that include a round of non-pumping water level measurements, transient changes in hydraulic heads during recovery-well pumping tests, and tidal responses in the recently installed MW-48 well cluster. For current transport modeling, a finer grid with small spacing was embedded in the calibrated flow-model using telescopic-mesh refinement (TMR).

Using TMR, the sub-regional model domain was subdivided into a finite-difference grid of 497 columns and 290 rows, with row and column spacings of 10 feet throughout the sub-regional model domain. The finer grid spacing in the local DRA zone of interest improved the simulation

---

accuracy of the transport model by reducing the potential effects of numerical dispersion. The details of the transport modeling approach, including the computer code, simulated chemicals of concern, and parameter values, are below.

#### **4.2.2.1 Computer Code**

The DRA numerical transport-model was developed using the well-known finite-difference code, *RT3D* (Clement, 1997). *RT3D* uses *MODFLOW*-2000 to simulate the flow field that provides the basis for representing (in *RT3D*) the advective transport of dissolved constituents. *RT3D* also directly accounts for other potentially significant transport mechanisms, including hydrodynamic dispersion, diffusion, sorption, and sequential first-order biodegradation.

#### **4.2.2.2 Simulated Chemicals of Concern**

The primary chemicals of concern (COC) simulated in the transport modeling are three chlorinated volatile organic compounds (cVOCs): trichloroethene (TCE), *cis*-1,2-dichloroethene (*cis*-1,2-DCE), and vinyl chloride (VC). Simulation of these chemicals allows the model to examine complete sequential degradation of the TCE-DCE-VC chain to ethene via reductive dechlorination, as observed in the field data (Tetra Tech 2002a; 2002b; 2004; 2013; 2015e).

#### **4.2.2.3 Transport Parameter Values**

Input parameters for the transport simulations include fraction of organic carbon (foc), partitioning coefficient (Koc), distribution coefficient (Kd), effective porosity, bulk density, retardation coefficient, dispersivity, and first-order degradation-rate constants. The parameter values used in the contaminant-mass fate and transport modeling are based on the Tetra Tech (2004) modeling and recent field data. A summary of the solute-transport model's parameter values is in Table 6.

The retardation factor (R) was calculated using the following equation:

$$R = 1 + (\text{bulk density/effective porosity}) \times \text{foc} \times K_{oc} \quad (1)$$

To calculate the retardation factor, total organic carbon value was estimated based on the average of the available data collected in the study area (Tetra Tech, 2004). Lateral, transverse, and vertical dispersivity values were estimated using best scientific judgment. A longitudinal dispersivity value of one foot was assigned to all model layers. By convention, the transverse and vertical dispersivities are set to 0.1 and 0.01 times the longitudinal dispersivity value, respectively.



---

A wide range of first-order aerobic and anaerobic biodegradation rates for VOCs (including TCE) is available in current literature (Aronson and Howard, 1997, and Wiedemeier et al., 1999). Under anaerobic conditions, reported ranges for biodegradation-rate constants are as follows (Aronson and Howard, 1997; Wiedemeier et al., 1999; Suarez and Rifai, 1999):

- TCE 0.053–0.90 year<sup>-1</sup> (0.053-0.90/year)
- *cis*-1,2 -DCE 0.0–3.3 year<sup>-1</sup>
- VC 0.12–2.6 year<sup>-1</sup>

The values of the half-lives (rate constants) for TCE, *cis*-1,2-DCE, and VC were assigned as 5.9 years (0.18 yr<sup>-1</sup>), 12 years (0.058 yr<sup>-1</sup>), and 4.2 years (0.17 yr<sup>-1</sup>), respectively, based on the calibrated Tetra Tech (2004) model. Although the degradation rates will vary over the duration of the site remedy, these calibrated degradation-rate values are reasonable for the five-year simulation period in this report. To improve the predictive ability of the transport-model simulations, the degradation-rate constant values will be refined as additional data are collected during the startup and future operation of the remedial system.

### 4.3 INITIALIZING MASS IN PLACE

The solute-transport model simulations were performed by predicting changes in contaminant distribution over time, based on an estimated initial distribution of TCE, *cis*-1,2-DCE, and VC concentrations in the model. The initial plume concentrations were estimated using groundwater data from the 2016 extraction well sampling, direct-push technology sampling data, and recent groundwater sampling data collected from the monitoring wells in 2013 and 2014. Each model layer has different initial-plume concentrations that are based on three-dimensional kriging<sup>12</sup> using *Mining Visualization Software*<sup>™</sup> (MVS). An exponential semi-variogram<sup>13</sup> model was used for the interpolation, with a one-tenth vertical to horizontal anisotropy<sup>14</sup> ratio. The initial TCE, *cis*-1,2-DCE, and VC concentrations for the upper (Layer 7), intermediate (Layer 11), and lower (Layer 14) zones of the surficial aquifer are shown in Figures 2, 3, and 4, respectively.

<sup>12</sup> *Kriging*: a regression technique used to interpolate data. Interpolation is a method of constructing new data points within the range of a discrete set of known data points.

<sup>13</sup> *Semivariogram*: a measure of the strength of a statistical correlation as a function of distance.

<sup>14</sup> *Anisotropy*: having a different value when measured in different directions.

---

## Section 5

# Analysis of Planned Remedial Action

Possible remedial alternatives were identified and evaluated during previous modeling analyses (GeoTrans, 2011; Tetra Tech, 2014a); these alternatives indicate (through predictive simulations) that the selected remedy of recovery-well pumping could prevent elevated concentrations of groundwater chemicals of concern (COC) from migrating toward Frog Mortar Creek (Tetra Tech, 2014a). The upcoming remedial action, which is planned to start in summer 2017, includes a line of 16 extraction wells (Figure 13 and Appendix A) along the western shore of Frog Mortar Creek (FMC). In preparation for the startup of these recovery wells, the primary objective of this modeling task is to predict both the extent of the hydraulic-capture zone and changes in COC plume concentrations over time during operation of the groundwater remediation system.

### 5.1 PREDICTIVE-SIMULATION METHODOLOGY

The updated numerical groundwater flow- and solute-transport model was applied to examine groundwater flow and plume transport for two scenarios: (1) no further action (base case) and (2) recovery well pumping for plume capture. Although the remedial action is planned to start in summer 2017, the no further action base-case simulation is useful to more fully assess the effects of recovery well pumping. For the hydraulic-capture scenario, the United States Geological Survey (USGS) particle-tracking code *MODPATH* (Pollock, 1989; 1994) was used to evaluate the effectiveness of hydraulic containment for impacted groundwater. Particle tracking simulates the movement of a groundwater particle from an initial starting point through a groundwater flow-field over time. Thus, particle-tracking techniques are useful tools for evaluating groundwater flow directions, dissolved-contaminant migration pathways, and hydraulic capture of groundwater recovery-well systems. Solute-transport modeling was subsequently applied to examine future trichloroethene (TCE), *cis*-1,2-DCE, and VC concentrations for both the base-case and hydraulic-capture scenarios. The results of the particle tracking and predictive solute-transport modeling analyses are discussed below.

---

## 5.2 PREDICTIVE-MODELING ANALYSES

### 5.2.1 Particle Tracking

Advective-particle tracking is a simple form of contaminant-transport analysis that does not account for effects due to dispersion, retardation, and chemical reactions. Using a groundwater flow-field simulated with *MODFLOW*, *MODPATH* computes groundwater velocities in the three principal coordinate-directions throughout the model domain, for each cell in the model grid. Then, *MODPATH* uses cell-by-cell three-dimensional (3D) velocities to simulate particle movement from one cell to the next, based on interpolated velocities at each cell phase.

Using *MODPATH*, forward particle-tracking was applied to simulate particle trajectories and travel times for the currently planned hydraulic-barrier well scenario. Particle tracking was performed by initially placing particles in the center of each cell in the model domain and determining which particles eventually migrated into a recovery well. The extent of hydraulic capture was delineated by identifying all model cells with initial particles that eventually reached a recovery well. Additional forward particle-tracking simulations were performed by initially placing particles in hot spots (i.e., high TCE-concentration areas) in the upper, intermediate, and lower zones, and then examining the particle pathways and travel times.

Figures 13 and 14 show the areal and cross-sectional (vertical) views (respectively) of both the simulated hydraulic-capture zone and the capture of particles initially placed in high concentration areas. These figures show that recovery well pumping creates a broad region of hydraulic capture in each monitoring zone that extends several hundred feet to the east and below FMC. Particle tracks show that all particles initially located in the high concentration zones will be captured by the recovery wells under the currently proposed groundwater-capture scenario. Particle tracks in the vertical cross-section indicate that extraction of impacted groundwater in the deep zone might take longer, because of slower upward transport to recovery wells pumping from the intermediate zone.

### 5.2.2 Solute-Transport Modeling

#### 5.2.2.1 Base Case (“No Further Remedial Action”)

Solute-transport model simulations under a “no further action” scenario (base case) were performed to better understand and interpret the predicted results for the planned remedial action. The predictive simulations for this base-case model were performed using calibrated groundwater-

---

flow and solute-transport modeling under the assumption that no further remedial action (i.e., no pumping) would occur. The initial extent of the TCE, *cis*-1,2-DCE, and VC plumes was estimated based on data collected from 2014–2016 (Figures 2, 3, and 4) for each monitoring zone. The solute-transport model was applied to predict the future extent of TCE and its degradation products (*cis*-1,2-DCE and VC) after five years. Figures 15 and 16 show simulated concentrations of TCE and its degradation product VC in the upper zone (Layer 7), intermediate zone (Layer 11), and lower zone (Layer 14) of the surficial aquifer after five years. Under this hypothetical no-further-action scenario, contaminant plumes would move downgradient to the east and eventually discharge into FMC (see Figures 15 and 16).

#### **5.2.2.2      Planned Remedial Action—Hydraulic Barrier Wells**

The hydraulic-barrier-well scenario was simulated using the solute-transport model to predict the future extent of TCE, *cis*-1,2-DCE, and VC after five years, based on planned recovery-well pumping rates (Table 7). Figures 17 and 18 show the simulated concentrations for TCE and VC in the upper zone (Layer 7), intermediate zone (Layer 11), and lower zone (Layer 14) of the surficial aquifer after pumping has continued for five years. In contrast to the no-further-action (base) case, recovery-well pumping will prevent upgradient plumes from discharging into Frog Mortar Creek. Model simulations also indicate that plume concentrations will decrease, from both mass-removal by the recovery wells and natural sequential-biodegradation of TCE, *cis*-1,2-DCE, and VC into ethene.

The solute-transport model was applied to estimate treatment-system influent concentrations of TCE, *cis*-1,2-DCE, and VC during startup of the groundwater recovery system. The average concentration of the blended water from each recovery well was calculated based on the estimated pumping rate and simulated concentration in each recovery well after 30 days. The estimated treatment-system-startup effluent concentrations for TCE, *cis*-1,2-DCE, and VC are 1174 micrograms per liter (µg/L), 207 µg/L, and 117 µg/L, respectively.

Model simulations were also applied to examine induced recharge from Frog Mortar Creek during operation of the groundwater-recovery well system. The groundwater-flow model simulations indicate that low rates (2.6 gallons per minute [gpm]) of induced inflow from Frog Mortar Creek will result from pumping of the recovery wells in comparison to the total recovery well pumping rate of 63.2 gpm. Thus, the simulations indicate that induced infiltration would be diluted by pumped freshwater at a ratio of about 24:1. Frog Mortar Creek is moderately brackish (its salinity

---

is approximately 15–20% that of seawater); it receives freshwater flow from Middle River and other local tributary streams and swales, and from groundwater base-flow. Therefore, the salinity in the groundwater from the recovery wells is expected to be diluted by a factor of approximately 120:1 to 160:1 in comparison to seawater.

---

## Section 6

# Summary and Next Steps

This report documents the further development and application of groundwater-flow and contaminant-transport modeling for the Martin State Airport site in Middle River, Maryland. Updated groundwater-flow and solute-transport modeling examined the future performance of the hydraulic-barrier remedy planned to address volatile organic compound contamination in groundwater at the Dump Road Area site. The primary objective of the remediation system is to control and capture contaminated groundwater, thereby preventing its migration and discharge into off-site areas, including to the surface waters of Frog Mortar Creek.

Numerous modeling simulations were performed to calibrate the groundwater-flow model to both static (non-pumping) conditions in March–2016 and to measured drawdown data from controlled variable-rate pumping tests of the recovery wells (AECOM, 2016). Results indicate that the calibration criteria have been met. The flow model adequately represents drawdown measured during recovery-well pumping tests. Further, the groundwater-flow model can adequately match the tidal responses in each zone of the surficial aquifer as observed on April 5–7 2015. These results provide additional confidence for applying the groundwater-flow and solute-transport model to assess and optimize remedial system performance.

Groundwater-flow and solute-transport modeling simulations were performed for two scenarios: (1) no further action (base case) scenario and (2) the hydraulic-barrier recovery-well remediation system. The base-case scenario is presented to more fully assess the effects of recovery well pumping, which is anticipated to start in summer 2017. Modeling results from the hydraulic-barrier scenario indicate that contaminated groundwater at the site would be effectively controlled.

The hydraulic barrier planned for the remedial action includes pumping 16 recovery wells arranged perpendicular to the plume and adjacent to Frog Mortar Creek. Seven recovery wells are in the upper zone, five are in the intermediate zone, and four are in the lower zone, resulting in a total system-wide pumping rate of 63.2 gallons per minute. Particle-tracking results indicate that particles initially placed in high concentration zones will be captured by recovery wells.

---

Solute-transport-model predictive simulations indicate that the recovery wells will reduce plume mass over time, and will prevent upgradient plumes from discharging into Frog Mortar Creek. During the startup of the recovery wells, the estimated treatment-system-effluent concentrations for trichloroethene (TCE), *cis*-1,2-DCE, and VC were 1174 µ/L, 207 µg/L, and 117 µg/L, respectively. Model simulations also indicate that low rates of induced inflow from Frog Mortar Creek will result from pumping.

Additional groundwater-flow model and particle tracking using measured transient hydraulic-head data collected in transducers during recovery-well-system startup will be conducted to more fully evaluate the extent of the hydraulic capture zone. These analyses will help refine pumping rates so that hydraulic capture, particularly during transient tidal fluctuations, can be ensured. We recommend additional updating of the groundwater-flow and solute-transport modeling using data collected during operation of the remedial system, so that mass-removal rates and overall remedial system performance can be optimized. Given that particles are migrating from high concentration areas in the deep zone to recovery wells in the intermediate zone, additional solute-transport modeling should be applied to refine pumping rates to ensure that the plumes move laterally within each zone toward recovery wells, with minimal transport between monitoring zones. We also recommend using calibrated groundwater-flow and solute-transport modeling as a decision-analysis tool for periodically analyzing and optimizing remedial system performance, to maintain hydraulic capture and efficient plume-mass reduction over the life cycle of the site remedy.

---

## Section 7

# References

1. AECOM, 2016. Technical memorandum, “Extraction Wells EW-01 through EW-16 Results, Airport Dump Road Area Groundwater IRA Treatment System, October 21, 2016.” Report prepared by AECOM for Lockheed Martin Corporation, Bethesda, Maryland.
2. Anderson, M. P. and W. W. Woessner, 1992. *Applied Groundwater Modeling: Simulation of Flow and Advective Transport*. San Diego: Academic Press.
3. Andreasen, D. C., A. W. Staley, and G. Achmad, 2013. “Maryland Coastal Plain Aquifer System Information: Hydrogeologic Framework,” *Maryland Geologic Survey Report of Investigations No. 12-02-20*.
4. Andreasen, D. C., 2007. “Optimization of Ground-Water Withdrawals in Anne Arundel County, Maryland, from the Upper Patapsco, Lower Patapsco, and Patuxent Aquifers, Projected through 2044,” *Maryland Geologic Survey Report of Investigations No. 77*.
5. Aronson, D. and P. Howard, 1997. *Anaerobic Biodegradation of Organic Chemicals in Groundwater: A Summary of Field and Laboratory Studies* (SRC TR-96-0223F), Environmental Science Center, Syracuse Research Corporation, 6225 Running Ridge Road, North Syracuse, New York 13212-2509.
6. ASTM International (ASTM) D5447-04 (2010). *Standard Guide for Application of a Groundwater-Flow Model to a Site-Specific Problem*.
7. ASTM International (ASTM) D5490-93 (2008). *Standard Guide for Comparing Groundwater-Flow Model Simulations to Site-Specific Information*.
8. ASTM International (ASTM) D5609-94 (2008). *Standard Guide for Defining Boundary Conditions in Groundwater-Flow Modeling*.
9. ASTM International (ASTM) D5610-94 (2008). *Standard Guide for Defining Initial Conditions in Groundwater-Flow Modeling*.
10. ASTM International (ASTM) D5611-94 (2008). *Standard Guide for Conducting a Sensitivity Analysis for a Groundwater-Flow-Model Application*.
11. ASTM International (ASTM) D5718-95 (2006). *Standard Guide for Documenting a Groundwater-Flow-Model Application*.
12. ASTM International (ASTM) D5880-95 (2006). *Standard Guide for Subsurface Flow- and Transport-Modeling*.



- 
13. ASTM International (ASTM) D5979-96 (2008). *Standard Guide for Conceptualization and Characterization of Groundwater Systems*.
  14. ASTM International (ASTM) D5981-96 (2008). *Standard Guide for Calibrating a Groundwater-Flow-Model Application*.
  15. Chapelle, F. H., 1985. "Hydrogeology, Digital Solute-Transport Simulation, and Geochemistry of the Lower Cretaceous Aquifer System near Baltimore, Maryland." *United States Geological Survey Report of Investigations No. 43*.
  16. Clement, T. P., 1997. *RT3D: A Modular Computer Code for Simulating Reactive Multispecies Transport in 3-Dimensional Groundwater Aquifers*, PNNL-SA-28967, Pacific Northwest National Laboratory, Richland, Washington.
  17. Fleck, W. B., and D. A. Vroblesky, 1996. "Simulation of ground-water flow of the coastal plain aquifers in parts of Maryland, Delaware, and the District of Columbia," *United States Geological Survey Professional Paper 1404-J*.
  18. Gelhar, L. W., C. Welty, and K. R. Rehfeldt, 1992. "A critical review of data on field-scale dispersion in aquifers." *Water Resources Research*, 28(7): 1955-1974.
  19. GeoTrans, 2011. *MSA Groundwater Feasibility Study—Appendix B: Refinement and Calibration of a Groundwater Flow Model at the "Dump Road Area Site" at Martin State Airport*. Report prepared by GeoTrans, for Lockheed Martin Corporation, Bethesda, Maryland. February.
  20. Handex Environmental Management, 1992. *Geophysical Survey Report, Taxiway Tango, Martin State Airport, Middle River, Maryland*. Report prepared by Handex Environmental Management, for Lockheed Martin Corporation, Bethesda, Maryland.
  21. Harbaugh, A. W., E. R. Banta, M. C. Hill, and M. G. McDonald, 2000a. "MODFLOW-2000: the U.S. Geological Survey Modular Groundwater Model—User's Guide to Modularization Concepts and the Groundwater-Flow Process," *United States Geological Survey Open-File Report 00-92*.
  22. Harbaugh, A. W., E. R. Banta, M. C. Hill, and M. G. McDonald, 2000b. "MODFLOW-2000: the U.S. Geological Survey Modular Groundwater Model—User's Guide to Observation, Sensitivity, and the Parameter-Estimation Process, and Three Post-Processing Programs," *United States Geological Survey Open-File Report 00-184*.
  23. Harbaugh, A. W., 2005. "MODFLOW-2005: the USGS Modular Ground-Water Model: The Ground-Water-Flow Process," *United States Geological Survey Techniques and Methods 6-A16*.
  24. Karickhoff, S. W., 1985. *Pollutant Sorption in Environmental Systems. Environmental Exposure from Chemicals, Vol. I*, Eds. W. B. Neely and G. E. Blau: Florida: Boca Raton, CRC Press, pp. 49–62.

- 
25. Maryland Environmental Service (MES), 1994. *Martin State Airport Preliminary Site Investigation of the Taxiway Tango, Martin State Airport, Middle River, Maryland*. Report prepared by MES, Annapolis, Maryland for the Maryland Aviation Administration, Baltimore, Maryland. May.
  26. McDonald, M. G., and A. W. Harbaugh, 1988. "A Modular Three-Dimensional Finite-Difference Ground-Water-Flow Model." *U.S. Geological Survey TWRI*, Book 6, Chapter A1.
  27. Newell, Charles J. and D. T. Adamson, 2005. "Planning-Level Source-Decay Models to Evaluate Impact of Source Depletion on Remediation Time Frame" in *Remediation*, 15(4), pp. 27-47.
  28. Pollock, D. W., 1989. "Documentation of Computer Programs to Compute and Display Pathlines Using Results from the U.S. Geological Survey Modular Three-Dimensional Finite-Difference Ground-Water-Flow Model." *United States Geological Survey Open File Report*, pp. 89–381.
  29. Pollock, D. W., 1994. "User's Guide for *MODPATH/MODPATH-PLOT*, version 3: A particle-tracking post-processing package for *MODFLOW*, the U.S. Geological Survey finite-difference ground-water-flow model." *United States Geological Survey Open-File Report* 94–464.
  30. Suarez, M. P. and H. S. Rifai, 1999. "Biodegradation rates of fuel hydrocarbons and chlorinated solvents," *Biorem. J.*, 3(4), pp. 337–362.
  31. Tenbus, F. J. and W. B. Fleck, 2001. "Simulation of Ground-Water Flow and Transport of Chlorinated Hydrocarbons at Graces Quarters, Aberdeen Proving Ground, Maryland," *United States Geological Survey Water Resources Investigation Report* 01-4106.
  32. Tetra Tech, Inc. (Tetra Tech), 1999. *Final Groundwater Monitoring Well Surveying and Sampling Report, Martin State Airport, Middle River, Maryland*. Report prepared by Tetra Tech, Inc., Germantown, Maryland for Lockheed Martin Corporation, Bethesda, Maryland.
  33. Tetra Tech, Inc. (Tetra Tech), 2002a. *Final Chemical Delineation and Groundwater Modeling Report, Martin State Airport, Middle River, Maryland, December 27, 2002*. Report prepared by Tetra Tech, Inc., Germantown, Maryland for Lockheed Martin Corporation, Bethesda, Maryland.
  34. Tetra Tech, Inc. (Tetra Tech), 2002b. *Interim Data-Summary Report, Martin State Airport, Middle River, Maryland, March 15, 2002*. Report prepared by Tetra Tech, Inc., Germantown, Maryland for Lockheed Martin Corporation, Bethesda, Maryland.
  35. Tetra Tech, Inc. (Tetra Tech), 2004. *Data-Gap Investigation and Modeling Report, Martin State Airport, Middle River, Maryland*. May. Report prepared by Tetra Tech, Inc., Germantown, Maryland for Lockheed Martin Corporation, Bethesda, Maryland.

- 
36. Tetra Tech, Inc. (Tetra Tech), 2013. *Dump Road Area Characterization of Possible Source Areas Report*, Martin State Airport, 701 Wilson Point Road, Middle River, Maryland. April. Report prepared by Tetra Tech, Inc., Germantown, Maryland for Lockheed Martin Corporation, Bethesda, Maryland.
  37. Tetra Tech, 2014a. *Groundwater-Flow and Solute-Transport Modeling for the Dump Road Area, Martin State Airport, July 2014*. Report prepared by Tetra Tech, Inc., Germantown, Maryland for Lockheed Martin Corporation, Bethesda, Maryland.
  38. Tetra Tech, Inc. (Tetra Tech), 2014b. *Dump Road Source-Areas Soil and Groundwater Characterization, Martin State Airport, 701 Wilson Point Road, Middle River, Maryland. January*. Report prepared by Tetra Tech, Inc., Germantown, Maryland for Lockheed Martin Corporation, Bethesda, Maryland.
  39. Tetra Tech, 2014c. *Dump Road Area Source-Areas Design-Characterization Groundwater-Investigation Report, Martin State Airport, November 2014*. Report prepared by Tetra Tech, Inc., Germantown, Maryland for Lockheed Martin Corporation, Bethesda, Maryland.
  40. Tetra Tech, 2015a. *Greater Strawberry Point Area Supplemental Soil and Groundwater Characterization Report, Martin State Airport, February 2015*. Report prepared by Tetra Tech, Inc., Germantown, Maryland for Lockheed Martin Corporation, Bethesda, Maryland.
  41. Tetra Tech, 2015b. *2014 Surface Water Monitoring Report for Frog Mortar Creek*. Report prepared by Tetra Tech, Inc., Germantown, Maryland for Lockheed Martin Corporation, Bethesda, Maryland. June.
  42. Tetra Tech, 2015c. *2015 Groundwater Monitoring Report for the Dump Road Area and Main Terminal Area, Martin State Airport*. Report prepared by Tetra Tech, Inc., Germantown, Maryland for Lockheed Martin Corporation, Bethesda, Maryland. December.
  43. Tetra Tech, 2015d. *Dump Road Area and Taxiway Tango Combined Soil and Waste Remedy Feasibility Study, Martin State Airport*. Report prepared by Tetra Tech, Inc., Germantown, Maryland for Lockheed Martin Corporation, Bethesda, Maryland. December.
  44. Tetra Tech, 2015e. *Frog Mortar Creek Groundwater Discharge Characterization Report*. Report prepared by Tetra Tech, Inc., Germantown, Maryland for Lockheed Martin Corporation, Bethesda, Maryland. December.
  45. Vroblesky D. A. and W. B Fleck, 1991. "Hydrogeologic framework of the coastal plain of Maryland, Delaware, and the District of Columbia," *United States Geological Survey Professional Paper 1404-E*, 45 p.
  46. Watermark Numerical Computing, 2004. *PEST: Model-Independent Parameter Estimation. User's Manual, 5th Edition*.
  47. Wiedemeier, T. H., H. S. Rifai, C. J. Newell, and J. W. Wilson, 1999. *Natural attenuation of fuels and chlorinated solvents*. John Wiley & Sons, New York.

- 
48. Xu, M. and Y. Eckstein, 1995. "Use of Weighted Least-Squares Method in Evaluation of the Relationship between Dispersivity and Field-scale." *Groundwater*, v. 33, No. 6, pp. 905–908.
  49. Zheng, C. and P. P. Wang, 1998. *MT3DMS: A Modular Three-Dimensional Multispecies Contaminant-Transport Document and User's Guide*. Technical Publication, U.S. Army Corps of Engineers Waterways Experiment Station, Vicksburg, Mississippi.
  50. Zheng, C., 2006. *MT3DMS v5.2. A Modular Three-Dimensional Multispecies Contaminant-Transport Model for Simulation of Advection, Dispersion, and Chemical Reactions of Contaminants in Groundwater Systems, Supplemental User's Guide*. Prepared for the U.S. Army Corps of Engineers Waterways Experiment Station, Vicksburg, Mississippi.

---

This page intentionally left blank.

---

## **ATTACHMENTS:**

**FIGURES**

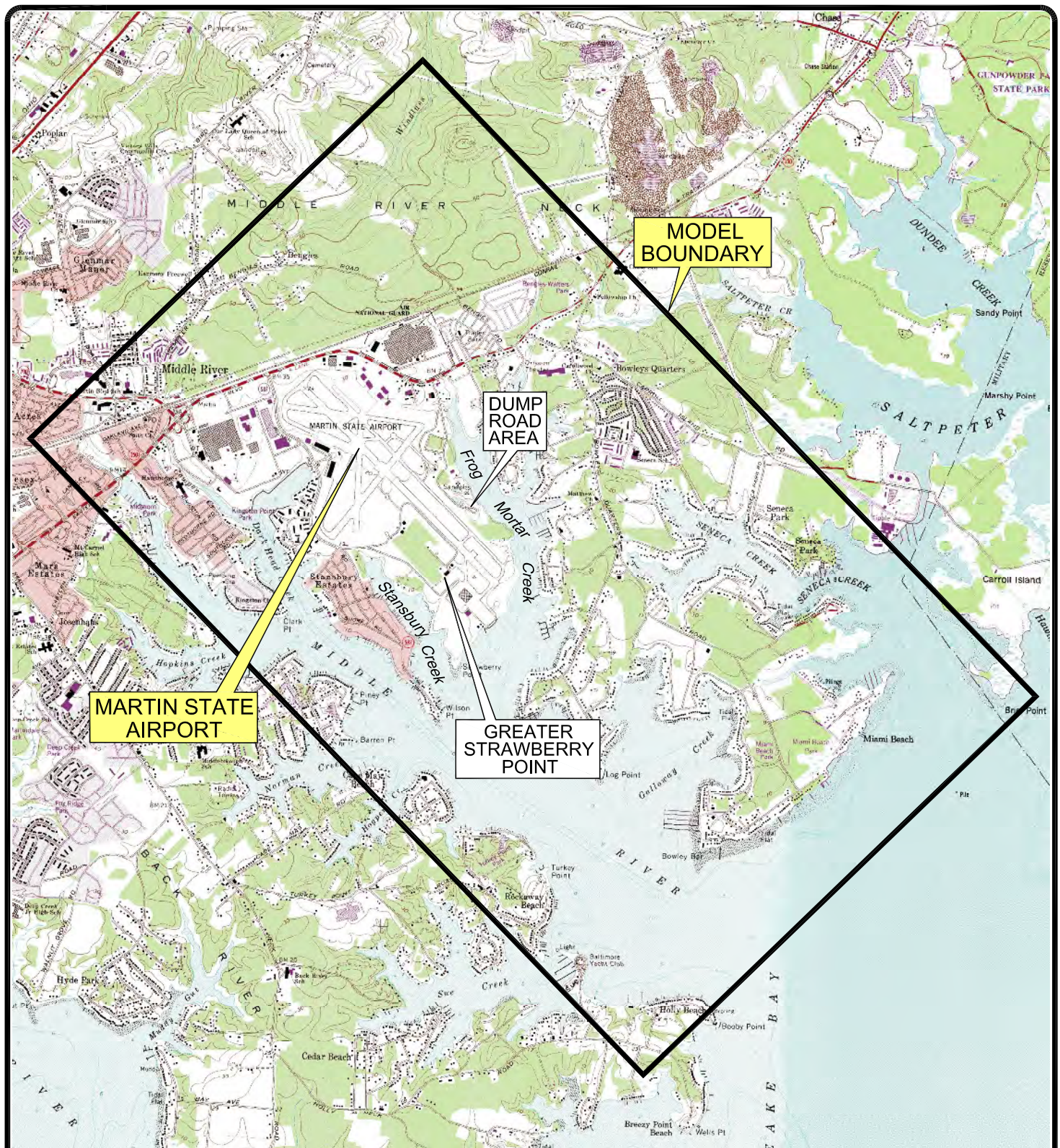
**TABLES**

**APPENDIX A**

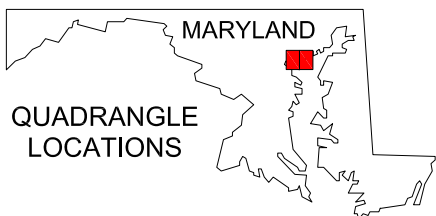
---


## FIGURES



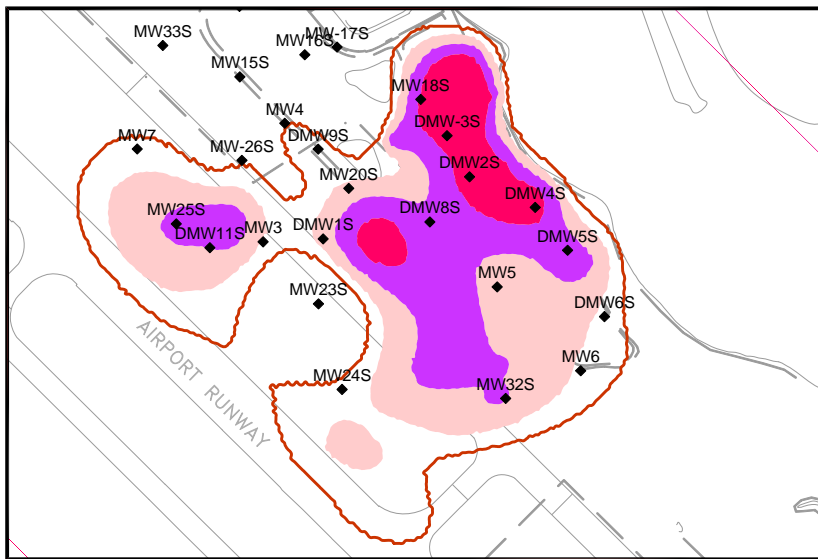


SOURCE:  
 U.S.G.S. QUADRANGLES MIDDLE RIVER, MD  
 (1969) PHOTOREVISED 1985 AND GUNPOWDER  
 NECK, MD (1949) PHOTOREVISED 1986.

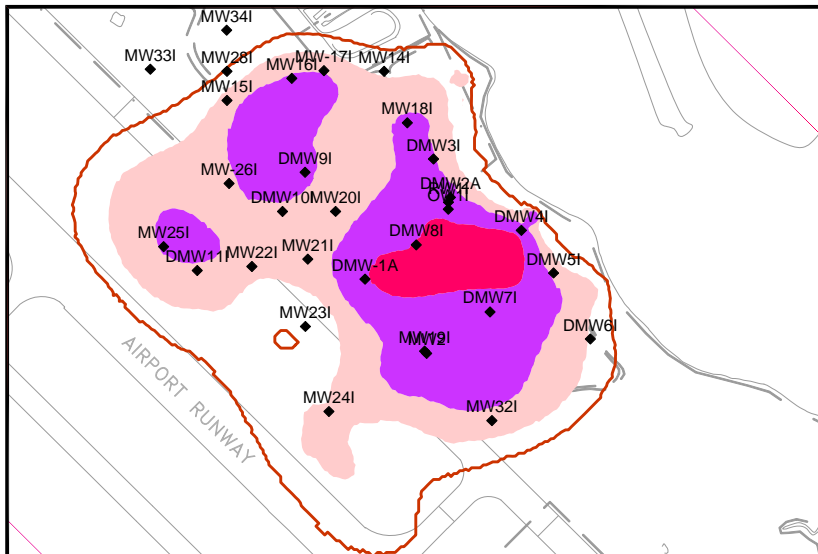
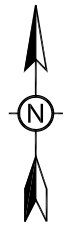


TITLE: <b>SITE LOCATION MAP</b>		
LOCATION: <b>Martin State Airport, Maryland</b>		
 <b>TETRA TECH</b>	APPROVED	DB
	DRAFTED	CP
	PROJECT#	117-0512128
	DATE	5-16-17
FIGURE <b>1</b>		

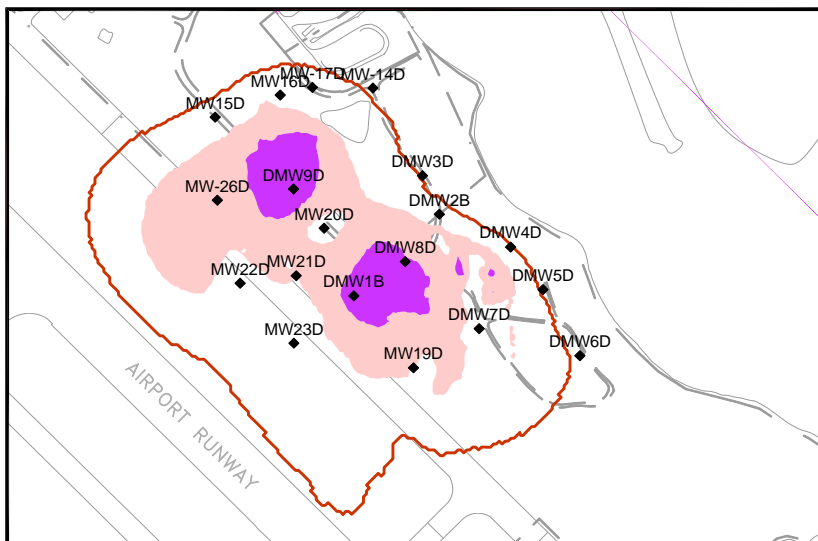
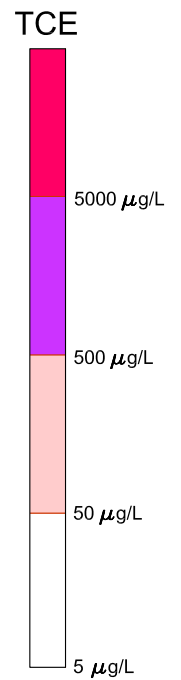




UPPER  
ZONE



INTERMEDIATE  
ZONE



LOWER  
ZONE



P:\ACAD\0512-128-MSA\0512128002A.DWG

TITLE:

**DISTRIBUTION OF TCE IN UPPER, INTERMEDIATE, AND  
LOWER ZONES OF SURFICIAL AQUIFER, 2013 - 2016**

LOCATION:

**Martin State Airport, Maryland**

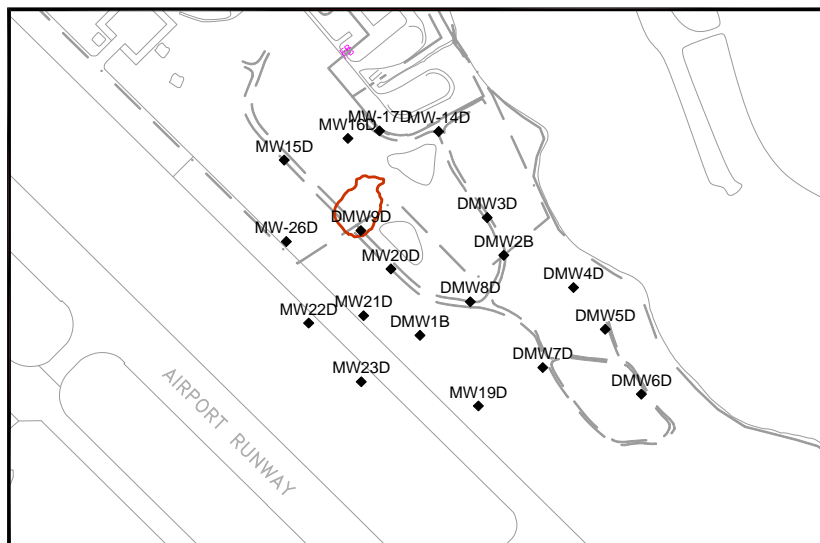
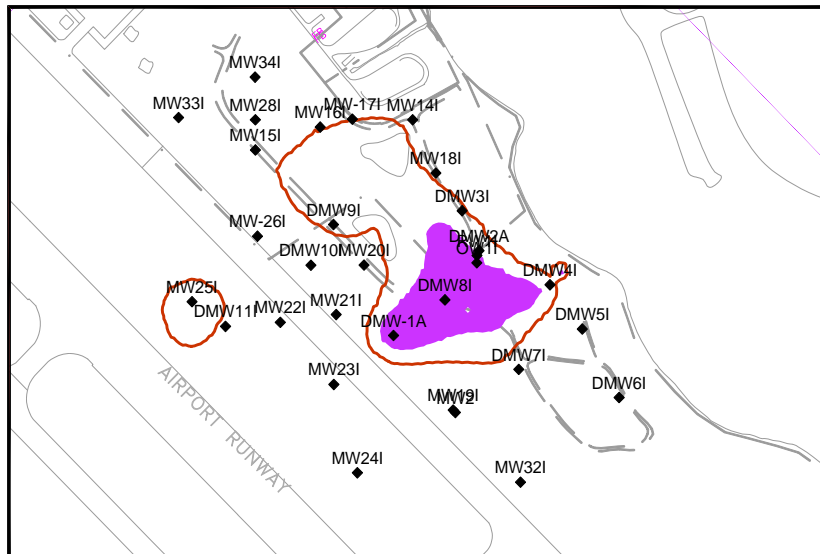
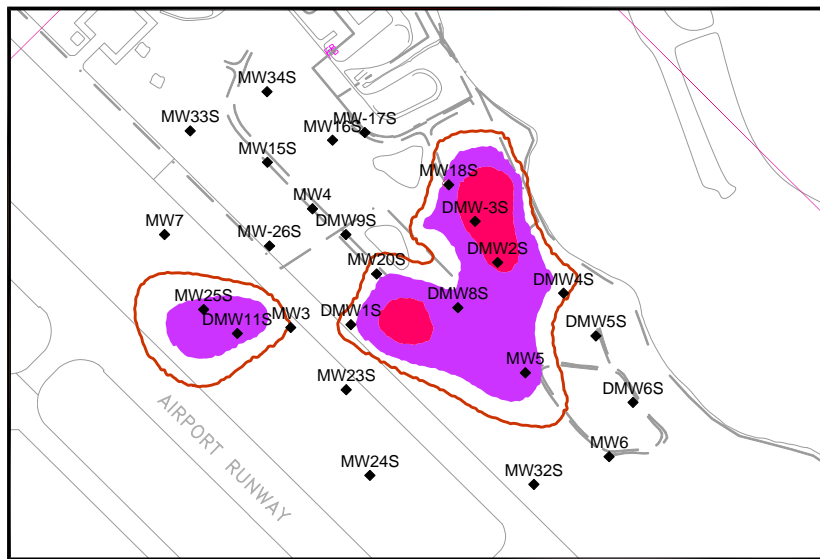


**TETRA TECH**

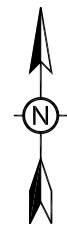
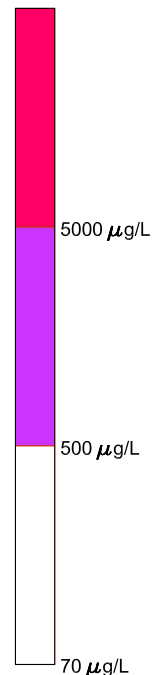
APPROVED	DB
DRAFTED	CP
PROJECT#	117-0507559
DATE	4-25-17

FIGURE

**2**



CIS 1,2-DCE



TITLE: **DISTRIBUTION OF CIS 1,2-DCE IN UPPER, INTERMEDIATE, AND LOWER ZONES OF SURFICIAL AQUIFER, 2013 - 2016**

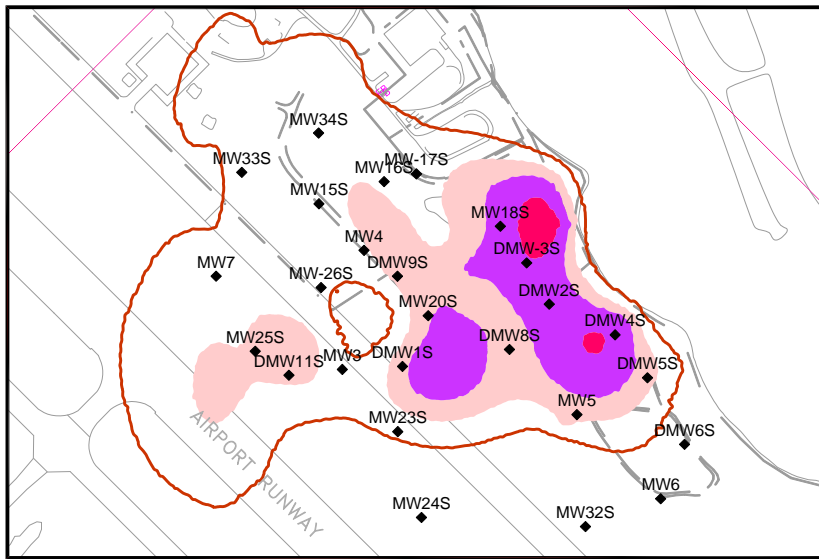
LOCATION: **Martin State Airport, Maryland**



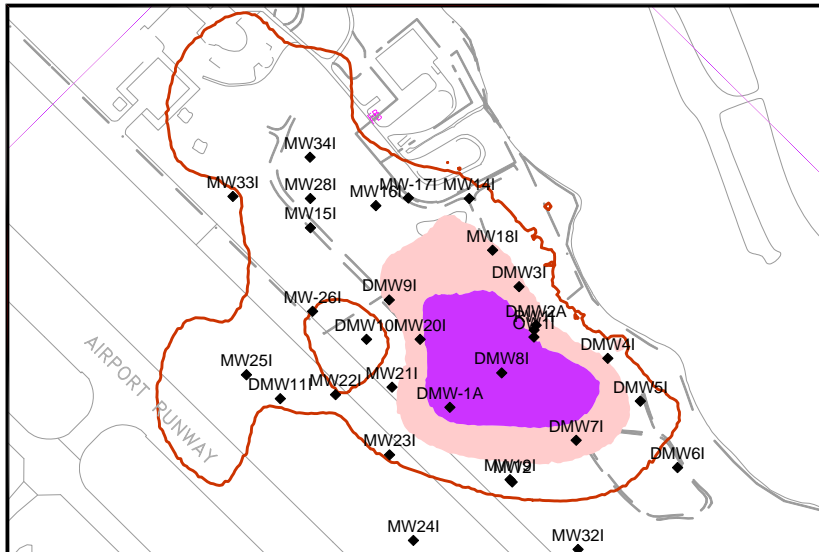
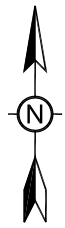
**TETRA TECH**

APPROVED	DB
DRAFTED	CP
PROJECT#	117-0512128
DATE	4-25-17

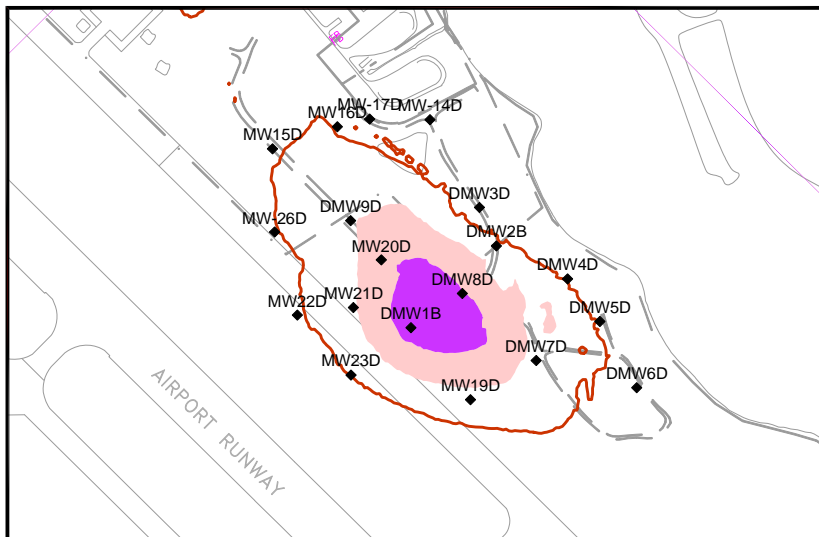
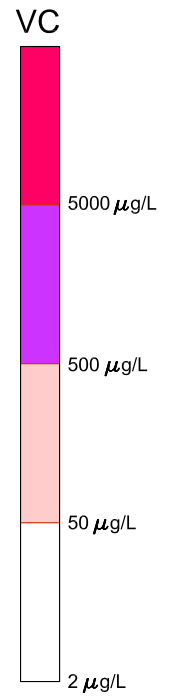
FIGURE  
**3**



UPPER  
ZONE



INTERMEDIATE  
ZONE



LOWER  
ZONE



TITLE:

**DISTRIBUTION OF VC IN UPPER, INTERMEDIATE, AND  
LOWER ZONES OF SURFICIAL AQUIFER, 2013 - 2016**

LOCATION:

**Martin State Airport, Maryland**



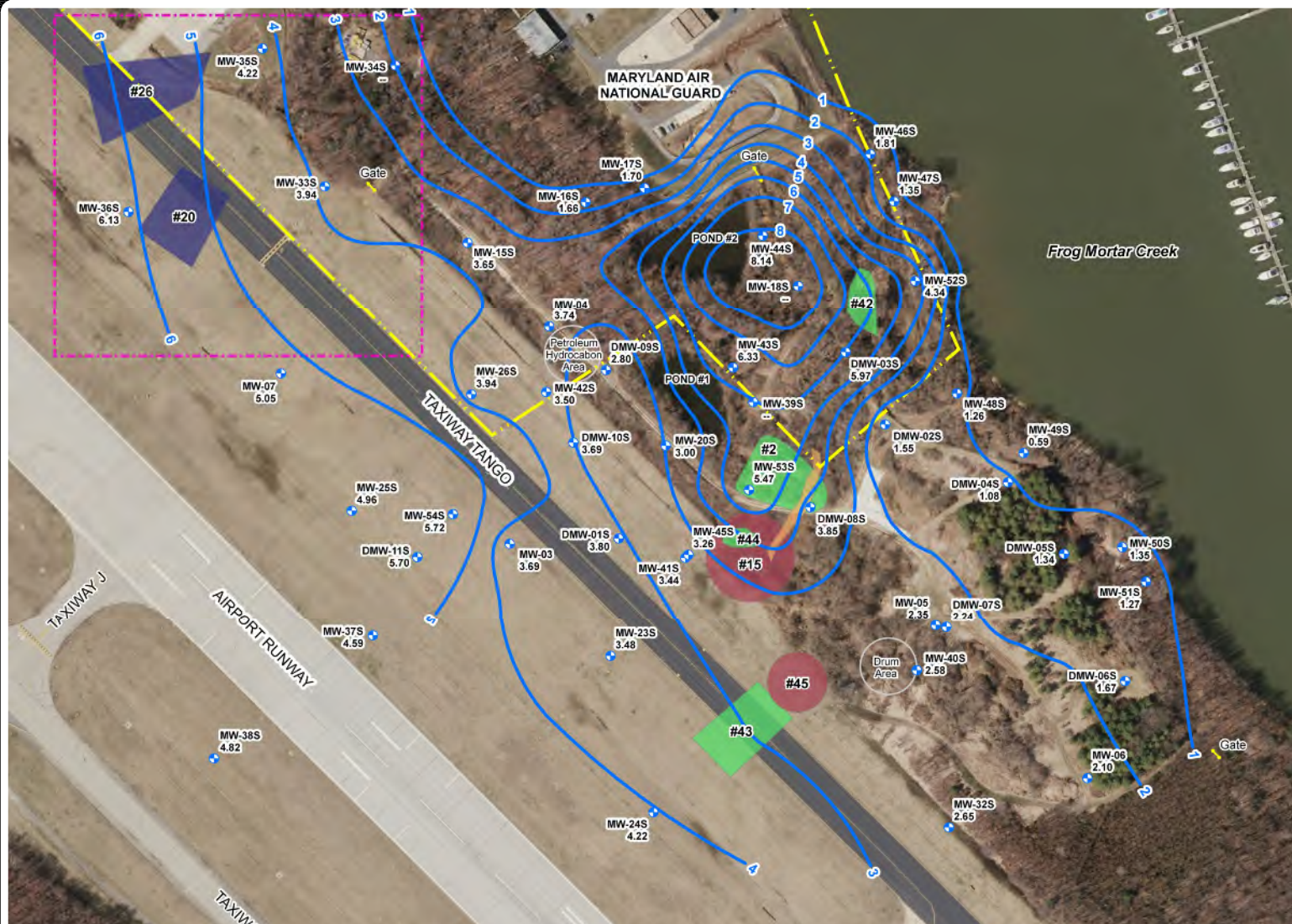
**TETRA TECH**

APPROVED	DB
DRAFTED	CP
PROJECT#	117-0507128
DATE	4-25-17

FIGURE

**4**





#### LEGEND

- UPPER SURFICIAL AQUIFER GROUNDWATER MONITORING WELL
  - 6.33 GROUNDWATER ELEVATION (IN FEET, NORTH AMERICAN VERTICAL DATUM, 1988)
  - NOT MEASURED
  - GROUNDWATER ELEVATION CONTOUR (CONTOUR INTERVAL = 1 FOOT, DASHED WHERE INFERRED)
  - MARYLAND AIR NATIONAL GUARD BOUNDARY
  - FORMER AMMUNITION BUNKER
  - FORMER OPEN BURNING AREA
  - FORMER POND/PIT
  - FORMER POND
  - TAXIWAY TANGO AREA - NORTH
  - EXTENT OF UNSATURATED CONTAMINATED SOIL AND LANDFILL MATERIAL
  - POND
  - #20 FORMER FEATURE NUMBER (FROM 2012 AERIAL PHOTOGRAPH STUDY)
- 2014 aerial photograph provided by U.S. Geological Survey.



#### TITLE:

**WATER TABLE MAP BASED ON GROUNDWATER LEVELS IN THE UPPER ZONE OF SURFICIAL AQUIFER, MARCH 2016**

#### LOCATION:

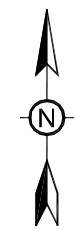
**Martin State Airport, Maryland**



**TETRA TECH**

APPROVED	DB	FIGURE <b>5</b>
DRAFTED	CP	
PROJECT#	117-0512128	
DATE	4-25-17	

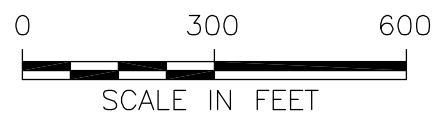





**LEGEND**

- SURFICIAL AQUIFER GROUNDWATER MONITORING WELL
- 3.37 GROUNDWATER ELEVATION (IN FEET, NORTH AMERICAN VERTICAL DATUM, 1988)
- NOT MEASURED
- GROUNDWATER ELEVATION CONTOUR (CONTOUR INTERVAL = 1 FOOT; DASHED WHERE INFERRED)
- MARYLAND AIR NATIONAL GUARD BOUNDARY
- FORMER AMMUNITION BUNKER
- FORMER OPEN BURNING AREA
- FORMER POND/PIT
- FORMER POND
- TAXIWAY TANGO AREA - NORTH
- EXTENT OF UNSATURATED CONTAMINATED SOIL AND LANDFILL MATERIAL
- POND
- #20 FORMER FEATURE NUMBER (FROM 2012 AERIAL PHOTOGRAPH STUDY)

2014 aerial photograph provided by U.S. Geological Survey.



TITLE: HYDRAULIC HEAD CONTOURS BASED ON GROUNDWATER LEVELS IN THE INTERMEDIATE ZONE OF SURFICIAL AQUIFER, MARCH 2016			
LOCATION: Martin State Airport, Maryland			
 <b>TETRA TECH</b>	APPROVED	DB	FIGURE  <b>6</b>
	DRAFTED	CP	
	PROJECT#	117-0512128	
	DATE	4-25-17	




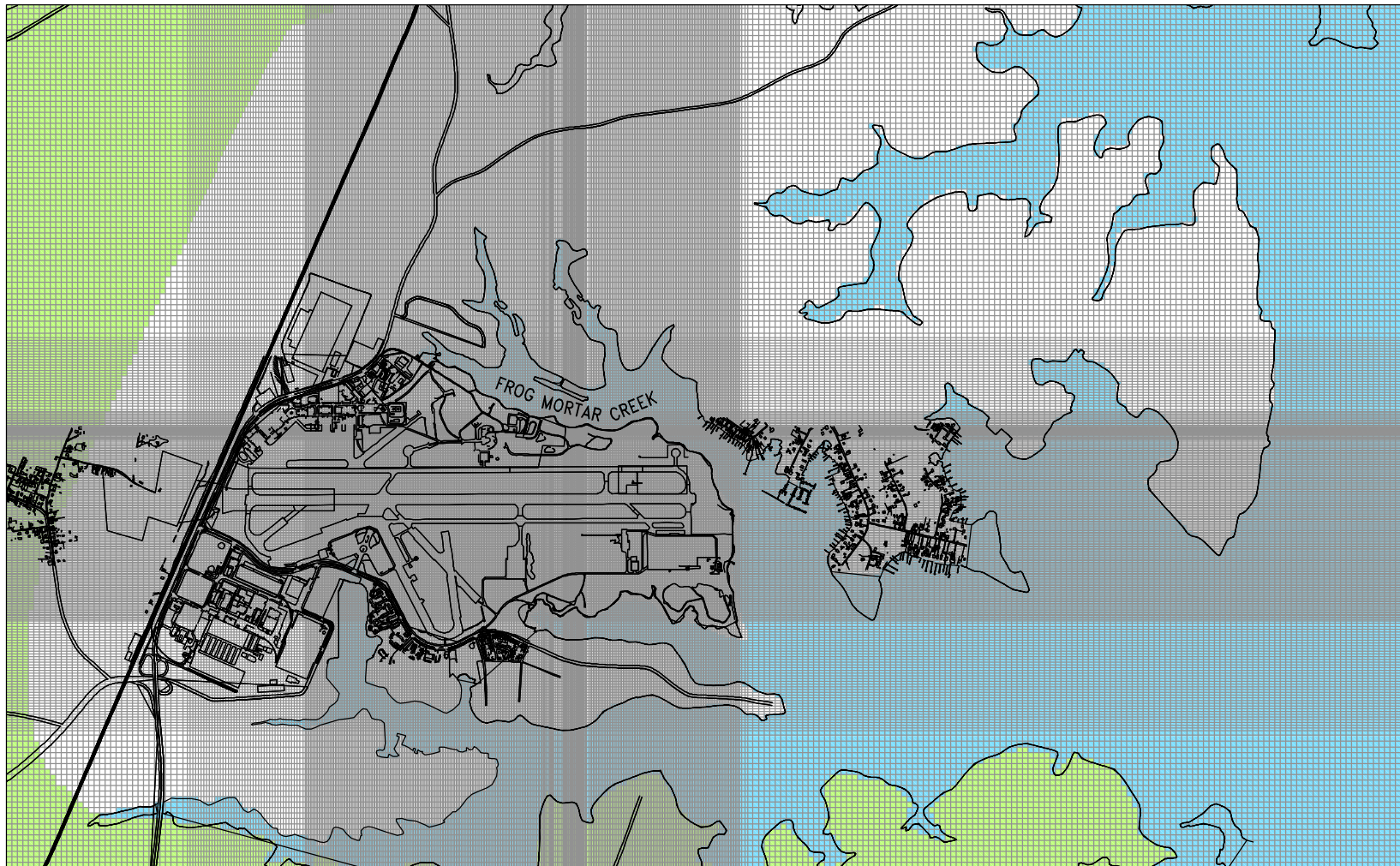


**LEGEND**

- SURFICIAL AQUIFER GROUNDWATER MONITORING WELL
- 1.58 GROUNDWATER ELEVATION (IN FEET, NORTH AMERICAN VERTICAL DATUM, 1988)
- NOT MEASURED
- 2- GROUNDWATER ELEVATION CONTOUR (CONTOUR INTERVAL = 1 FOOT, DASHED WHERE INFERRED)
- MARYLAND AIR NATIONAL GUARD BOUNDARY
- FORMER AMMUNITION BUNKER
- FORMER OPEN BURNING AREA
- FORMER POND/PIT
- FORMER POND
- TAXIWAY TANGO AREA - NORTH
- EXTENT OF UNSATURATED CONTAMINATED SOIL AND LANDFILL MATERIAL
- POND
- #20 FORMER FEATURE NUMBER (FROM 2012 AERIAL PHOTOGRAPH STUDY)

2014 aerial photograph provided by U.S. Geological Survey.

TITLE: HYDRAULIC HEAD CONTOURS BASED ON GROUNDWATER LEVELS IN THE LOWER ZONE OF SURFICIAL AQUIFER, MARCH 2016			
LOCATION: Martin State Airport, Maryland			
 <b>TETRA TECH</b>	APPROVED	DB	FIGURE <b>7</b>
	DRAFTED	CP	
	PROJECT#	117-0512128	
	DATE	4-25-17	



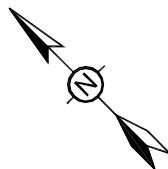
**LEGEND**


■ NO FLOW

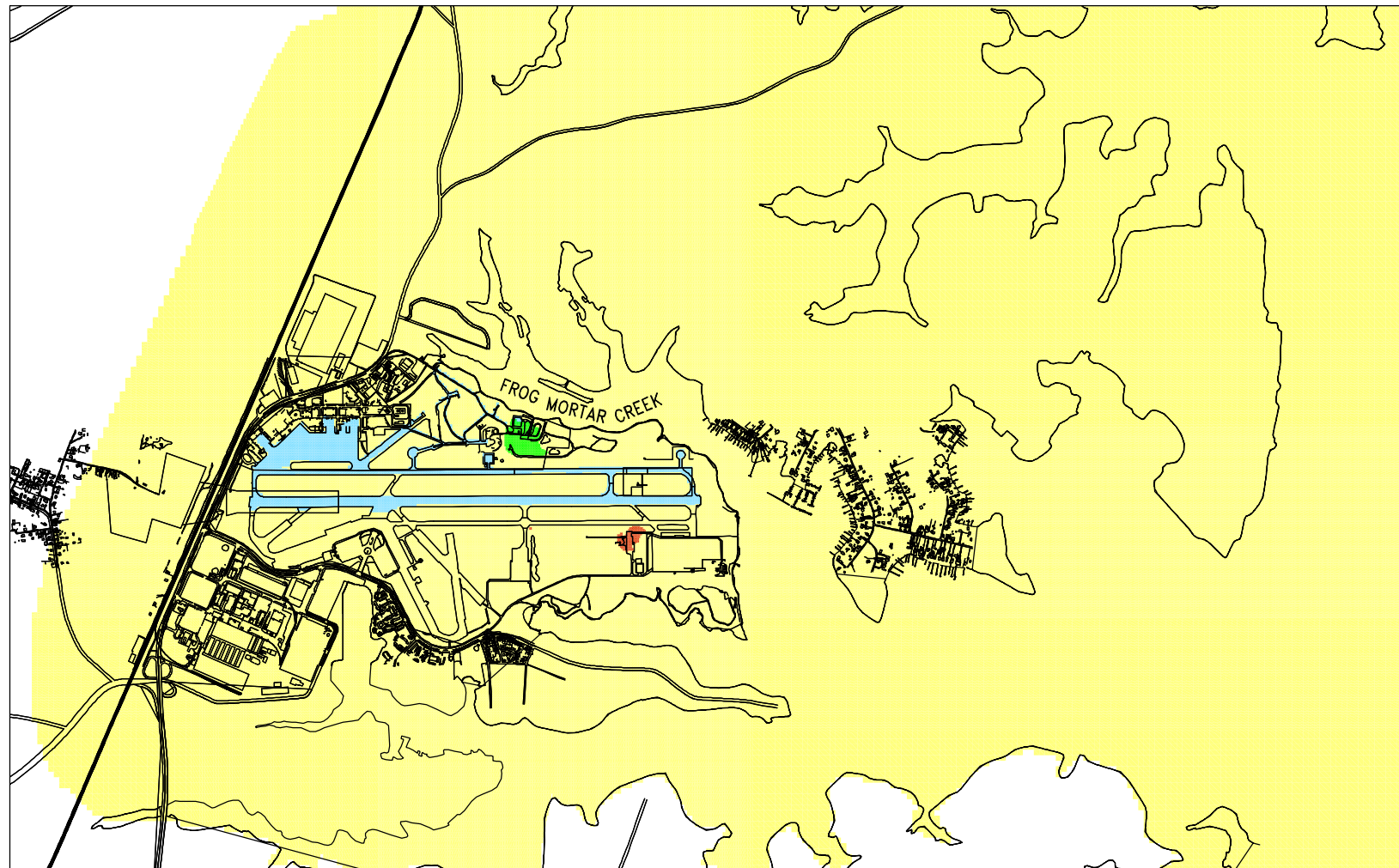
■ RIVER BOUNDARY  
CONDITION  
H = 0.32 FT MSL  
CONDUCTIVITY = 20 FT/DAY

**NOTE:**  
RIVER BOUNDARY CONDITION  
IS ONLY IN LAYERS 1, 2,  
AND 3.

0 3000 6000  
SCALE IN FEET



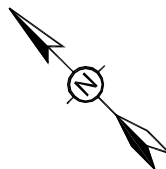
TITLE: <b>MODEL GRID AND BOUNDARY CONDITIONS</b>			
LOCATION: <b>Martin State Airport, Maryland</b>			
 <b>TETRA TECH</b>	APPROVED	DB	FIGURE  <b>8</b>
	DRAFTED	CP	
	PROJECT#	117-0512128	
	DATE	4-25-17	



**LEGEND**

- ET:
- 21.9 IN/YR
- RECHARGE:
- 4.03 IN/YR
  - 7.54 IN/YR
  - 394.2 IN/YR

0 3000 6000  
SCALE IN FEET



**TITLE:**  
**SIMULATED DISTRIBUTION OF GROUNDWATER RECHARGE  
AND EVAPOTRANSPIRATION IN THE CALIBRATED MODEL**

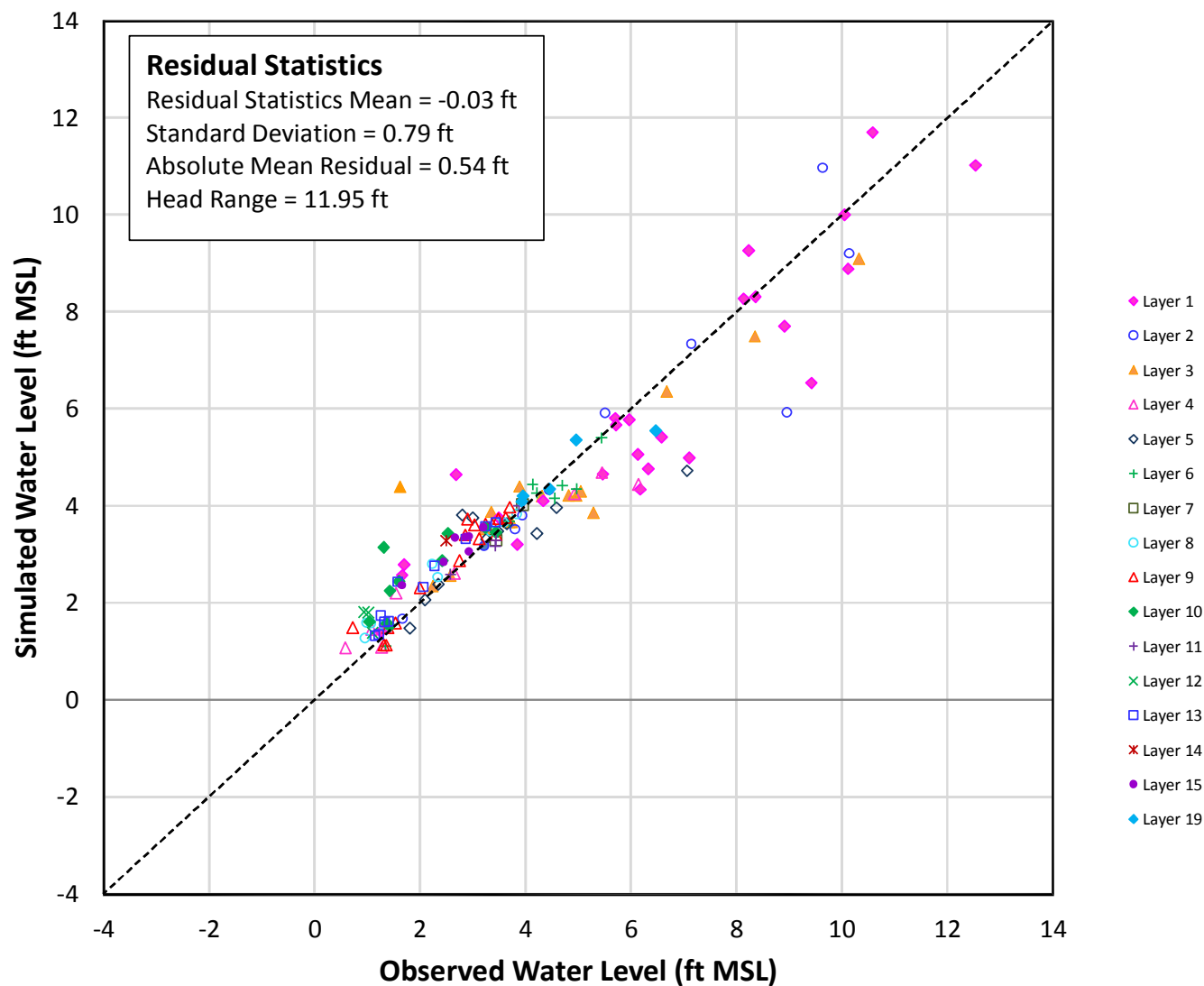
**LOCATION:**  
**Martin State Airport, Maryland**



**TETRA TECH**

APPROVED	DB	FIGURE  <b>9</b>
DRAFTED	CP	
PROJECT#	117-0512128	
DATE	4-25-17	





TITLE: **PLOT OF MEASURED VERSUS SIMULATED  
GROUNDWATER LEVELS, MARCH 2016**

LOCATION: **Martin State Airport, Maryland**



**TETRA TECH**

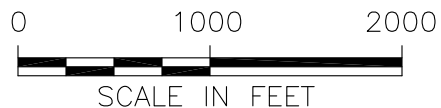
APPROVED	DB
DRAFTED	CP
PROJECT#	117-0512128
DATE	4-25-17

FIGURE  
**10**

This map shows the Frog Mortar Creek area with stream flow indicated by blue arrows. Elevation contours are shown in blue, with values ranging from 2 to 6. Sampling points are marked with black dots and labeled with their elevations. The elevations range from 0.0 to 0.6. The map also shows a road and some buildings.

1. RESIDUALS ARE FOR ALL MODEL LAYERS IN THE UPPER, INTERMEDIATE, AND LOWER ZONE.
2. SIMULATED HEADS ARE FOR MODEL LAYERS 2, 9, AND 14, RESPECTIVELY.
3. UPPER ZONE (LAYERS 1-6), INTERMEDIATE ZONE (LAYERS 7-9), AND LOWER ZONE (LAYERS 10-12).

— 4.0 POTENTIOMETRIC CONTOUR (ft MSL)  
0.76+ SIMULATED < OBSERVED RESIDUAL (FT)  
-0.74+ SIMULATED > OBSERVED RESIDUAL (FT)



**SIMULATED POTENTIOMETRIC SURFACE AND RESIDUALS IN THE UPPER (LAYER 2), INTERMEDIATE (LAYER 9), AND LOWER (LAYER 14) ZONES OF THE SURFICIAL AQUIFER**

### Martin State Airport, Maryland

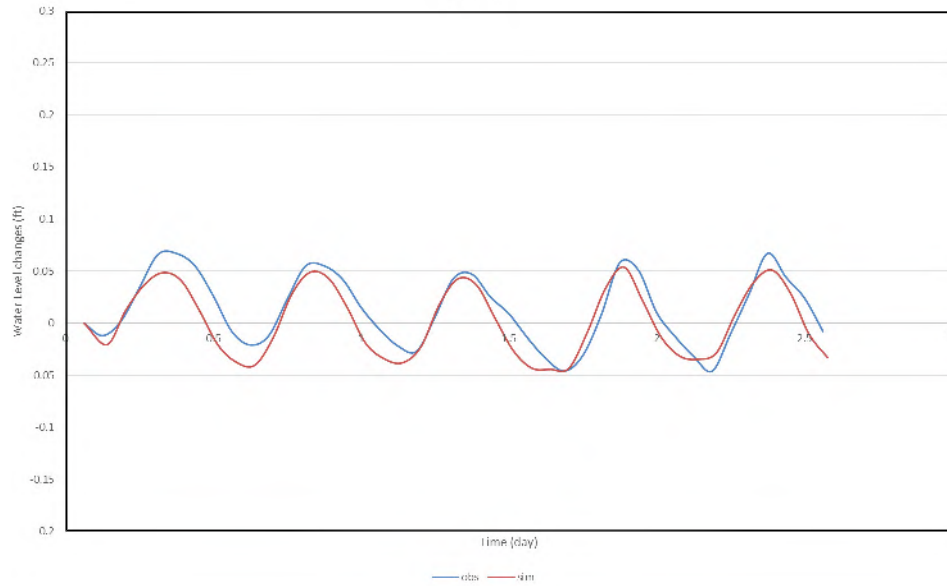


**TETRA TECH**

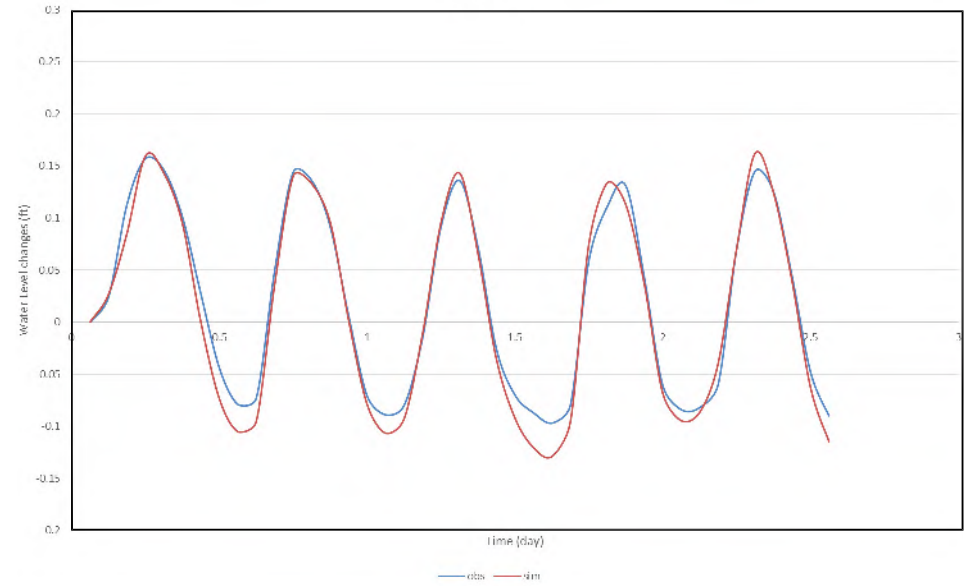
FIGURE

11

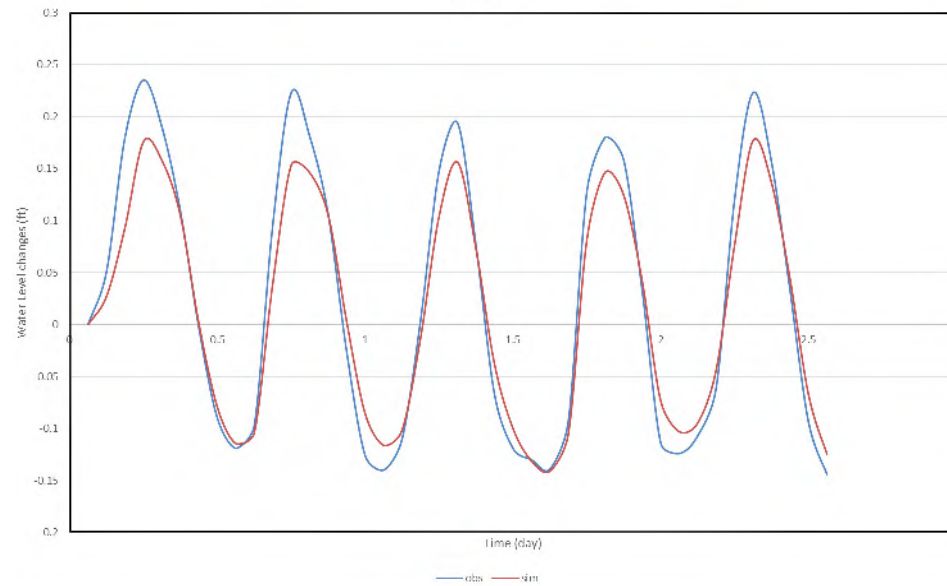
MW48S



MW48I



MW48D



TITLE:  
**SIMULATED AND OBSERVED HYDRAULIC HEAD CHANGES  
AT MW48S, MW48I, AND MW48D DURING TIDAL  
FLUCTUATION FROM APRIL 5, 2015 AND APRIL 7, 2015**

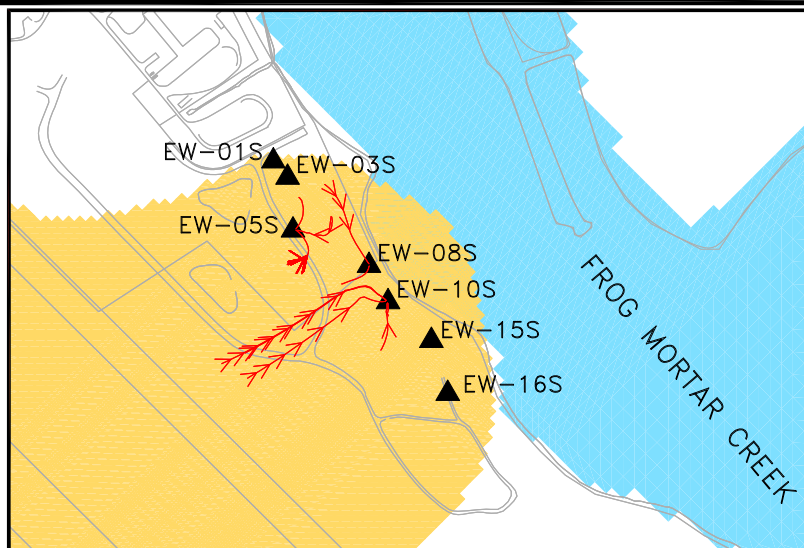
LOCATION:

**Martin State Airport, Maryland**

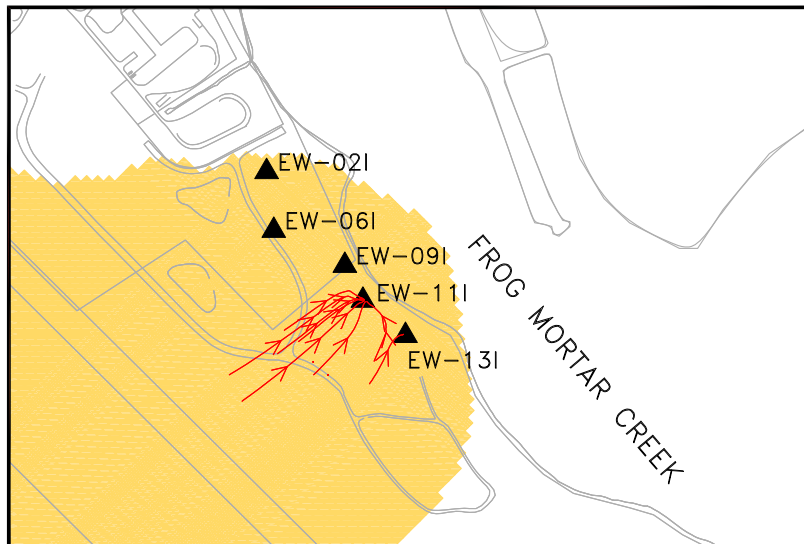
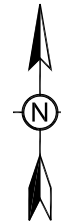


**TETRA TECH**

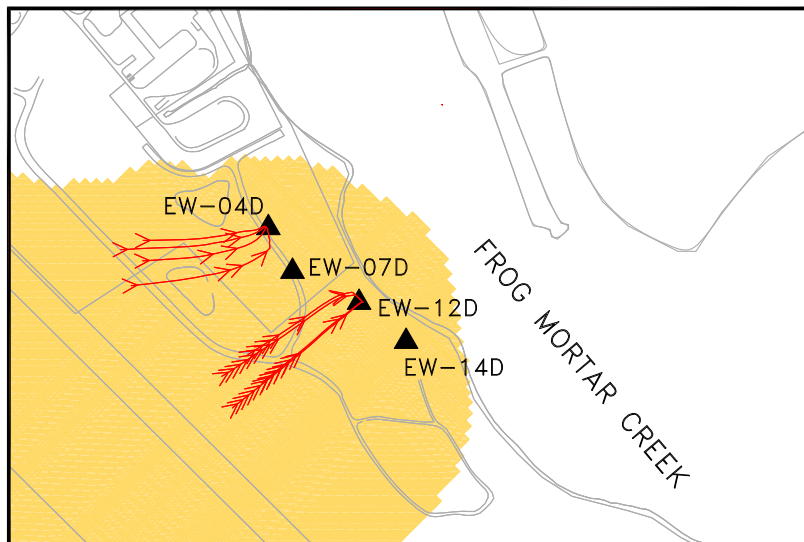
APPROVED	DB	FIGURE <b>12</b>
DRAFTED	CP	
PROJECT#	117-0512128	
DATE	4-25-17	



UPPER  
ZONE



INTERMEDIATE  
ZONE



LOWER  
ZONE

#### LEGEND

- ▲ EXTRACTION WELL
- EXTENT OF CAPTURE ZONE
- RIVER
- PARTICLE TRACE

#### NOTES:

1. EACH ARROW REPRESENTS A 1 YEAR TRAVEL TIME.
2. PARTICLE TRACES WERE STARTED IN AREAS OF HIGH CONCENTRATION.



TITLE: **PREDICTED STEADY-STATE CAPTURE ZONE FOR REMEDIAL SYSTEM STARTUP PUMPING RATES IN THE UPPER (LAYERS 1-7), INTERMEDIATE (LAYERS 8-11), AND LOWER (LAYERS 12-15) ZONES OF THE SURFICIAL AQUIFER**

LOCATION:

**Martin State Airport, Maryland**

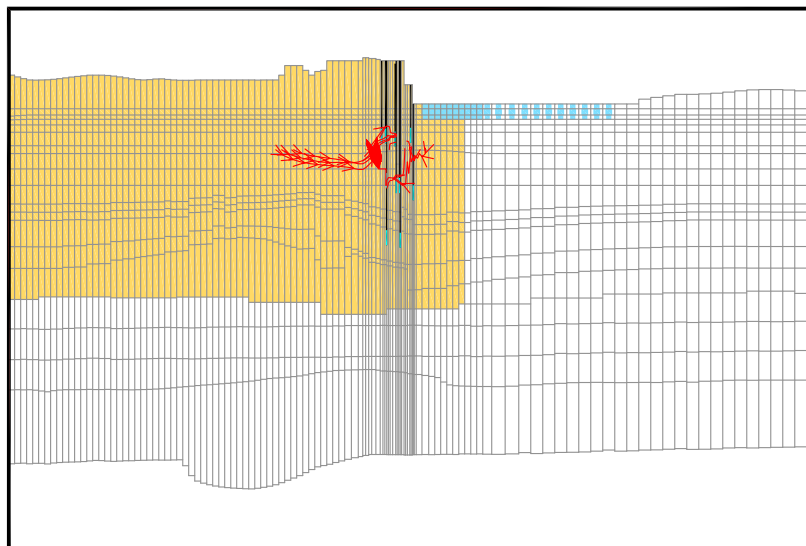


**TETRA TECH**

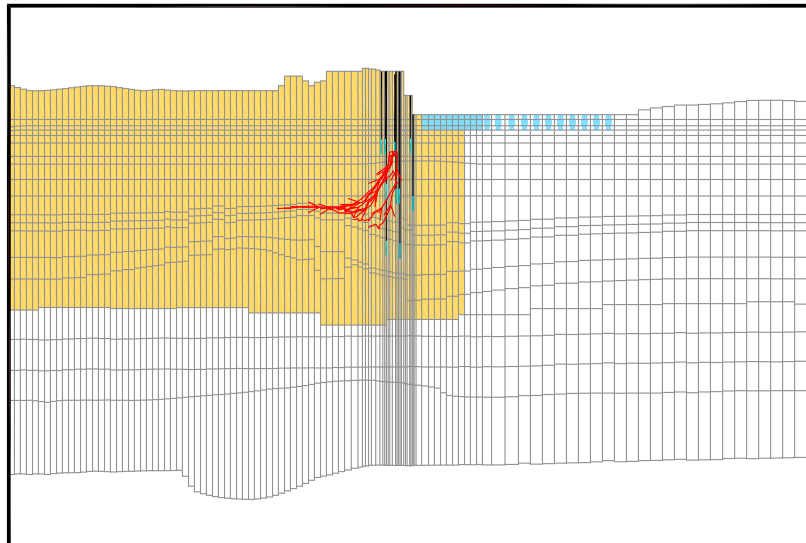
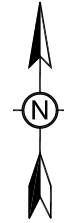
APPROVED	DB
DRAFTED	CP
PROJECT#	117-0512128
DATE	4-25-17

FIGURE

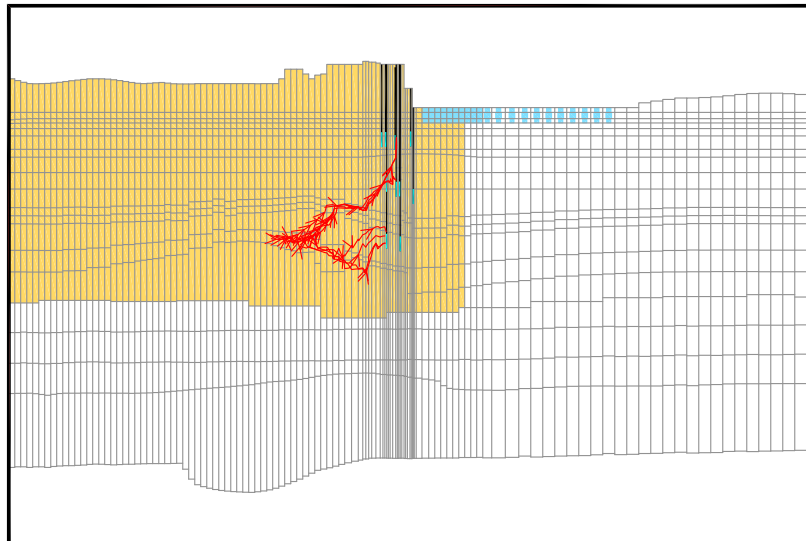
**13**



UPPER  
ZONE







INTERMEDIATE  
ZONE



LOWER  
ZONE

#### LEGEND

-  EXTRACTION WELL
-  EXTENT OF CAPTURE ZONE
-  RIVER
-  PARTICLE TRACE

#### NOTES:

1. EACH ARROW REPRESENTS A 1 YEAR TRAVEL TIME.
2. PARTICLE TRACES WERE STARTED IN AREAS OF HIGH CONCENTRATION.

0 800 1600  
  
 SCALE IN FEET  
 VERTICAL EXAGGERATION 10X

TITLE: **VERTICAL CROSS SECTIONAL VIEW OF SIMULATED FORWARD PARTICLE-TRACKING RESULTS FOR CONDITIONS DURING REMEDIAL SYSTEM PUMPING**

LOCATION: **Martin State Airport, Maryland**

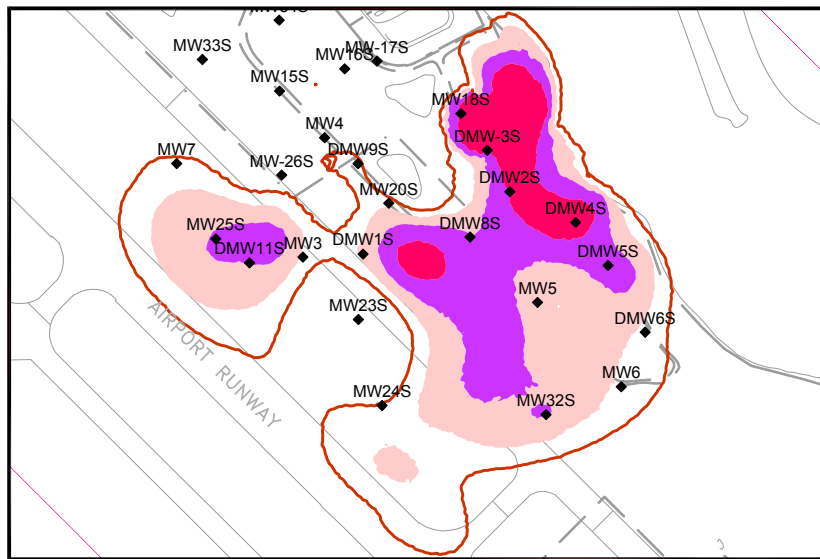


**TETRA TECH**

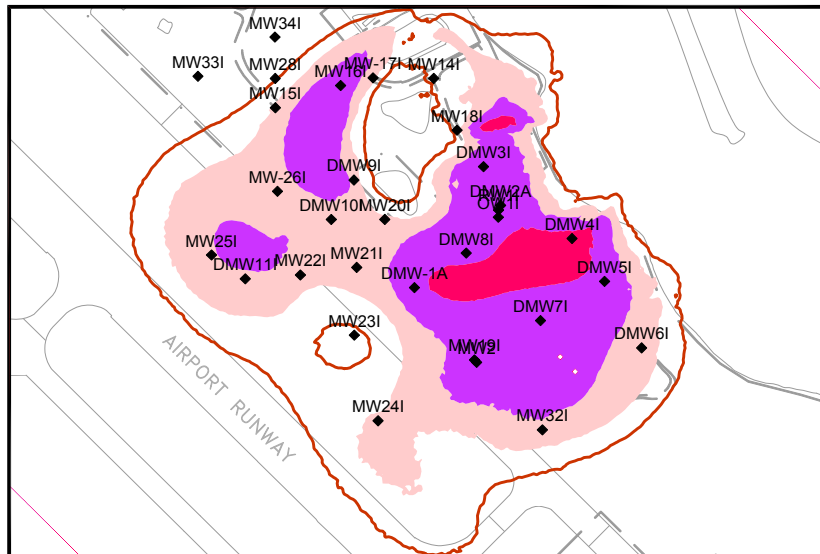
APPROVED	DB
DRAFTED	CP
PROJECT#	117-0512128
DATE	4-25-17

FIGURE

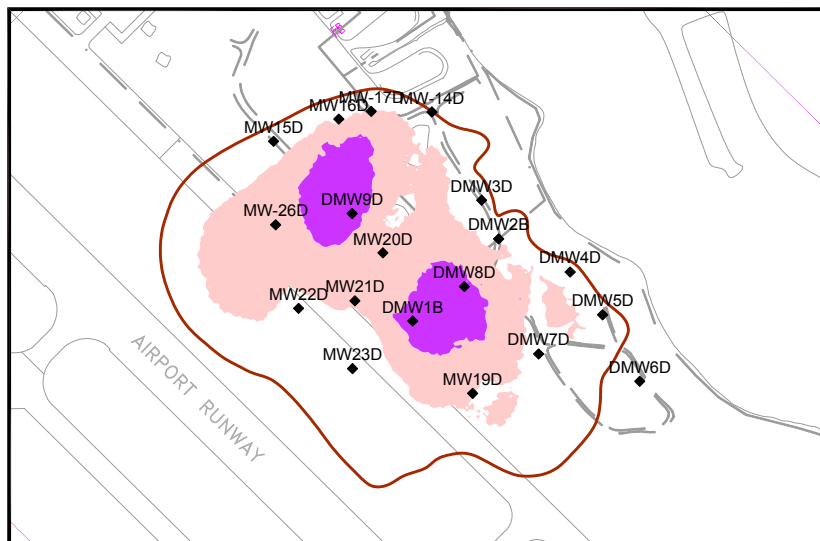
**14**



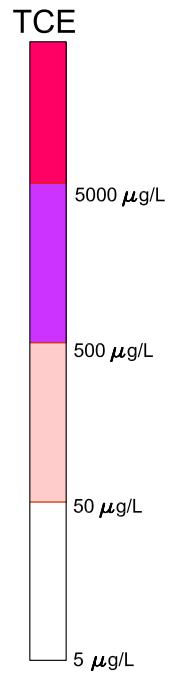
UPPER  
ZONE



INTERMEDIATE  
ZONE



LOWER  
ZONE



TITLE:

**PREDICTED TCE UNDER NO FURTHER REMEDIAL ACTION IN THE  
UPPER (LAYER 7), INTERMEDIATE (LAYER 11), AND LOWER  
(LAYER 14) ZONES OF THE SURFICIAL AQUIFER AFTER 5 YEARS**

LOCATION:

**Martin State Airport, Maryland**



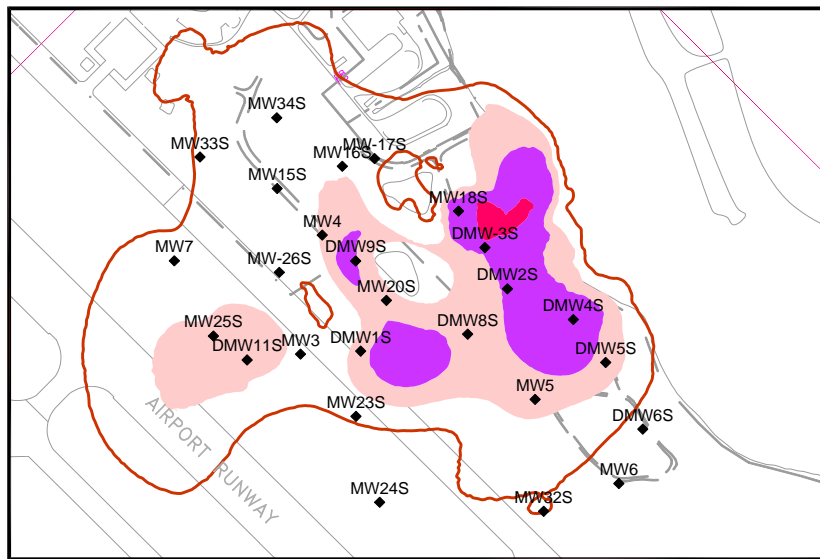
**TETRA TECH**

APPROVED	DB
DRAFTED	CP
PROJECT#	117-0512128
DATE	4-25-17

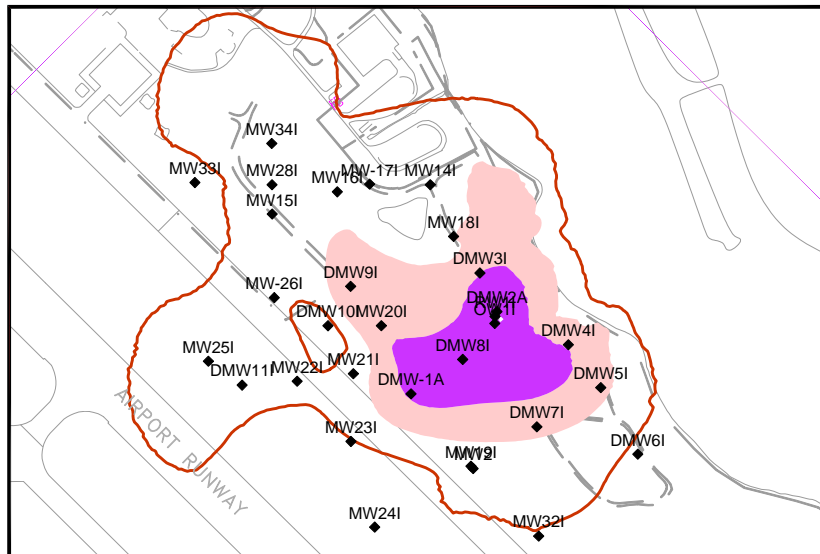
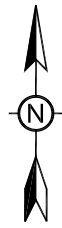
FIGURE

**15**

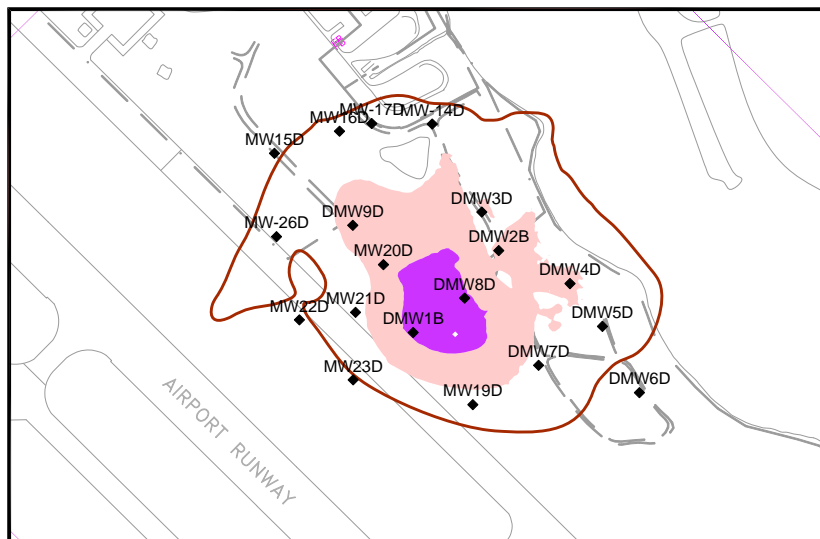
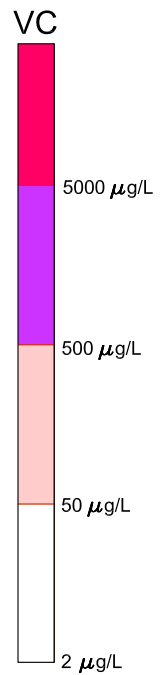




UPPER  
ZONE



INTERMEDIATE  
ZONE



LOWER  
ZONE



TITLE:

**PREDICTED VC UNDER NO FURTHER REMEDIAL ACTION IN THE  
UPPER (LAYER 7), INTERMEDIATE (LAYER 11), AND LOWER  
(LAYER 14) ZONES OF THE SURFICIAL AQUIFER AFTER 5 YEARS**

LOCATION:

**Martin State Airport, Maryland**

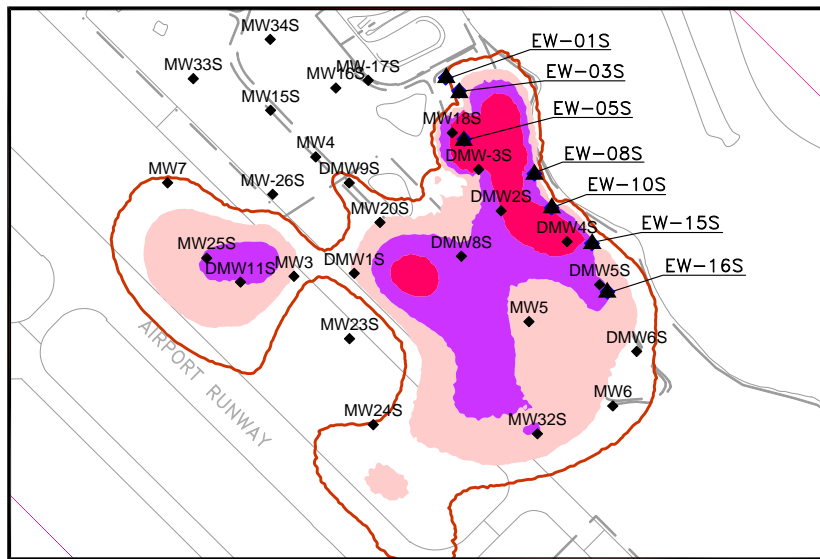


**TETRA TECH**

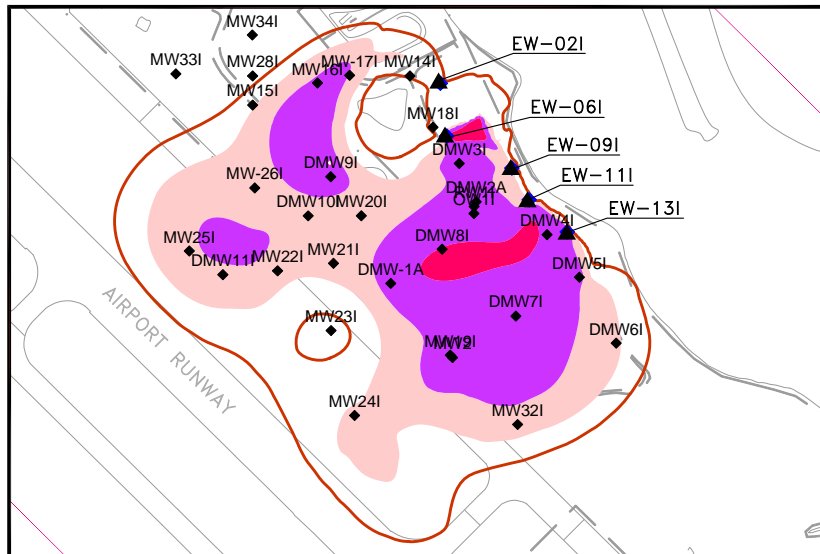
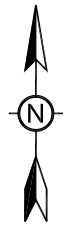
APPROVED	DB
DRAFTED	CP
PROJECT#	117-0512128
DATE	4-25-17

FIGURE

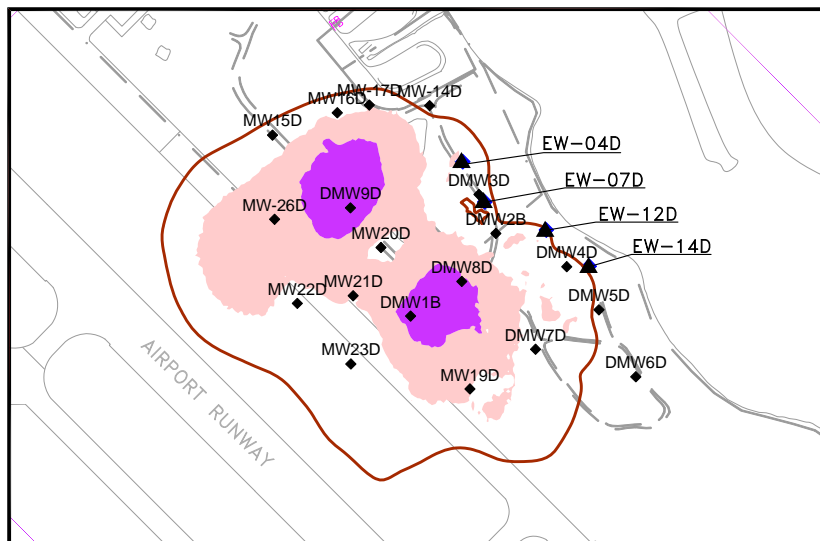
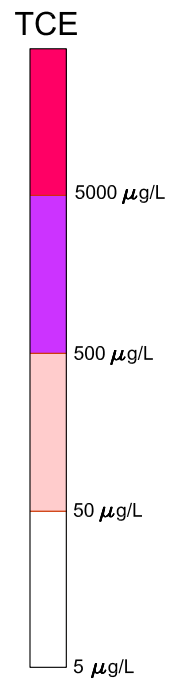
**16**



UPPER  
ZONE



INTERMEDIATE  
ZONE



LOWER  
ZONE



TITLE:  
**PREDICTED TCE UNDER PLANNED PUMPING CONDITIONS IN THE  
UPPER (LAYER 7), INTERMEDIATE (LAYER 11), AND LOWER  
(LAYER 14) ZONES OF THE SURFICIAL AQUIFER AFTER 5 YEARS**

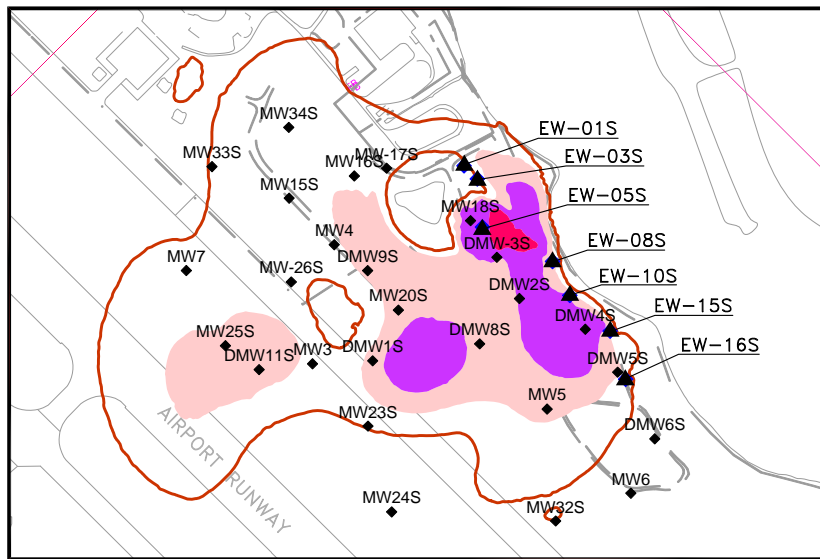
LOCATION: **Martin State Airport, Maryland**



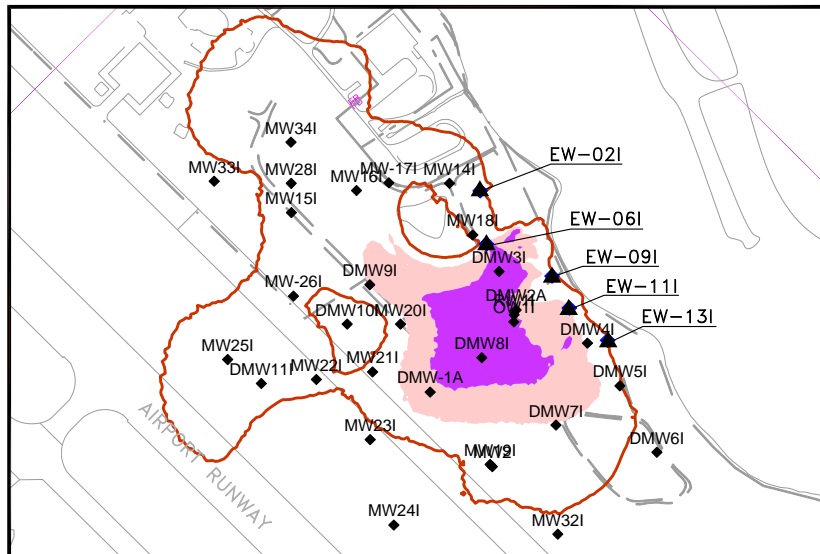
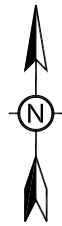
**TETRA TECH**

APPROVED	DB	FIGURE <b>17</b>
DRAFTED	CP	
PROJECT#	117-0512128	
DATE	4-25-17	

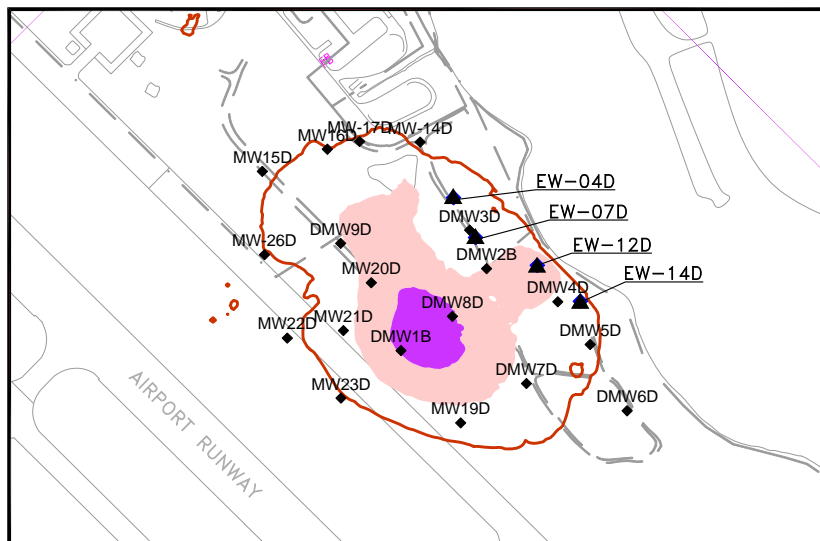
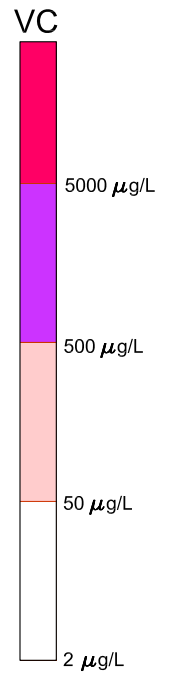




UPPER  
ZONE



INTERMEDIATE  
ZONE



LOWER  
ZONE



TITLE:

**PREDICTED VC UNDER PLANNED PUMPING CONDITIONS IN THE  
UPPER (LAYER 7), INTERMEDIATE (LAYER 11), AND LOWER  
(LAYER 14) ZONES OF THE SURFICIAL AQUIFER AFTER 5 YEARS**

LOCATION:

**Martin State Airport, Maryland**



**TETRA TECH**

APPROVED	DB	FIGURE  <b>18</b>
DRAFTED	CP	
PROJECT#	117-0512128	
DATE	4-25-17	

---

## TABLES

Table 1 Summary of Groundwater Flow Model Parameter Values

Flow Model Parameter Values					
Unit	Layer	Horizontal Hydraulic Conductivity $K_h$ (ft/day)	Vertical Hydraulic Conductivity $K_z$ (ft/day)	Specific Yield $S_y$	Storativity $S$ (-)
Upper	1	0.025-3.5	0.0025-0.35	0.25	1.0E-04
	2	0.025-1.5	0.0025-0.15		
	3	0.025-4.5	0.0025-0.45		
	4	0.025-4.5	0.0025-0.45		
	5	8	0.8		
	6	8	0.7		
	7	7	0.139		
Intermediate	8	10	1		1.0E-05
	9	10	1		
	10	10	1		
	11	35	3.5		
Lower	12	1.39	0.139		1.0E-05
	13	5.5	0.55		
	14	6.5	0.65		
	15	100	10		
Intermediate Aquitard	16	0.025	0.0025		1.0E-05
	17	0.044	0.0044		
	18	0.0033	0.00033		
Deep confined	19	10	1		1.0E-05

Note: The recharge rate for unpaved area is 7.54 in/yr; for the paved area is 4.03 in/yr; for mounding area is 394.2 in/yr. The rate for high ET area is 21.9 in/yr.

Table 2. March 23, 2016 Measured Groundwater Elevations and Vertical Hydraulic Gradients versus Simulated Values in the Calibrated Groundwater Flow Model

Well Name	X	Y	Aquifer Unit	Observed WL	Computed WL	Residual	Observed Vertical Head Difference	Computed Vertical Head Difference
DMW-1S	1479310.5	604458.6	U	3.8	3.57	0.23	0.37 0.50	0.35 0.12
DMW-1A	1479498.3	604398.6	I	3.43	3.22	0.21		
DMW-1B	1479498.3	604398.6	D	2.93	3.10	-0.17		
DMW-2S	1479807.5	604670.4	U	1.55	2.23	-0.68	0.12 -0.23	-0.05 -0.12
DMW-2A	1479789.4	604678.8	I	1.43	2.28	-0.85		
DMW-2B	1479789.4	604678.8	D	1.66	2.40	-0.74		
DMW-3S	1479733.9	604804.9	U	5.97	5.83	0.14	4.37 0.02	3.35 0.00
DMW-3I	1479731.1	604810.5	I	1.6	2.48	-0.88		
DMW-3D	1479731.1	604810.5	D	1.58	2.48	-0.90		
DMW-4S	1480036.3	604563.0	U	1.08	1.48	-0.40	-0.35 0.17	-0.08 -0.21
DMW-4I	1480031.5	604566.0	I	1.43	1.56	-0.13		
DMW-4D	1480031.5	604566.0	D	1.26	1.77	-0.51		
DMW-5S	1480141.1	604430.0	U	1.34	1.54	-0.20	-0.05 0.06	0.02 -0.12
DMW-5I	1480140.5	604431.1	I	1.39	1.52	-0.13		
DMW-5D	1480140.6	604431.1	D	1.33	1.64	-0.31		
DMW-6S	1480255.0	604190.5	U	1.67	1.70	-0.03	0.13 0.13	0.08 -0.03
DMW-6I	1480266.2	604193.6	I	1.54	1.62	-0.08		
DMW-6D	1480266.2	604193.6	D	1.41	1.65	-0.24		
DMW-7I	1479924.2	604287.2	I	2	2.35	-0.35	-0.06	-0.01
DMW-7D	1479924.2	604287.2	D	2.06	2.36	-0.30		
DMW-8S	1479667.8	604516.6	U	3.85	3.24	0.61	1.62 -0.05	0.40 0.04
DMW-8I	1479673.6	604516.0	I	2.23	2.84	-0.61		
DMW-8D	1479673.6	604516.0	D	2.28	2.80	-0.52		
DMW-9S	1479286.9	604771.6	U	2.8	3.85	-1.05	-0.10 0.24	0.09 0.38
DMW-9I	1479293.4	604764.9	I	2.9	3.77	-0.87		
DMW-9D	1479293.4	604764.9	D	2.66	3.39	-0.73		

Table 2. March 23, 2016 Measured Groundwater Elevations and Vertical Hydraulic Gradients versus Simulated Values in the Calibrated Groundwater Flow Model

Well Name	X	Y	Aquifer Unit	Observed WL	Computed WL	Residual	Observed Vertical Head Difference	Computed Vertical Head Difference
DMW-10S	1479225.8	604636.8	U	3.69	3.71	-0.02	0.32	0.06
DMW-10I	1479217.3	604630.7	I	3.37	3.66	-0.29		
DMW-11S	1478934.9	604424.2	U	5.7	5.80	-0.10	1.86	1.97
DMW-11I	1478930.8	604429.3	I	3.84	3.83	0.01		
MW-14I	1479550.7	605129.9	I	1.31	3.19	-1.88	-3.65	-2.26
MW-14D	1479550.7	605129.9	DD	4.96	5.44	-0.48		
MW-15S	1479028.3	605011.0	U	3.65	3.68	-0.03	0.41	0.01
MW-15I	1479028.3	605011.0	I	3.24	3.67	-0.43		
MW-15D	1479028.3	605011.0	D	3.24	3.63	-0.39	0.00	0.05
MW-16S	1479248.8	605086.4	U	1.66	2.60	-0.94	-1.20	-0.84
MW-16I	1479248.8	605086.4	I	2.86	3.45	-0.59		
MW-16D	1479248.8	605086.4	D	2.87	3.36	-0.49	-0.01	0.09
MW-17S	1479358.3	605112.7	U	1.7	2.82	-1.12		
MW-17I	1479358.3	605112.7	I	2.53	3.48	-0.95	-0.83	-0.65
MW-19I	1479701.2	604152.7	I	2.42	2.92	-0.50	-0.03	0.03
MW-19D	1479701.2	604152.7	D	2.45	2.89	-0.44		
MW-20S	1479397.9	604631.0	U	3	3.79	-0.79	-0.03	0.14
MW-20I	1479397.9	604631.0	I	3.03	3.65	-0.62		
MW-20D	1479397.9	604631.0	D	2.5	3.32	-0.82	0.53	0.33
MW-21I	1479303.2	604467.8	I	3.34	3.52	-0.18	0.48	0.12
MW-21D	1479303.2	604467.8	D	2.86	3.40	-0.54		
MW-22I	1479112.8	604442.1	I	3.59	3.71	-0.12	0.39	0.09
MW-22D	1479112.8	604442.1	D	3.2	3.61	-0.41		

Table 2. March 23, 2016 Measured Groundwater Elevations and Vertical Hydraulic Gradients versus Simulated Values in the Calibrated Groundwater Flow Model

Well Name	X	Y	Aquifer Unit	Observed WL	Computed WL	Residual	Observed Vertical Head Difference	Computed Vertical Head Difference
MW-23S	1479295.1	604237.1	U	3.48	3.53	-0.05	0.04 0.51	0.03 0.07
MW-23I	1479295.1	604237.1	I	3.44	3.50	-0.06		
MW-23D	1479295.1	604237.1	D	2.93	3.43	-0.50		
MW-24S	1479375.2	603945.7	U	4.22	3.43	0.79	0.78	0.02
MW-24I	1479375.2	603945.7	I	3.44	3.40	0.04		
MW-25S	1478812.4	604510.1	U	4.96	4.26	0.70	1.26	0.24
MW-25I	1478812.4	604510.1	I	3.7	4.02	-0.32		
MW-26S	1479035.4	604726.4	U	3.94	3.85	0.09	0.45 0.05	0.06 0.08
MW-26I	1479035.4	604726.4	I	3.49	3.78	-0.29		
MW-26D	1479035.4	604726.4	D	3.44	3.71	-0.27		
MW-28I	1479027.9	605110.6	I	3.24	3.60	-0.36	-3.23	-2.03
MW-27D	1479032.0	605114.3	DD	6.47	5.63	0.84		
MW-30I	1479473.5	603824.9	I	3.12	3.38	-0.26	-1.34	-1.03
MW-30D	1479645.7	603825.5	DD	4.46	4.42	0.04		
MW-32S	1479926.5	603917.7	U	2.65	2.65	0.00	0.07	0.02
MW-32I	1479926.5	603917.7	I	2.58	2.64	-0.06		
MW-33S	1478762.0	605115.6	U	3.94	4.07	-0.13	0.06	0.02
MW-33I	1478762.0	605115.6	I	3.88	4.05	-0.17		
MW-40S	1479866.6	604210.6	U	2.58	2.60	-0.02	0.24	0.03
MW-40I	1479866.6	604210.6	I	2.34	2.57	-0.23		
MW-41S	1479434.6	604422.9	U	3.44	3.34	0.10	0	0.01
MW-41I	1479434.6	604422.9	I	3.44	3.33	0.11		
MW-42S	1479175.2	604730.8	U	3.5	3.80	-0.30	0.07	0.10
MW-42I	1479175.2	604730.8	I	3.43	3.70	-0.27		
MW-46S	1479779.9	605175.5	U	1.81	1.52	0.29	1.09 -0.3	-0.01 -0.31
MW-46I	1479779.9	605175.5	I	0.72	1.54	-0.82		
MW-46D	1479784.5	605173.6	D	1.02	1.84	-0.82		

Table 2. March 23, 2016 Measured Groundwater Elevations and Vertical Hydraulic Gradients versus Simulated Values in the Calibrated Groundwater Flow Model

Well Name	X	Y	Aquifer Unit	Observed WL	Computed WL	Residual	Observed Vertical Head Difference	Computed Vertical Head Difference
MW-47S	1479824.2	605088.2	U	1.35	1.66	-0.31	0.36 0.05	0.03 -0.22
MW-47I	1479824.2	605088.2	I	0.99	1.63	-0.64		
MW-47D	1479826.2	605083.0	D	0.94	1.85	-0.91		
MW-48S	1479941.3	604728.2	U	1.26	1.44	-0.18	-0.06 -0.05	-0.13 -0.04
MW-48I	1479941.3	604728.2	I	1.32	1.58	-0.26		
MW-48D	1479944.1	604724.2	D	1.37	1.61	-0.24		
MW-49S	1480065.8	604617.6	U	0.59	1.10	-0.51	-0.37 -0.14	-0.20 -0.11
MW-49I	1480065.8	604617.6	I	0.96	1.30	-0.34		
MW-49D	1480070.9	604615.7	D	1.1	1.41	-0.31		
MW-50S	1480249.7	604442.4	U	1.35	1.14	0.21	0.04 0.09	-0.02 -0.22
MW-50I	1480249.7	604442.4	I	1.31	1.16	0.15		
MW-50D	1480246.2	604445.9	D	1.22	1.38	-0.16		
MW-51S	1480293.9	604378.6	U	1.27	1.11	0.16	-0.09 0.21	-0.04 -0.20
MW-51I	1480293.9	604378.6	I	1.36	1.15	0.21		
MW-51D	1480296.1	604373.7	D	1.15	1.35	-0.20		
MW-52S	1479863.6	604940.2	U	4.34	4.14	0.20	3.27 0.03	2.52 -0.04
MW-52I	1479863.6	604940.2	I	1.07	1.62	-0.55		
MW-52D	1479858.8	604938.9	D	1.04	1.66	-0.62		
MW-53S	1479553.3	604548.7	U	5.47	4.69	0.78	2.25	1.48
MW-53I	1479553.3	604548.7	I	3.22	3.21	0.01		
MW-54S	1479001.2	604503.7	U	5.72	5.71	0.01	2.09	1.90
MW-54I	1479001.2	604503.7	I	3.63	3.81	-0.18		
MW-29D	1480488.4	603774.8	DD	3.93	4.09	-0.16		
MW-31D	1480099.6	603747.8	DD	3.95	4.20	-0.25		
MW-35S	1478645.8	605371.6	U	4.22	4.27	-0.05		
MW-36S	1478395.9	605068.5	U	6.13	5.06	1.07		
MW-37S	1478851.7	604275.3	U	4.59	3.96	0.63		

Table 2. March 23, 2016 Measured Groundwater Elevations and Vertical Hydraulic Gradients versus Simulated Values in the Calibrated Groundwater Flow Model

Well Name	X	Y	Aquifer Unit	Observed WL	Computed WL	Residual	Observed Vertical Head Difference	Computed Vertical Head Difference
MW-38S	1478555.3	604045.9	U	4.82	4.22	0.60		
MW-43S	1479523.7	604776.0	U	6.33	4.76	1.57		
MW-44S	1479579.2	605023.9	U	8.14	8.27	-0.13		
MW-45S	1479440.4	604428.4	U	3.26	3.31	-0.05		
MW-2	1479708.3	604144.3	U	2.75	2.86	-0.11		
MW-3	1479107.2	604448.8	U	3.69	3.68	0.01		
MW-4	1479180.8	604852.9	U	3.74	3.66	0.08		
MW-5	1479901.9	604294.7	U	2.35	2.38	-0.03		
MW-6	1480184.7	604009.3	U	2.1	2.06	0.04		
MW-7	1478680.4	604765.2	U	5.05	4.30	0.75		
GSP-MW-1	1478204.7	603998.1	U	7.11	4.99	2.12		
GSP-MW-2	1478149.4	604048.1	U	5.45	4.68	0.77		
GSP-MW-3	1478158.2	603920.3	U	3.89	4.40	-0.51		
GSP-MW-4	1478020.4	603801.7	U	4.45	4.32	0.13		
GSP-MW-5	1478737.1	603313.3	U	6.14	4.44	1.70		
GSP-MW-6	1478705.1	603358.9	U	8.36	8.31	0.05		
GSP-MW-7	1479296.3	602920.0	U	6.58	5.41	1.17		
GSP-MW-8	1479055.4	603086.9	U	6.18	4.34	1.84		
GSP-MW-9	1479195.2	602854.4	U	8.91	7.70	1.21		
GSP-MW-10	1479357.3	602812.3	U	6.68	6.36	0.32		
GSP-MW-11	1479265.7	602756.0	U	10.05	10.00	0.05		
GSP-MW-12	1479141.9	602597.5	U	10.14	9.20	0.94		
GSP-MW-13	1479249.8	602668.0	U	10.32	9.09	1.23		
GSP-MW-14	1479384.8	602642.4	U	10.58	11.69	-1.11		
GSP-MW-15	1479259.9	602509.3	U	10.12	8.88	1.24		
GSP-MW-16	1479131.3	602440.1	U	9.42	6.53	2.89		
GSP-MW-17	1477996.6	603757.0	U	4.31	4.20	0.11		



Table 2. March 23, 2016 Measured Groundwater Elevations and Vertical Hydraulic Gradients versus Simulated Values in the Calibrated Groundwater Flow Model

Well Name	X	Y	Aquifer Unit	Observed WL	Computed WL	Residual	Observed Vertical Head Difference	Computed Vertical Head Difference
GSP-MW-18	1478068.0	603791.3	U	4.93	4.24	0.69		
GSP-MW-19	1478209.9	603924.9	U	1.63	4.39	-2.76		
GSP-MW-20	1478261.2	603984.8	U	2.69	4.64	-1.95		
GSP-MW-21I	1479080.3	602400.8	U/I	4.97	4.35	0.62		
GSP-MW-22I	1479084.6	602540.4	U/I	5.44	5.39	0.05		
GSP-MW-23I	1479313.1	602969.5	U/I	7.07	4.72	2.35		
GSP-MW-24I	1478079.5	603738.8	U/I	4.55	4.15	0.40		
GSP-MW-25I	1478127.6	603997.5	U/I	4.14	4.44	-0.30		
GSP-MW-26I	1478241.6	604035.8	U/I	4.70	4.42	0.28		
MT-MW-01S	1475440.7	606556.7	U	12.54	11.01	1.53		
MT-MW-02S	1475383.5	606333.0	U	8.23	9.26	-1.03		
MT-MW-03S	1475540.0	605940.4	U	3.22	3.52	-0.30		
MT-MW-04S	1475744.1	605222.4	U	8.96	5.92	3.04		
MT-MW-05S	1475990.7	605775.4	U	7.15	7.33	-0.18		
MT-MW-06S	1475763.2	605723.9	U	5.51	5.91	-0.40		
MT-MW-08S	1475339.0	606408.0	U	8.35	7.49	0.86		
MT-MW-09S	1476159.2	605416.3	U	9.64	10.96	-1.32		
MT-MW-010S	1475841.0	605210.0	U	3.35	3.88	-0.53		
MT-MW-011S	1475717.2	605506.5	U	5.29	3.86	1.43		

Note:

- 1) Residual = Observed Water Level- Simulated Water Level.
- 2) Vertical Head Difference = Water level in the upper unit - Water level in the lower unit.
- 3) S - Upper surficial aquifer  
I - Intermediate surficial aquifer  
D - Lower surficial aquifer  
DD - Deep confined aquifer or below the lower surficial aquifer

Table 3 Summary Statistics for Steady-State Flow Model Simulation for March 2016 Conditions

Model Layer	Unit	# Targets	Range of Water Levels (ft)	Residual Mean (ft)	Absolute Residual Mean (ft)	Residual Standard Deviation (ft)	Standard Deviation / Range
	Entire Model	150	11.95	-0.03	0.54	0.79	6.6%
	Entire DRA	113	7.55	-0.22	0.39	0.47	6.2%
1-7	Upper Zone	81	11.95	0.24	0.66	0.94	7.9%
8-11	Intermediate Zone	42	3.16	-0.30	0.35	0.38	12.0%
12-15	Lower Zone	22	2.60	-0.44	0.44	0.23	8.8%
16-18	Basal Confining Unit	0	-	-	-	-	-
19	Deep Confined Zone	5	2.54	0.05	0.37	0.47	18.5%

Table 4. Comparison of Simulated and Measured Drawdowns at the End of the Step-Drawdown Tests

Test A			
Well I.D.	Distance to pumped well	Maximum Drawdown (feet)	
	(feet)	Observed	Modeled
EW-13I*	0	22.27	20.53
DMW-4I	68.5	0.94	1.31
EW-14D	11	0.34	0.43
EW-15S	22	0.68	0.85
MW-49S	53.7	0.05	0.27
MW-49I	53.7	1.2	1.44
Test B			
Well I.D.	Distance to pumped well	Maximum Drawdown (feet)	
	(feet)	Observed	Modeled
EW-14D*	0	48.49	46.39
DMW-4D	75.6	2.01	1.24
EW-13I	11	0.36	0.42
EW-15S	11	0.05	0.15
MW-49I	64.6	0.19	0.33
MW-49D	60.1	0.65	0.45
Test C			
Well I.D.	Distance to pumped well	Maximum Drawdown (feet)	
	(feet)	Observed	Modeled
EW-15S*	0	17.16	12.79
DMW-4S	78.6	0.15	0.22
EW-13I	22	0.65	0.62
EW-14D	11	0.29	0.29
MW-49S	75.6	0.19	0.15
MW-49I	75.5	0.63	0.25
Test D			
Well I.D.	Distance to pumped well	Maximum Drawdown (feet)	
	(feet)	Observed	Modeled
EW-16S*	0	11.82	7.84
DMW-5S	43	0.26	0.43
DMW-5I	44.2	0.3	0.54
EW-15S	172.1	0.08	0.08
MW-50S	94.4	0.33	0.33
Test E			
Well I.D.	Distance to pumped well	Maximum Drawdown (feet)	
	(feet)	Observed	Modeled
EW-10S*	0	6.0	6.68
MW-48S	60.1	0.46	0.28
MW-48I	60.1	0.96	0.97
MW-49S	107.9	0.23	0.19

Note: The monitoring wells in the table were all of the wells monitored for drawdowns.

\* Pumping well in the test

Table 4. Comparison of Simulated and Measured Drawdowns at the End of the Step-Drawdown Tests

Well I.D.	Distance to pumped well	Maximum Drawdown (feet)	
	(feet)	Observed	Modeled
DMW-04S	131.2	0.17	0.17
EW-08S	128.9	0.77	0.55
EW-09I	132.4	0.55	0.6
EW-11I	10.1	0.64	0.67
EW-12D	19.5	0.48	0.19
Test F			
Well I.D.	Distance to pumped well	Maximum Drawdown (feet)	
	(feet)	Observed	Modeled
EW-11I*	0	7.73	8.78
MW-48I	43.4	0.76	1.1
MW-48S	43.4	0.18	0.12
MW-49I	126.9	0.79	0.62
EW-10S	9.3	0.43	0.65
EW-12D	19.4	0.64	0.48
DMW-04I	142.2	0.61	0.5
EW-13I	179	0.68	0.33
RW-01I	181.1	0.70	0.39
Test G			
Well I.D.	Distance to pumped well	Maximum Drawdown (feet)	
	(feet)	Observed	Modeled
EW-12D*	0	27.43	27.76
MW-48I	60.5	0.5	0.17
MW-48D	55.7	0.83	0.26
MW-49D	112.8	0.71	0.32
EW-07D	249.8	1.18	0.2
EW-10S	10.1	0.27	0.15
EW-11I	19.4	0.81	0.35
EW-14D	170.9	1.81	0.51
Test H			
Well I.D.	Distance to pumped well	Maximum Drawdown (feet)	
	(feet)	Observed	Modeled
EW-09I*	0	9.6	9.48
EW-08S	8.9	1.03	1.17
MW-48S	72.9	0.06	0.1
MW-48I	72.9	0.79	0.76
EW-07D	159.6	0.7	0.5
EW-10S	123.8	0.35	0.37
EW-11I	116.2	1.29	0.74
Test I			
Well I.D.	Distance to pumped well	Maximum Drawdown (feet)	

Note: The monitoring wells in the table were all of the wells monitored for drawdowns.

\* Pumping well in the test

Table 4. Comparison of Simulated and Measured Drawdowns at the End of the Step-Drawdown Tests

Well I.D.	Distance to pumped well	Maximum Drawdown (feet)	
	(feet)	Observed	Modeled
	(feet)	Observed	Modeled
EW-08S*	0	8.86	7.64
EW-09I	9.5	1.01	1.21
MW-48S	70.9	0.31	0.23
MW-48I	70.9	1.76	1.2
DMW-03S	186.5	0.015	0.078
MW-52S	155.1	0.012	0.04
EW-10S	128.9	0.71	0.64
EW-11I	120.6	0.95	0.61
Test J			
Well I.D.	Distance to pumped well	Maximum Drawdown (feet)	
	(feet)	Observed	Modeled
EW-07D*	0	14.4	13.82
DMW-2B	112.7	2.01	0.48
DMW-03I	32.7	0.95	1.08
DMW-03D	32.7	4.46	4.87
MW-52D	187.4	0.83	0.31
EW-04D	155.4	2.26	1.1
EW-06I	134.7	1.61	0.7
EW-08S	168.7	0.65	0.27
EW-09I	159.3	0.77	0.37
Test K			
Well I.D.	Distance to pumped well	Maximum Drawdown (feet)	
	(feet)	Observed	Modeled
EW-06I*	0	13.98	13.5
MW-18I	51.3	2.55	3.1
MW-18D	55.6	1.84	1.47
MW-47D	225.4	0.41	0.45
MW-52D	173.3	0.6	0.56
EW-02I	182.5	0.64	0.6
EW-04D	20.9	2.16	1.98
EW-05S	10.5	0.24	0.2
EW-09I	247.4	0.45	0.3
Test M			
Well I.D.	Distance to pumped well	Maximum Drawdown (feet)	
	(feet)	Observed	Modeled
EW-04D*	0	12.89	12.81
MW-18I	33.1	1.31	1.24
MW-18D	36.9	4.81	4.42
MW-46D	274.4	0.68	0.38
MW-47D	220.3	0.67	0.41

Note: The monitoring wells in the table were all of the wells monitored for drawdowns.

\* Pumping well in the test

Table 4. Comparison of Simulated and Measured Drawdowns at the End of the Step-Drawdown Tests

Well I.D.	Distance to pumped well	Maximum Drawdown (feet)	
	(feet)	Observed	Modeled
MW-52D	182.9	0.75	0.39
EW-06I	20.9	2.32	2.36
EW-07D	155.4	2.16	1.28
EW-09I	266	0.61	0.32
Test O			
Well I.D.	Distance to pumped well	Maximum Drawdown (feet)	
	(feet)	Observed	Modeled
EW-02I*	0	14.83	15.01
MW-14I	125	0.16	0.12
MW-44S	107.7	0.01	0.00
MW-46D	146.4	2.06	1.32
MW-47D	158.7	1.33	1.14
EW-01S	59.3	0.02	0.02
EW-04D	164.6	0.72	0.66
EW-06I	182.5	0.76	0.61

Note: The monitoring wells in the table were all of the wells monitored for drawdowns.

\* Pumping well in the test

Table 5 Summary of Flow Model Sensitivity Analysis

Model Parameter	Multiplier	Normalized RSS
Recharge Rate (unpaved area)	0.5	2.22
Recharge Rate (unpaved area)	1.5	3.14
Recharge Rate (paved area)	0.5	1.06
Recharge Rate (paved area)	1.5	0.99
Recharge Rate (mounding area)	0.5	2.83
Recharge Rate (mounding area)	1.5	2.28
Horizontal Hydraulic Conductivity of Upper Zone	0.5	1.07
Horizontal Hydraulic Conductivity of Upper Zone	1.5	1.21
Horizontal Hydraulic Conductivity of Intermediate Zone	0.5	1.15
Horizontal Hydraulic Conductivity of Intermediate Zone	1.5	1.14
Horizontal Hydraulic Conductivity of Lower Zone	0.5	3.14
Horizontal Hydraulic Conductivity of Lower Zone	1.5	1.57
Vertical Hydraulic Conductivity of Upper Zone	0.5	1.92
Vertical Hydraulic Conductivity of Upper Zone	1.5	1.40
Vertical Hydraulic Conductivity of Intermediate Zone	0.5	1.00
Vertical Hydraulic Conductivity of Intermediate Zone	1.5	1.00
Vertical Hydraulic Conductivity of Lower Zone	0.5	1.09
Vertical Hydraulic Conductivity of Lower Zone	1.5	1.04
Vertical Hydraulic Conductivity Intermediate Aquitard (Layer 16, 17, and 18)	0.5	1.05
Vertical Hydraulic Conductivity Intermediate Aquitard (Layer 16, 17, and 18)	1.5	1.02
Horizontal Hydraulic Conductivity of Deep Confined Zone (Layer 19)	0.5	1.02
Horizontal Hydraulic Conductivity of Deep Confined Zone (Layer 19)	1.5	1.02
Vertical Hydraulic Conductivity of Deep Confined Zone (Layer 19)	0.5	1.00
Vertical Hydraulic Conductivity of Deep Confined Zone (Layer 19)	1.5	1.00

Note:

1) Normalized RSS (residual sum of squares) is the new RSS divided by calibrated model RSS

Table 6. Summary of Solute Transport Model Parameter Values

Bulk density	Effective	$K_d$ (ml/g)			Dispersivity (ft)			Retardation Factor R			Half Life (yr)		
	Porosity										TCE	DCE	VC
110	0.28	0.015	0.003	0.0016	1	0.1	0.01	6.9	2.2	3.7	5.9	12	4.2

Note:

- (1) Transport model parameter values used in the table are based on transport model (Tetra Tech, 2004) and field data.
- (2) Retardation factors were calculated based on  $k_{oc}$  of 166 ml/g for TCE, 35.5 ml/g for cis 1,2-DCE, and 57 ml/g for VC.



Table 7. Summary of Pumping Rates (gpm) of the Recovery Wells

<b>Recovery Well</b>	<b>Recommended System Startup Pumping Rate (gpm)</b>	<b>Well Screen (Depth, ft bgs)</b>
<b>EW-13I</b>	2.2	45-55
<b>EW-14D</b>	1.0	70-80
<b>EW-15S</b>	2.2	25-35
<b>EW-16S</b>	4.7	25-29
<b>EW-10S</b>	8.4	22-32
<b>EW-08S</b>	5.7	25-35
<b>EW-09I</b>	5.2	50-60
<b>EW-11I</b>	6.8	45-55
<b>EW-12D</b>	1.7	70-80
<b>EW-07D</b>	3.5	70-80
<b>EW-06I</b>	7.1	45-55
<b>EW-05S</b>	0.1	15-25
<b>EW-04D</b>	7.8	65-75
<b>EW-03S</b>	0.1	15-25
<b>EW-02I</b>	6.8	45-55
<b>EW-01S</b>	0.1	15-25

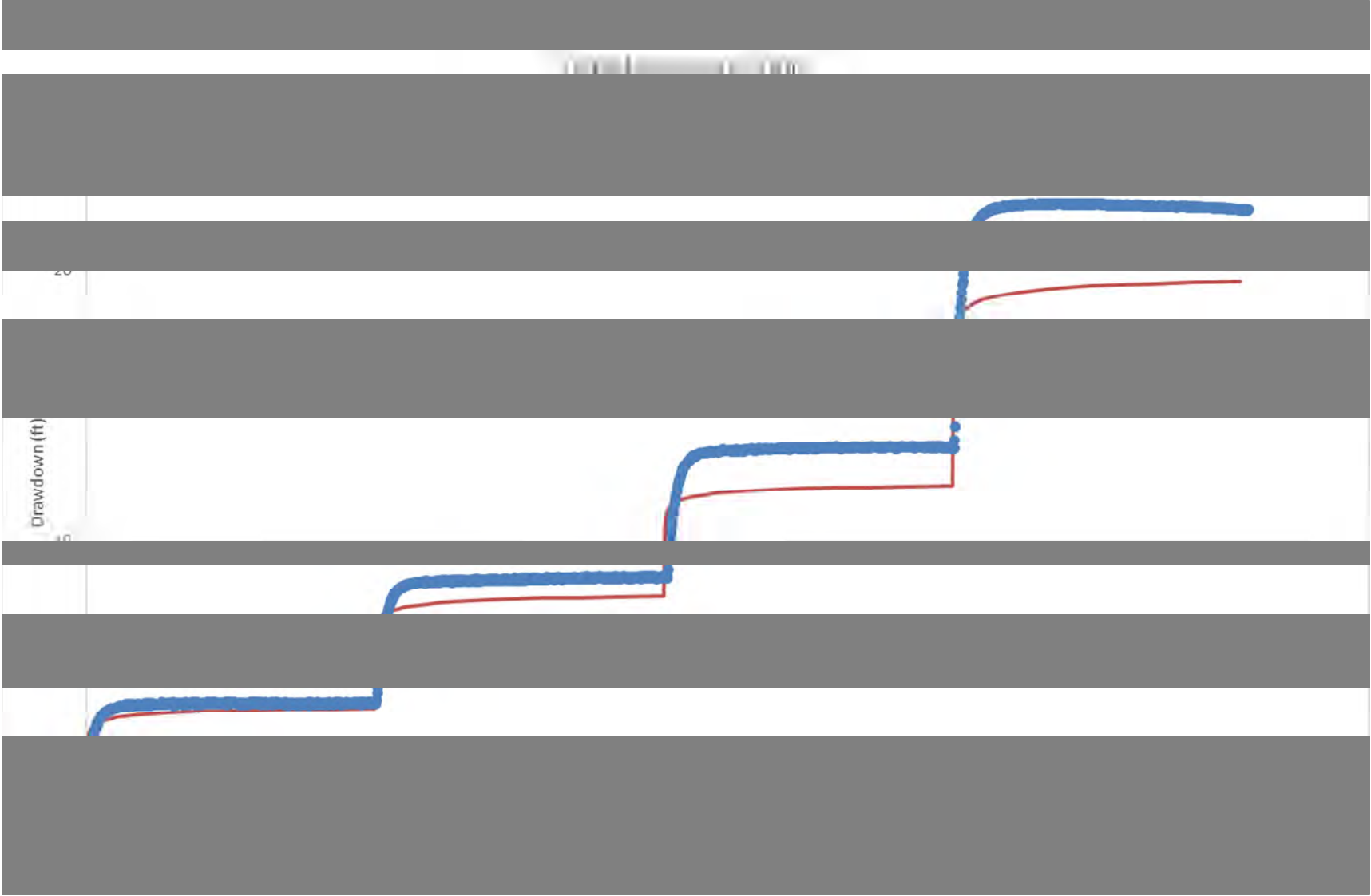
---

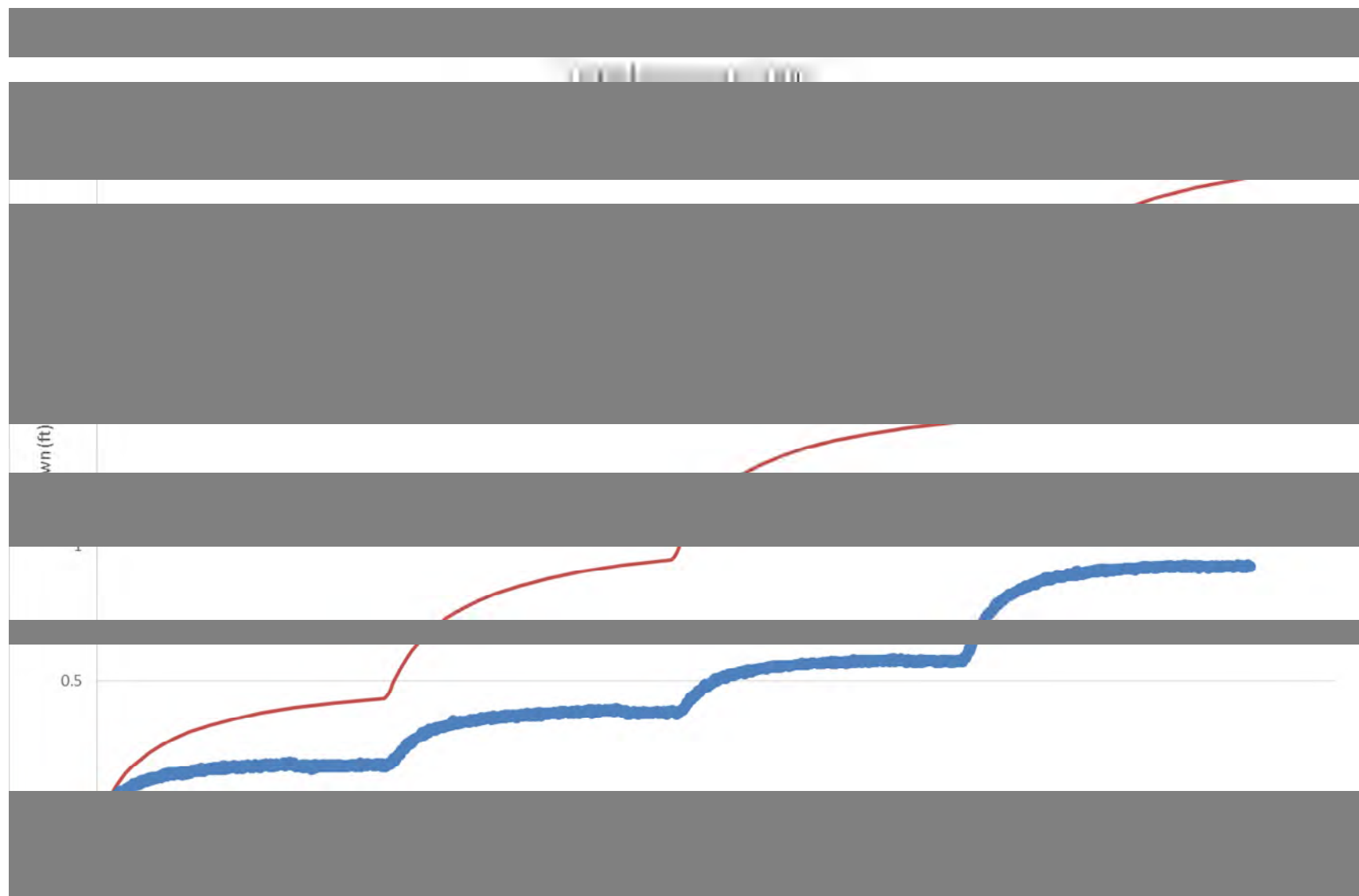
## **APPENDIX A—TRANSIENT MODELING-ANALYSIS OF RECOVERY WELL VARIABLE-RATE PUMPING TESTS**

# Appendix A

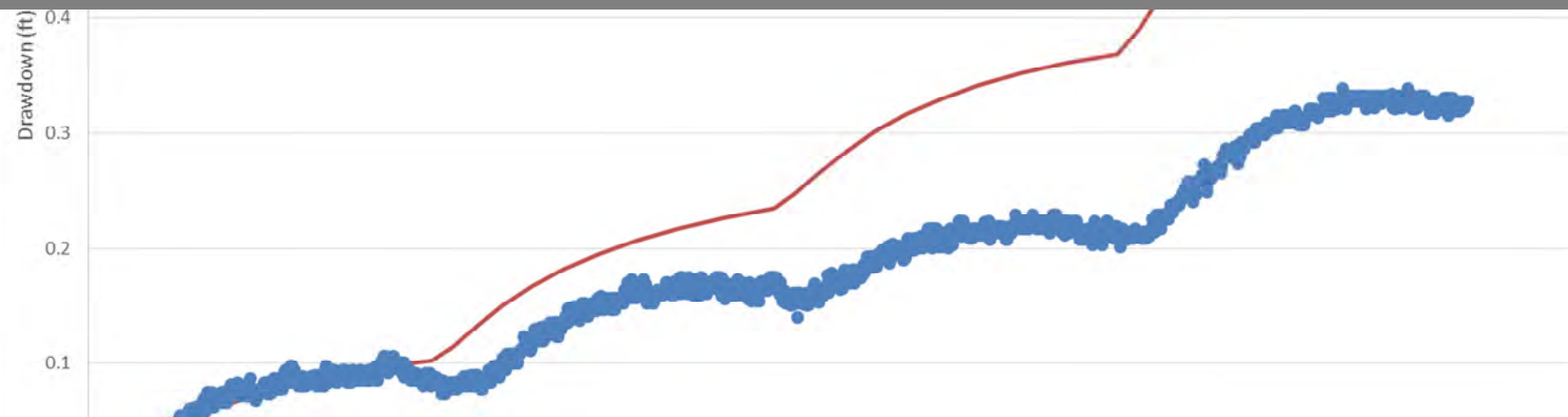
## Step-Drawdown Test A

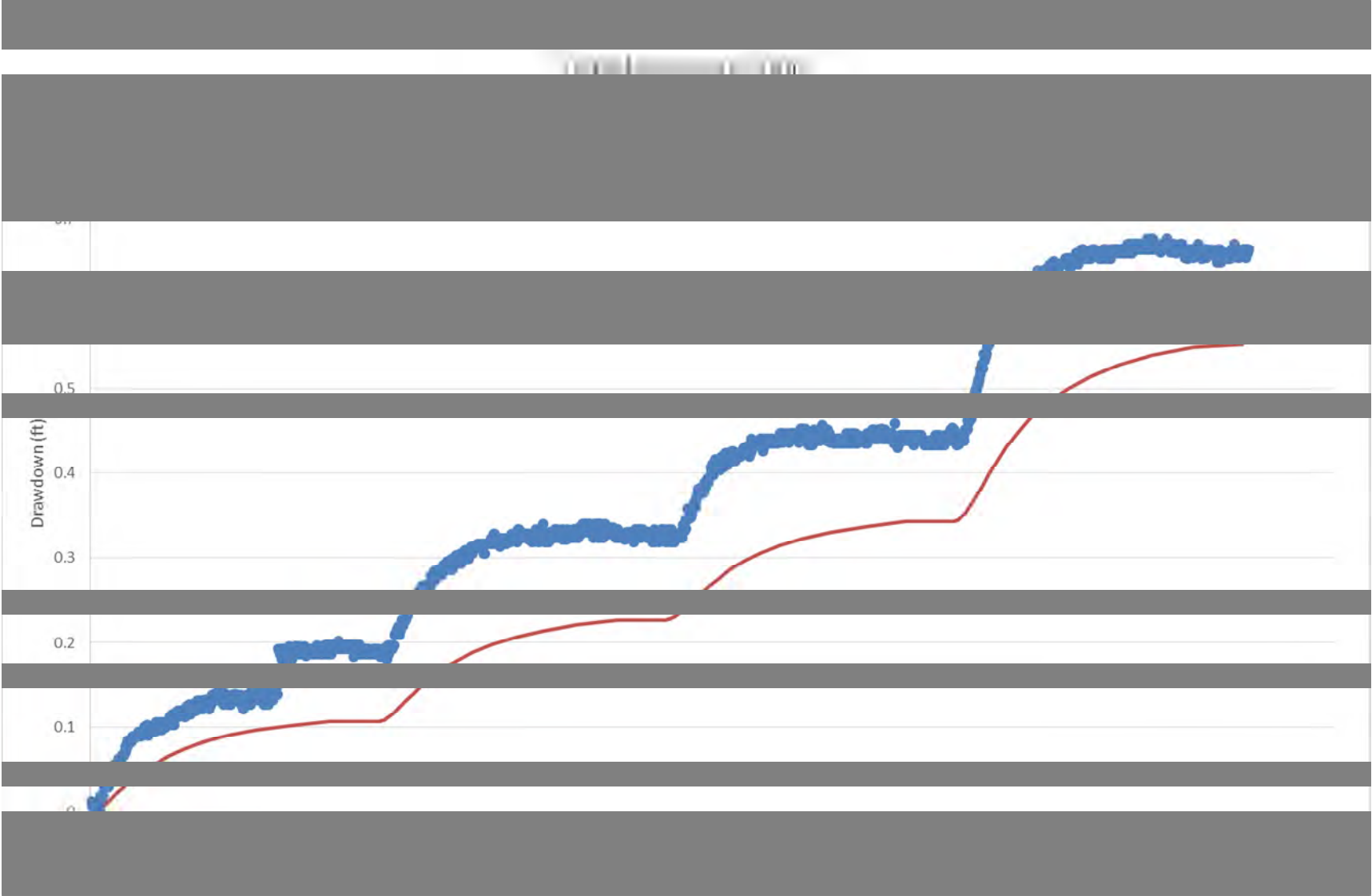
EW-13I Step Test	Average Rate (gpm)
Step 1	5.45
Step 2	11.34
Step 3	17.14
Step 4	27.96



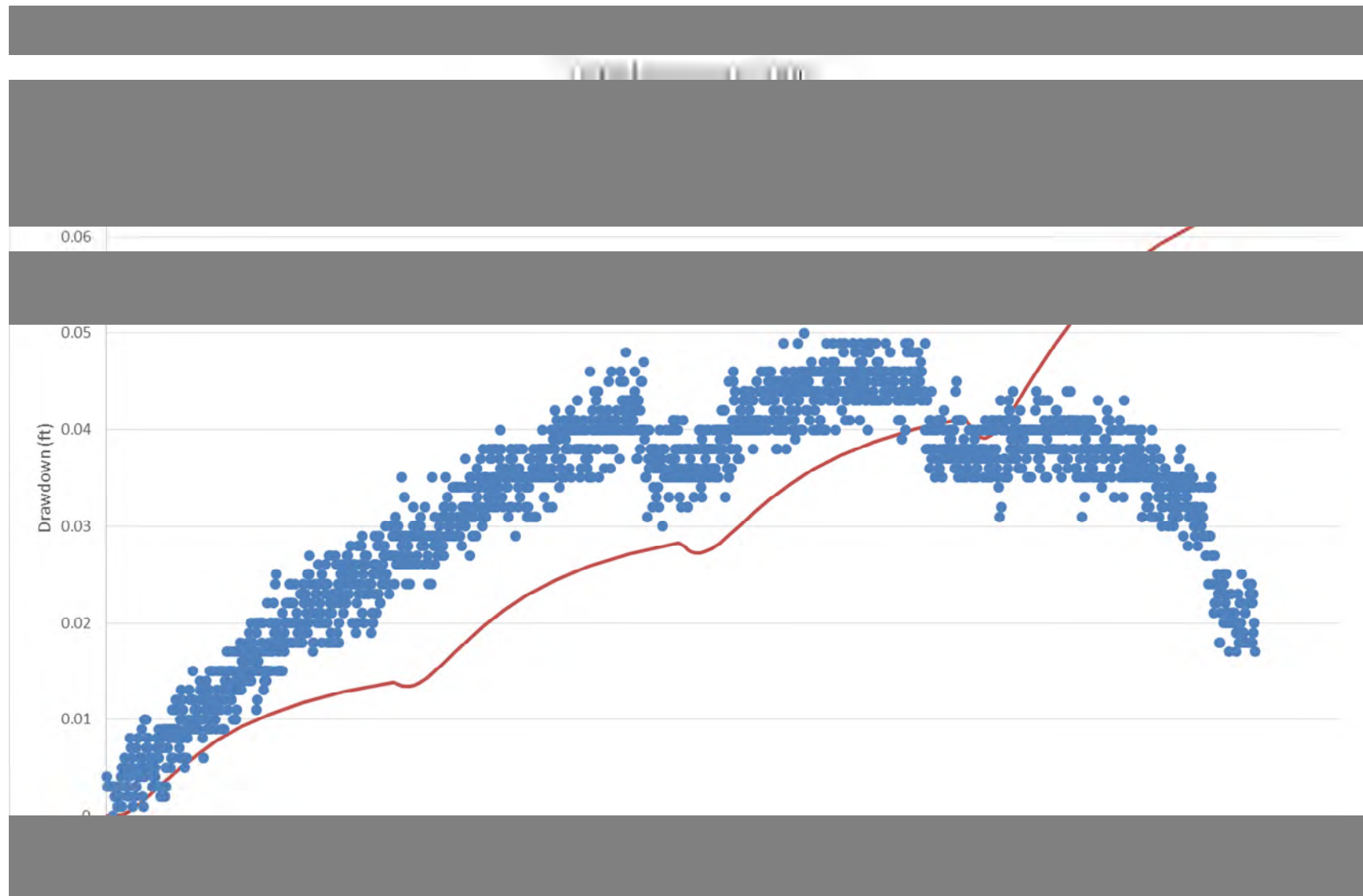


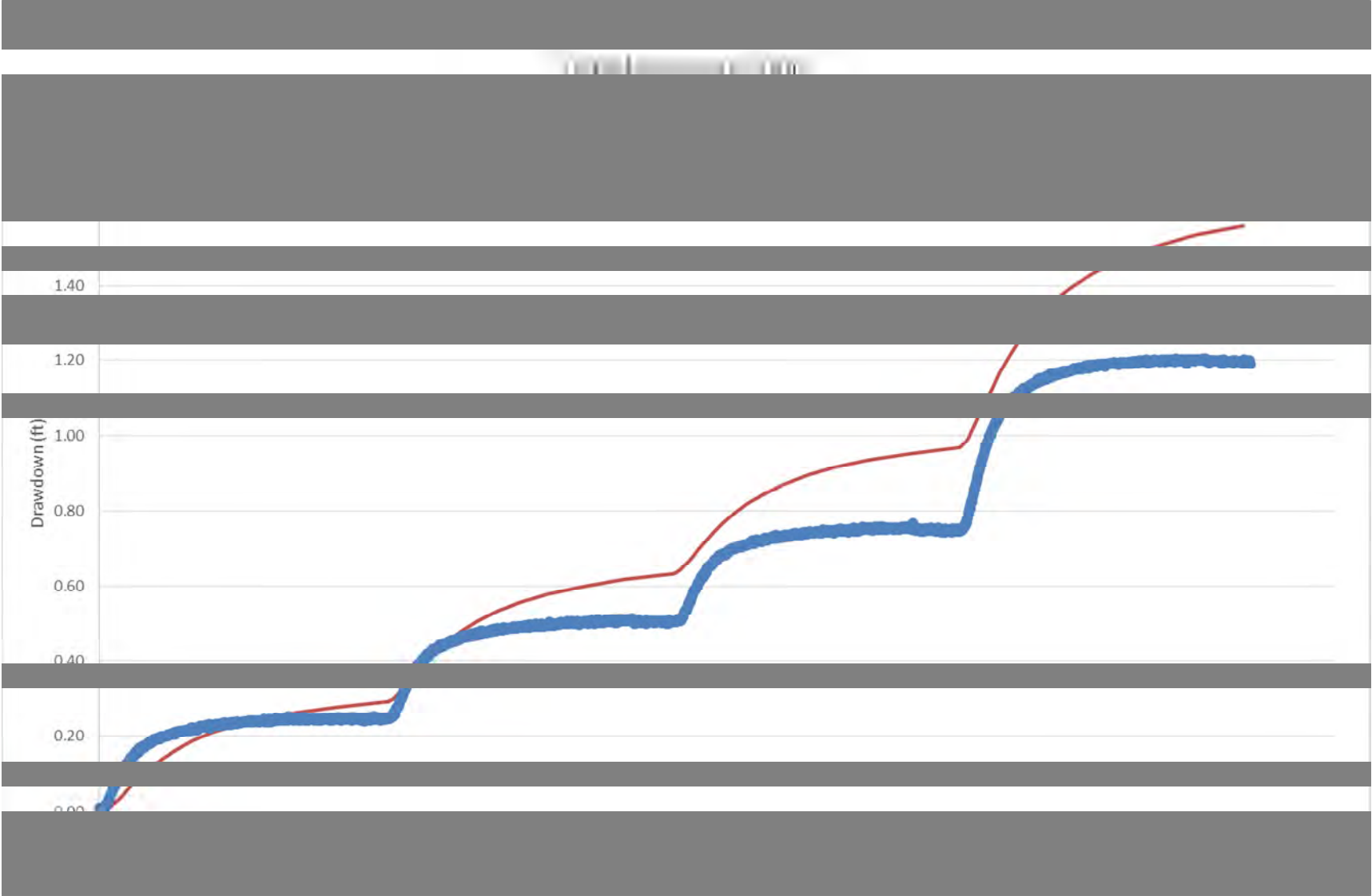
# Graph 1





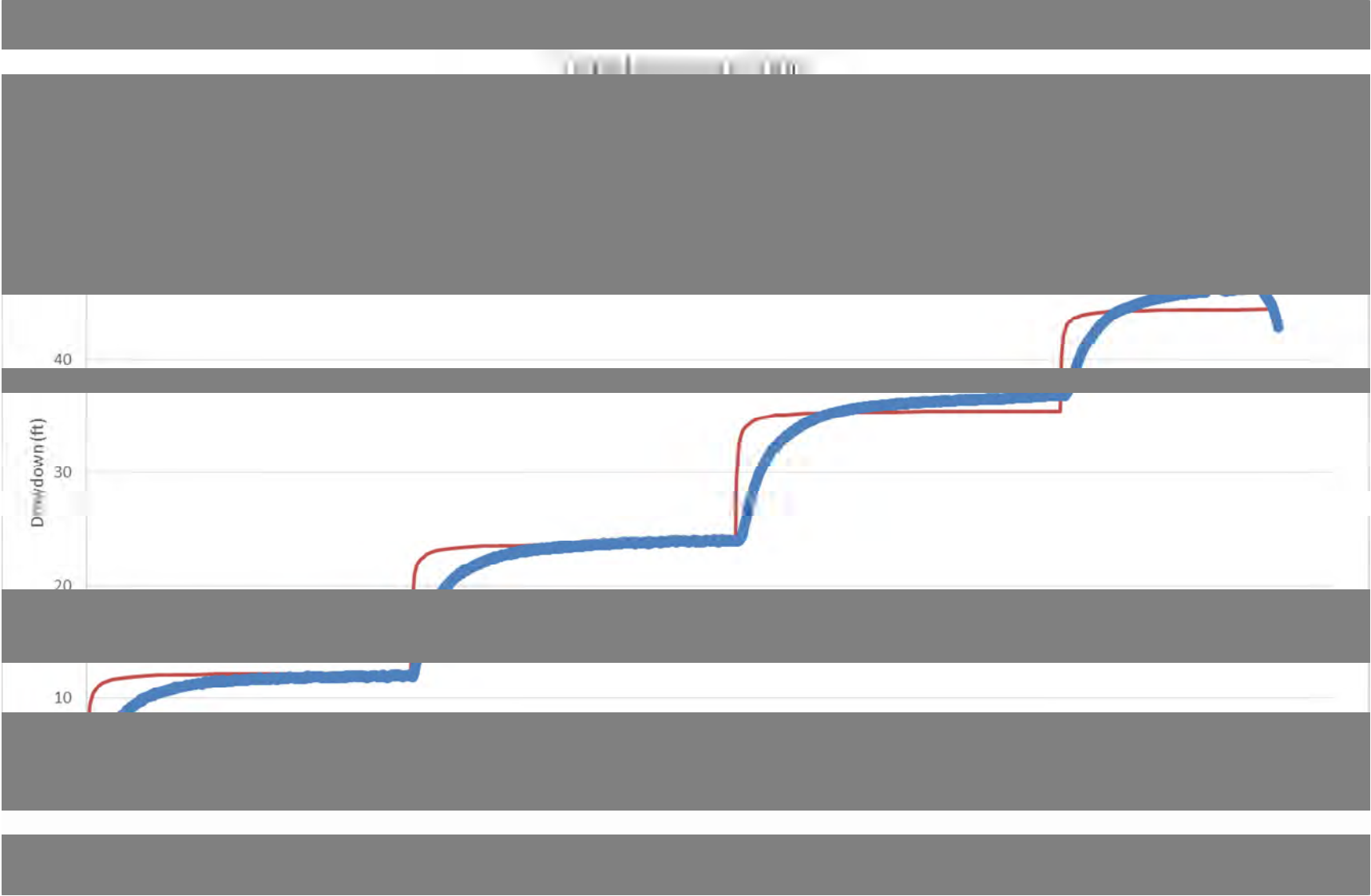


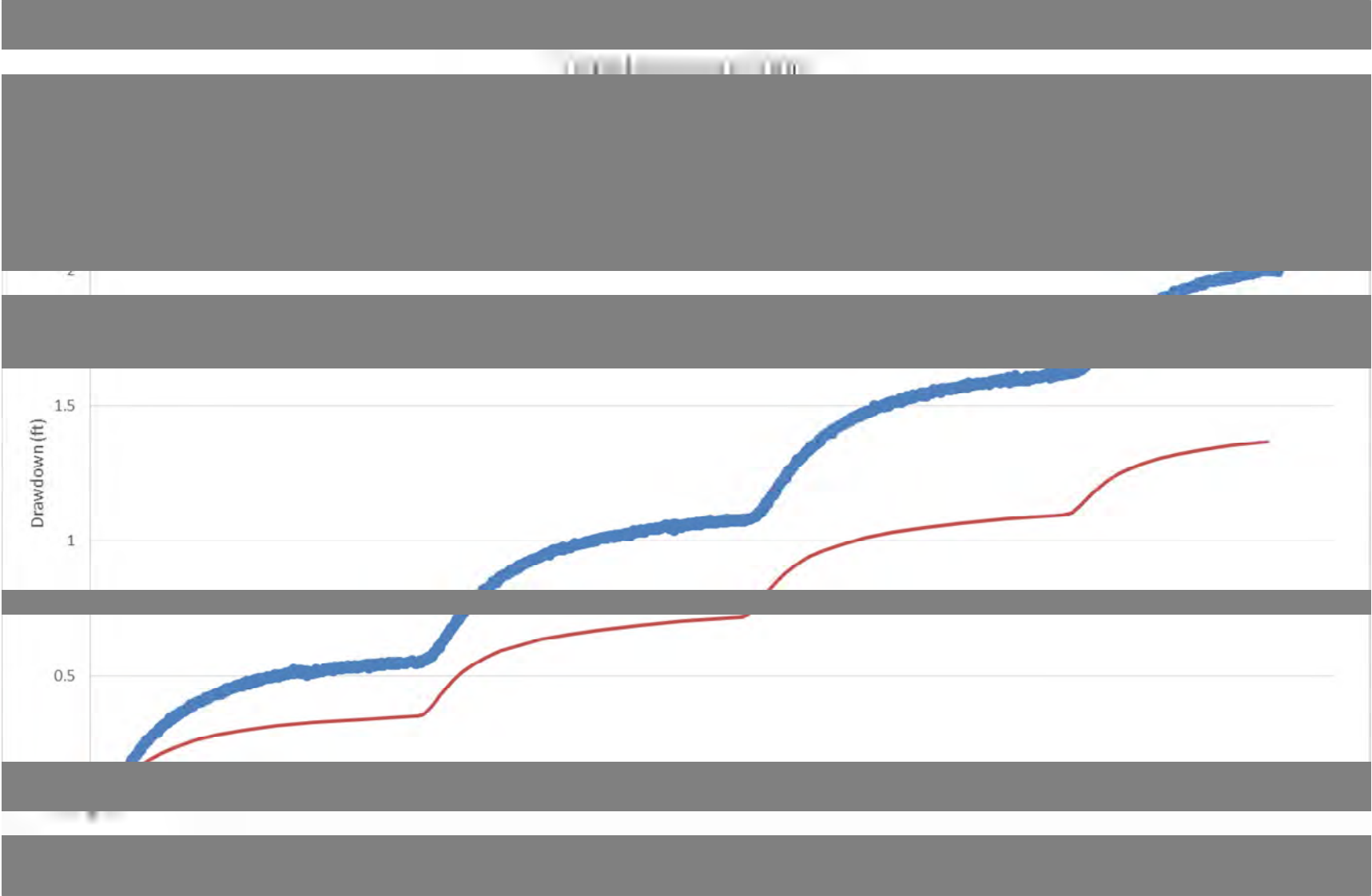


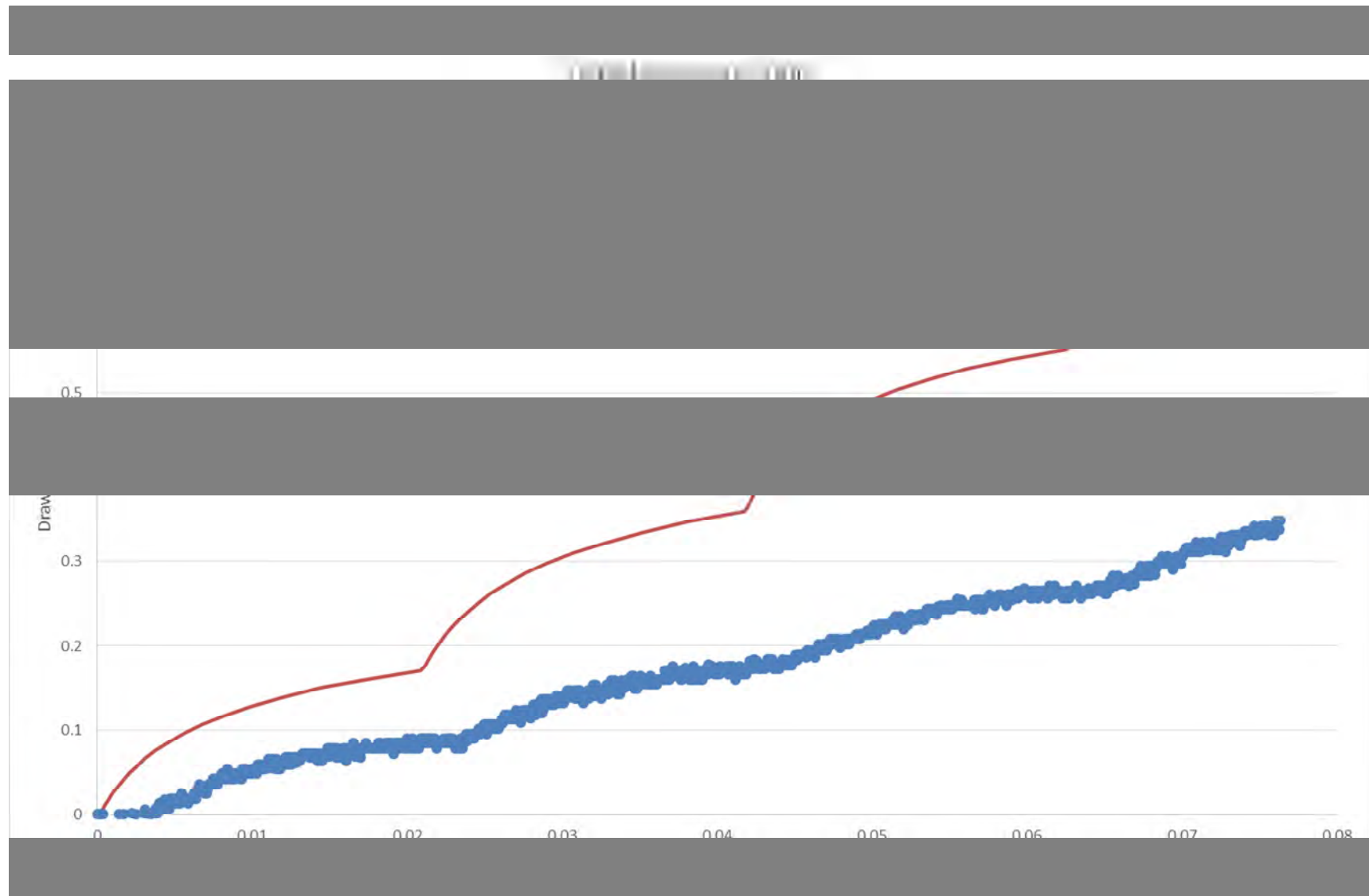


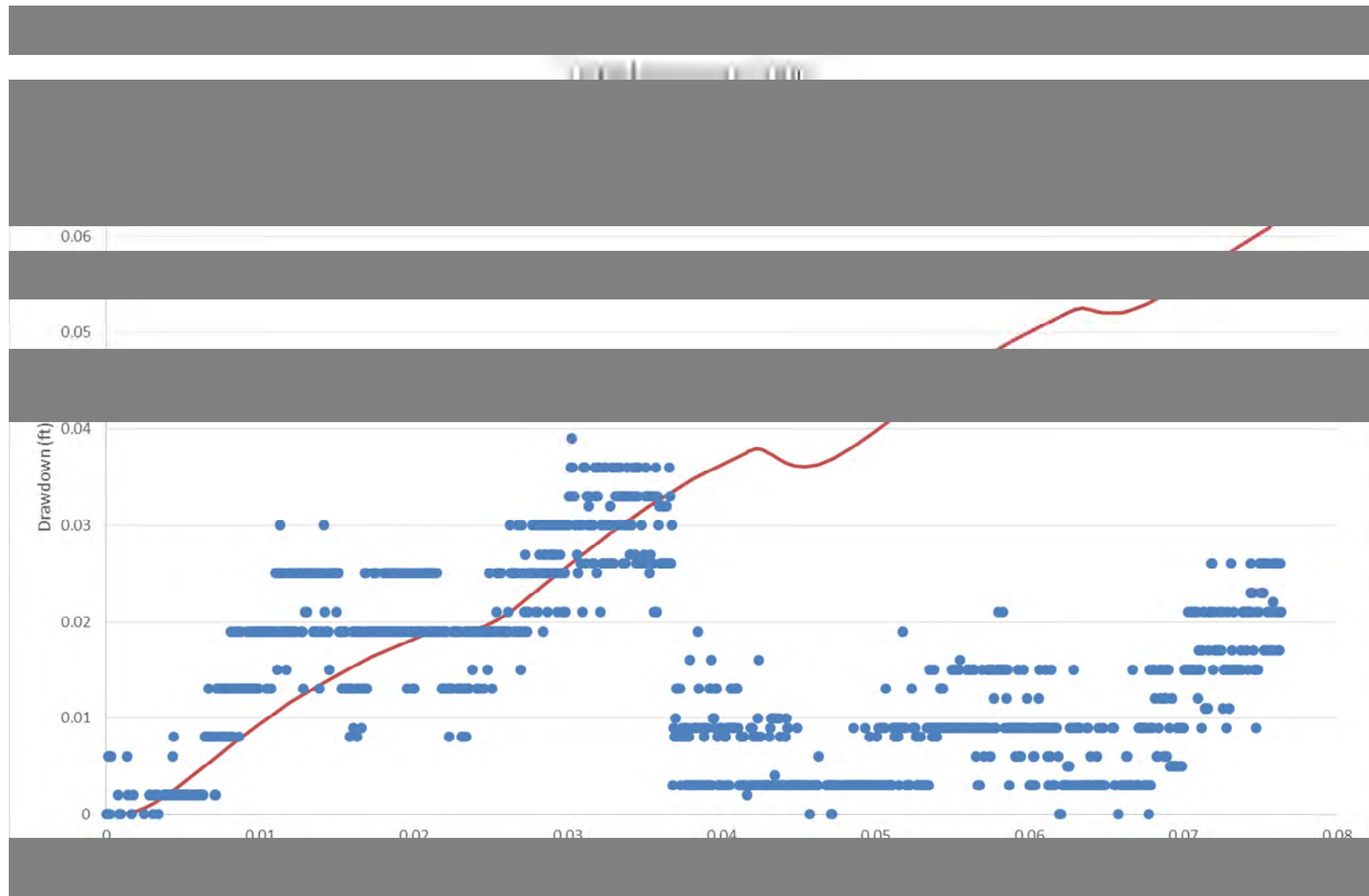
## Step-Drawdown Test B

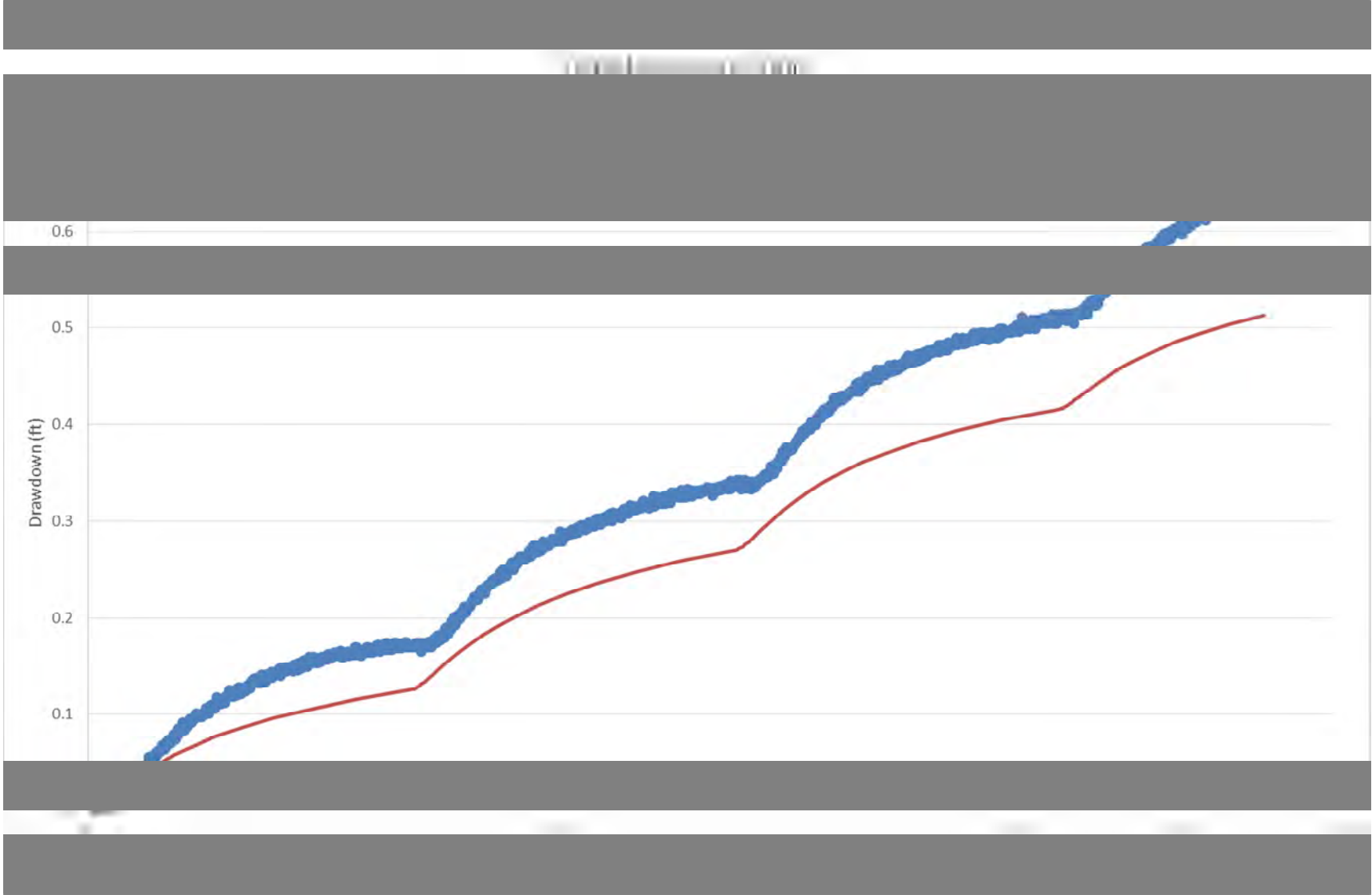
EW-14D Step Test	Average Rate (gpm)
Step 1	7.25
Step 2	14.06
Step 3	21.06
Step 4	26.43



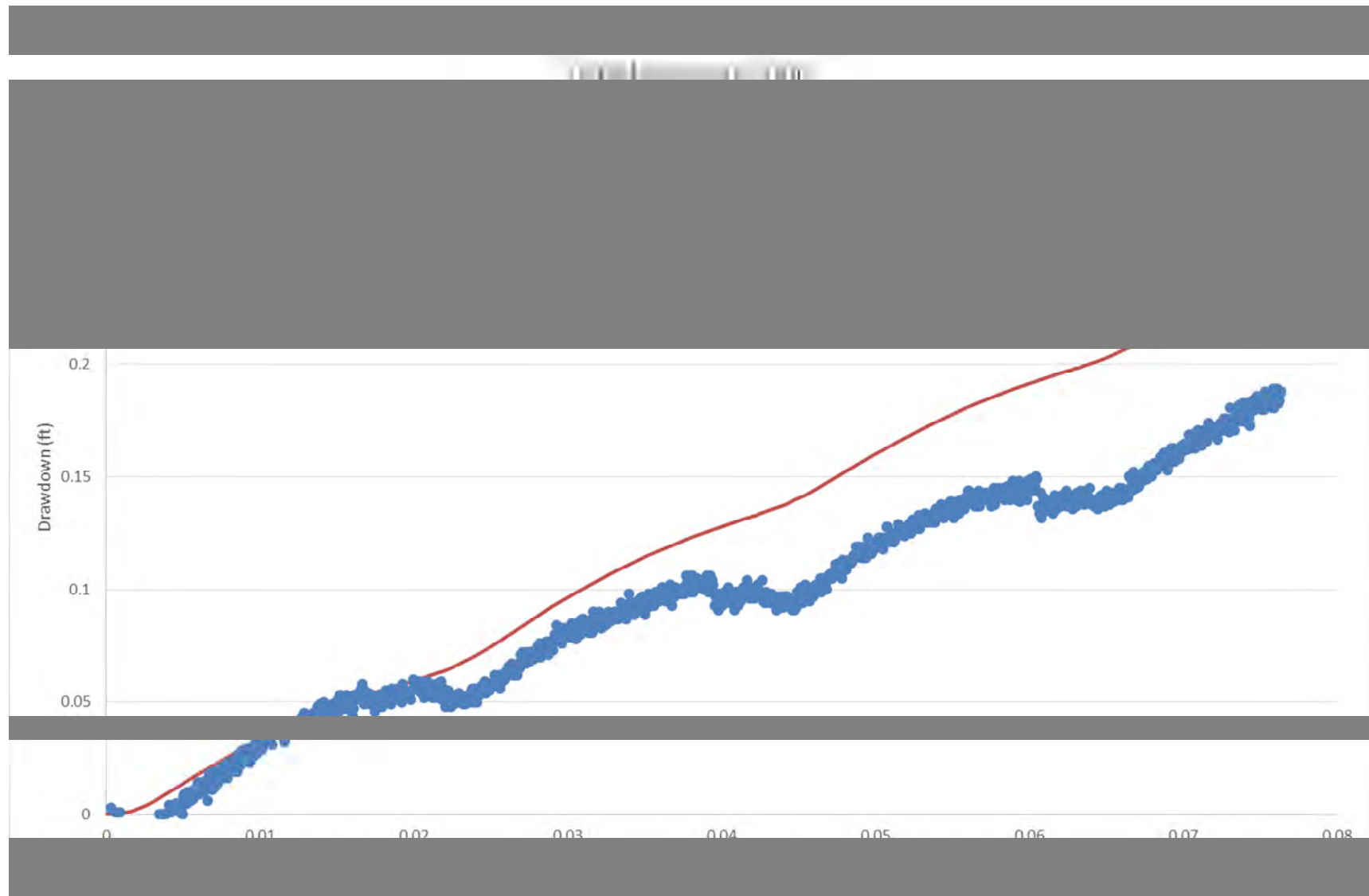






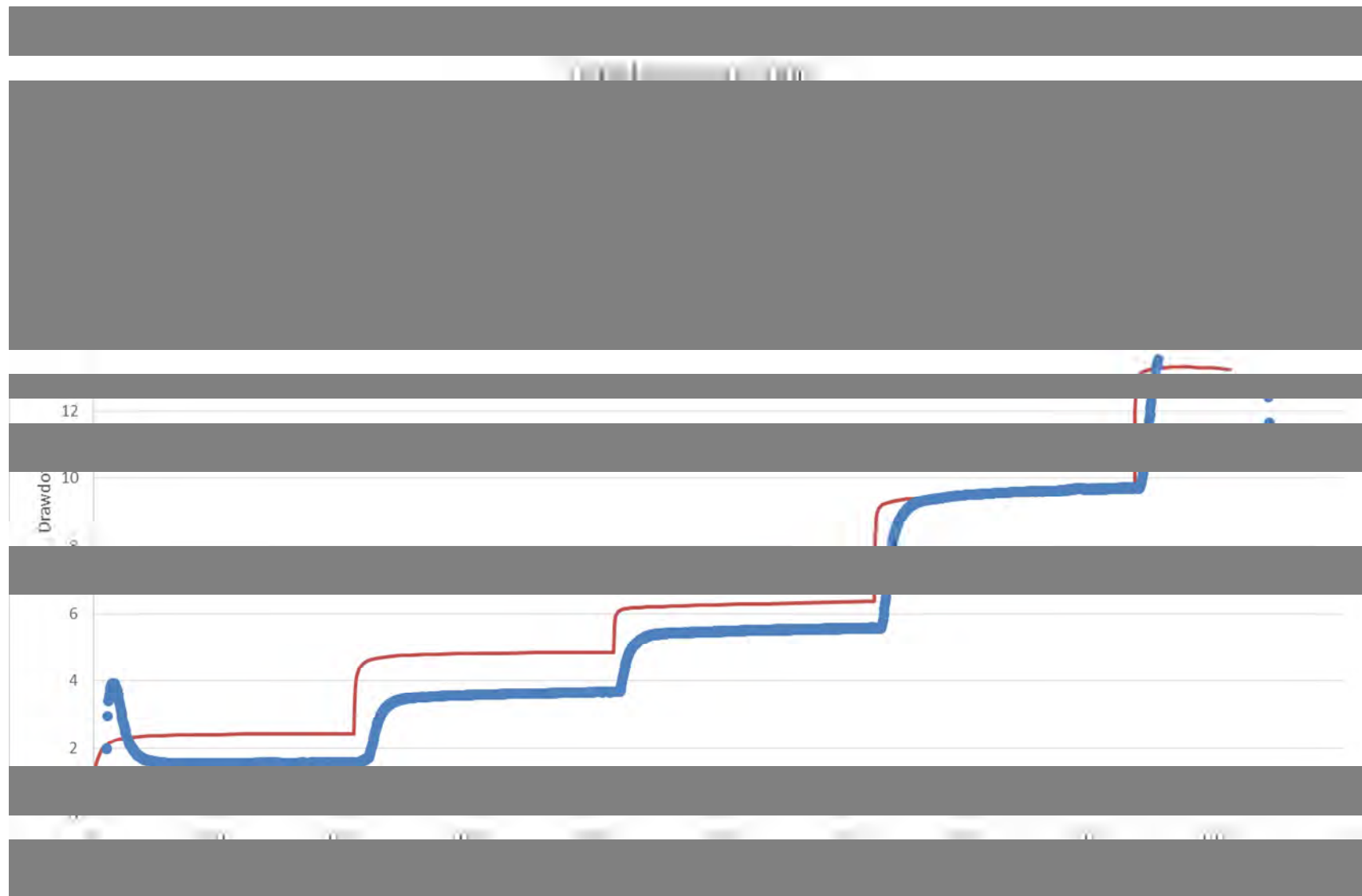


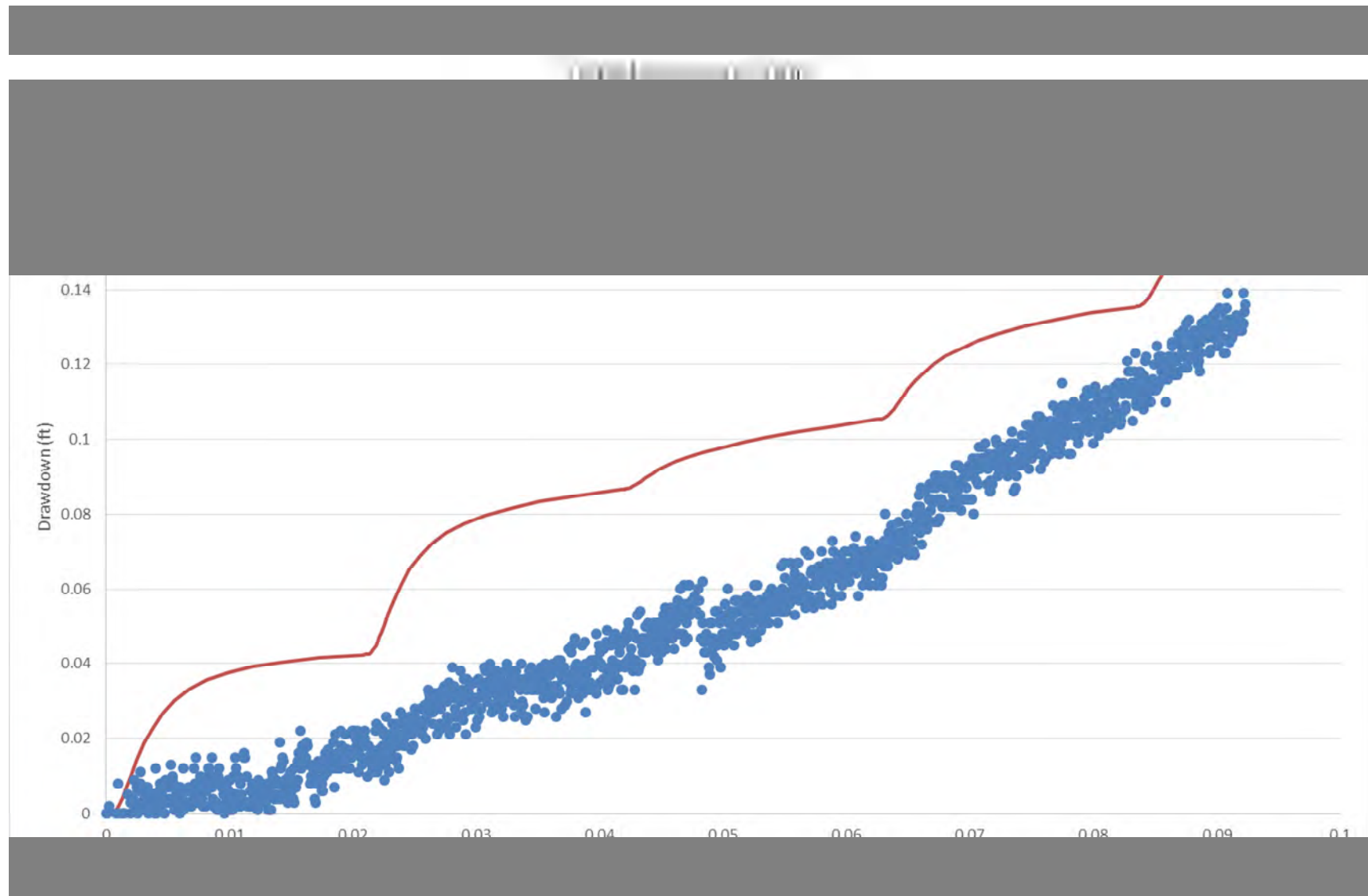


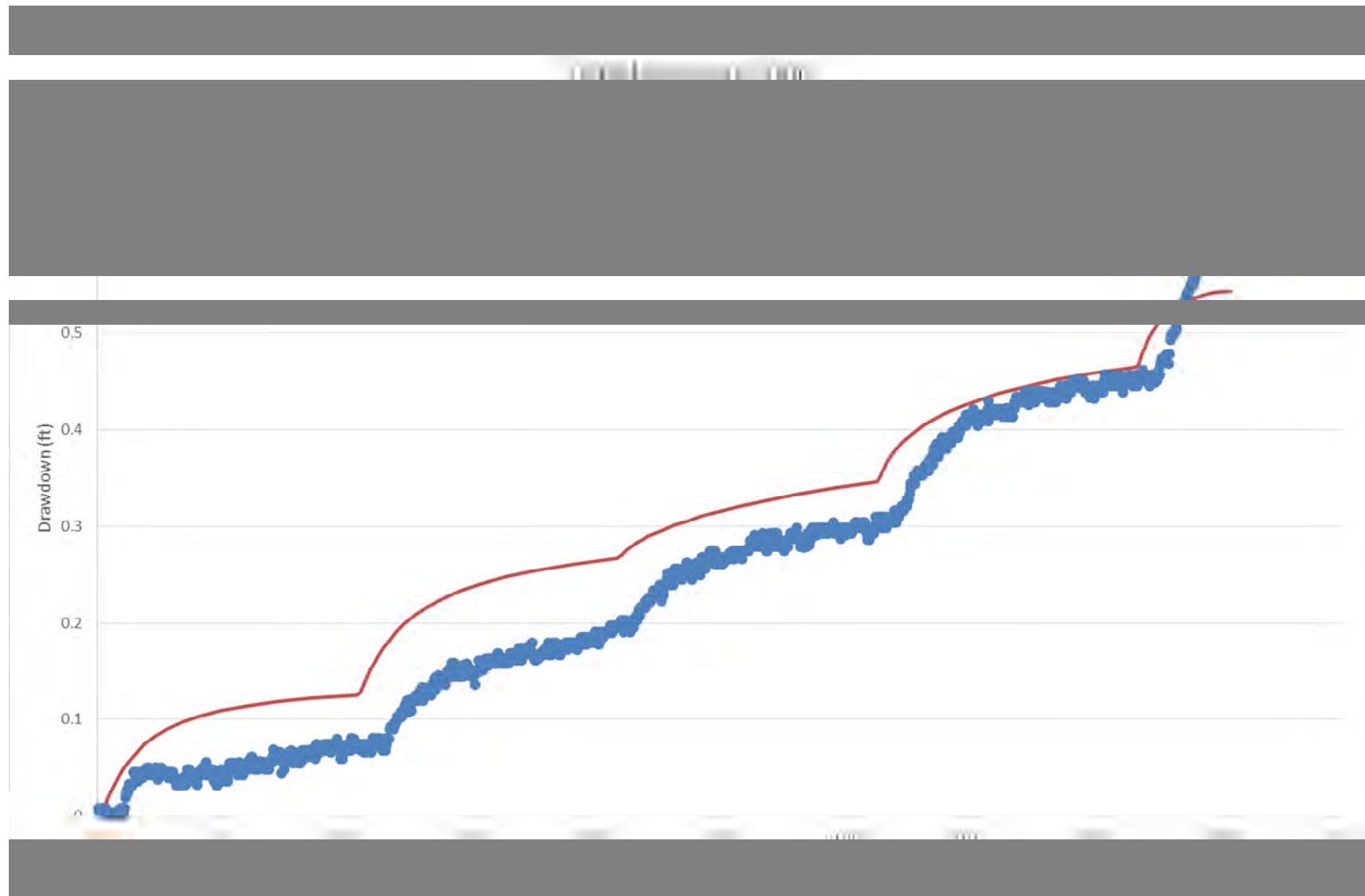


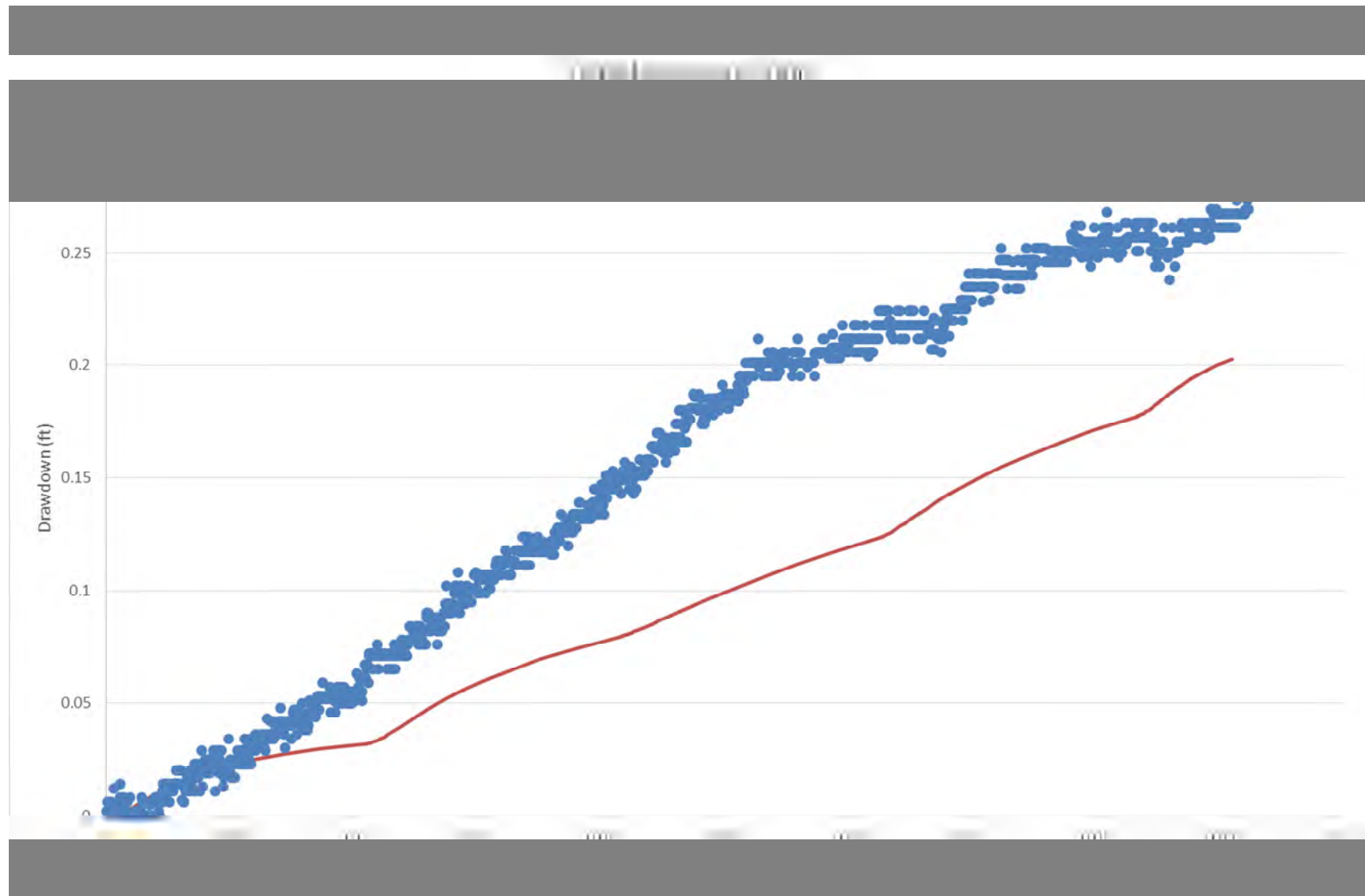
## Step-Drawdown Test C

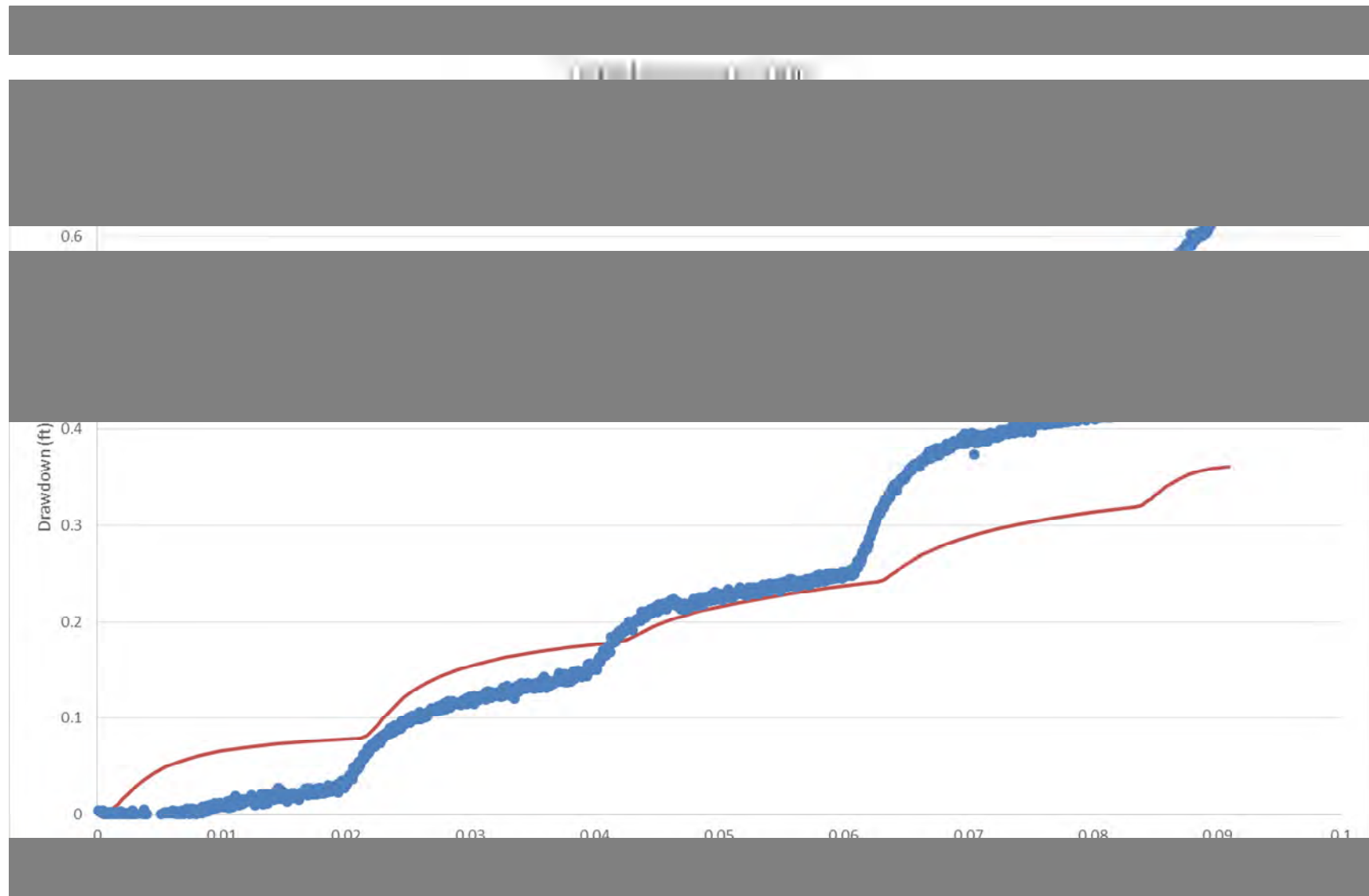
EW-15S Step Test	Average Rate (gpm)
Step 1	2.40
Step 2	5.12
Step 3	7.53
Step 4	13.01
Step 5	19.87

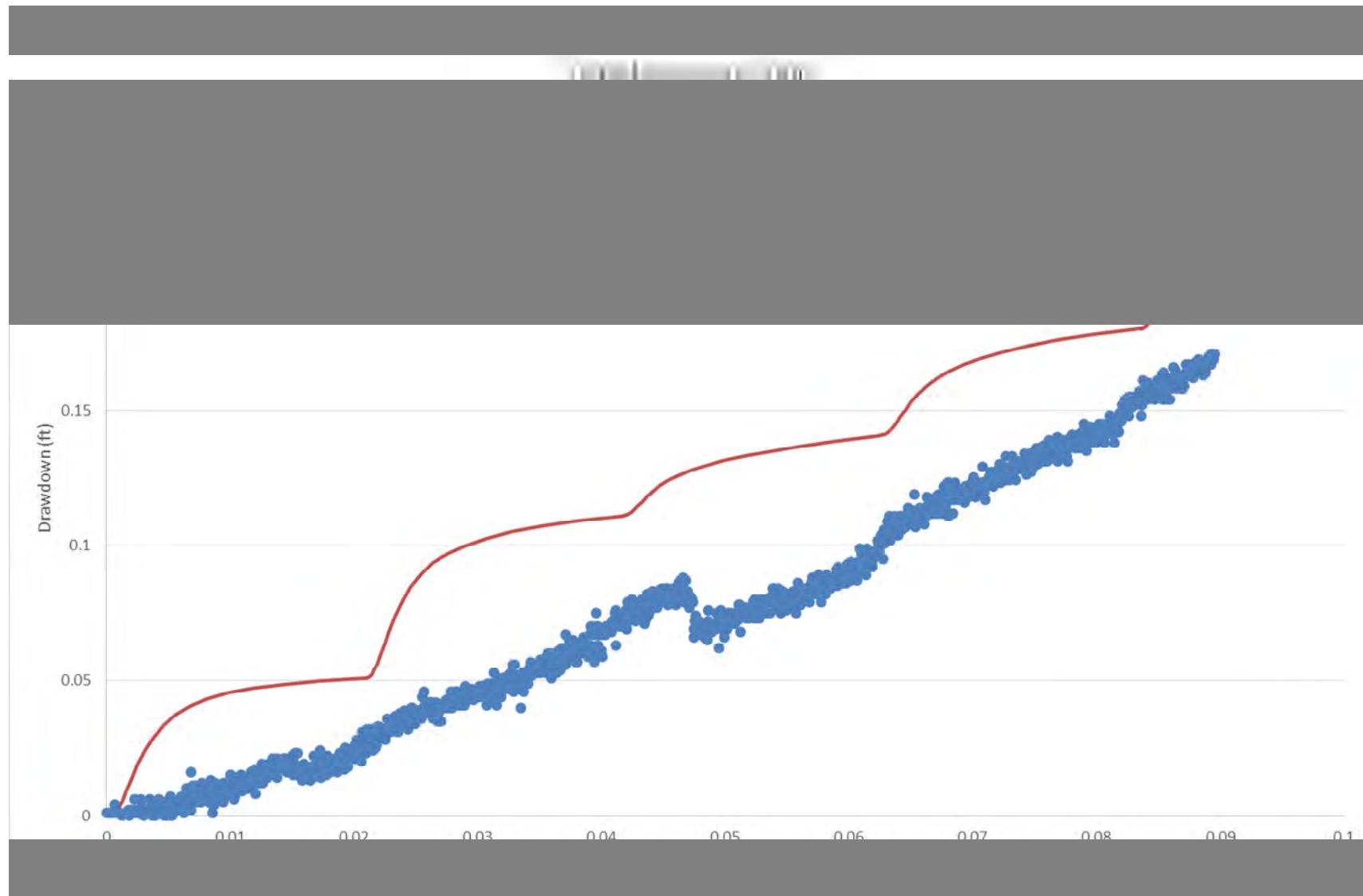








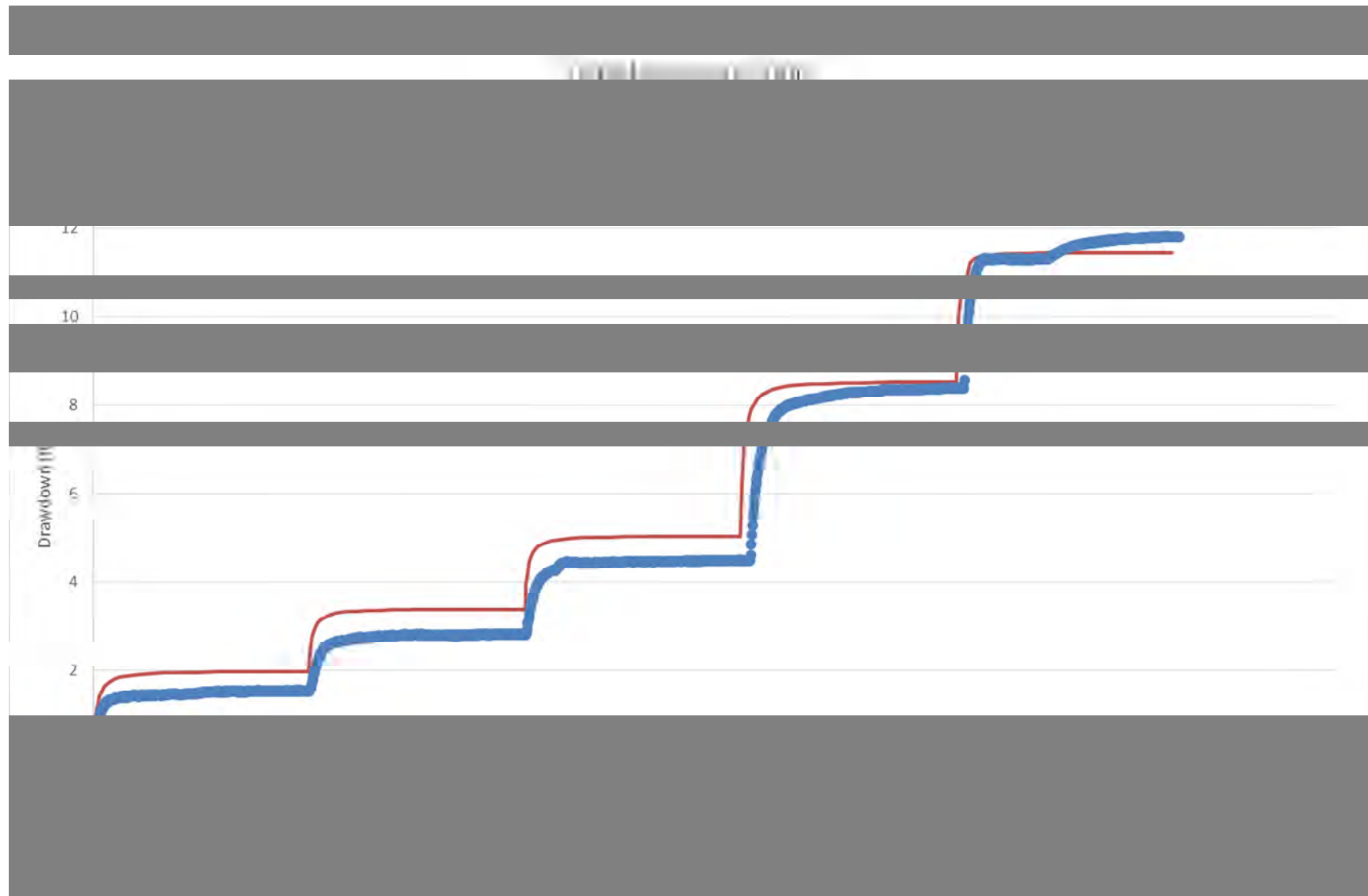


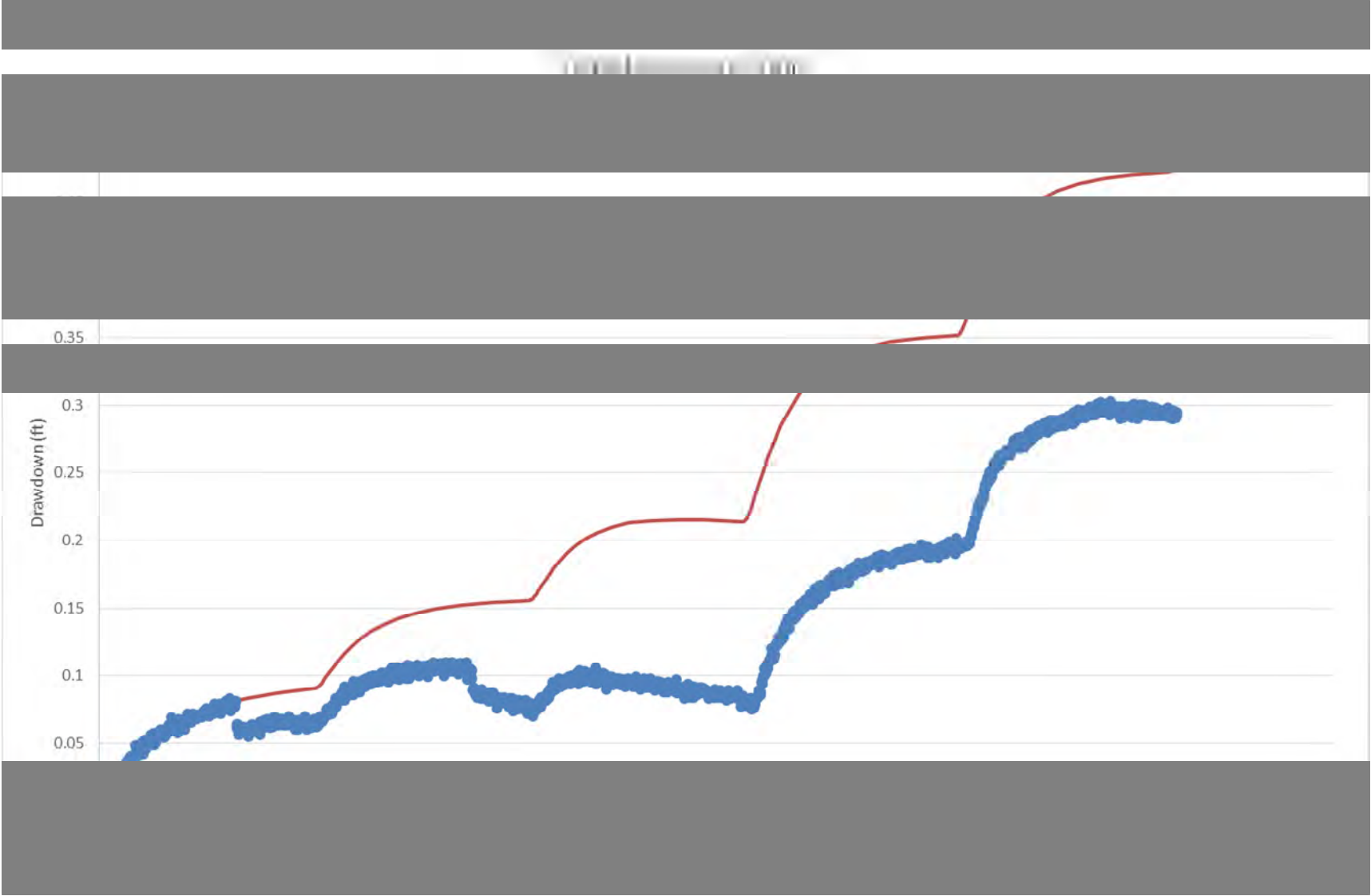


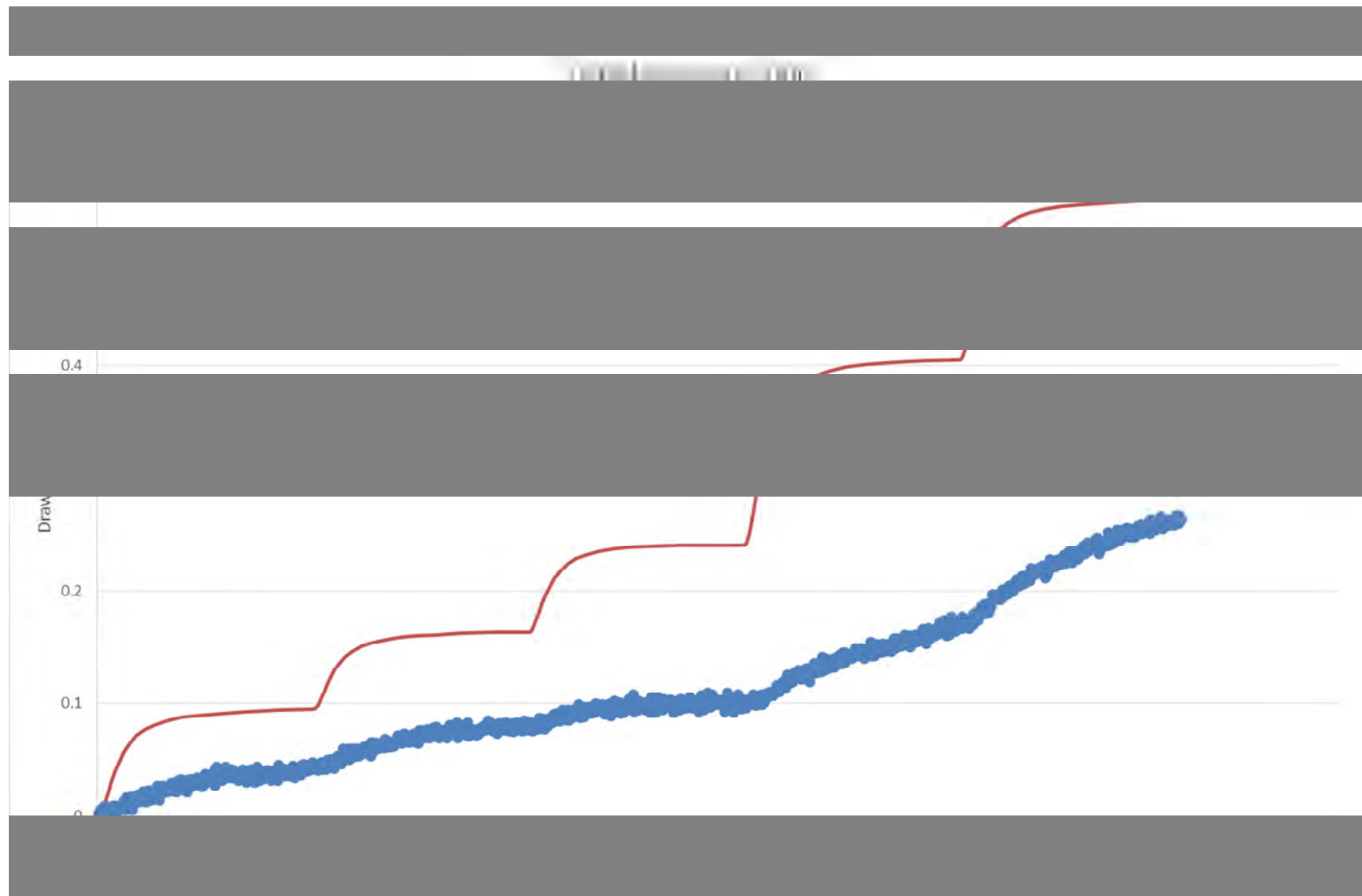


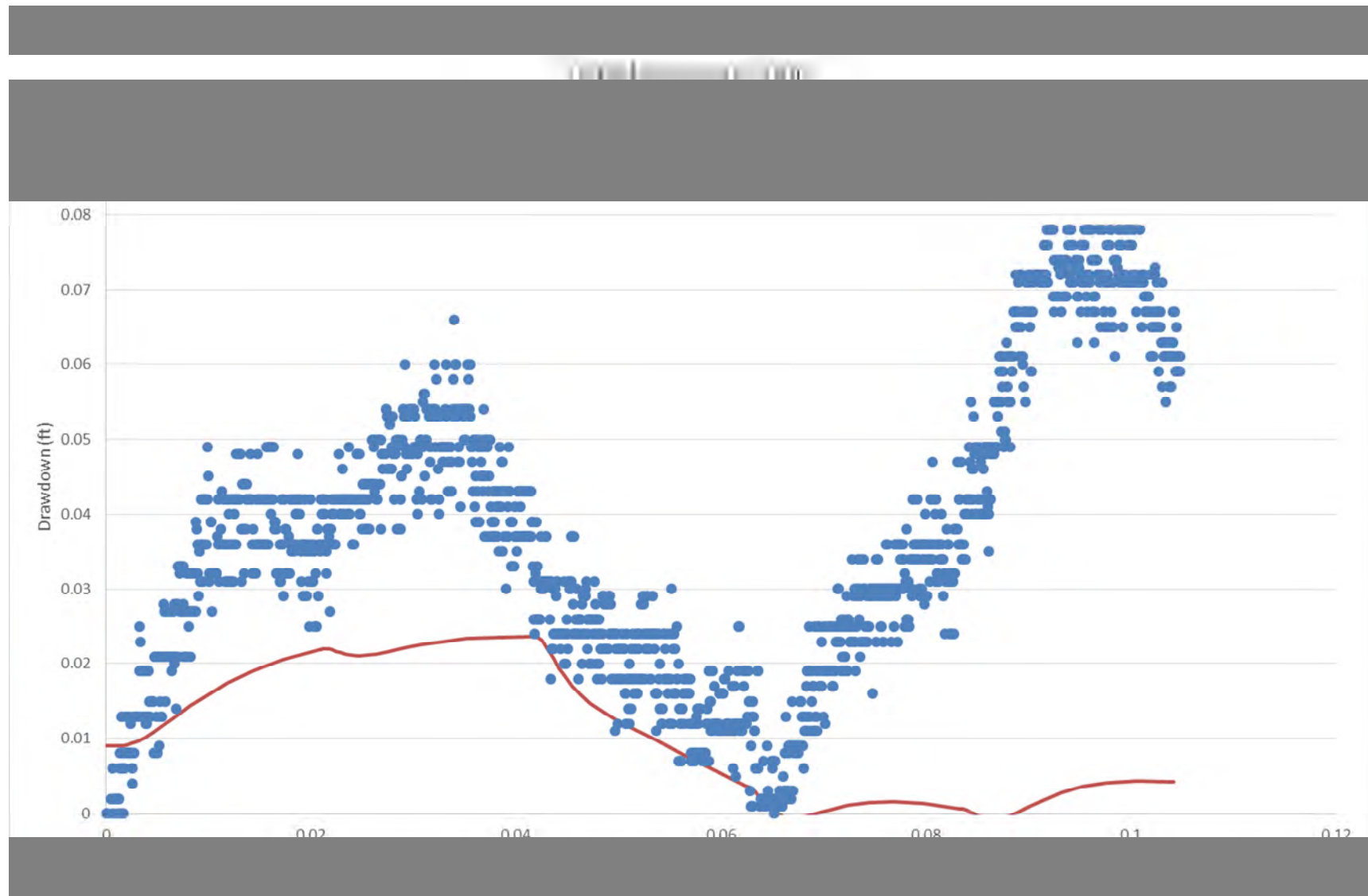
## Step-Drawdown Test D

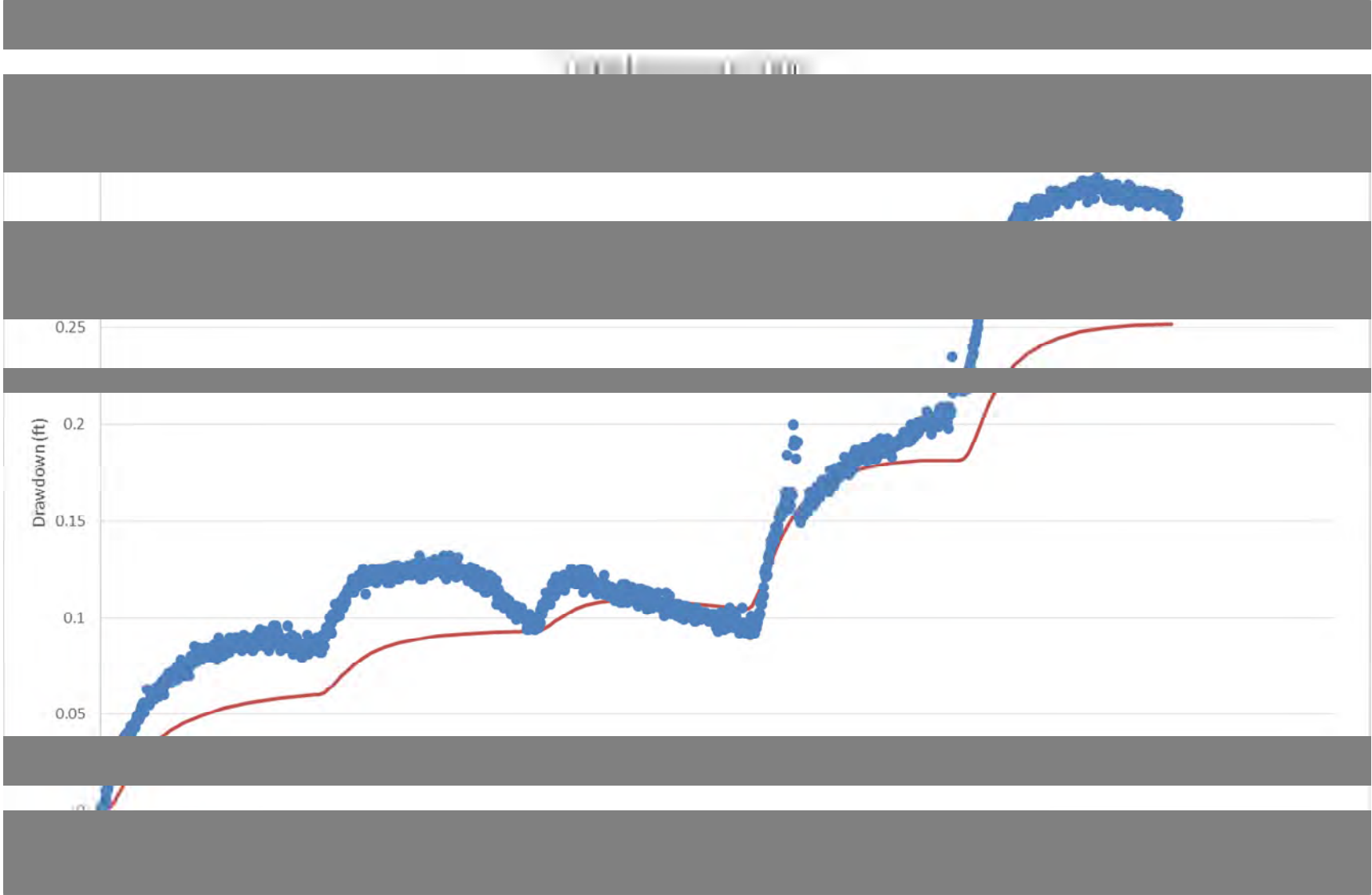
EW-16S Step Test	Average Rate (gpm)
Step 1	2.34
Step 2	4.02
Step 3	5.99
Step 4	10.13
Step 5	13.85





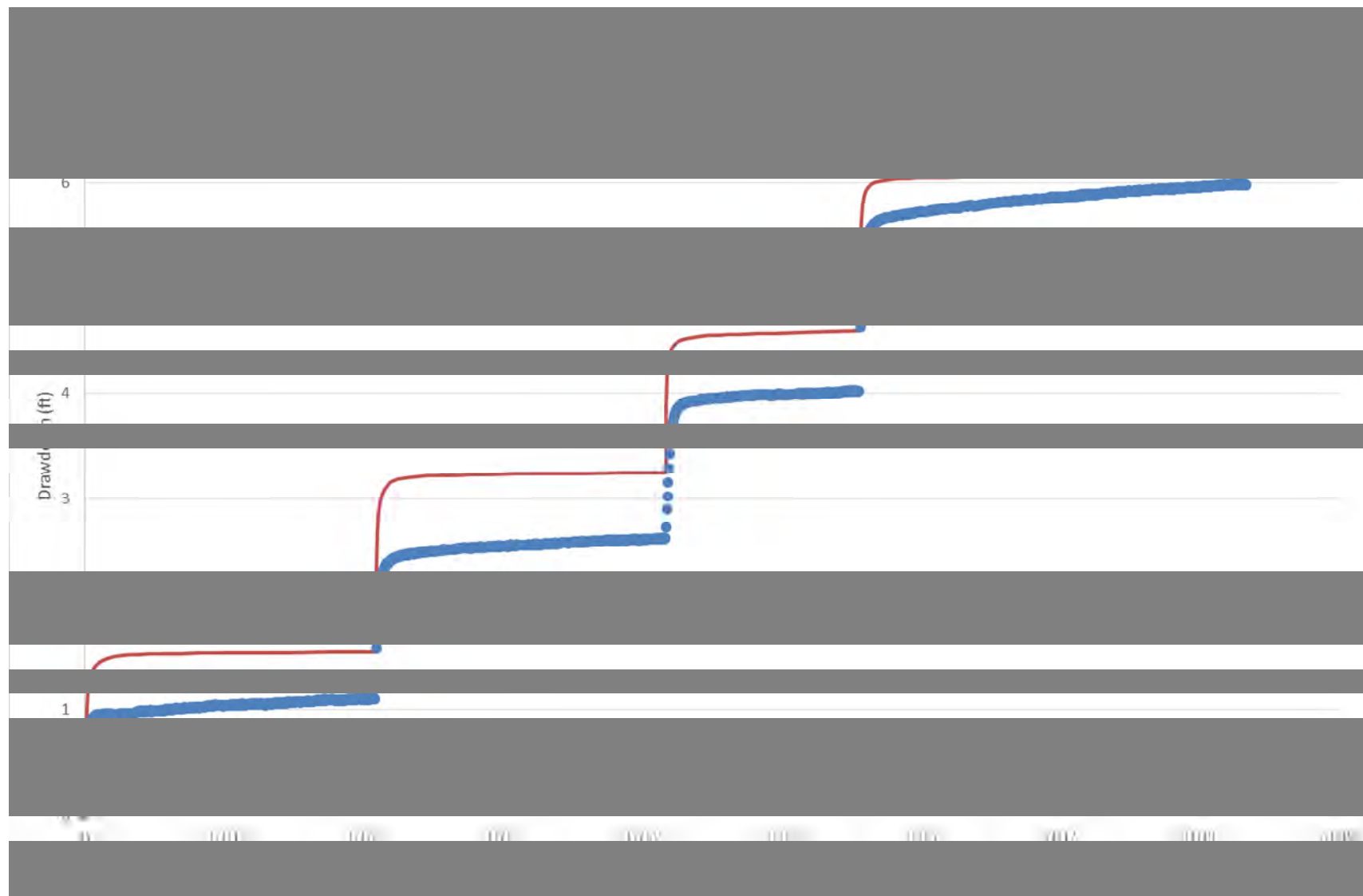




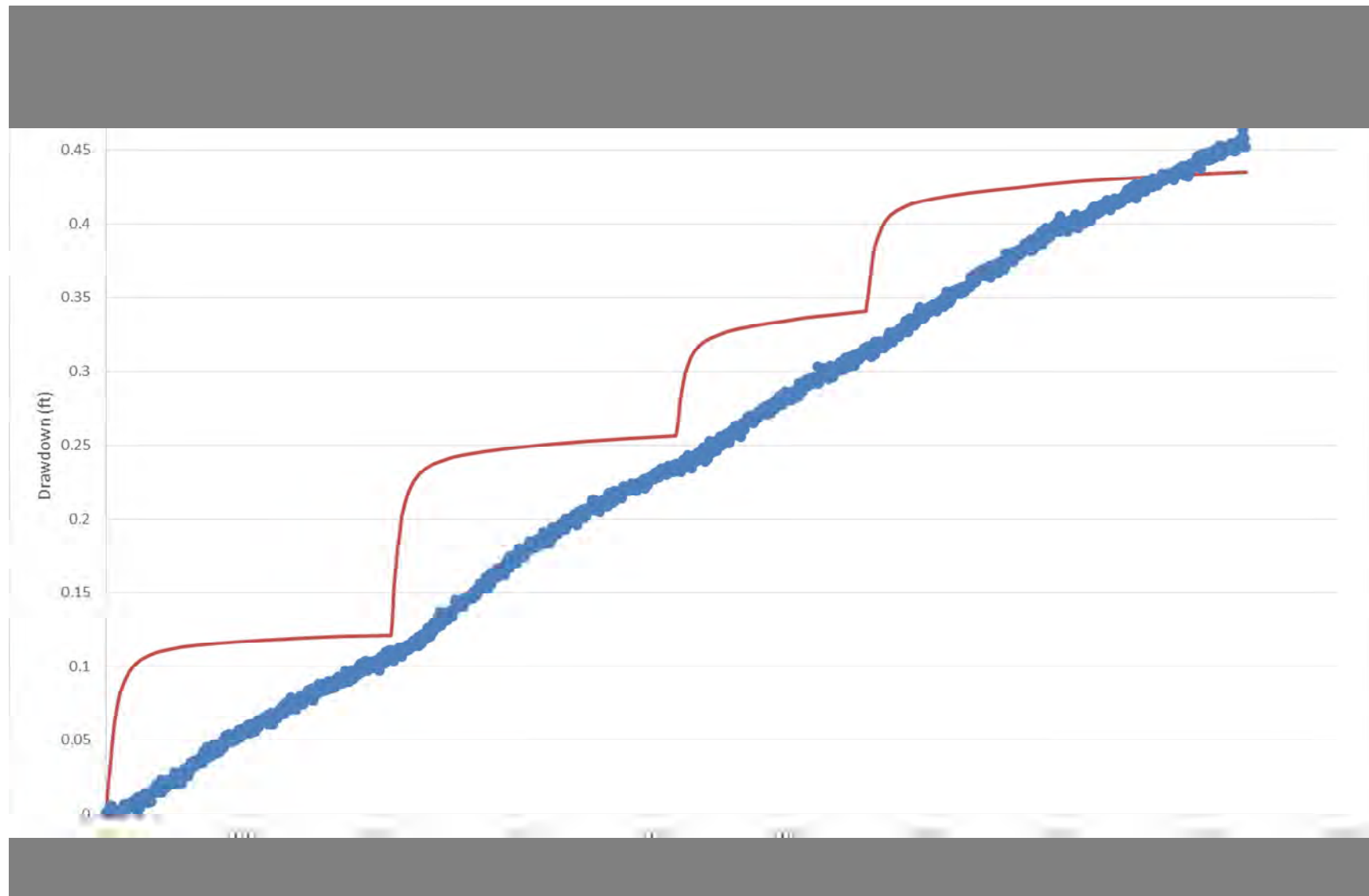


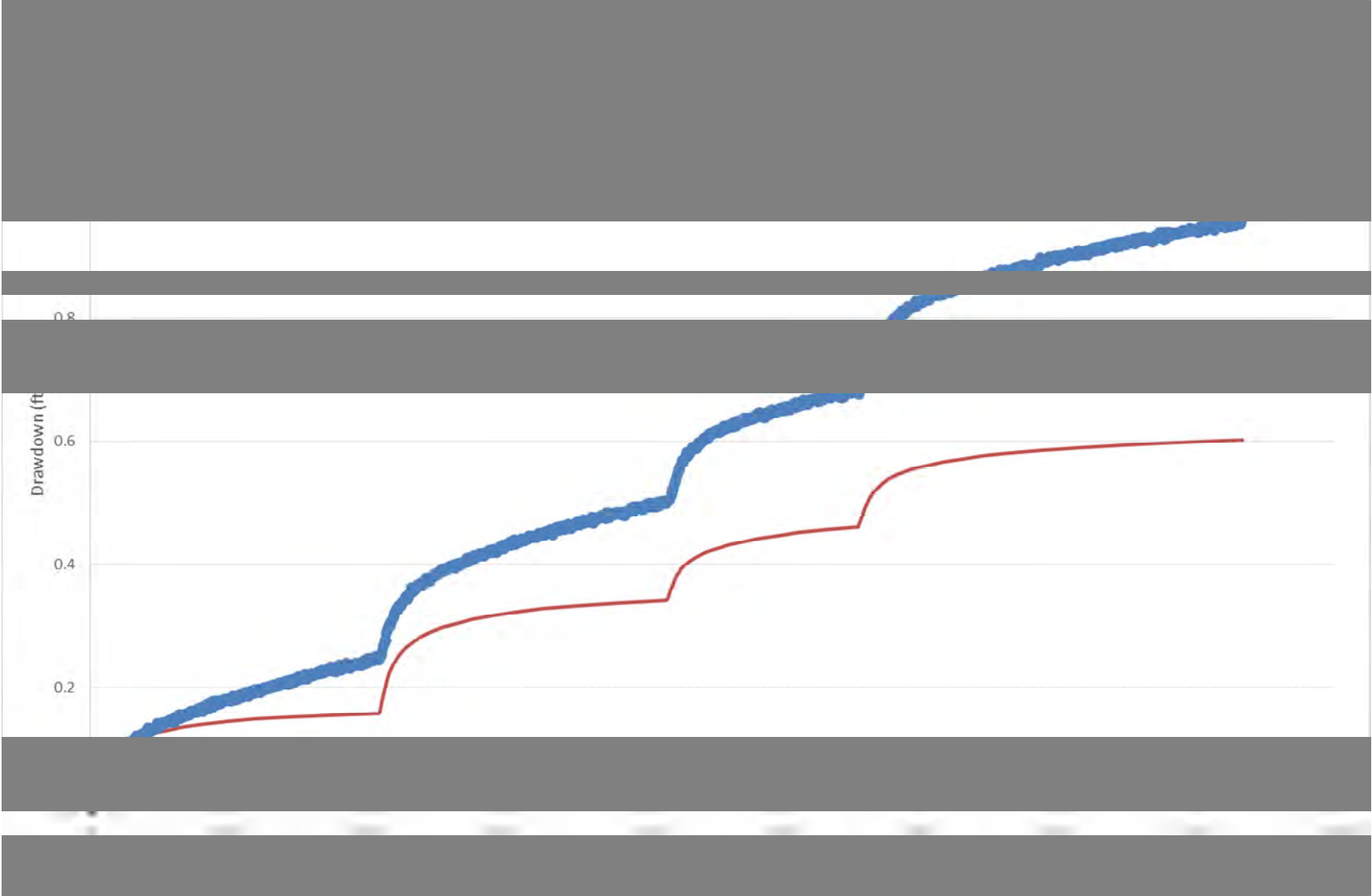
## Step-Drawdown Test E

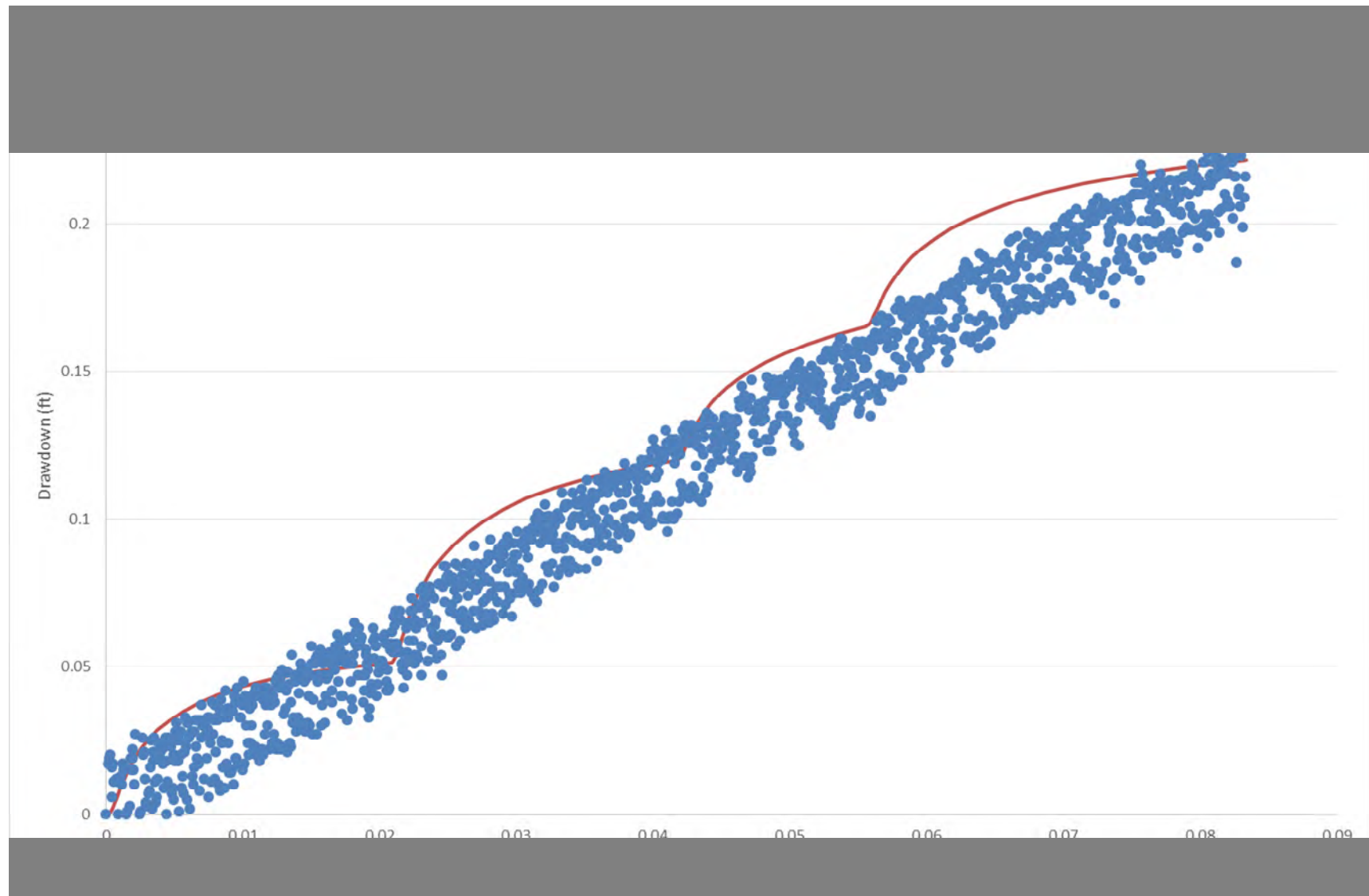
EW-10S Step Test	Average Rate (gpm)
Step 1	6.63
Step 2	14.06
Step 3	21.05
Step 4	29.29

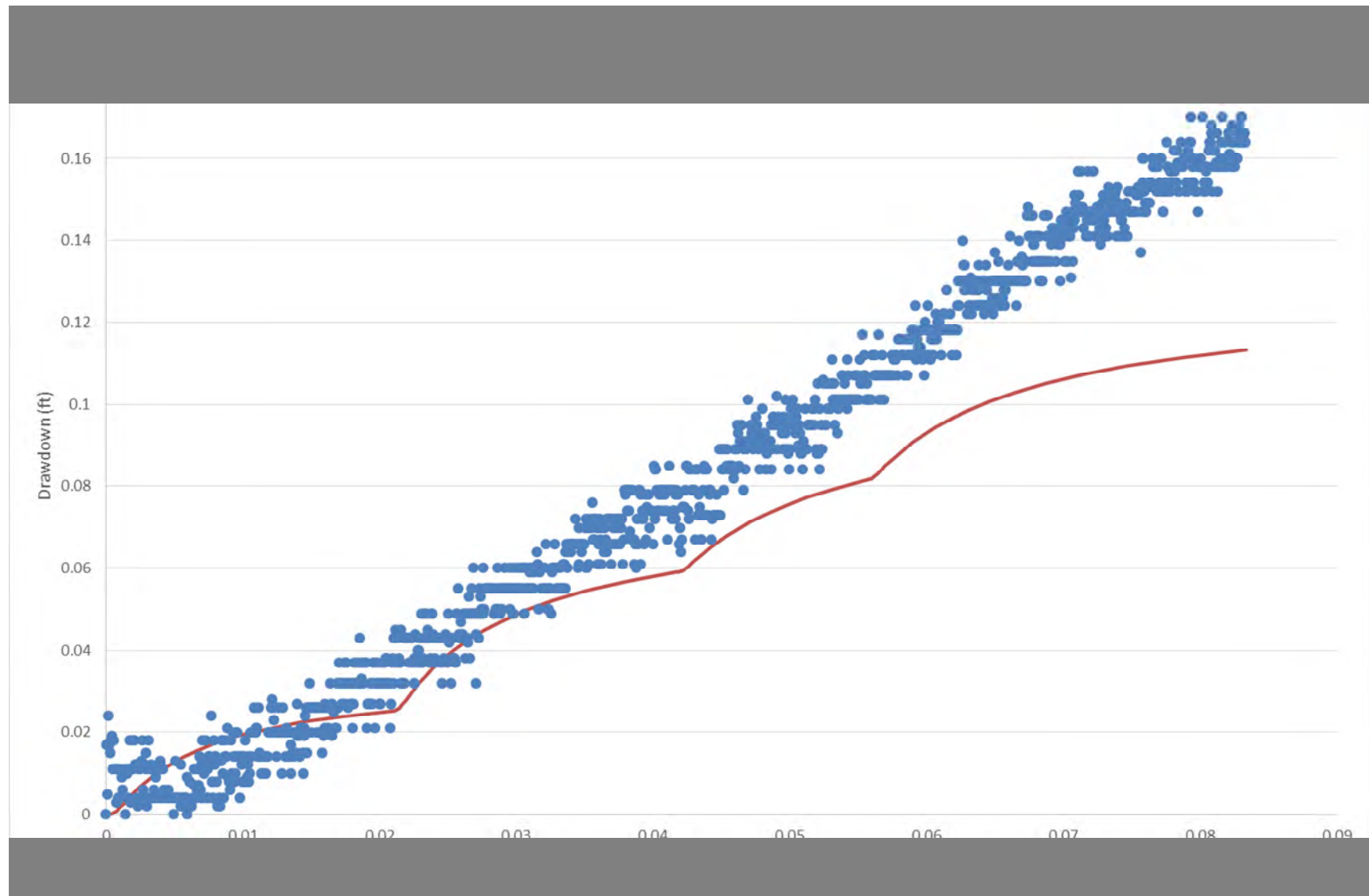


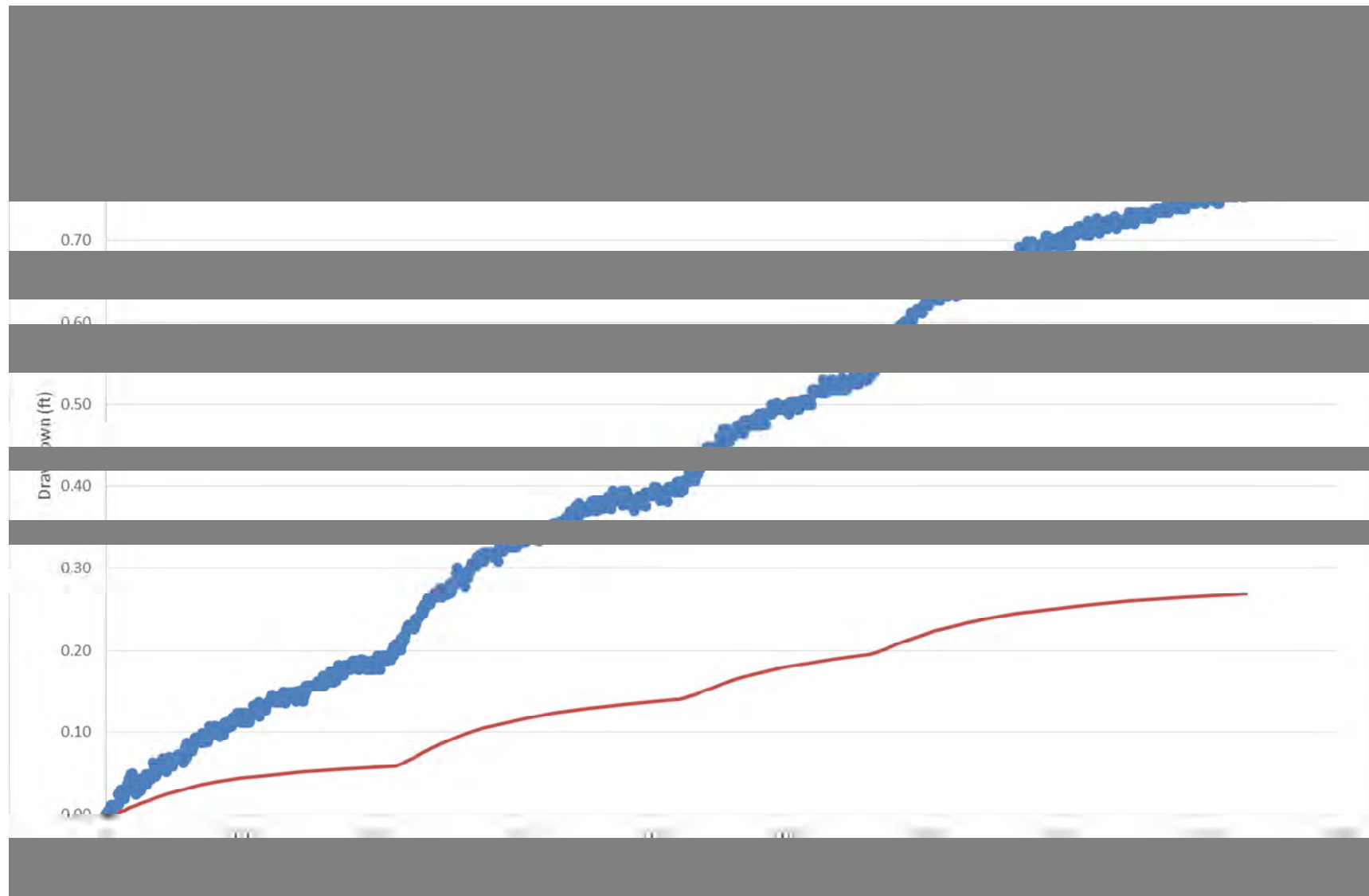


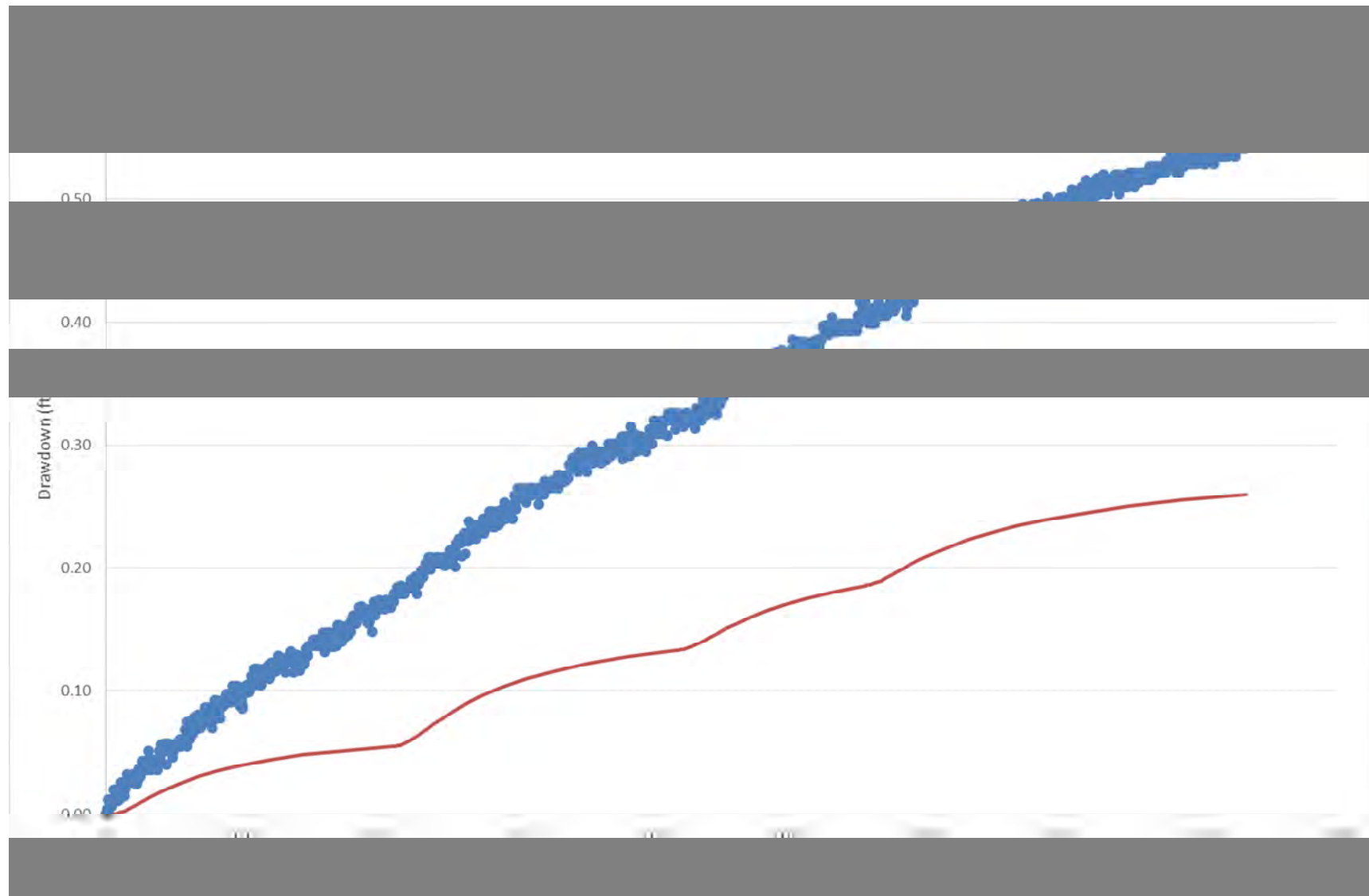


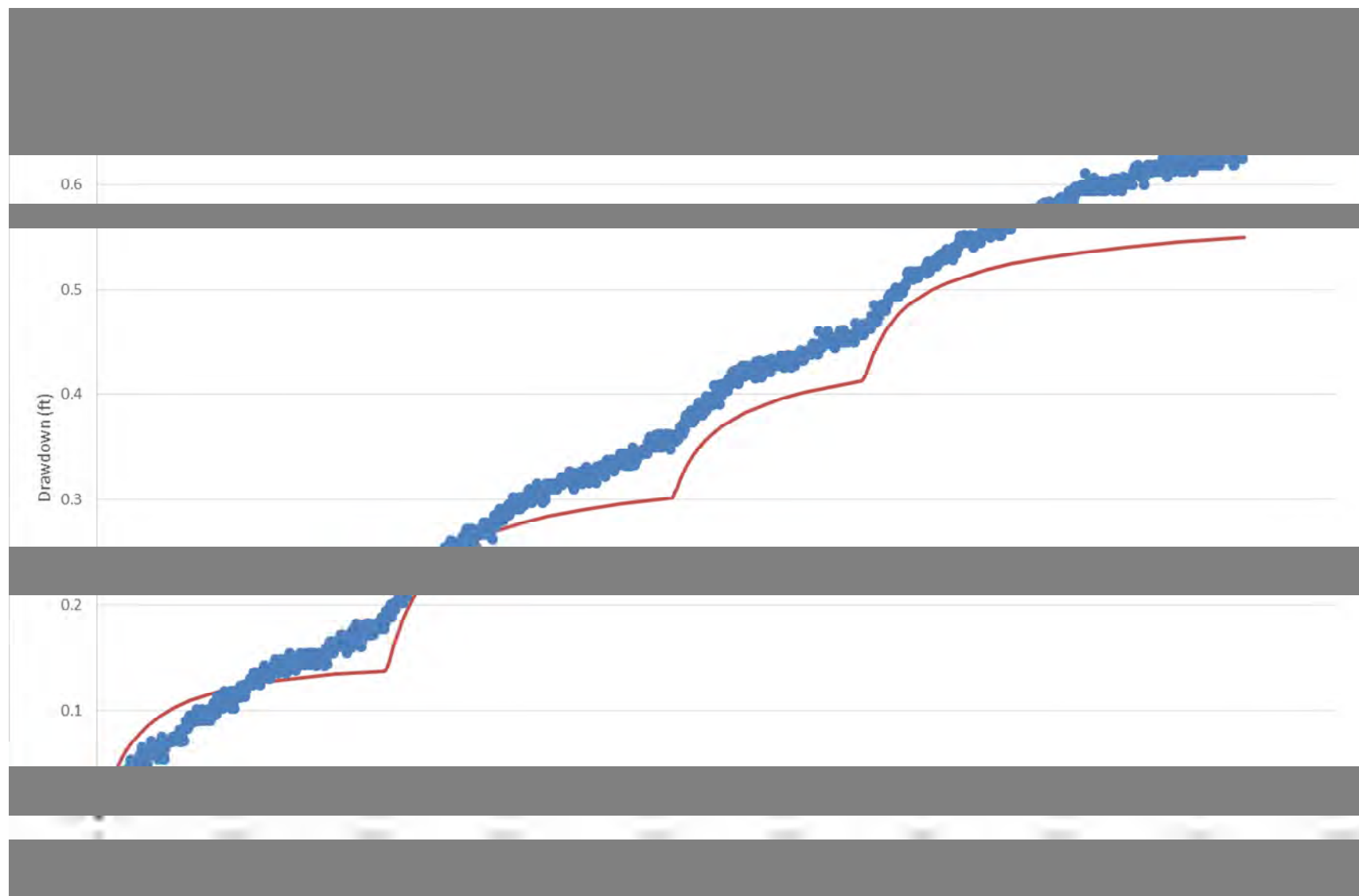


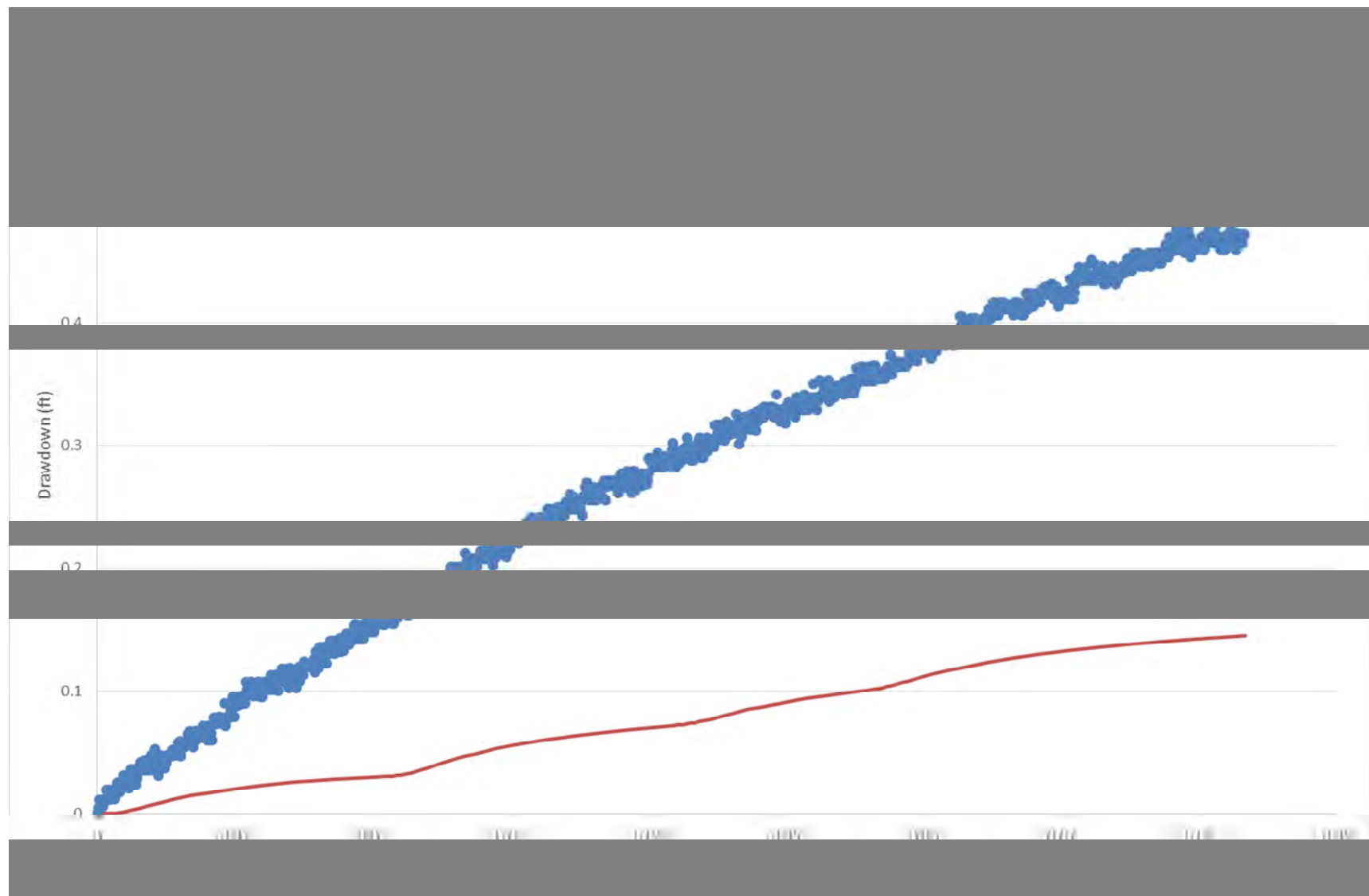








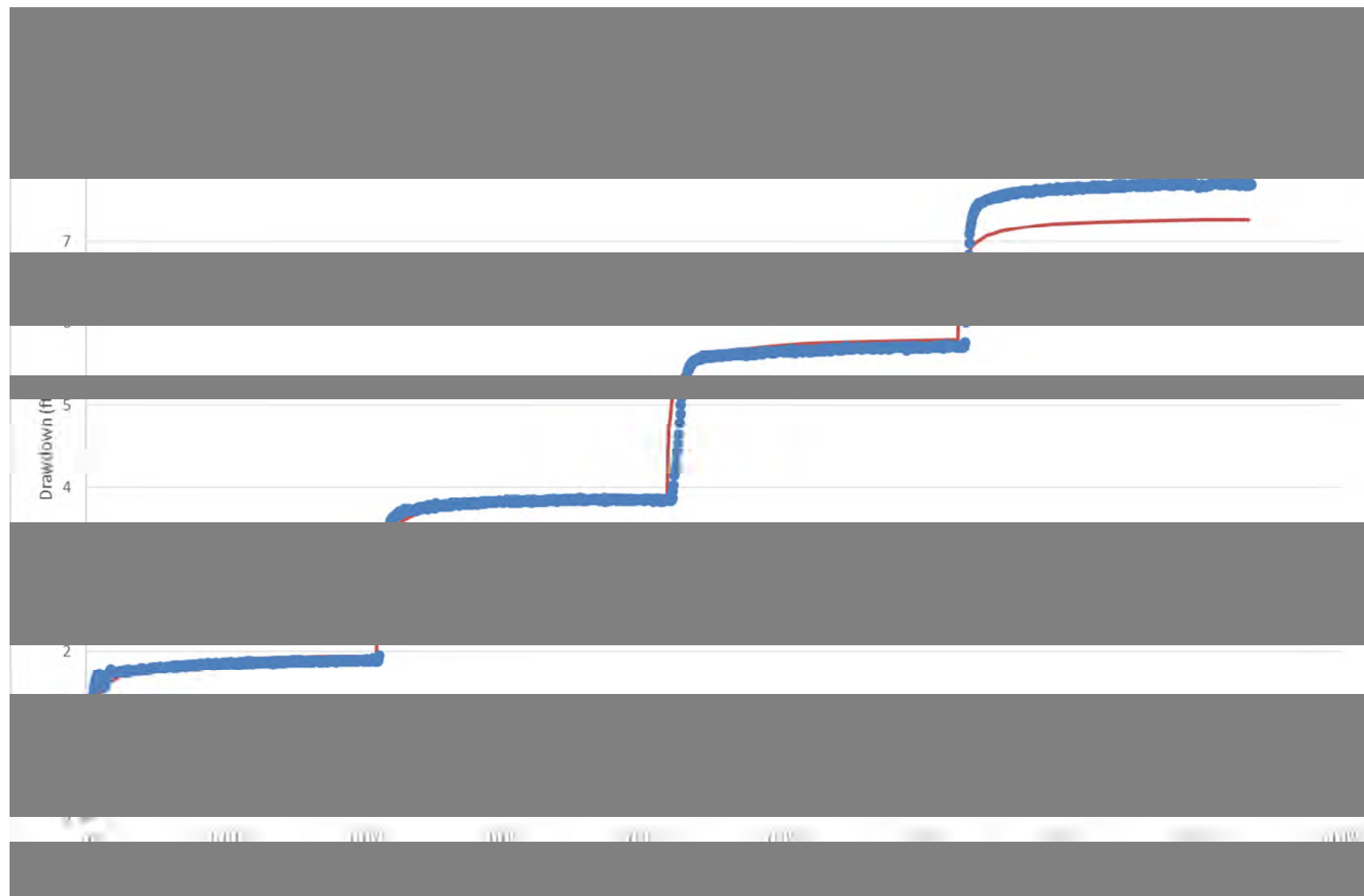


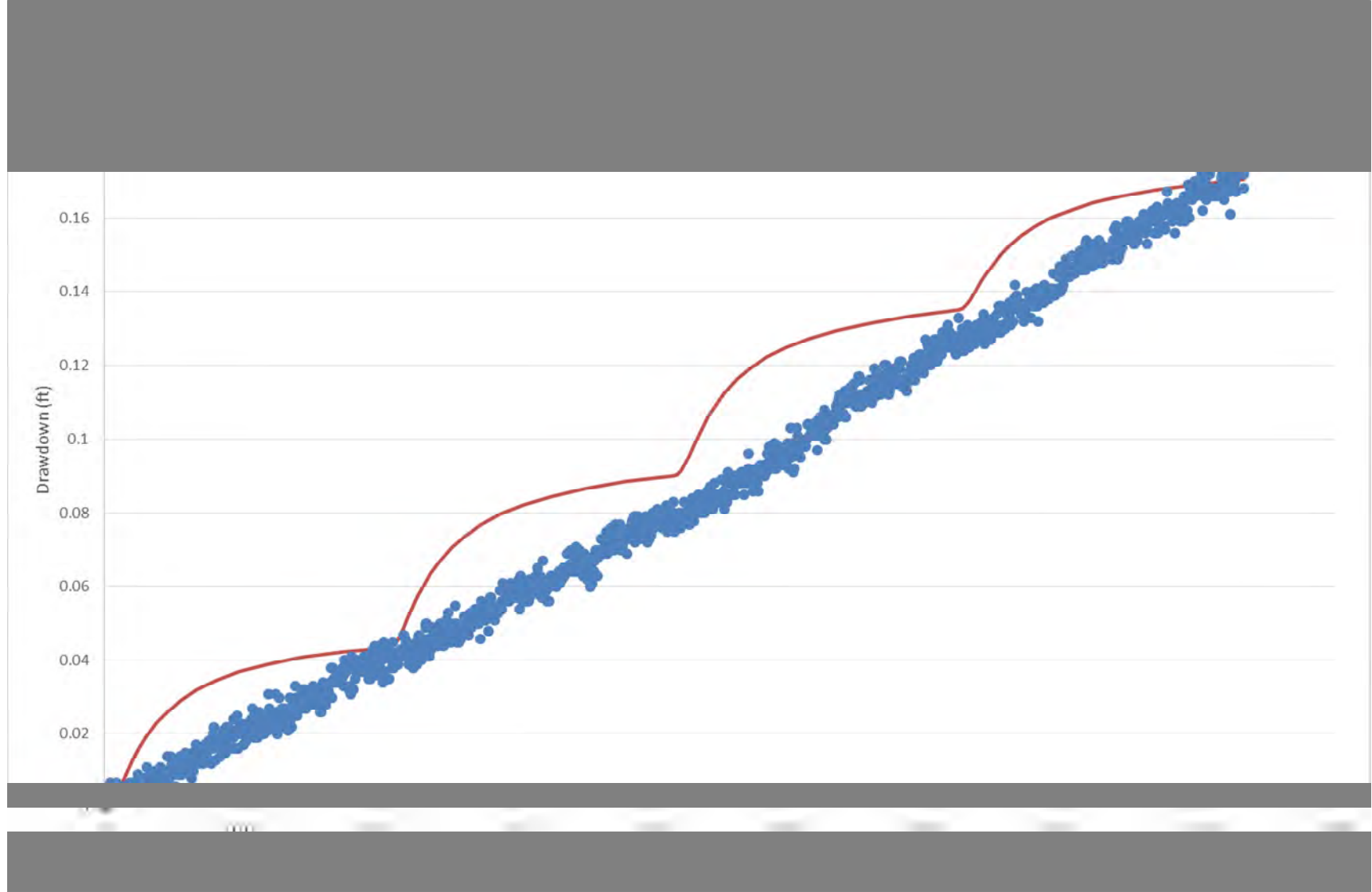


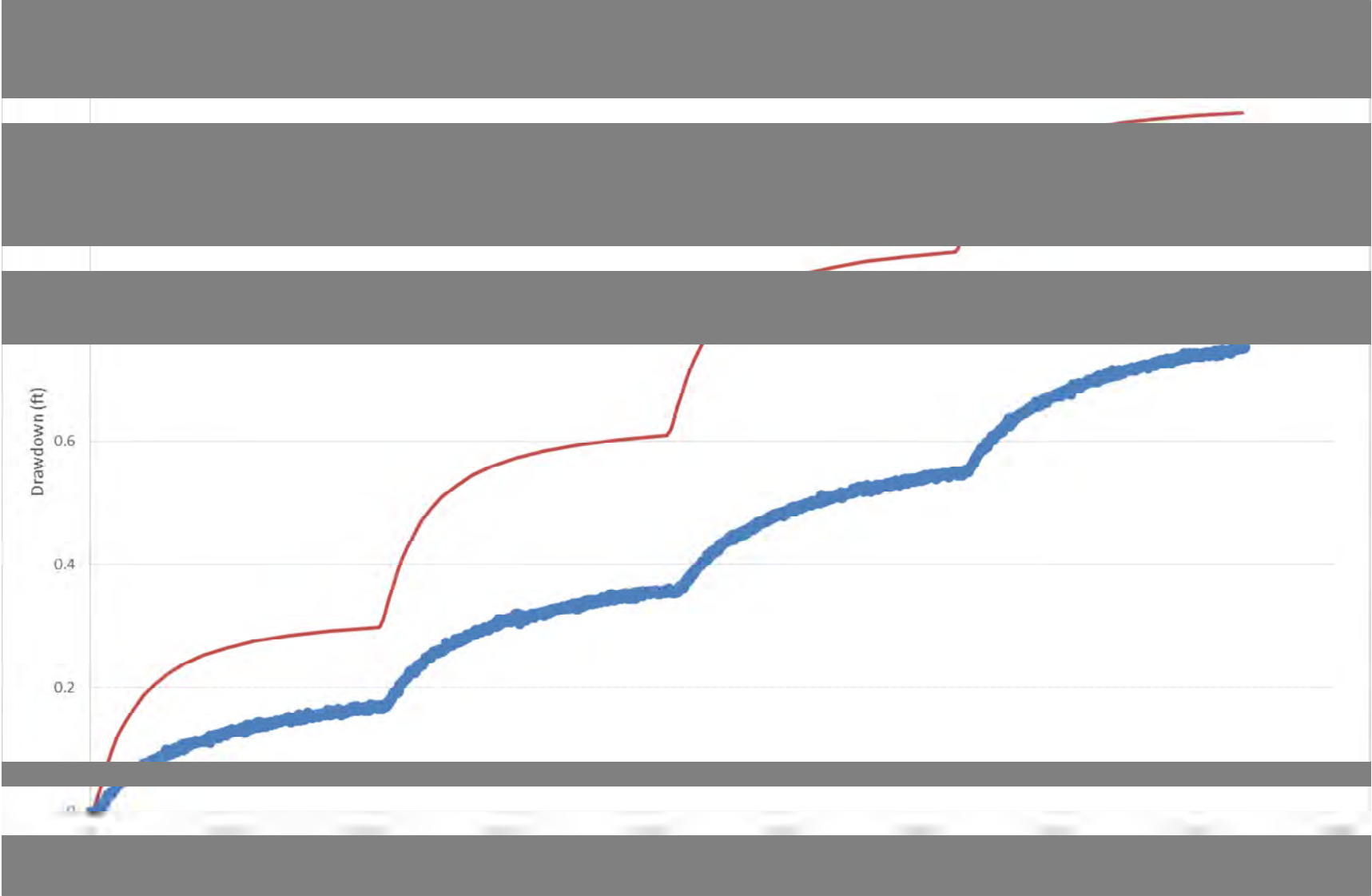


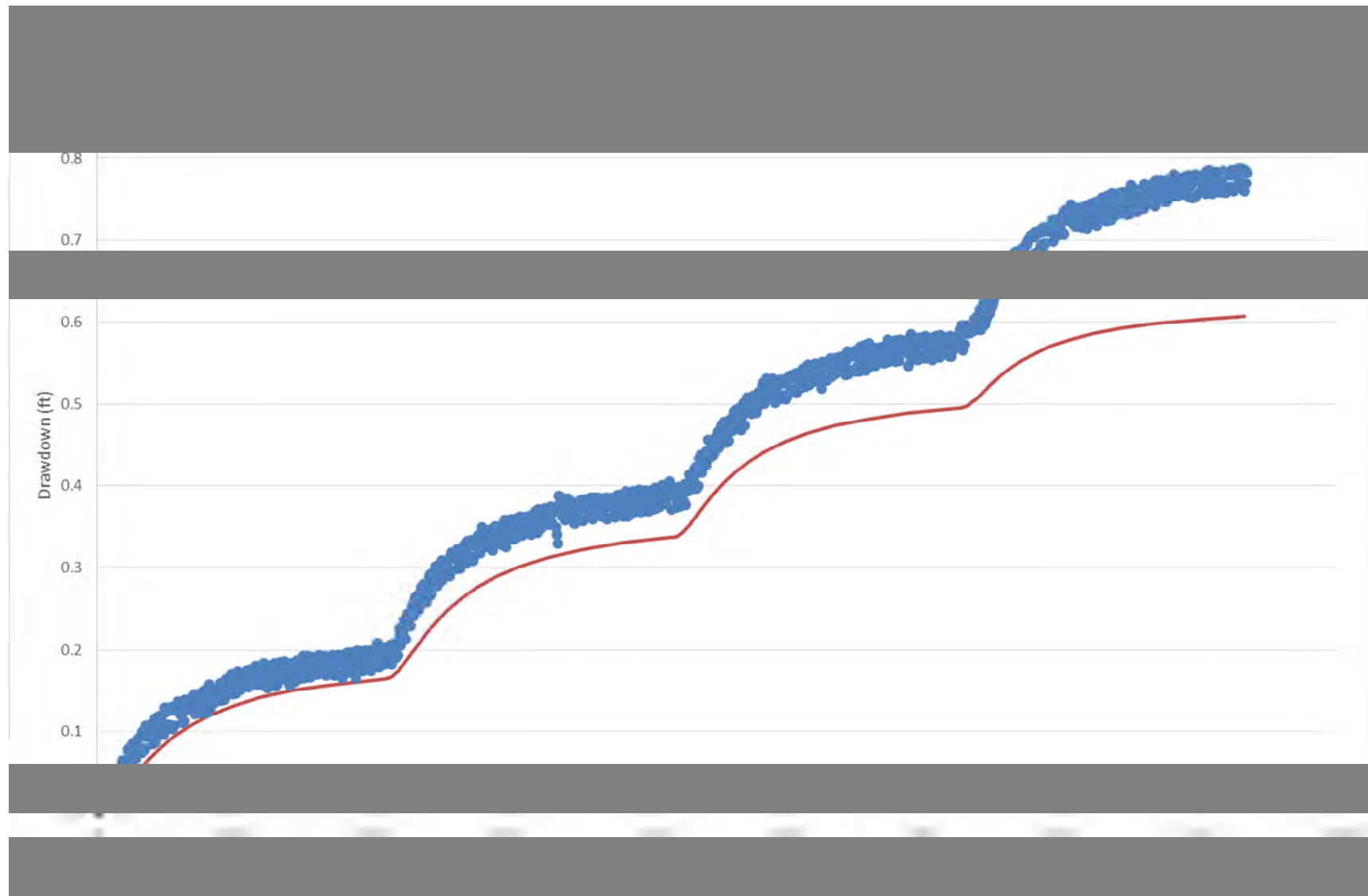
## Step-Drawdown Test F

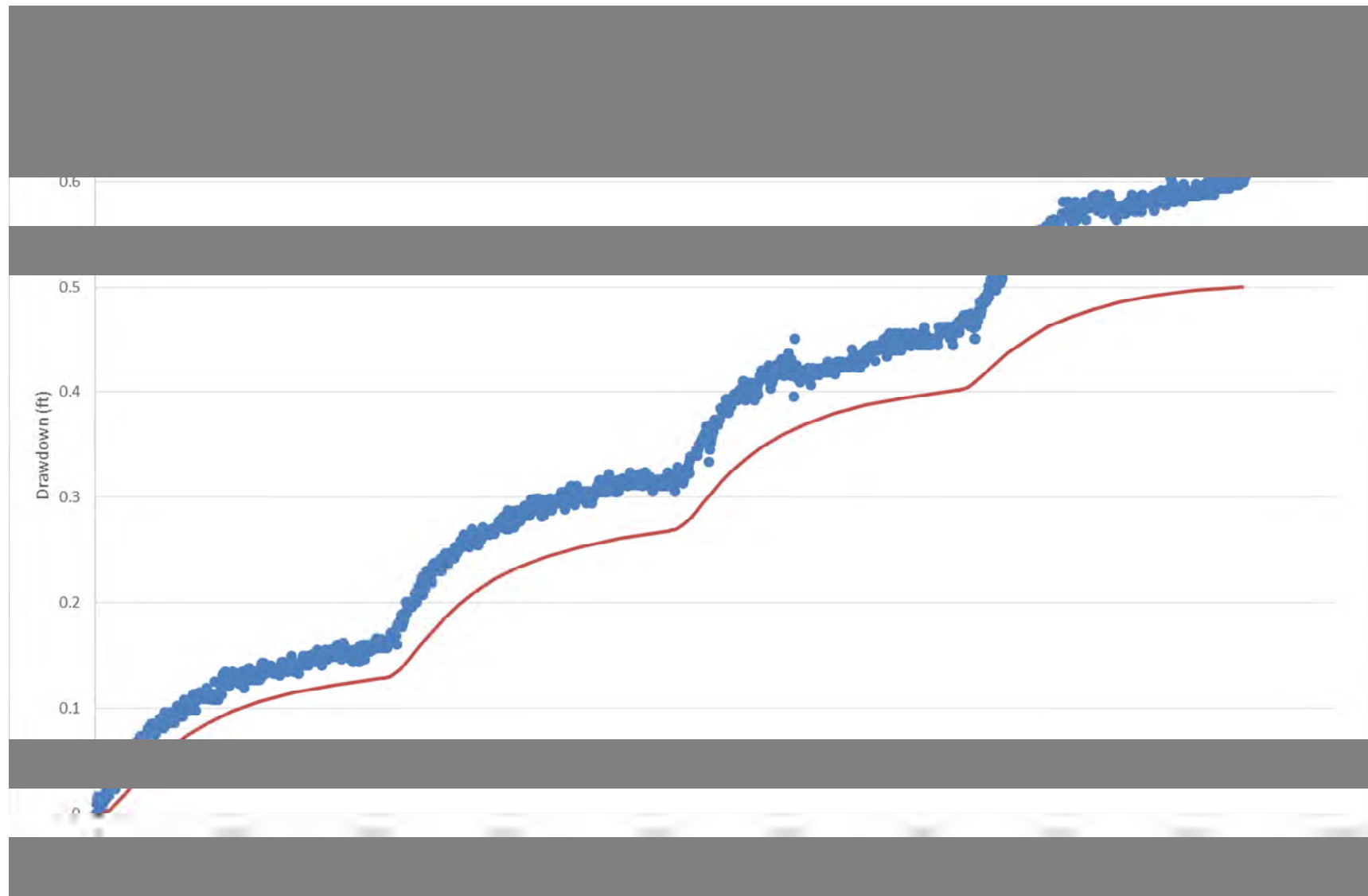
EW-11I Step Test	Average Rate (gpm)
Step 1	7.15
Step 2	14.27
Step 3	21.00
Step 4	26.60

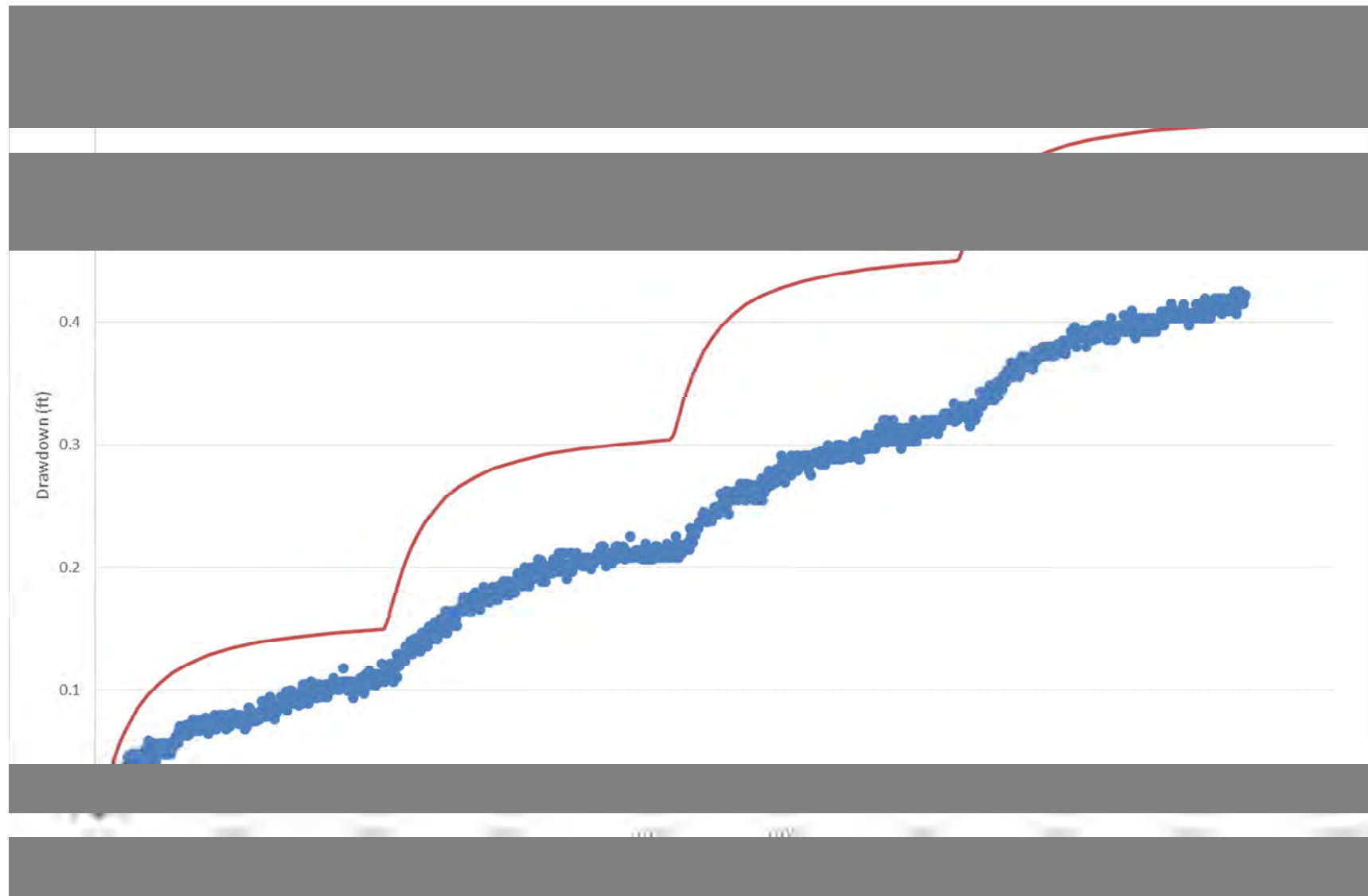


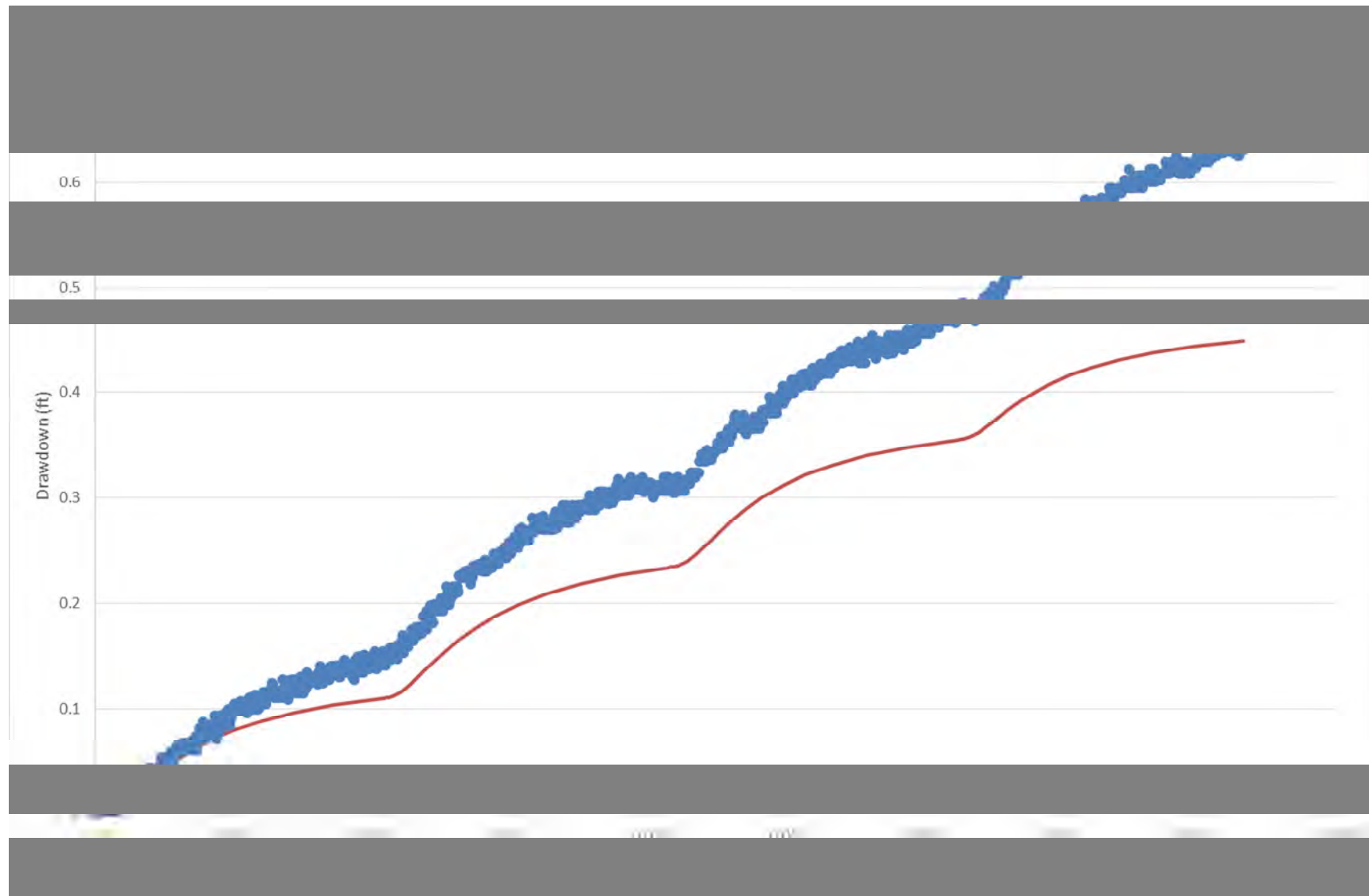






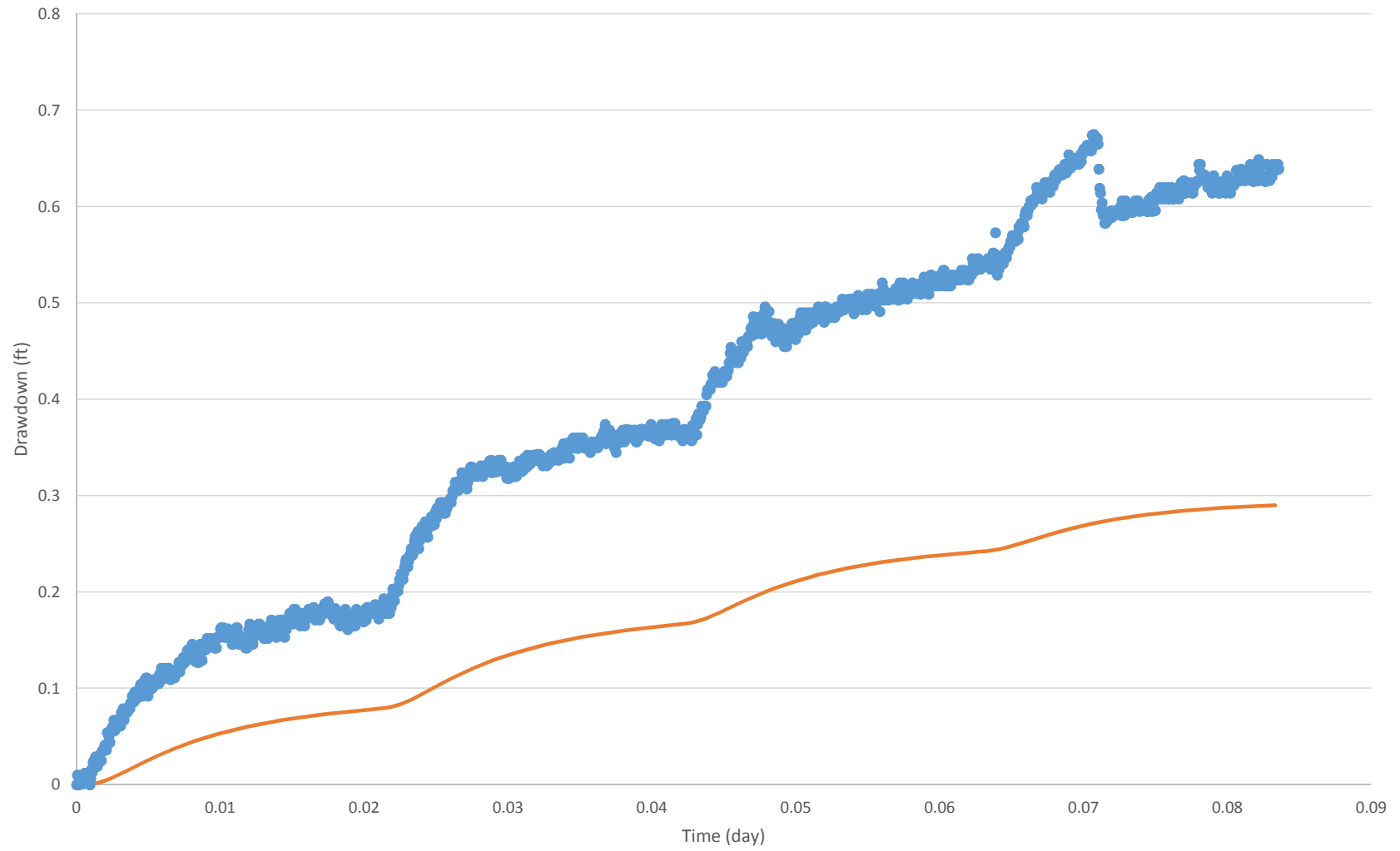


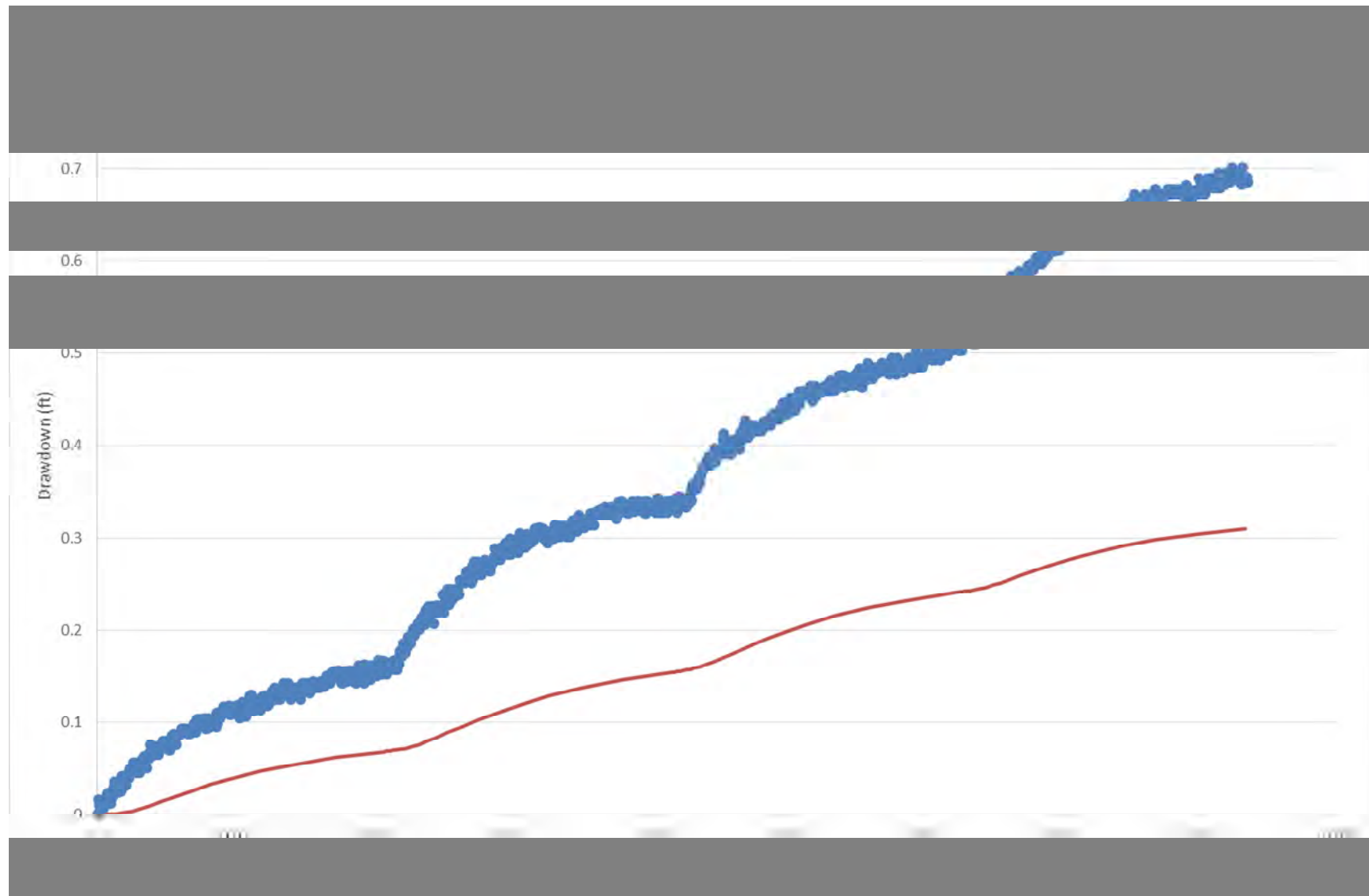






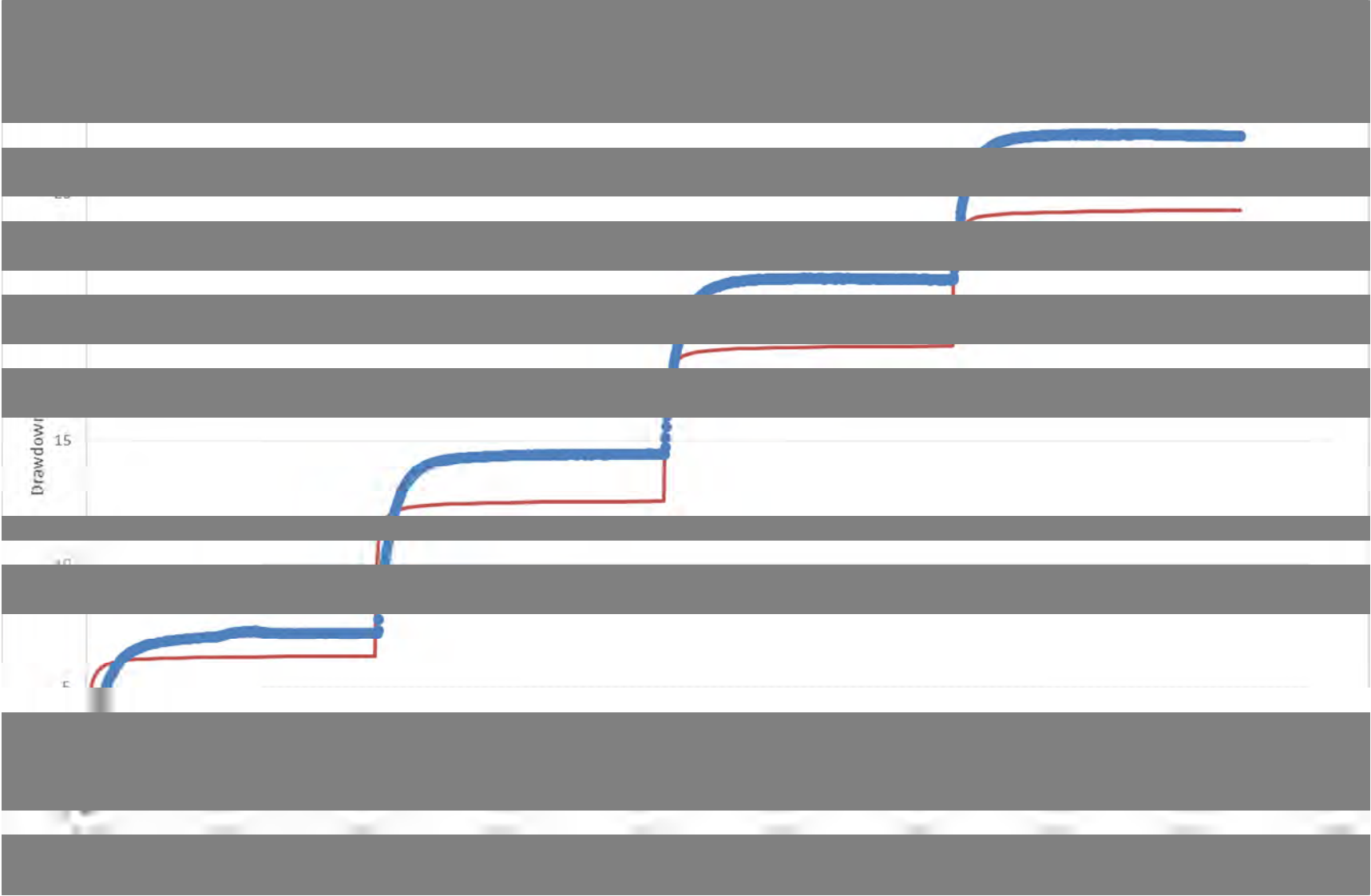
EW-13I

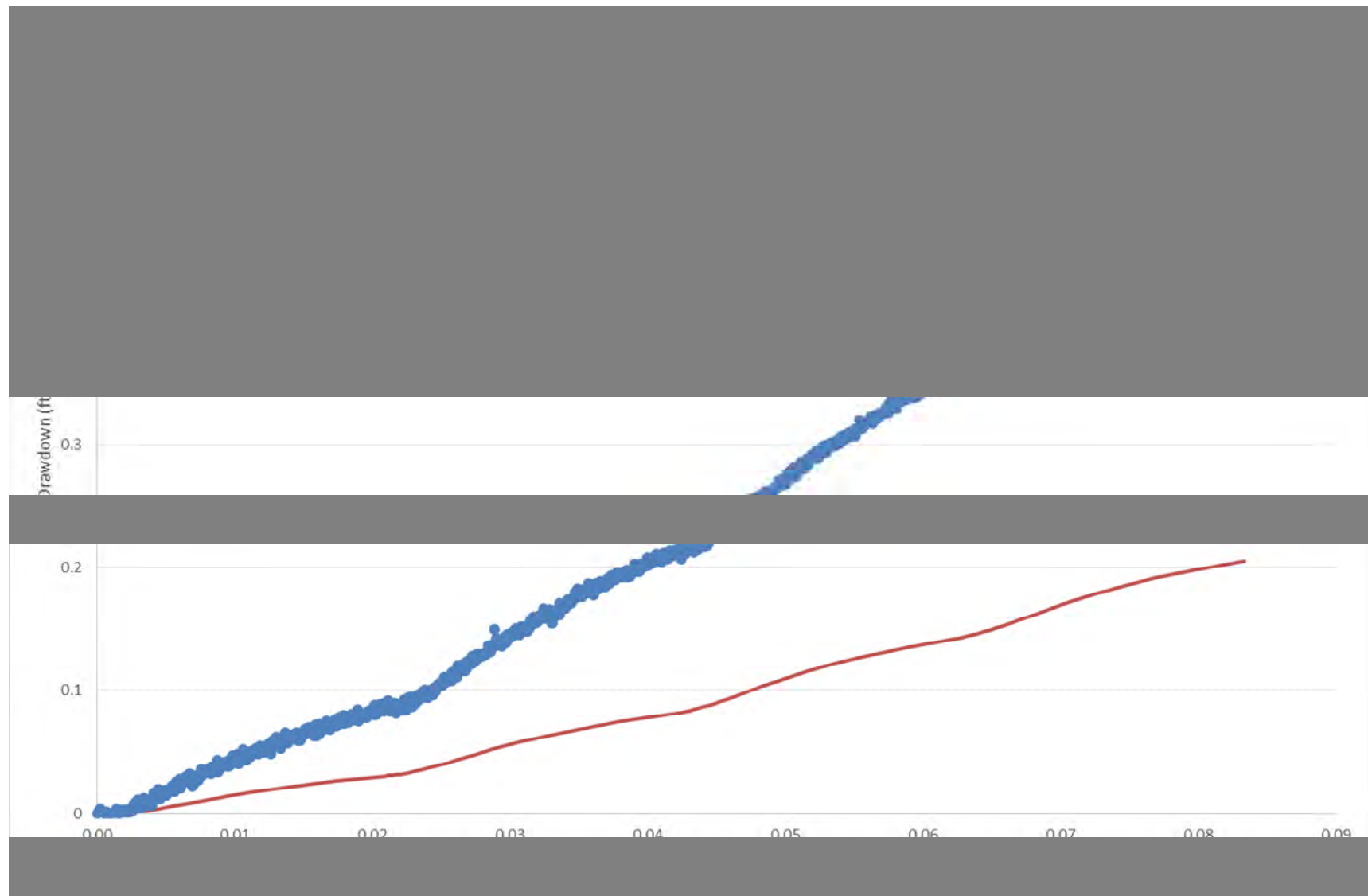


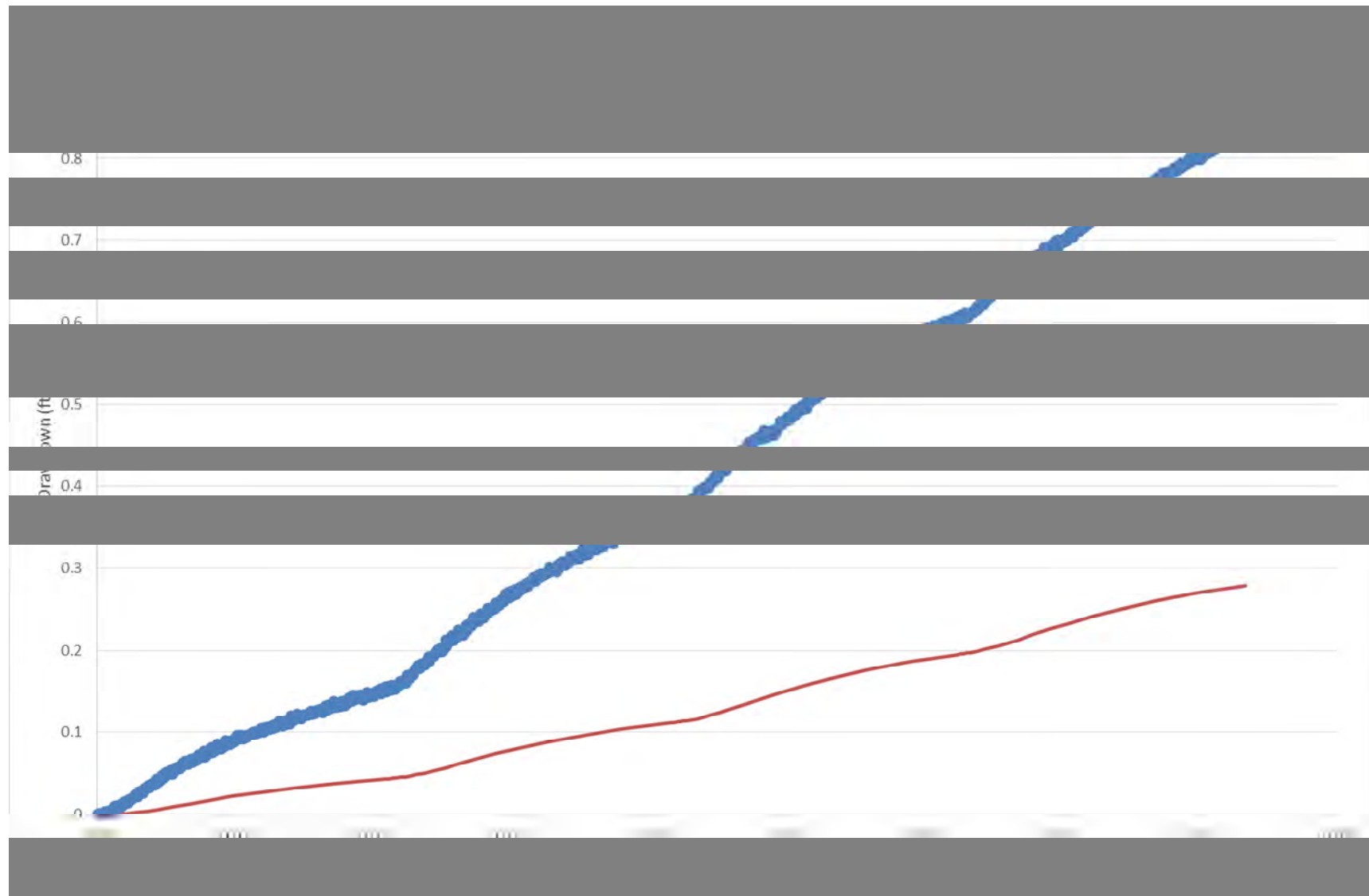


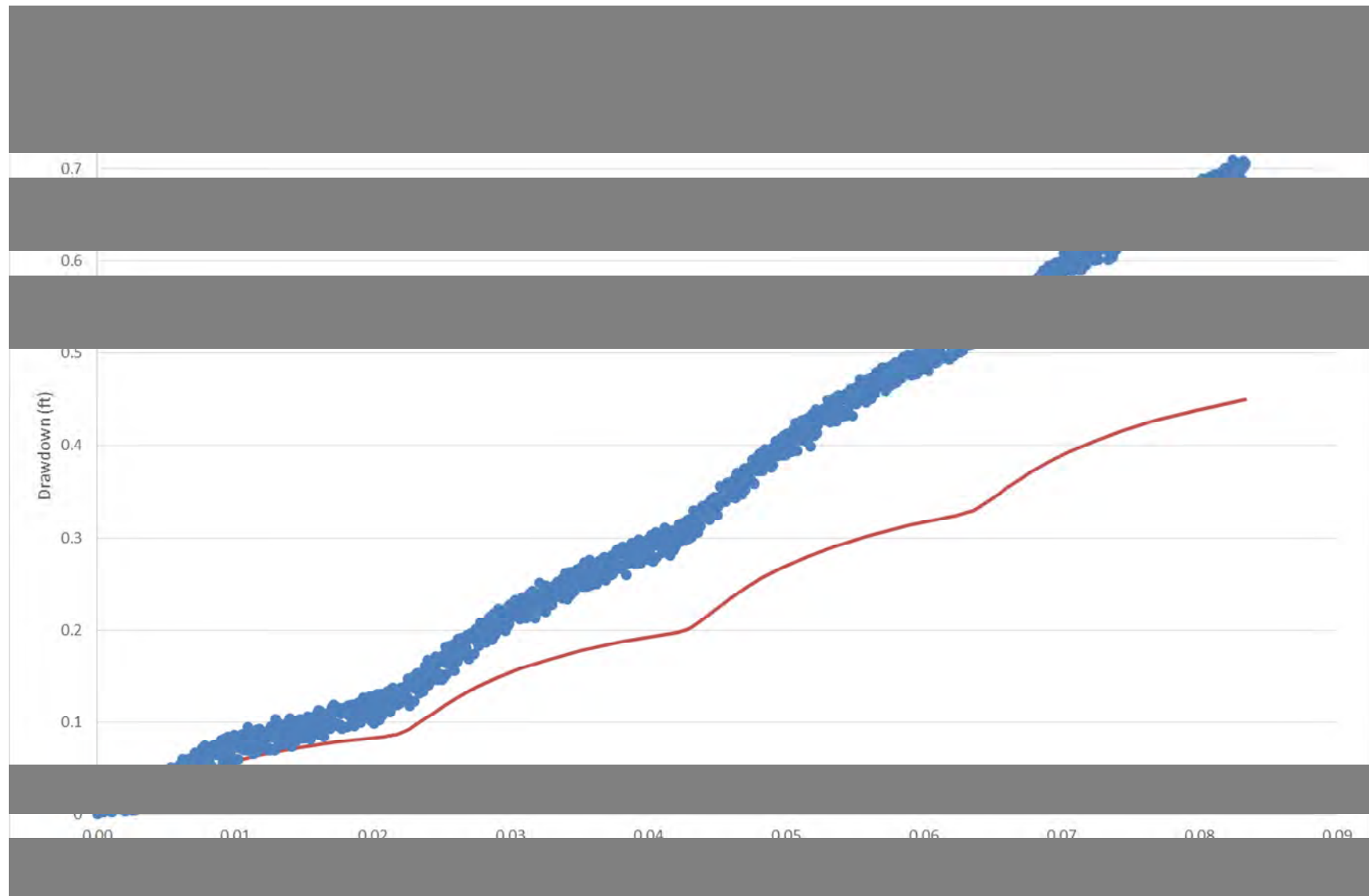
## Step-Drawdown Test G

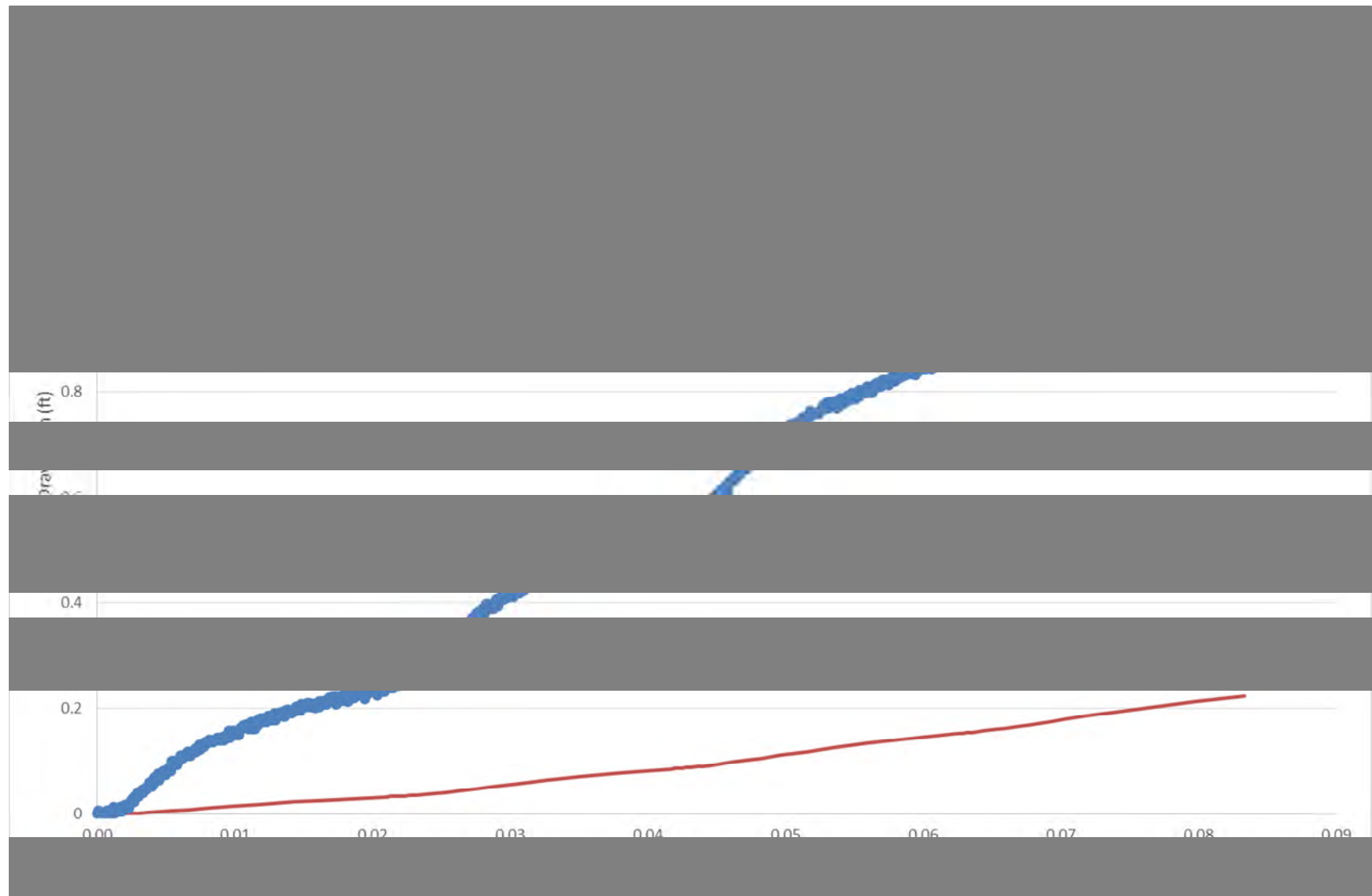
EW-12D Step Test	Average Rate (gpm)
Step 1	7.04
Step 2	14.05
Step 3	21.07
Step 4	27.20



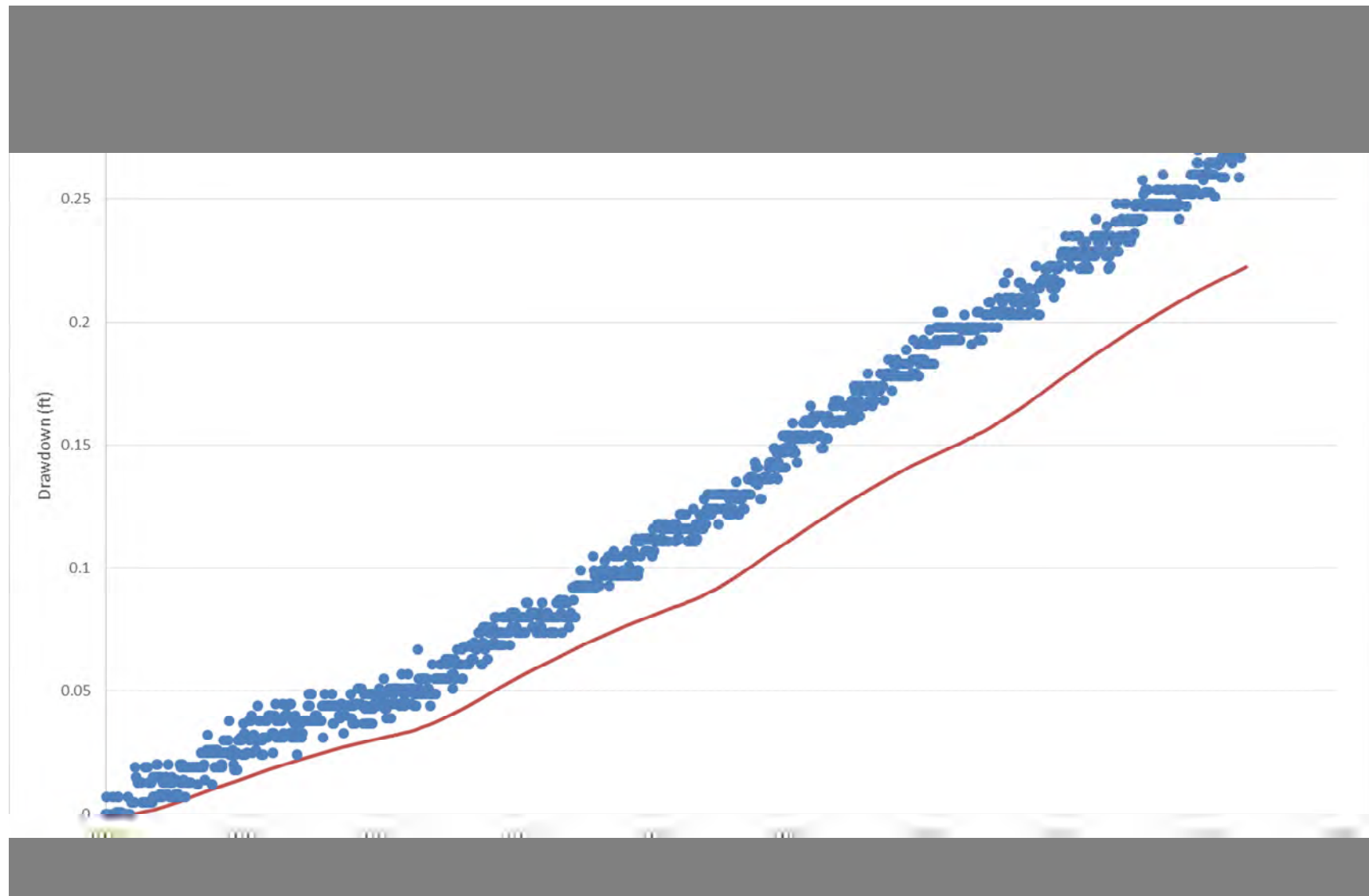


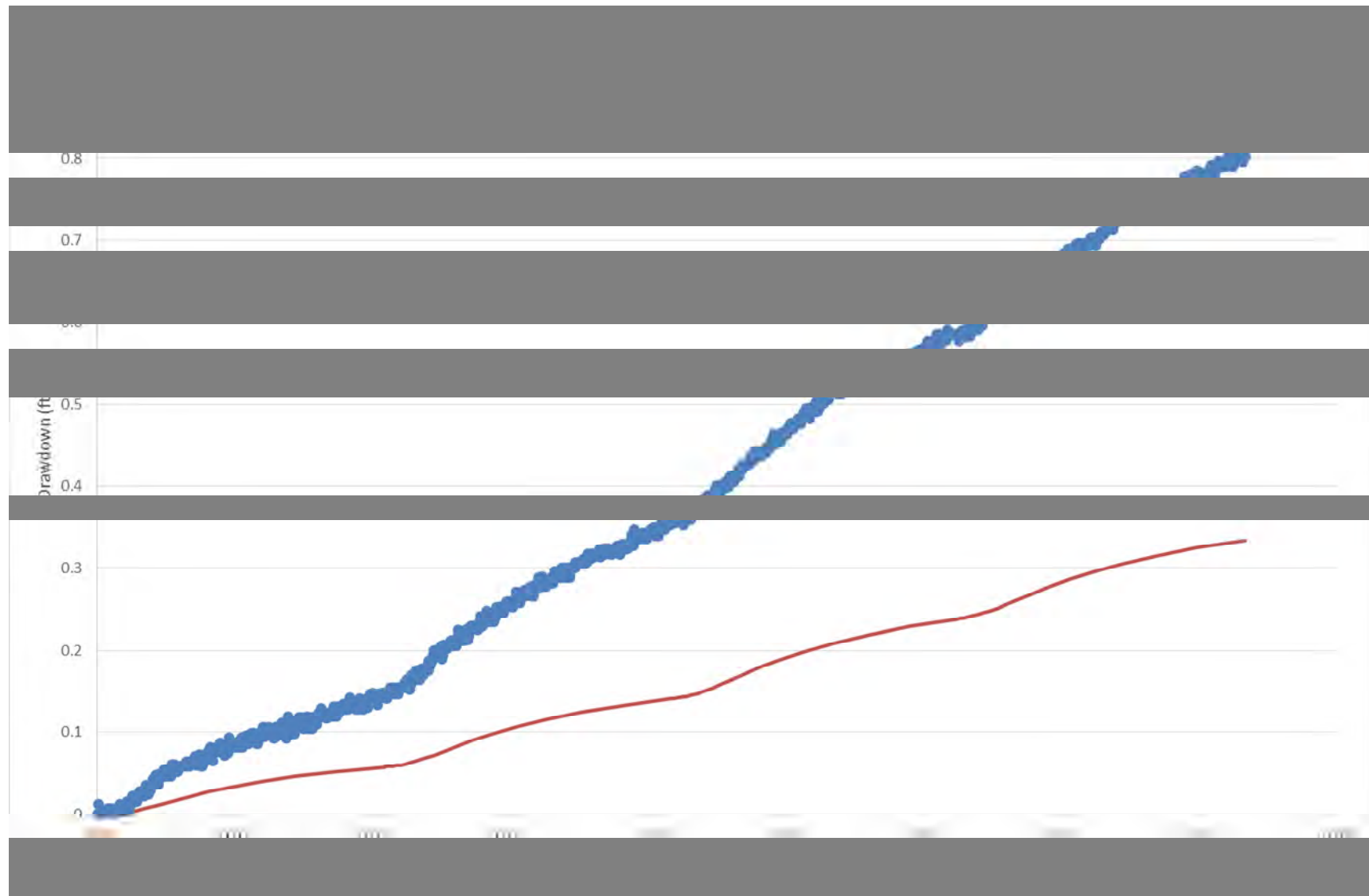


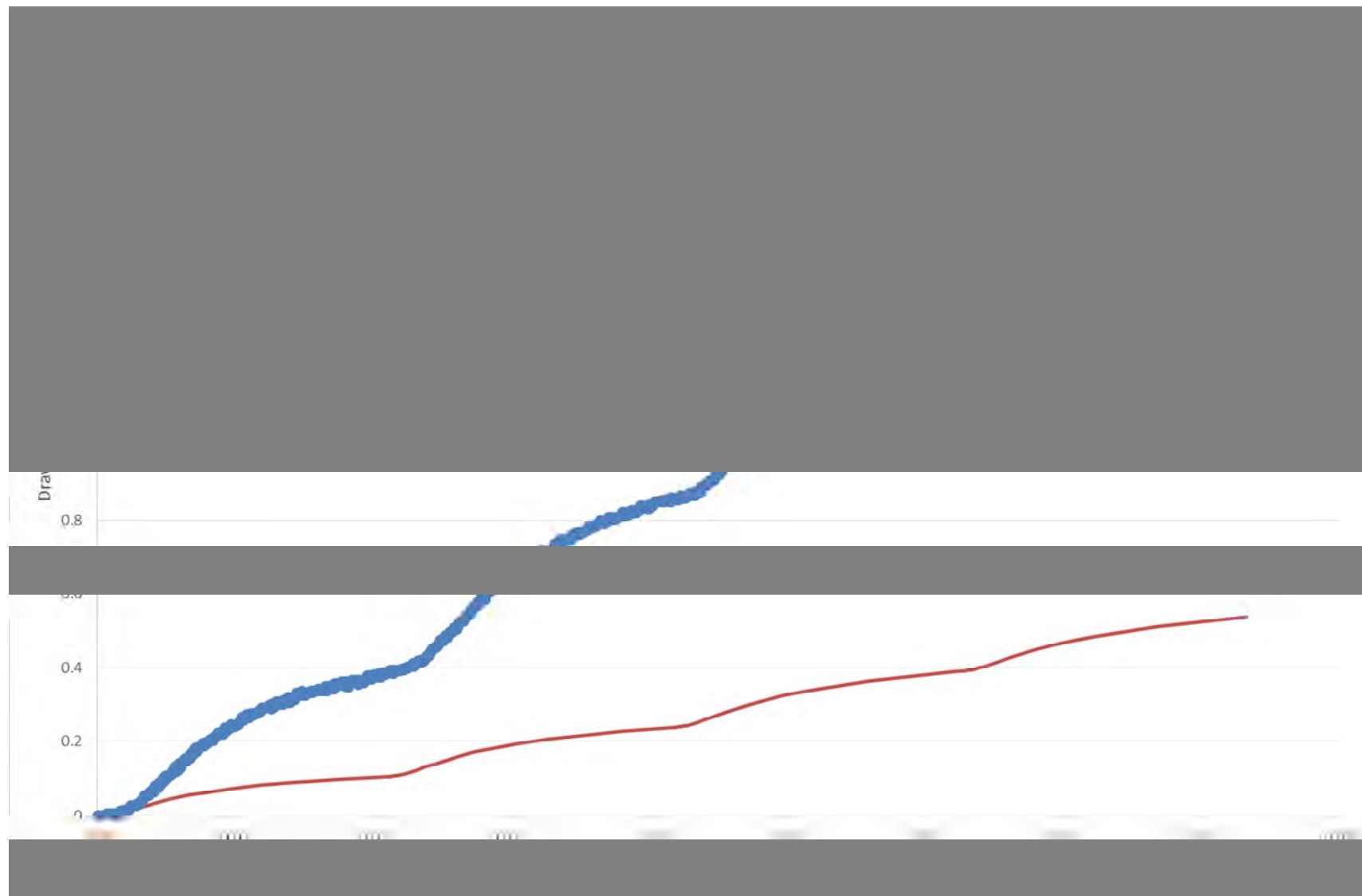






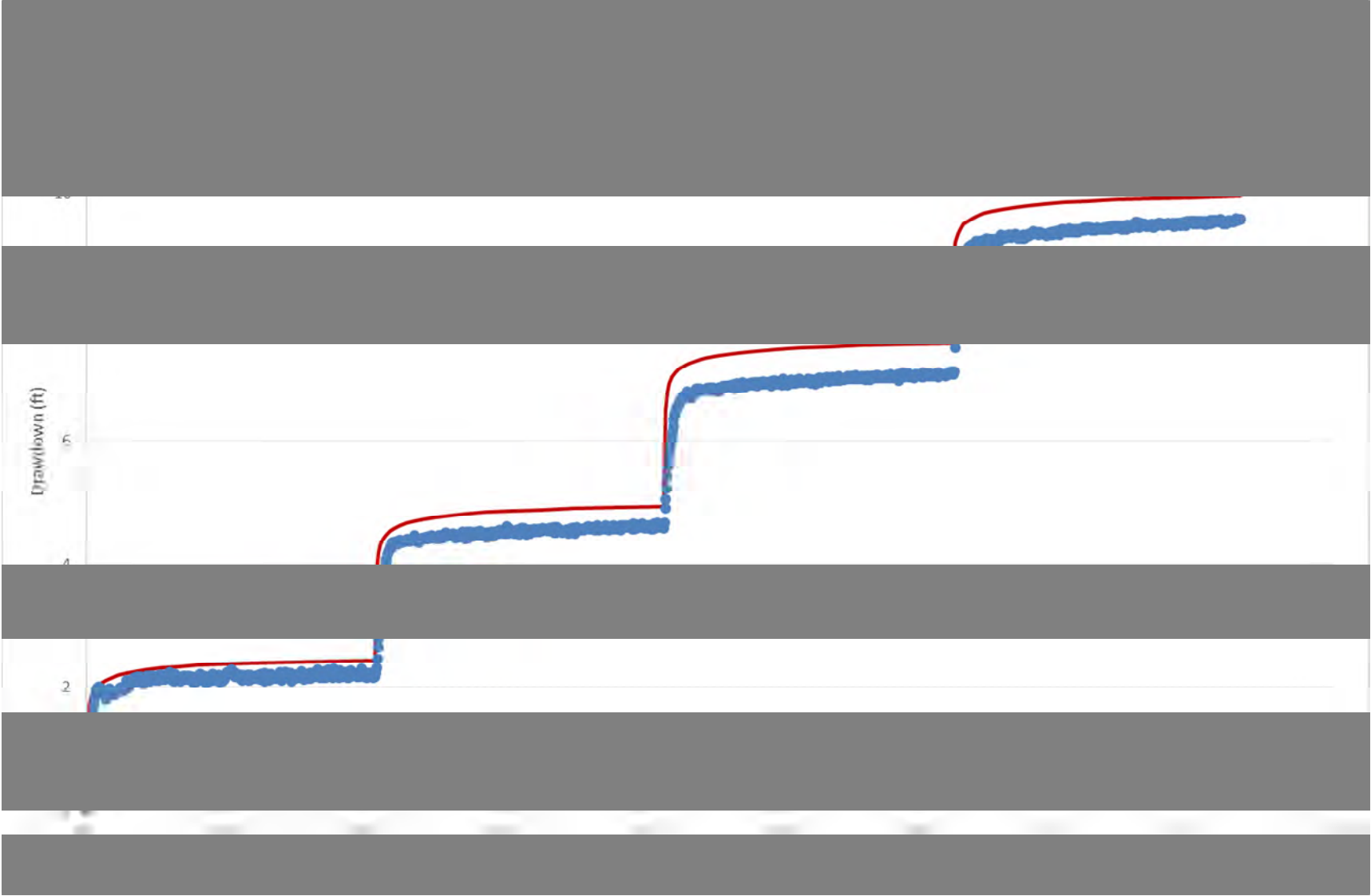


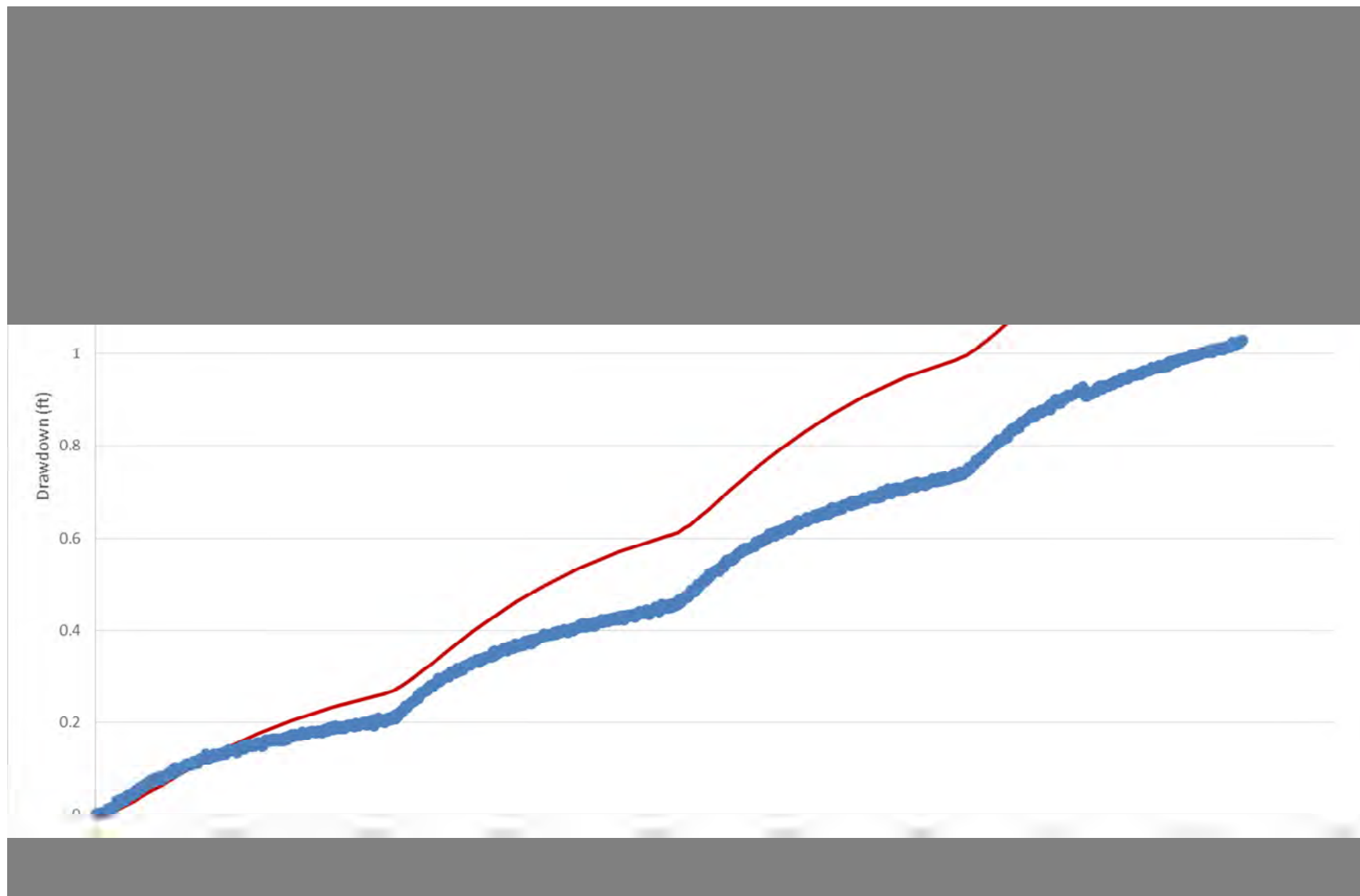


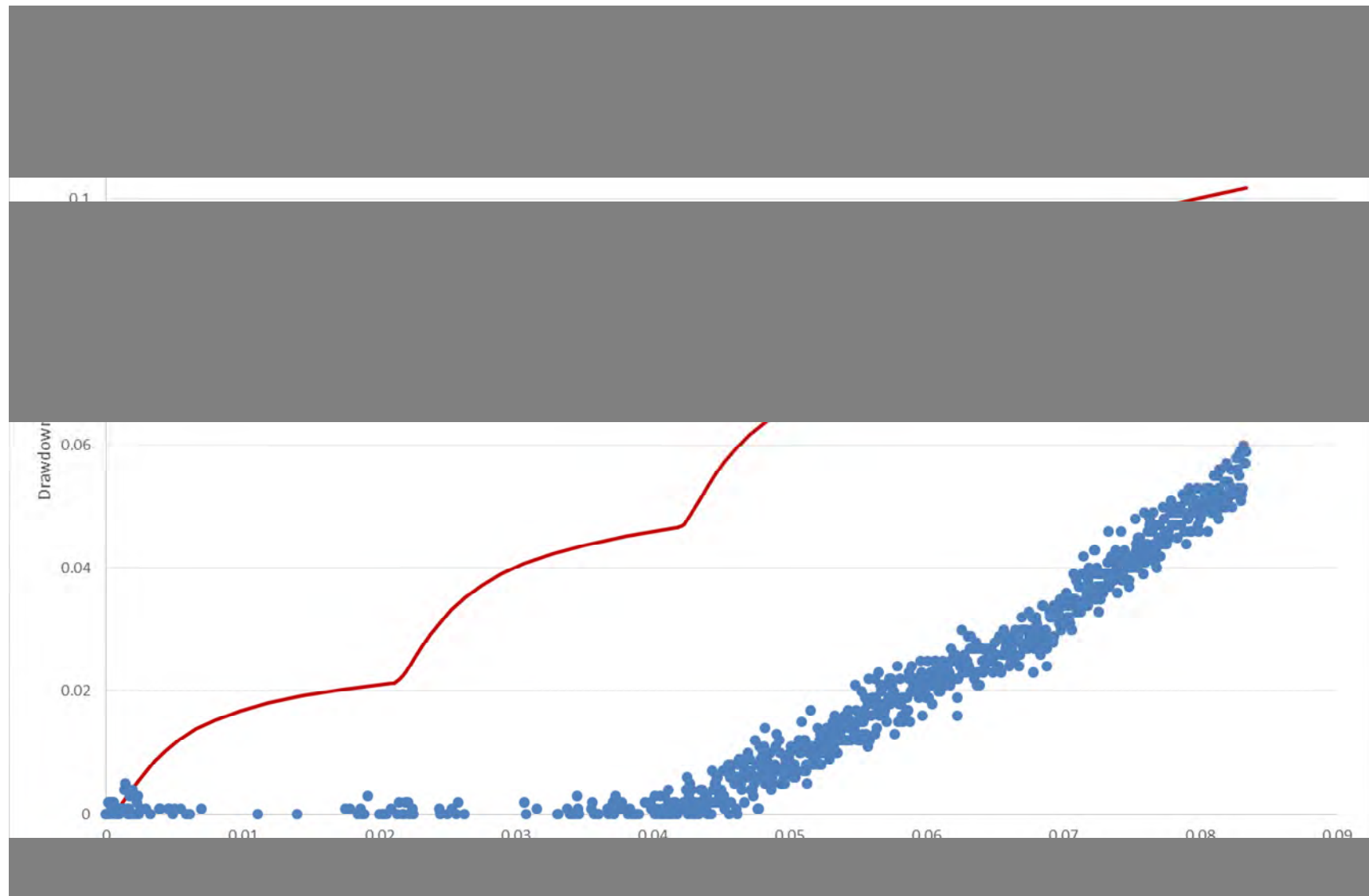


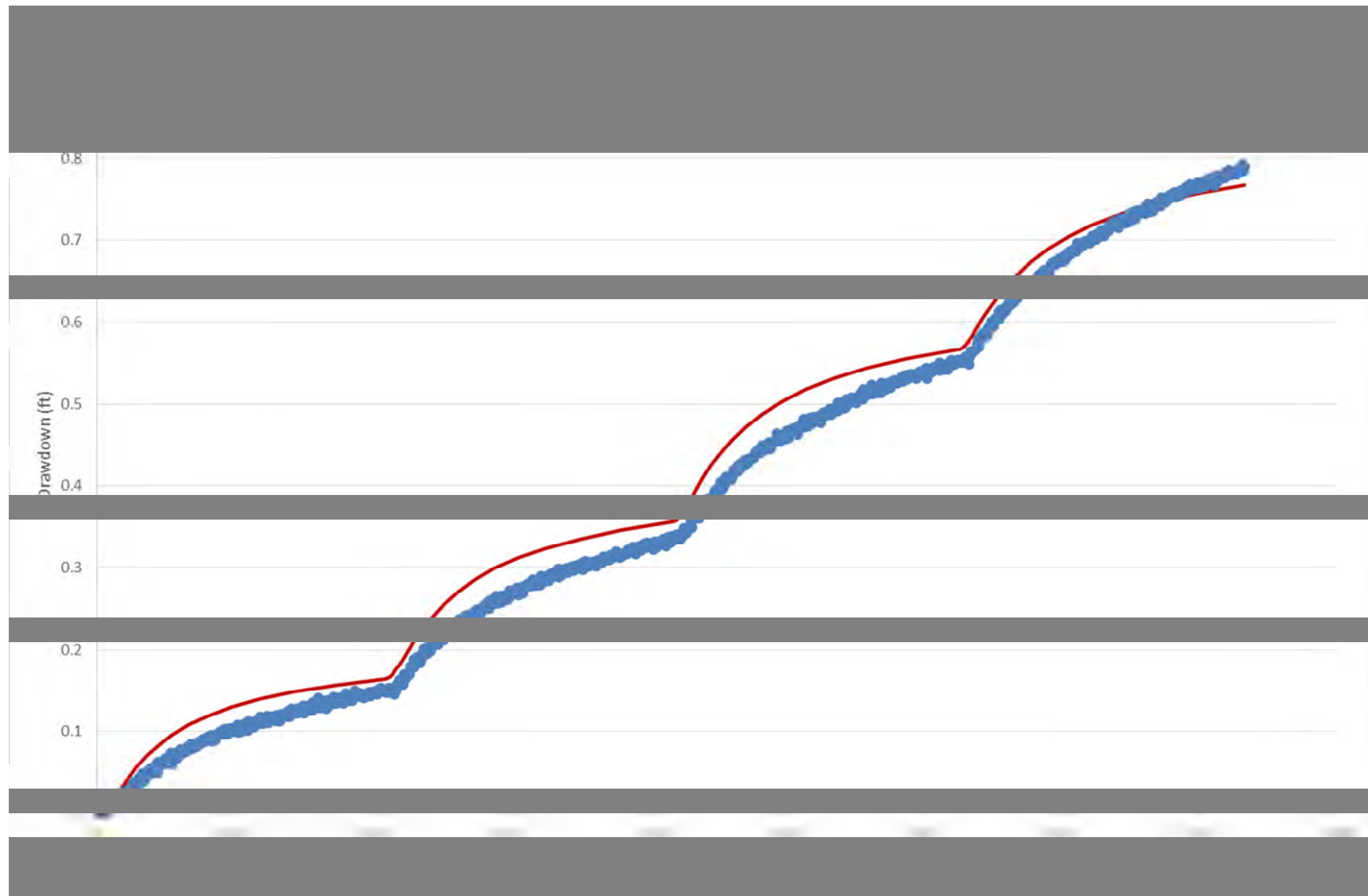
## Step-Drawdown Test H

EW-9I Step Test	Average Rate (gpm)
Step 1	7.01
Step 2	14.13
Step 3	21.63
Step 4	28.29

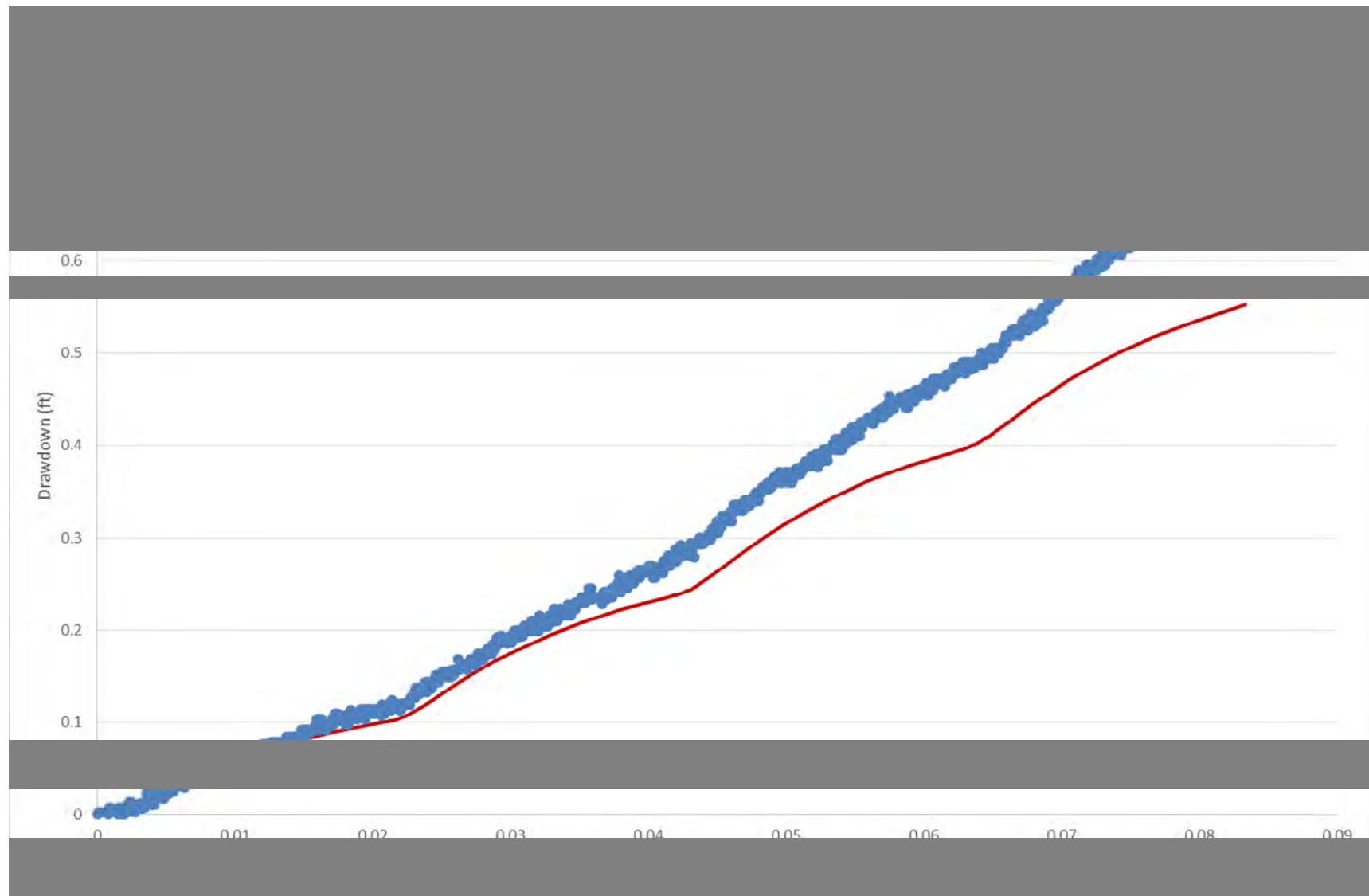


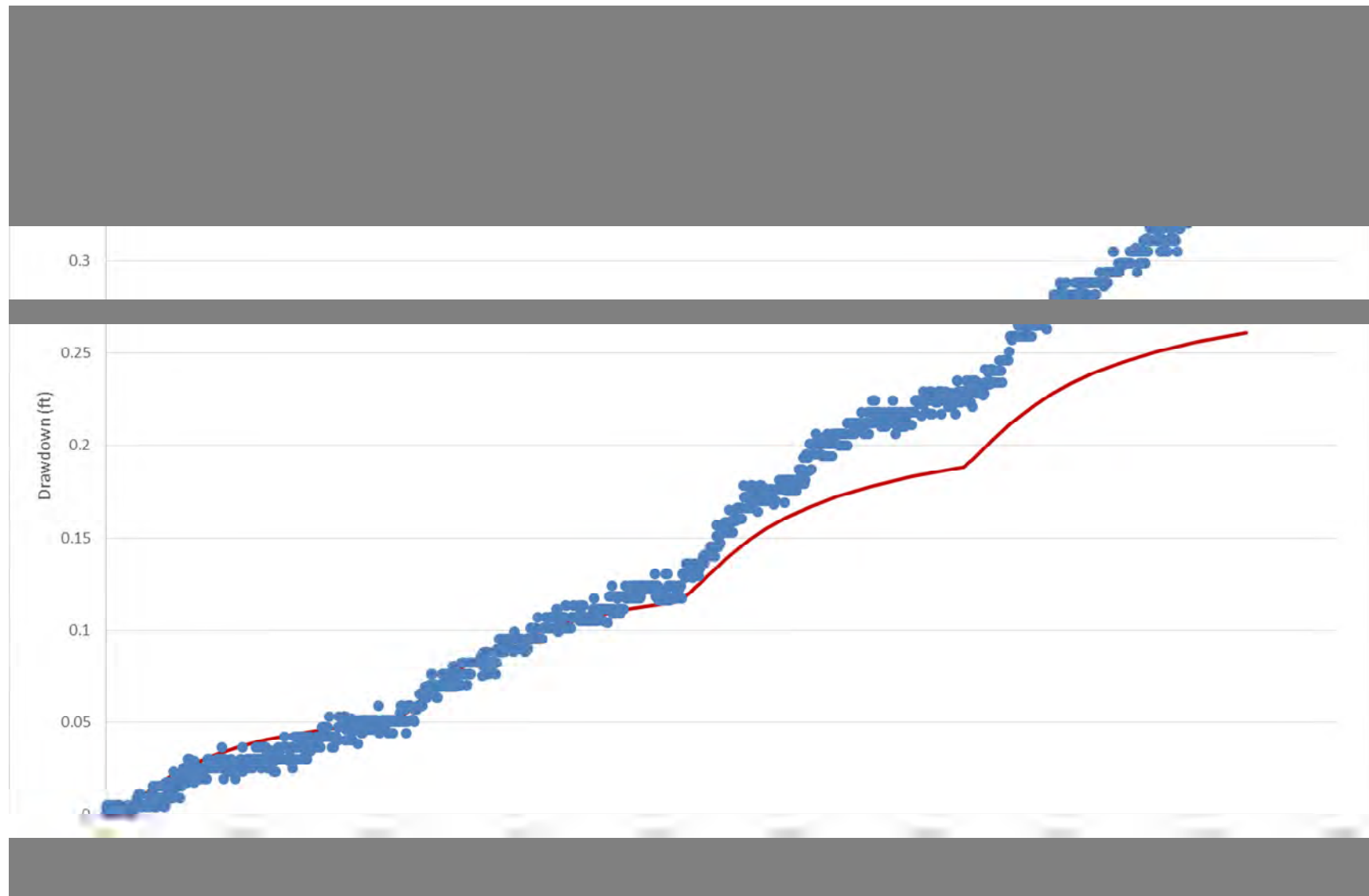


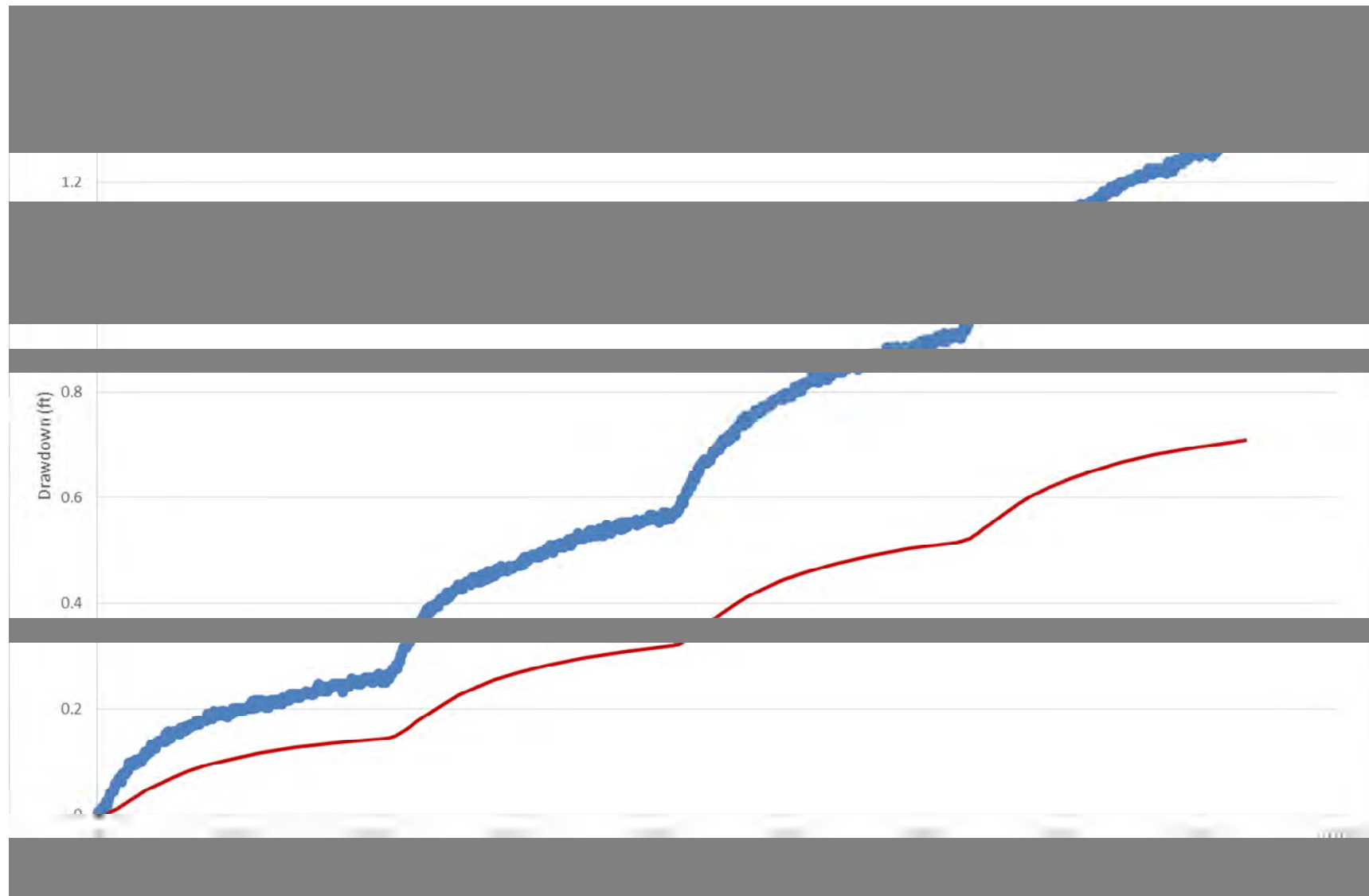






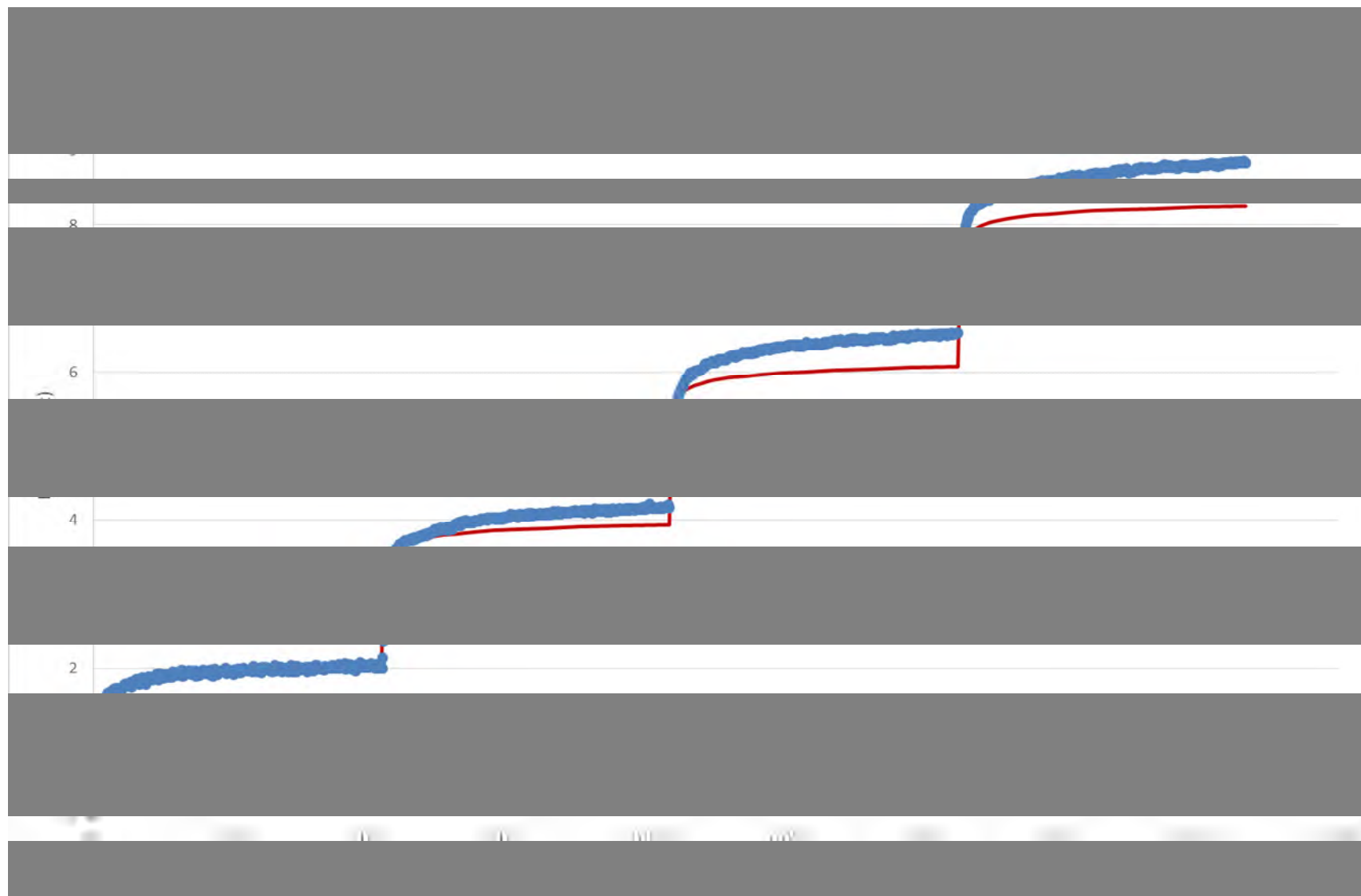


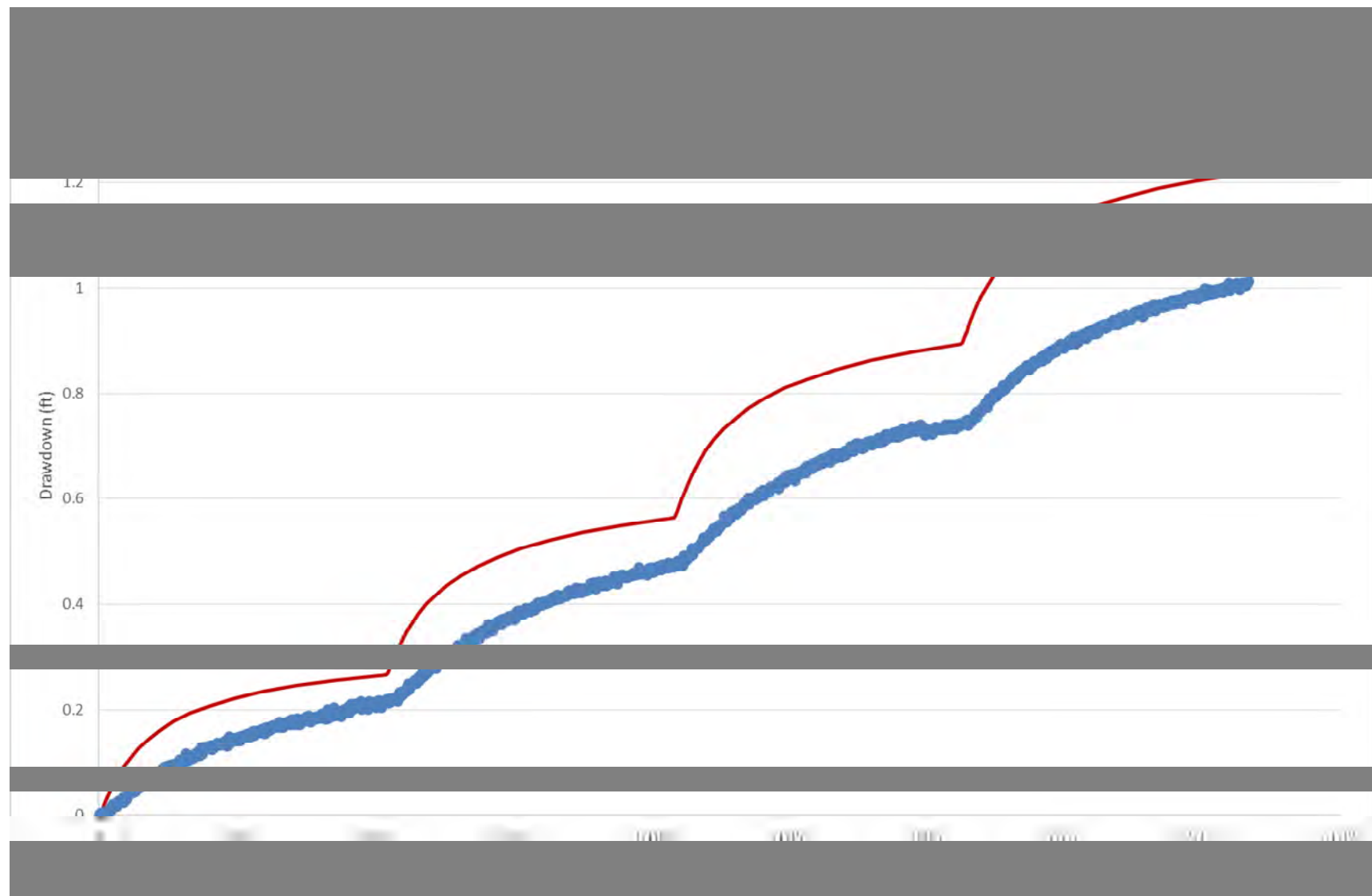


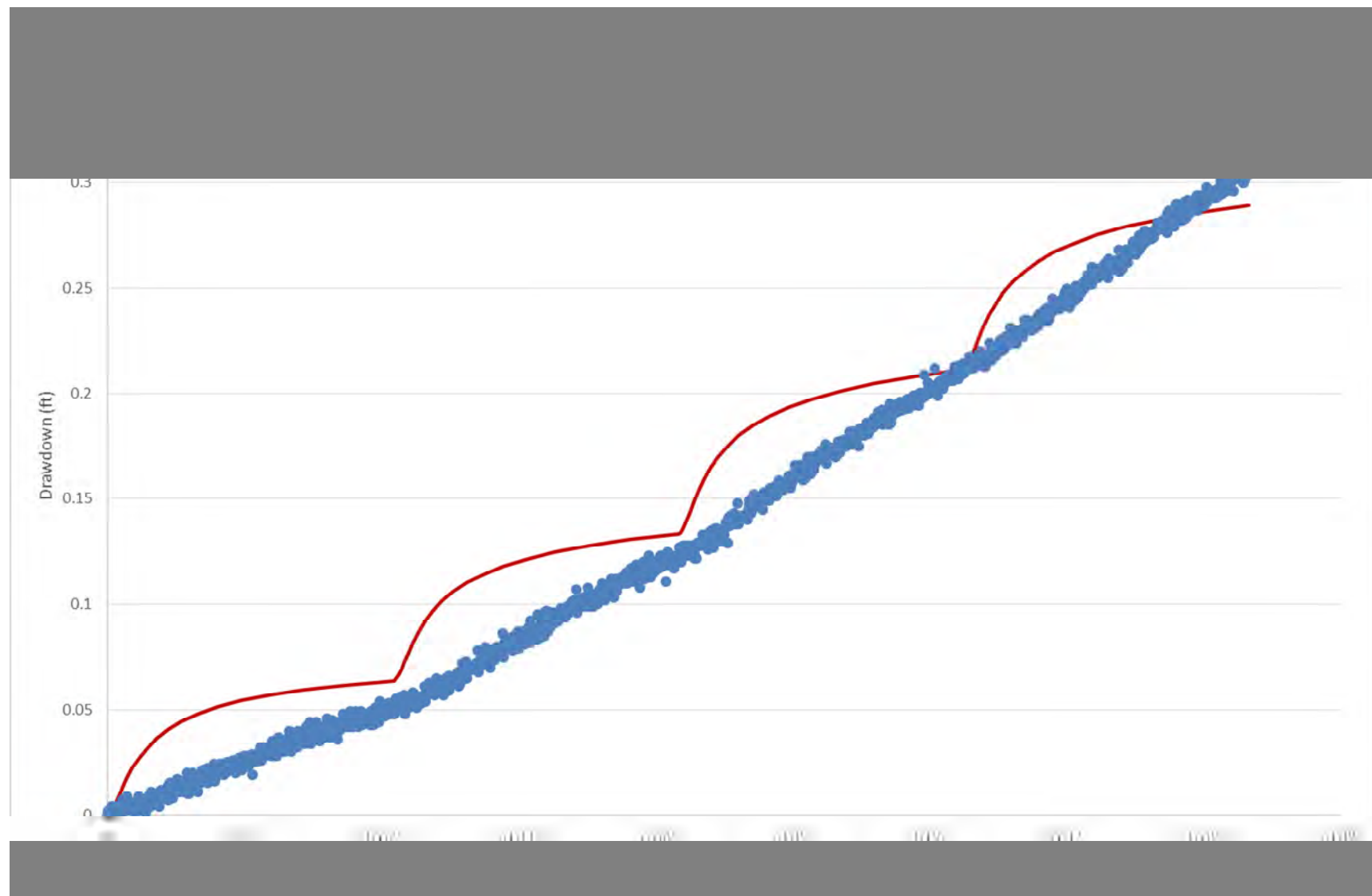


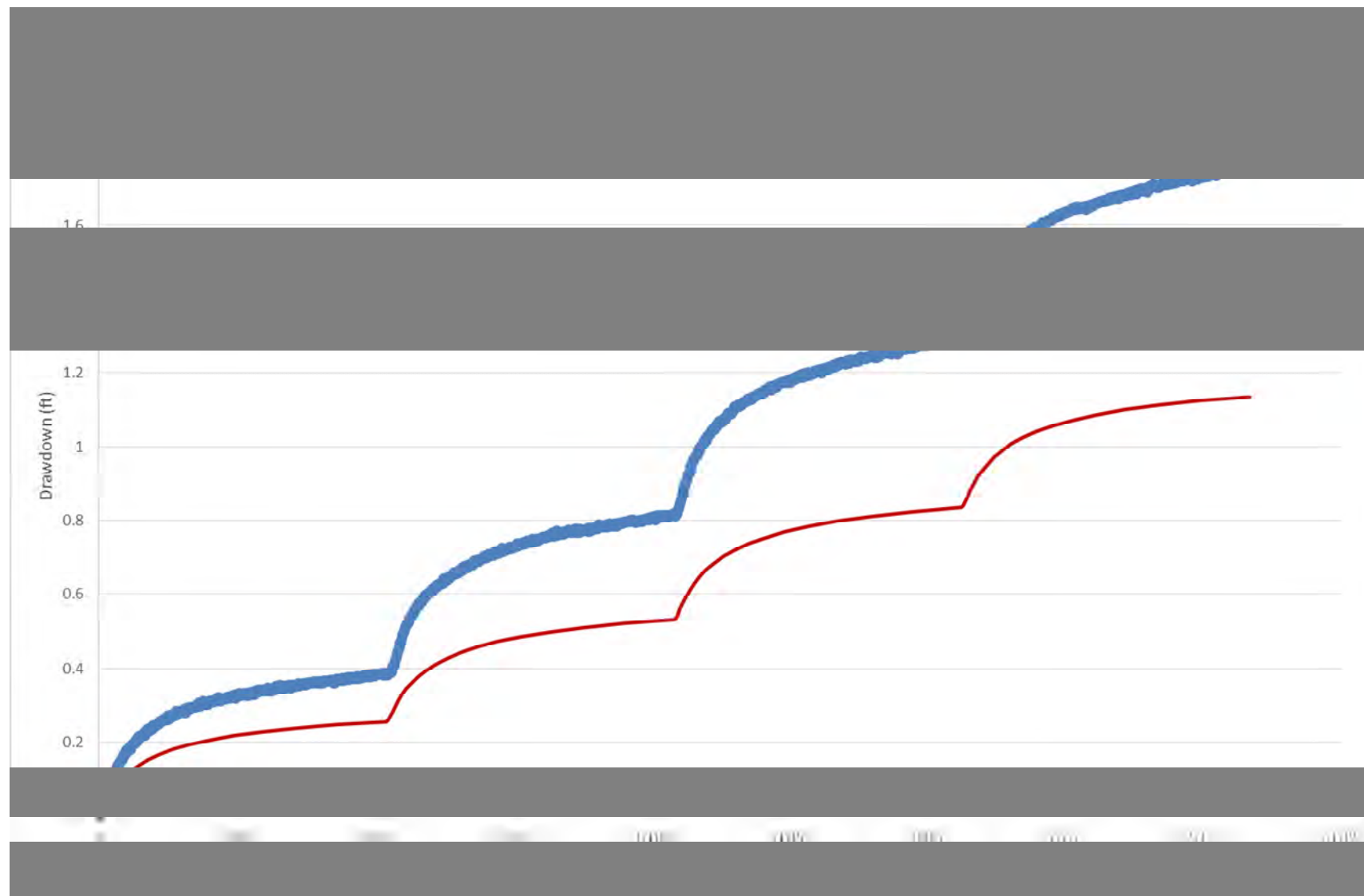
## Step-Drawdown Test I

EW-08S Step Test	Average Rate (gpm)
Step 1	7.10
Step 2	14.10
Step 3	21.74
Step 4	29.50

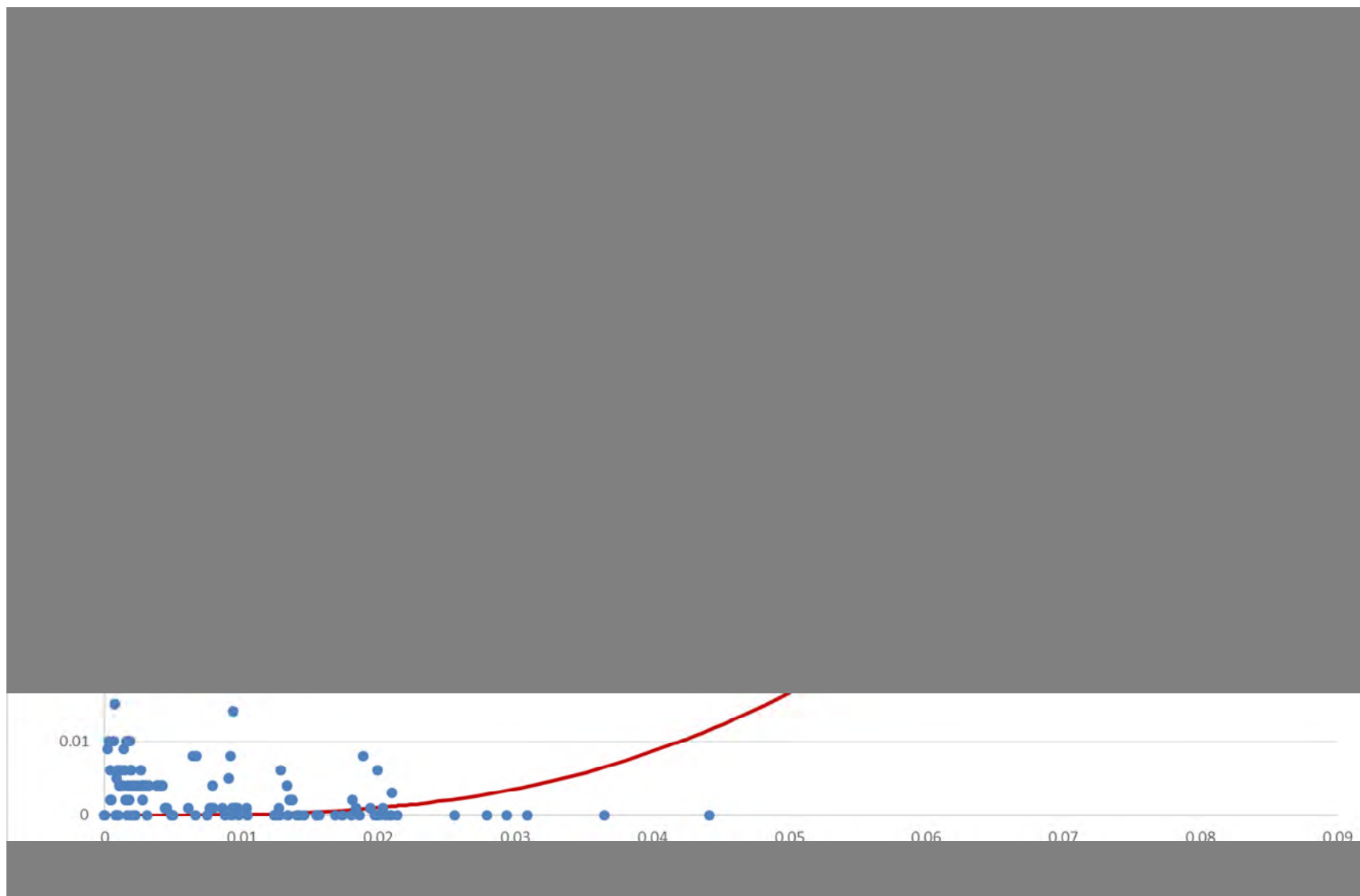


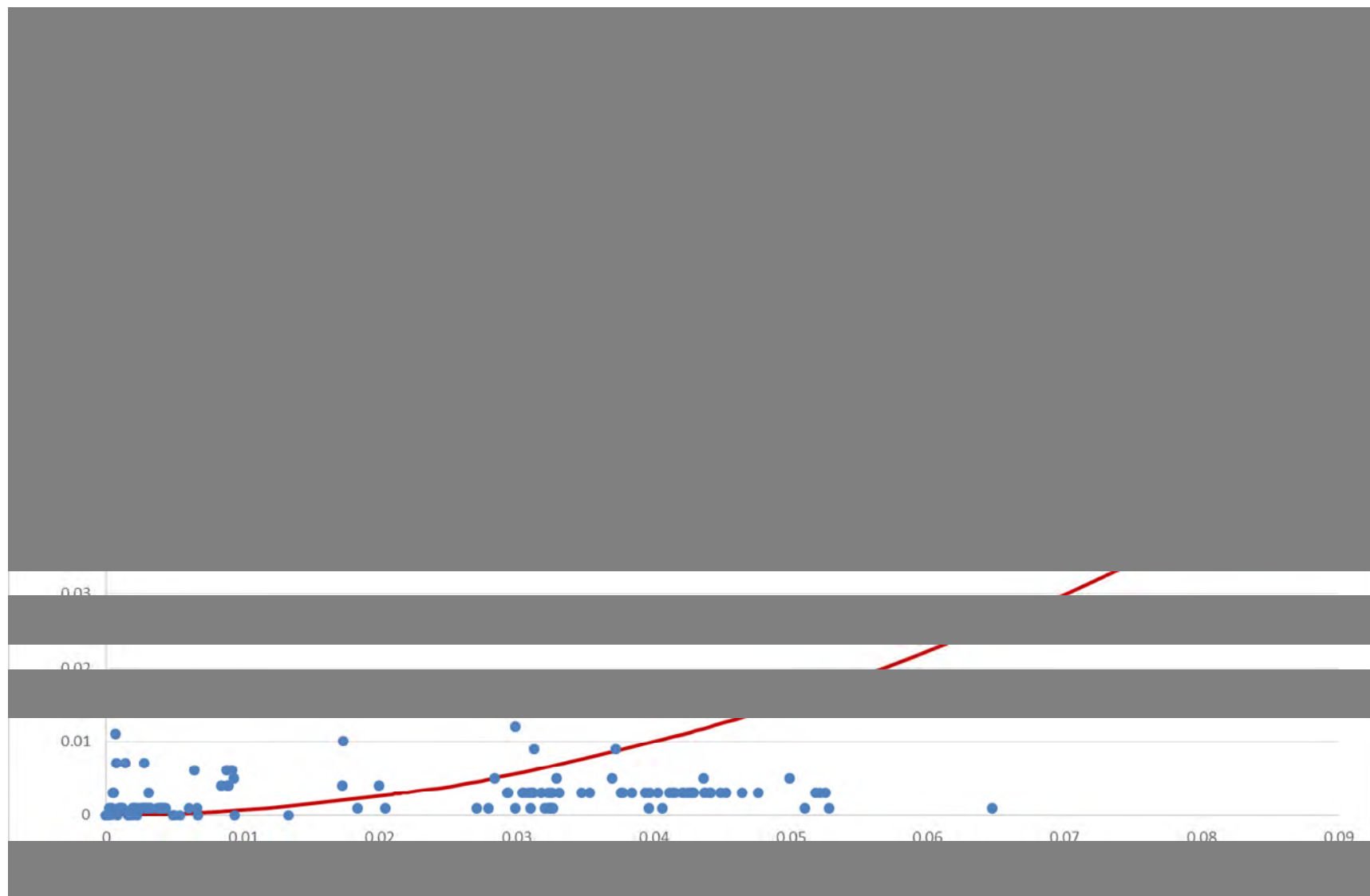


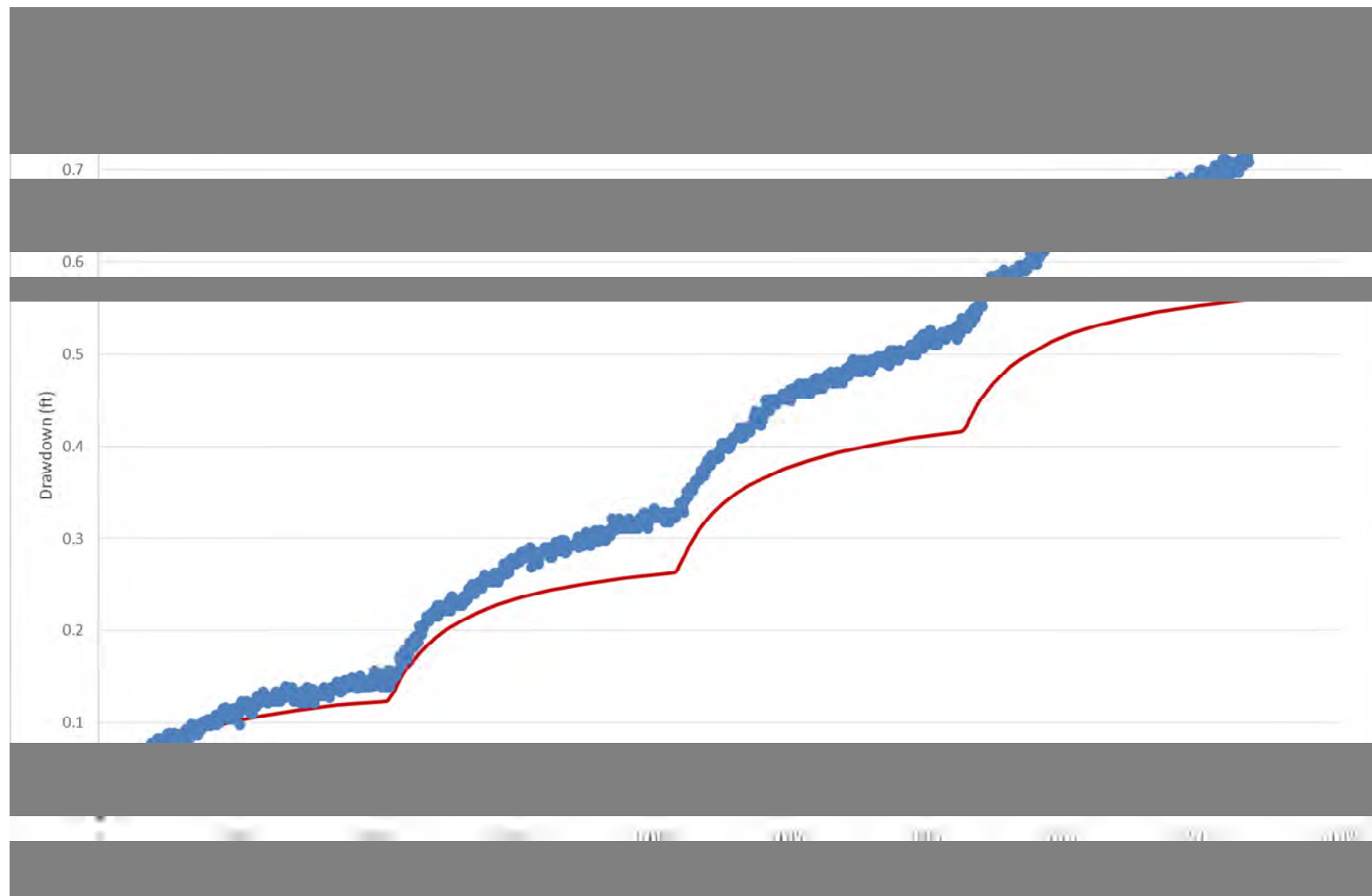


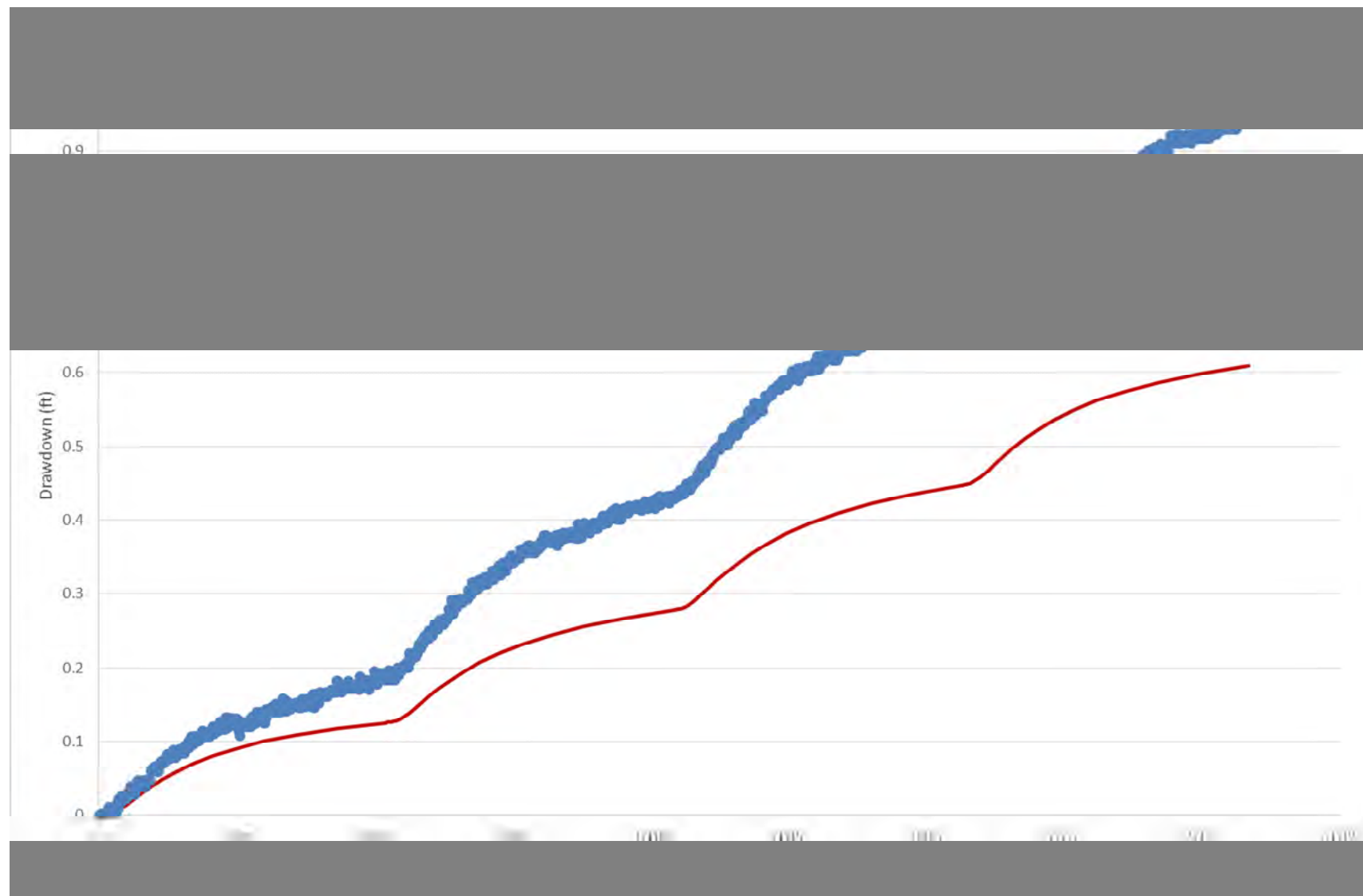






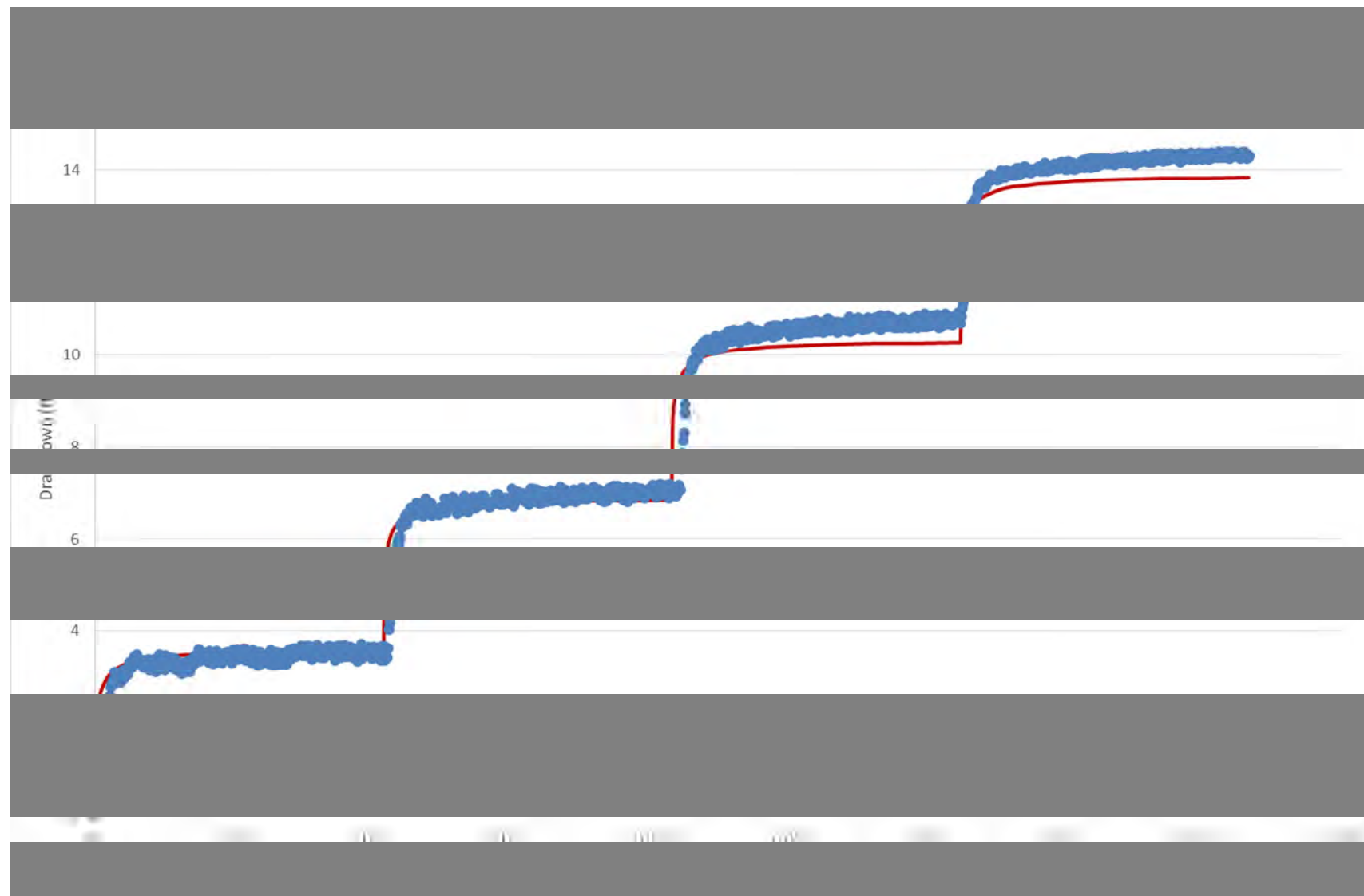


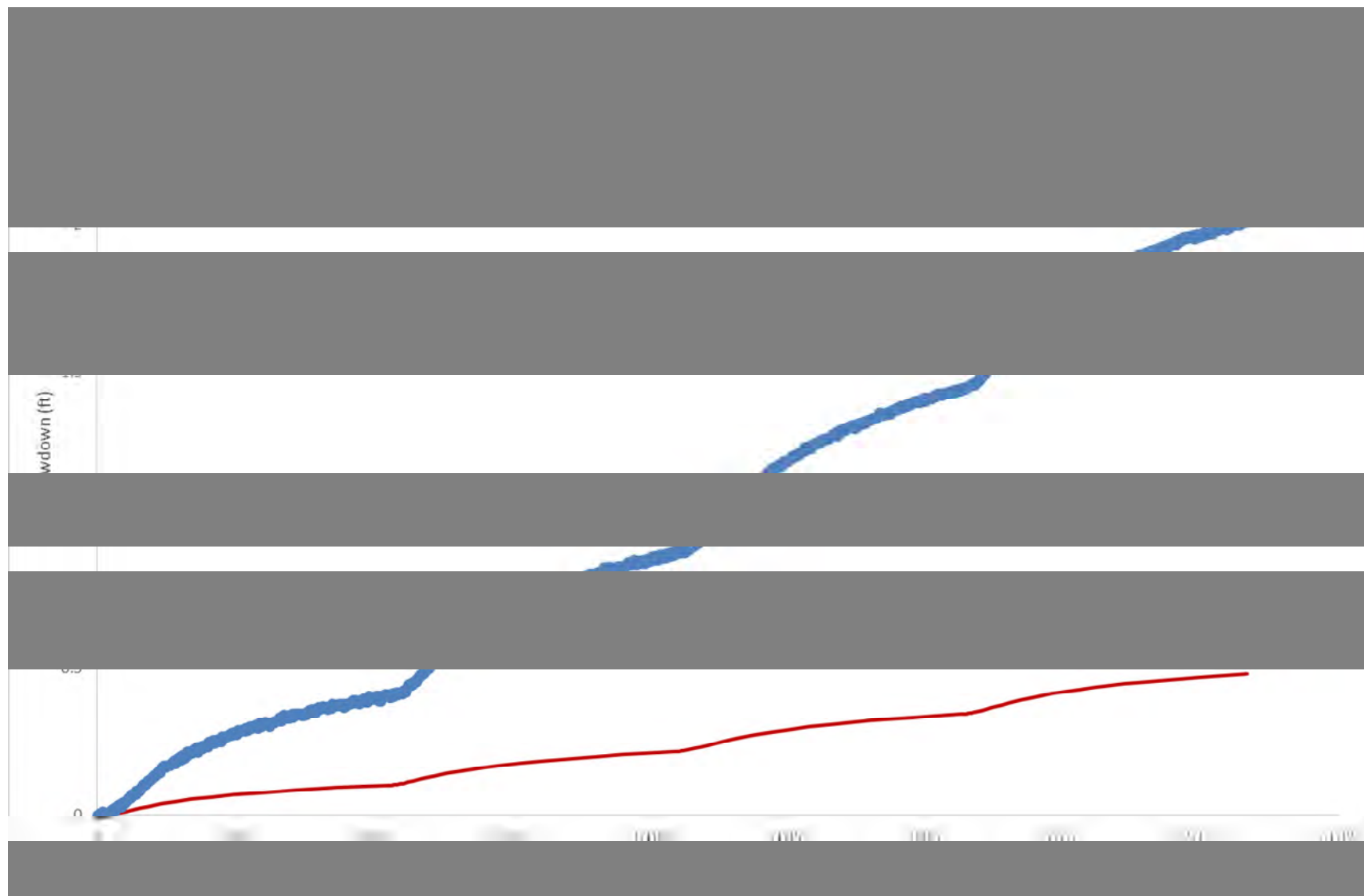


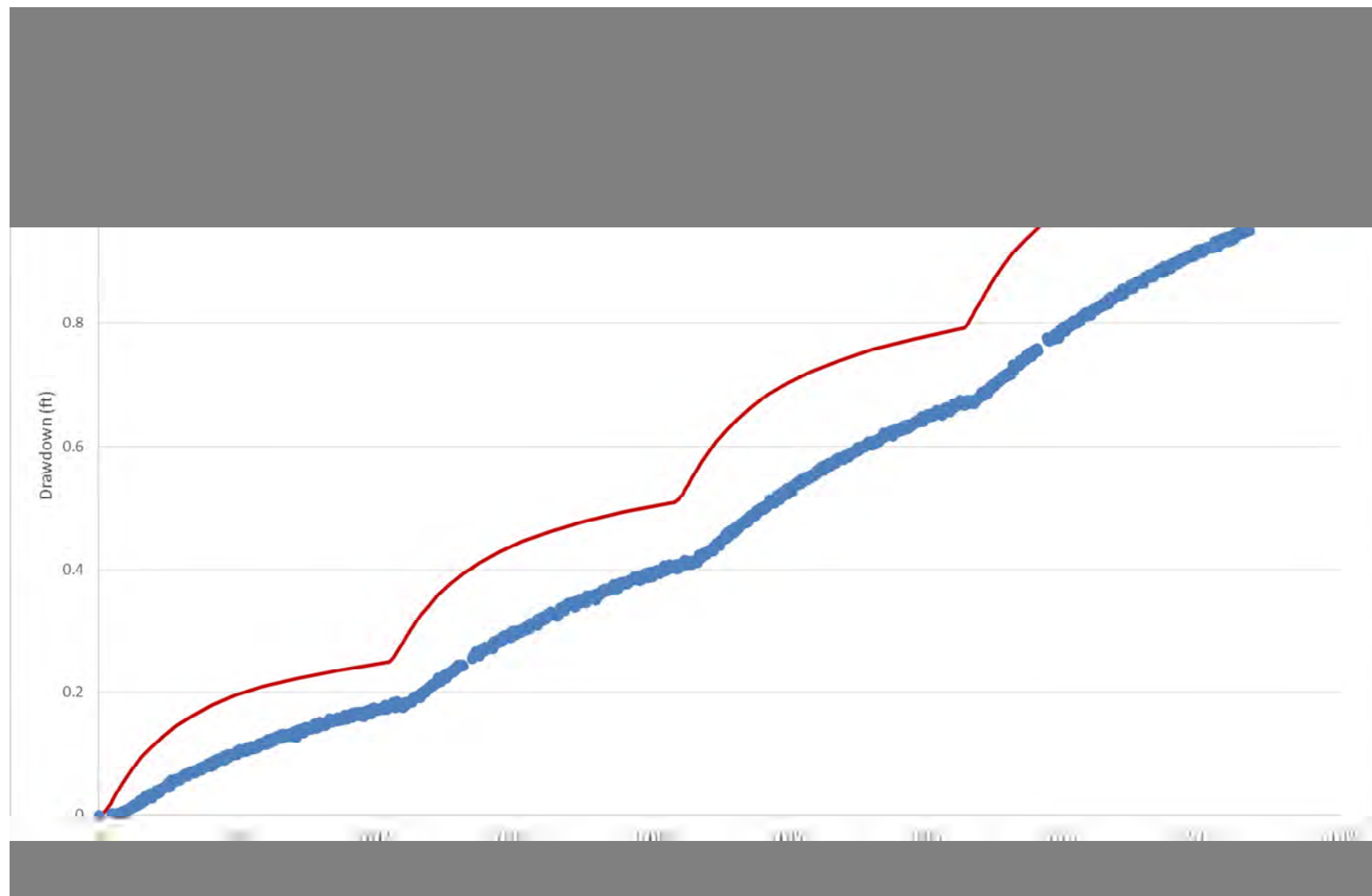


# Step-Drawdown Test J

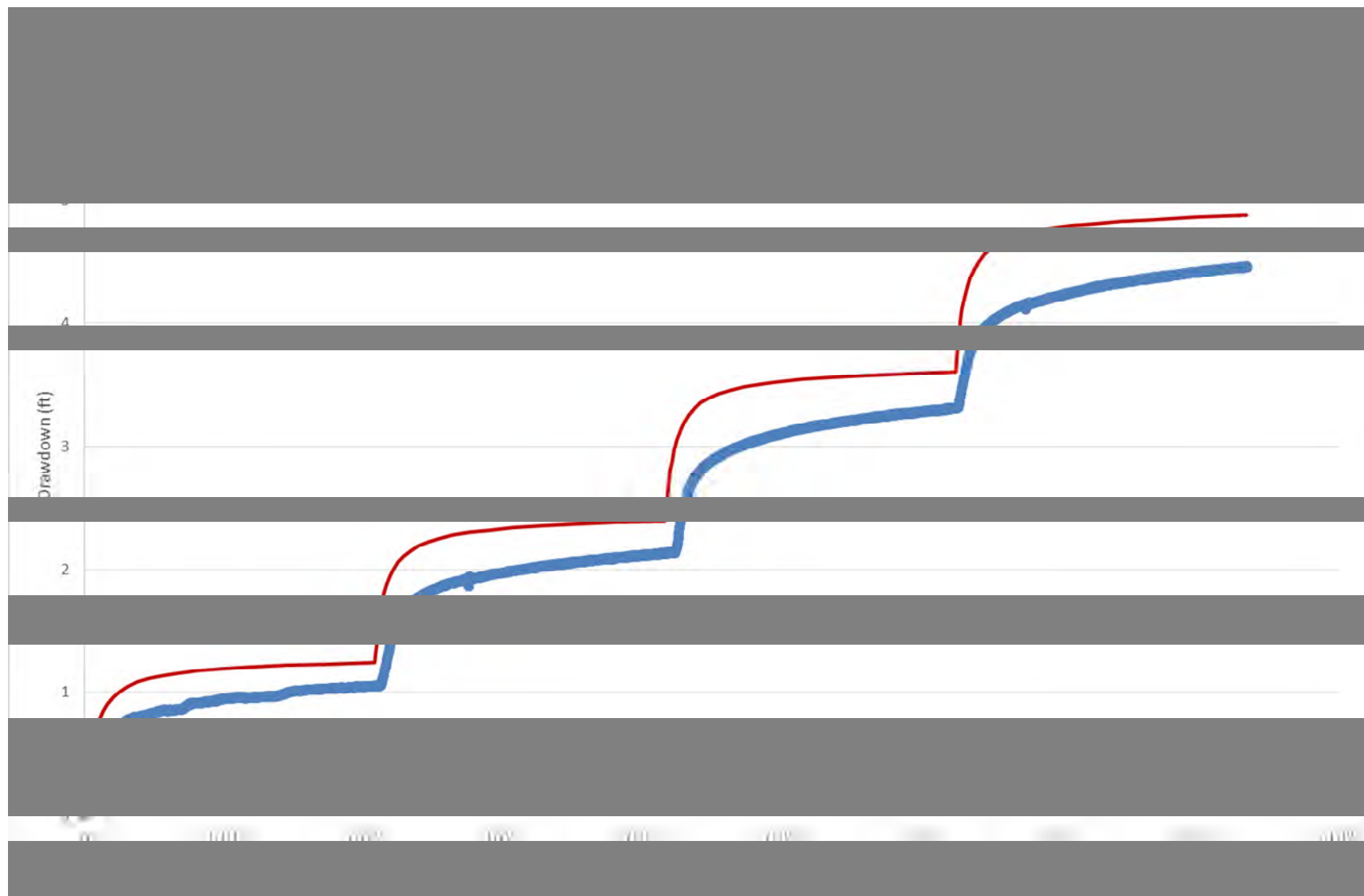
EW-07D Step Test	Average Rate (gpm)
Step 1	7.40
Step 2	14.03
Step 3	21.01
Step 4	28.28

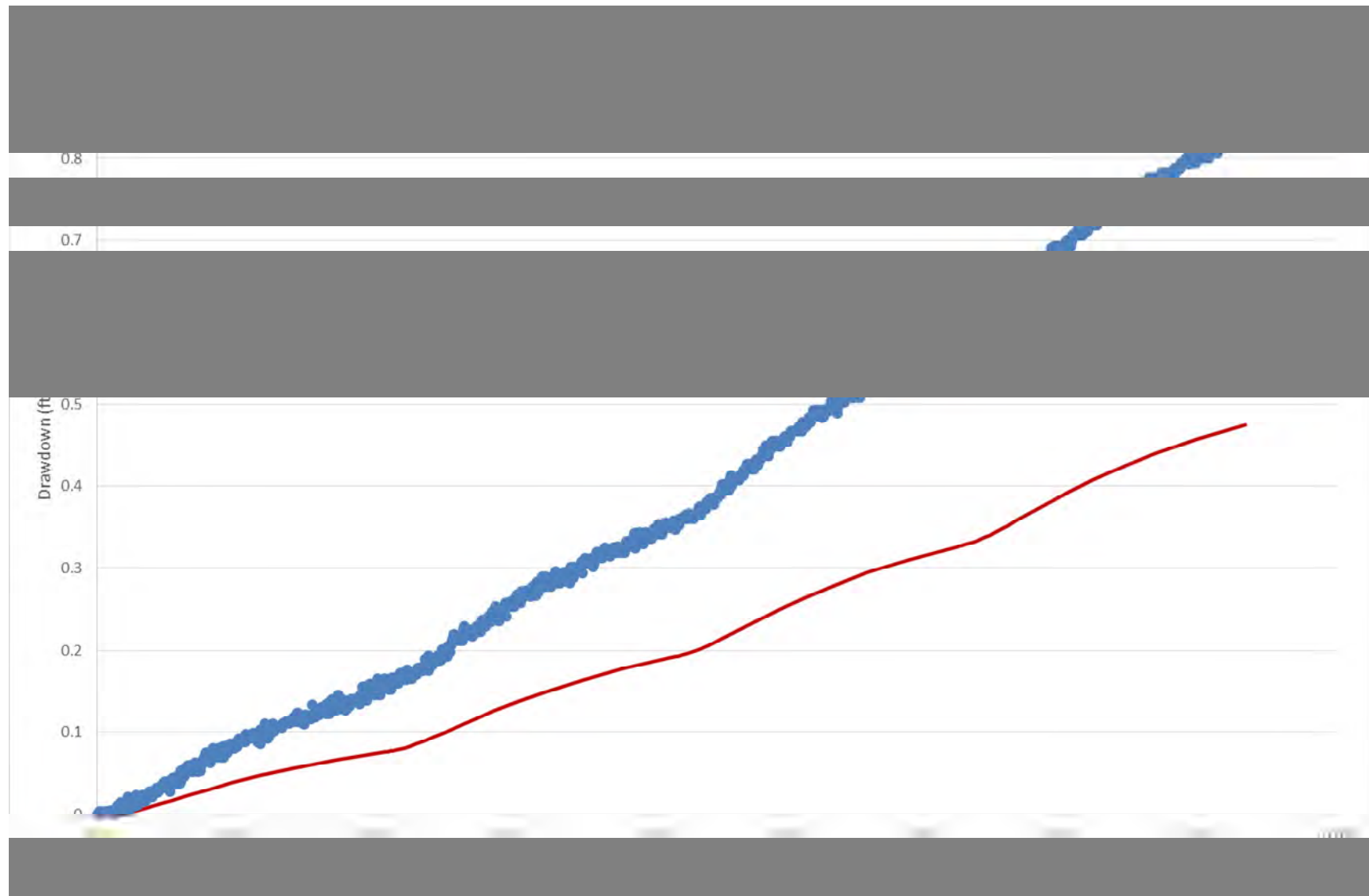


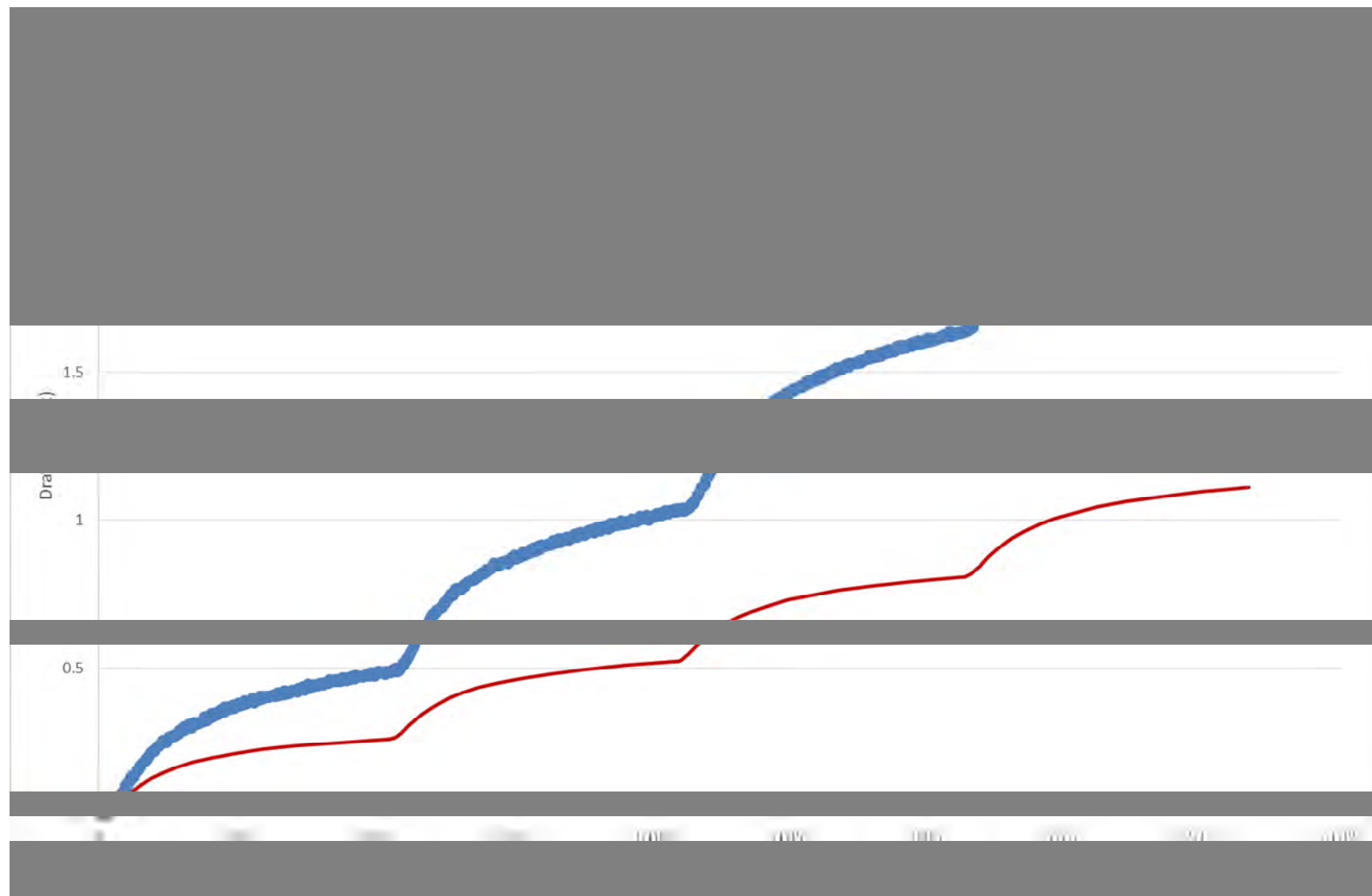


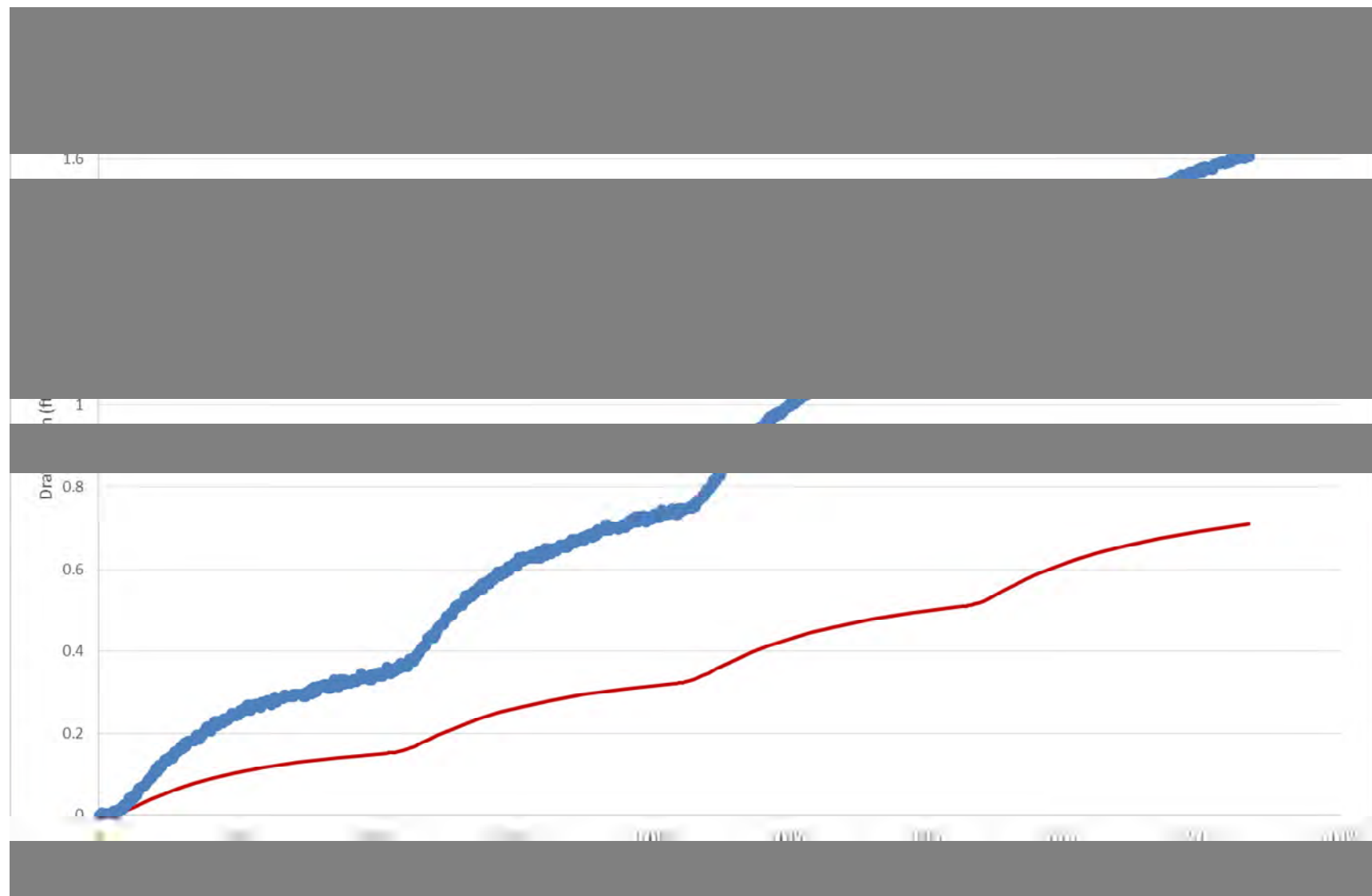


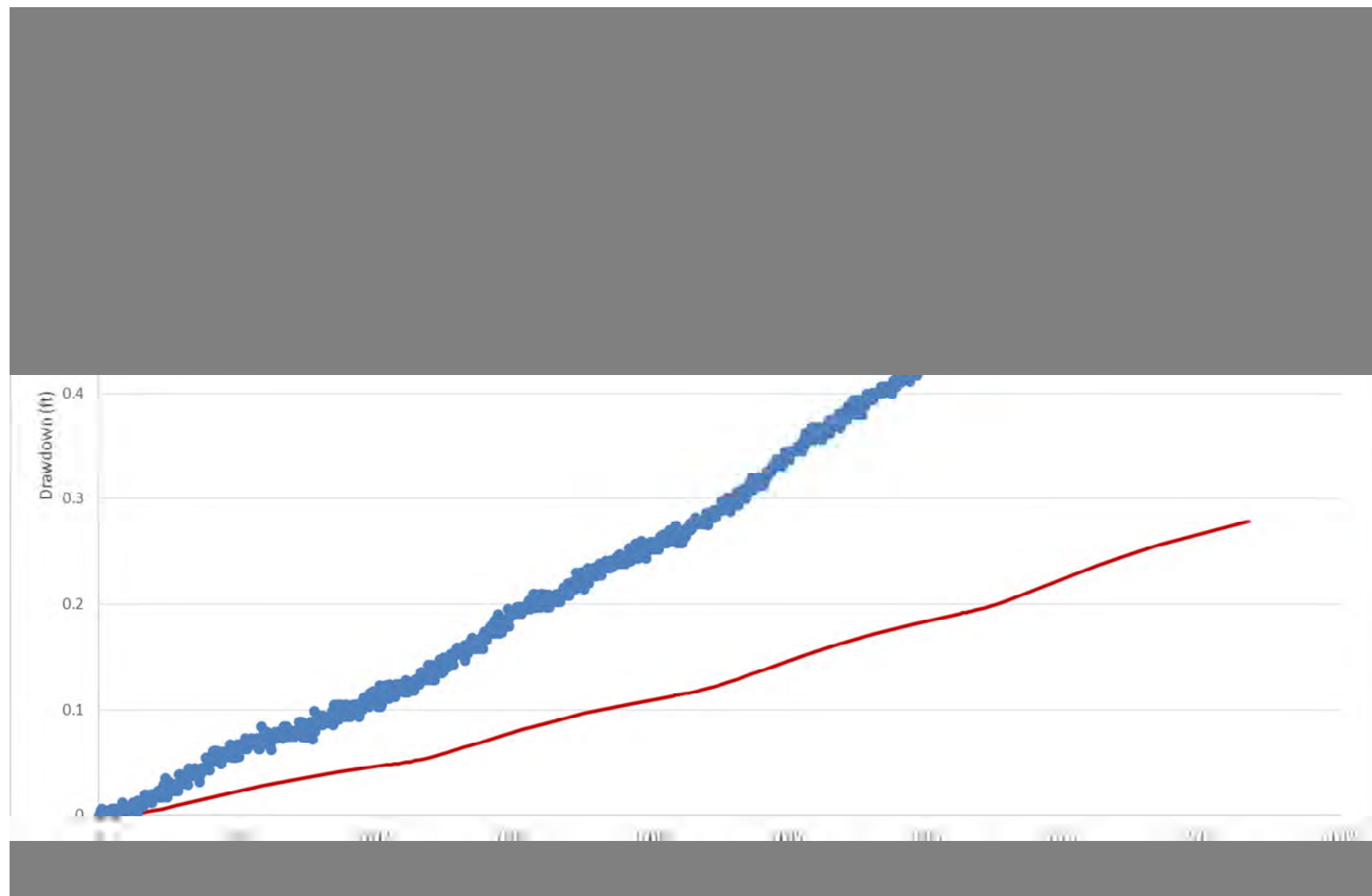


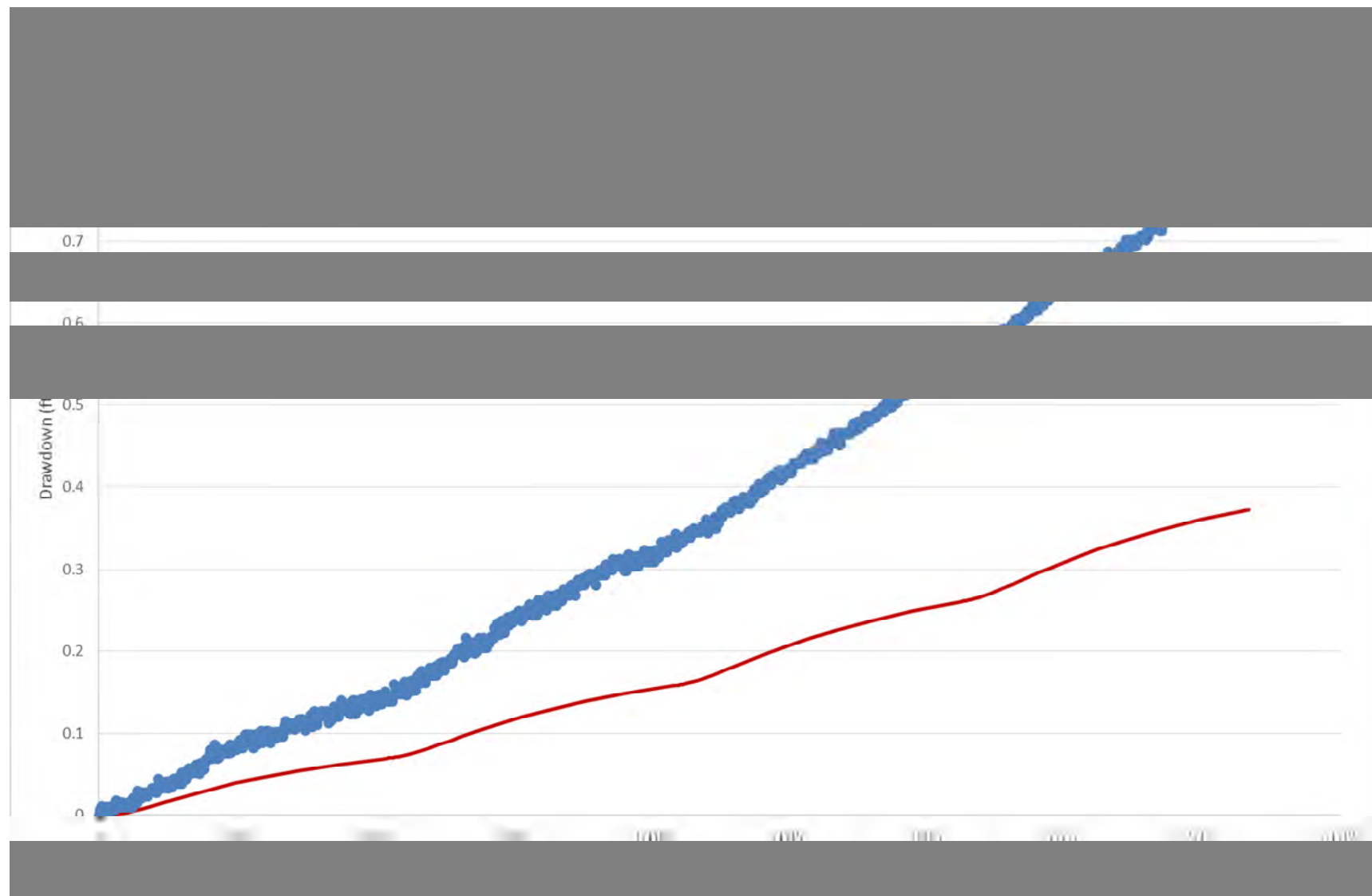






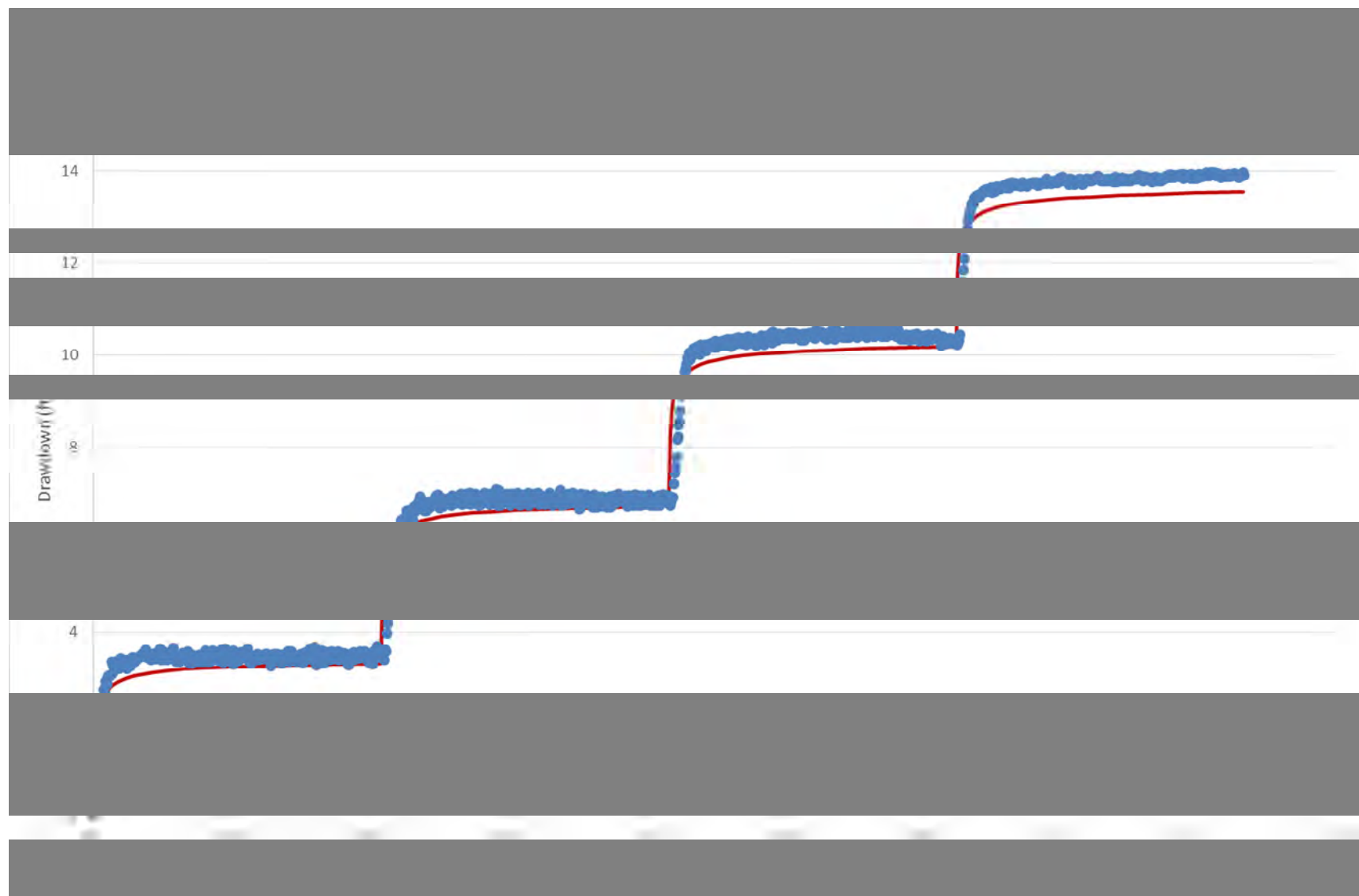




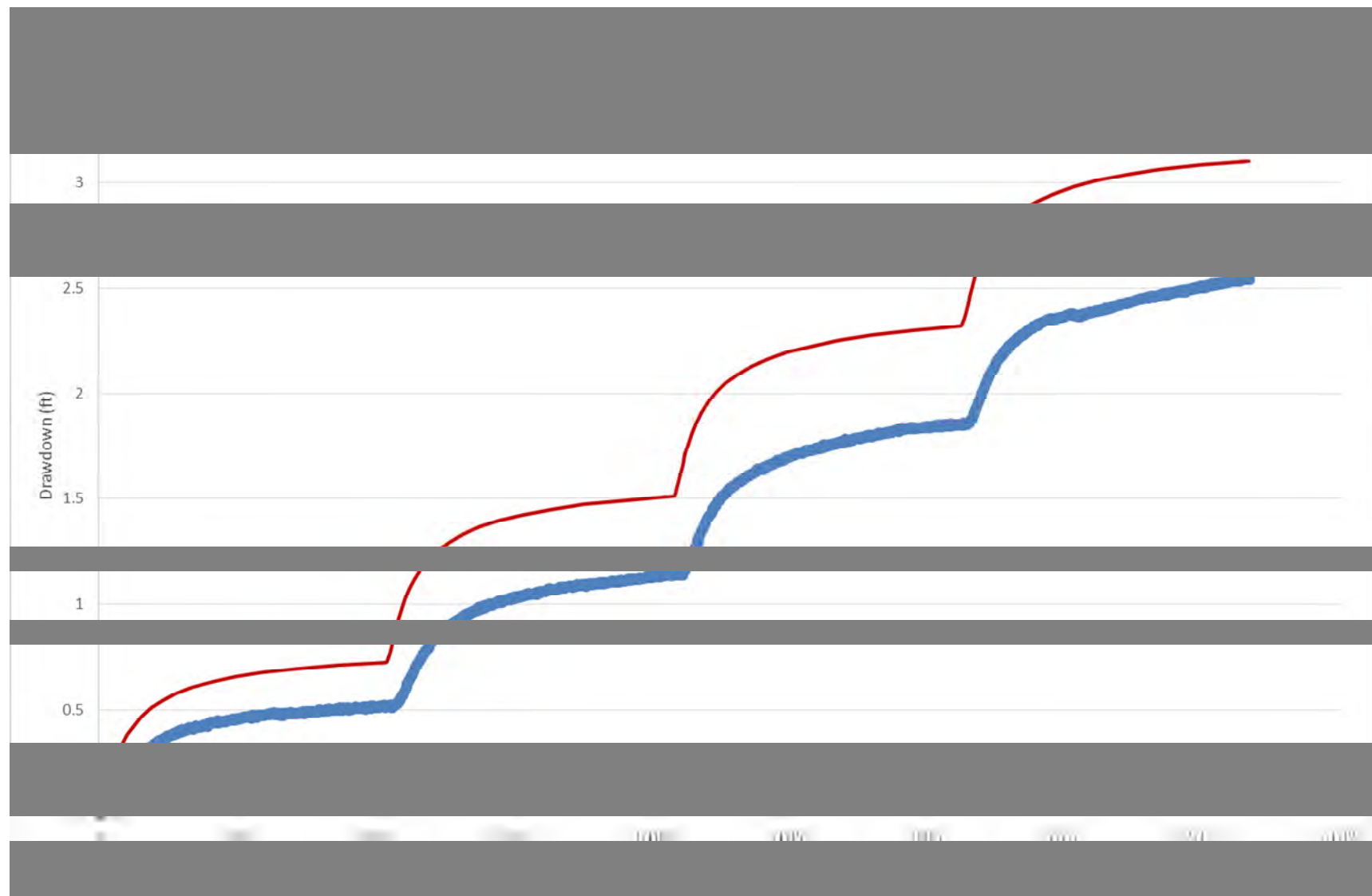


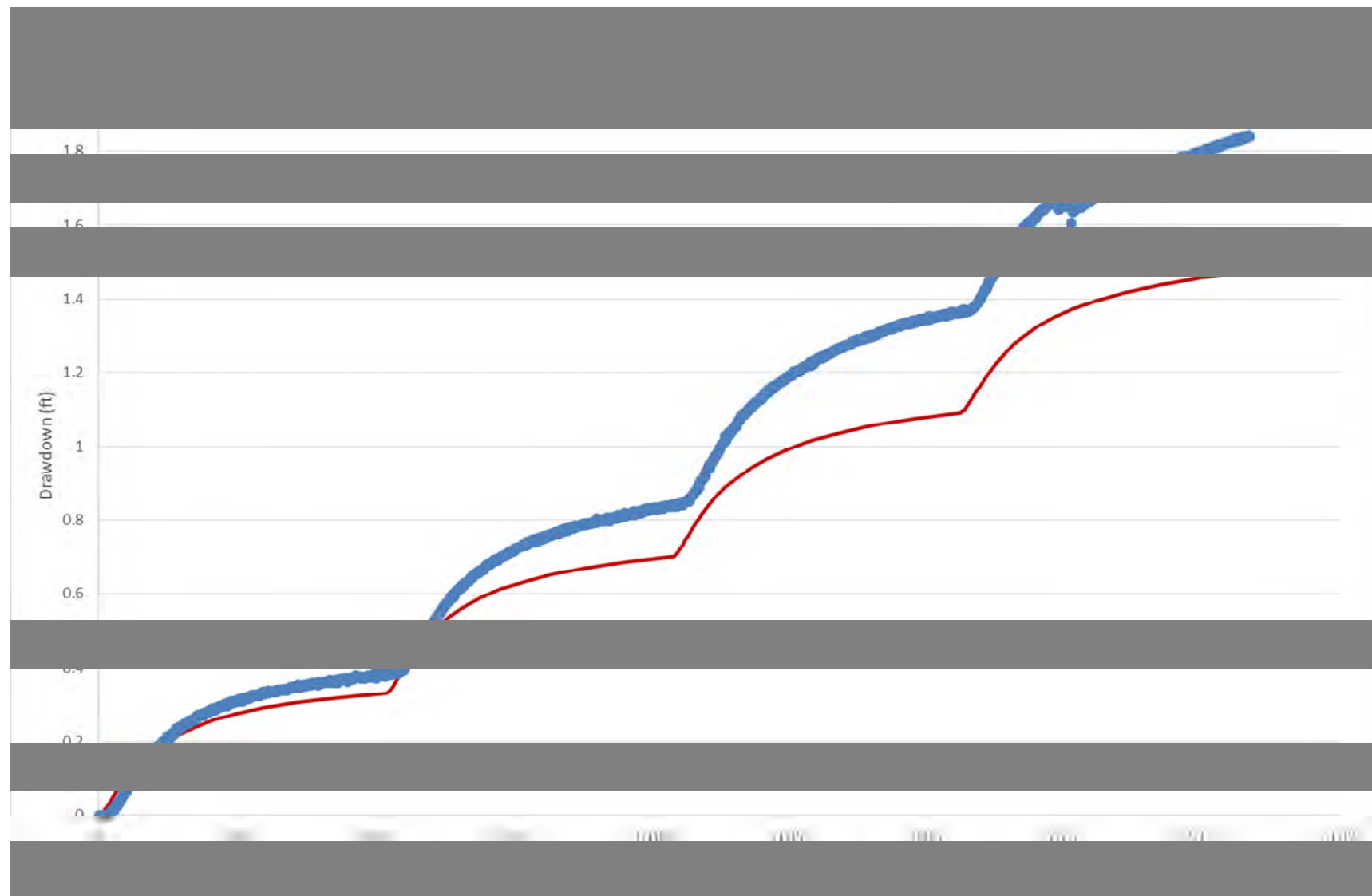
## Step-Drawdown Test K

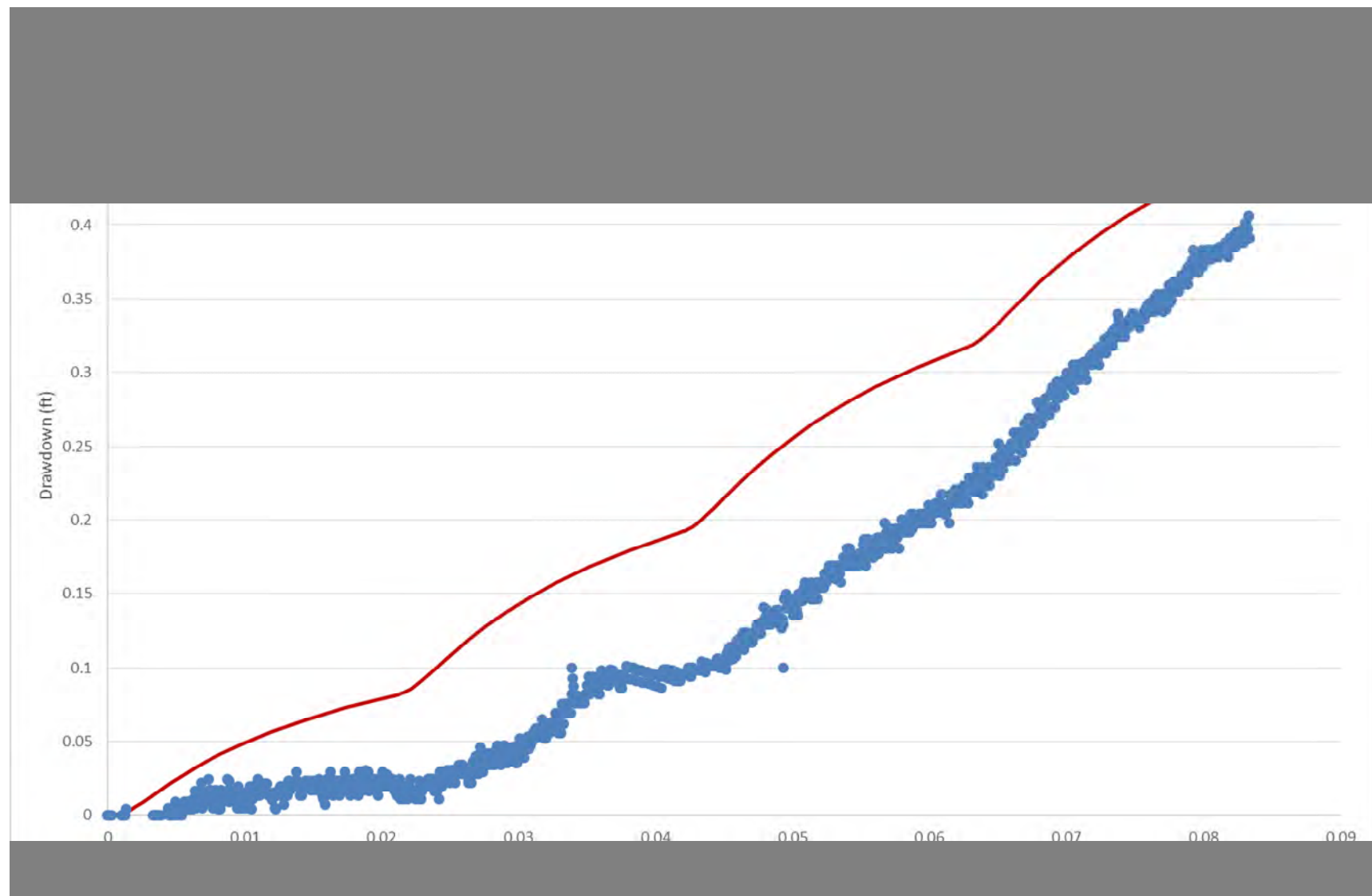
EW-06I Step Test	Average Rate (gpm)
Step 1	7.06
Step 2	14.27
Step 3	21.52
Step 4	28.49

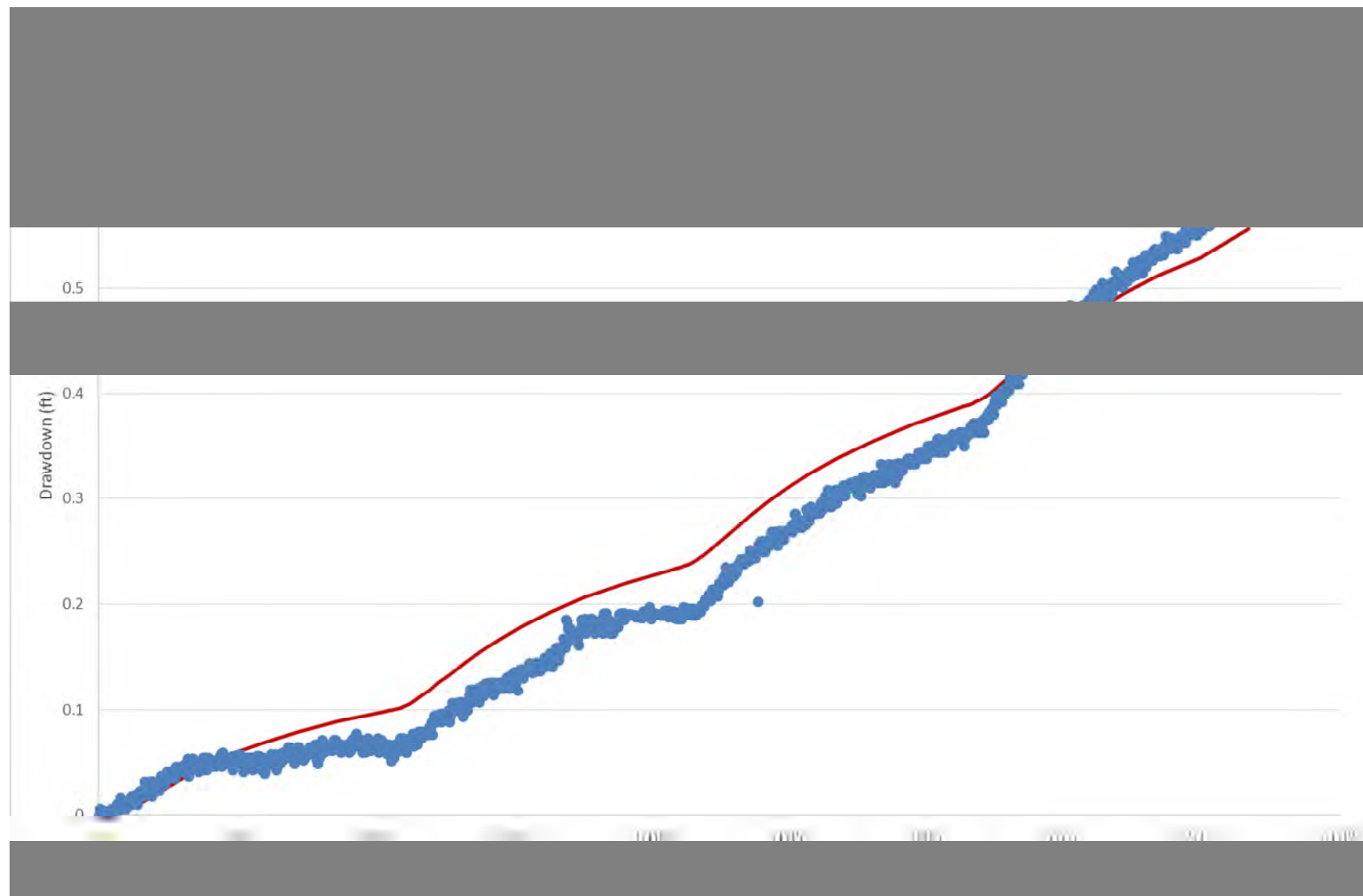


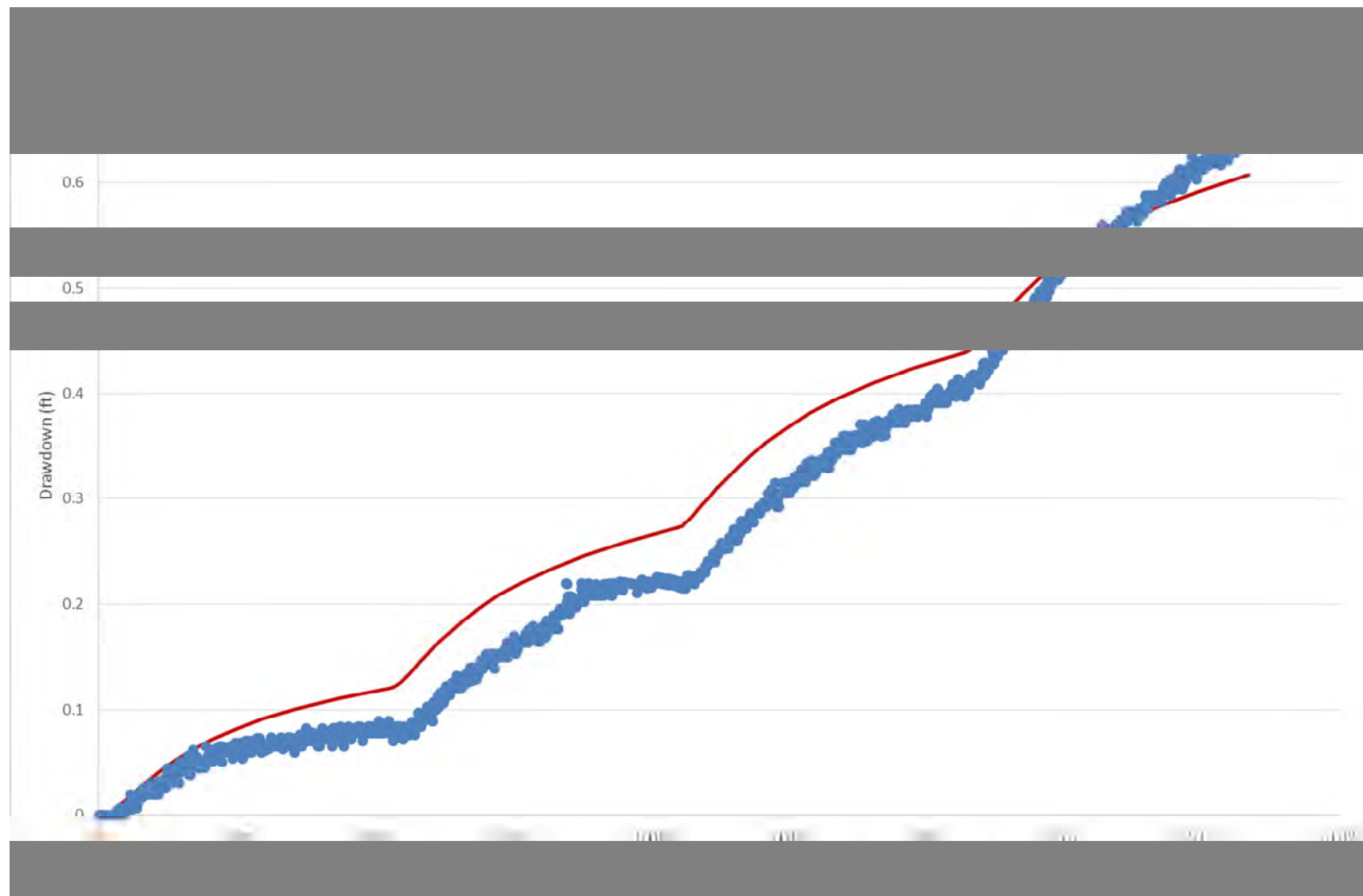


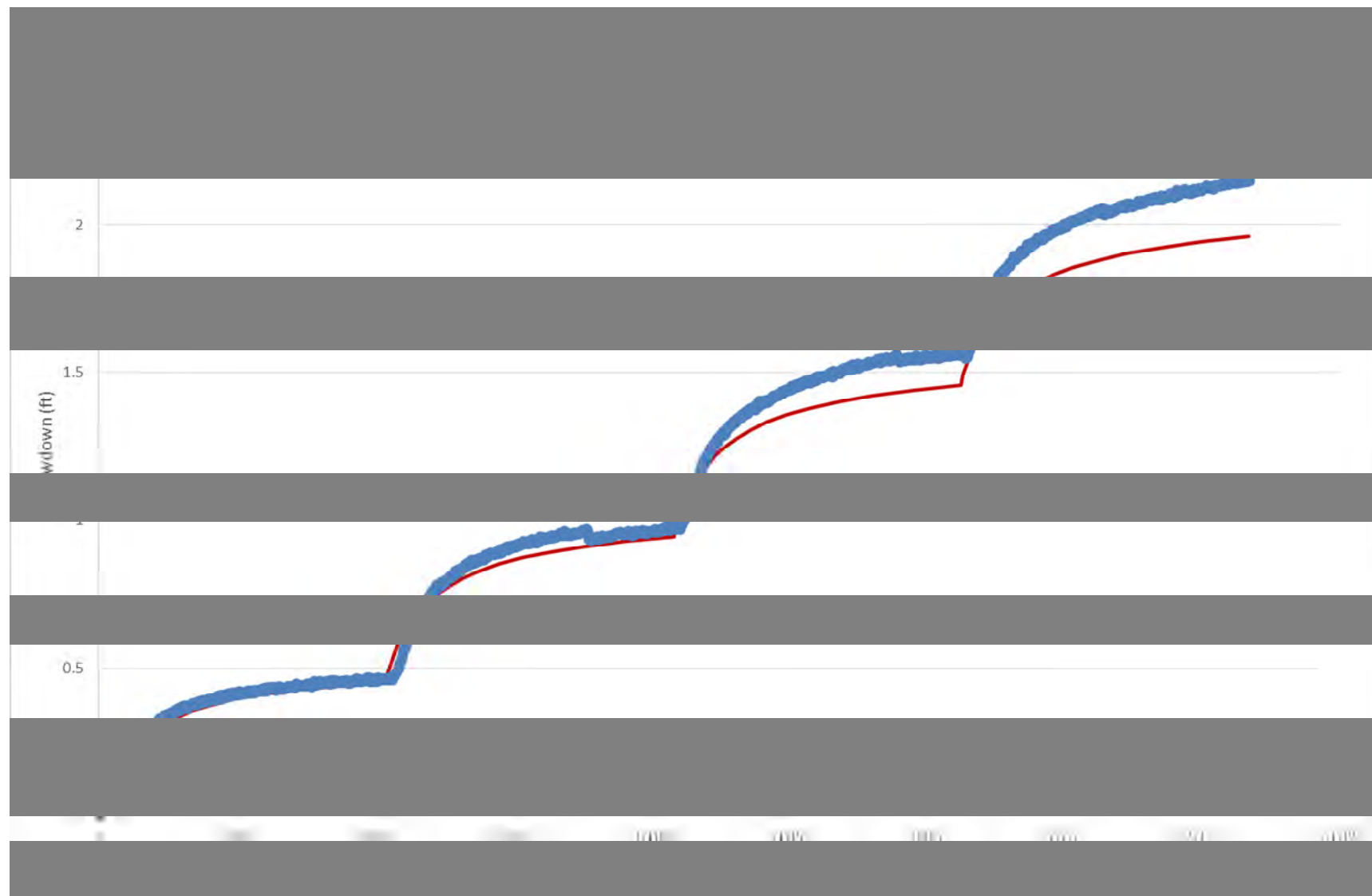


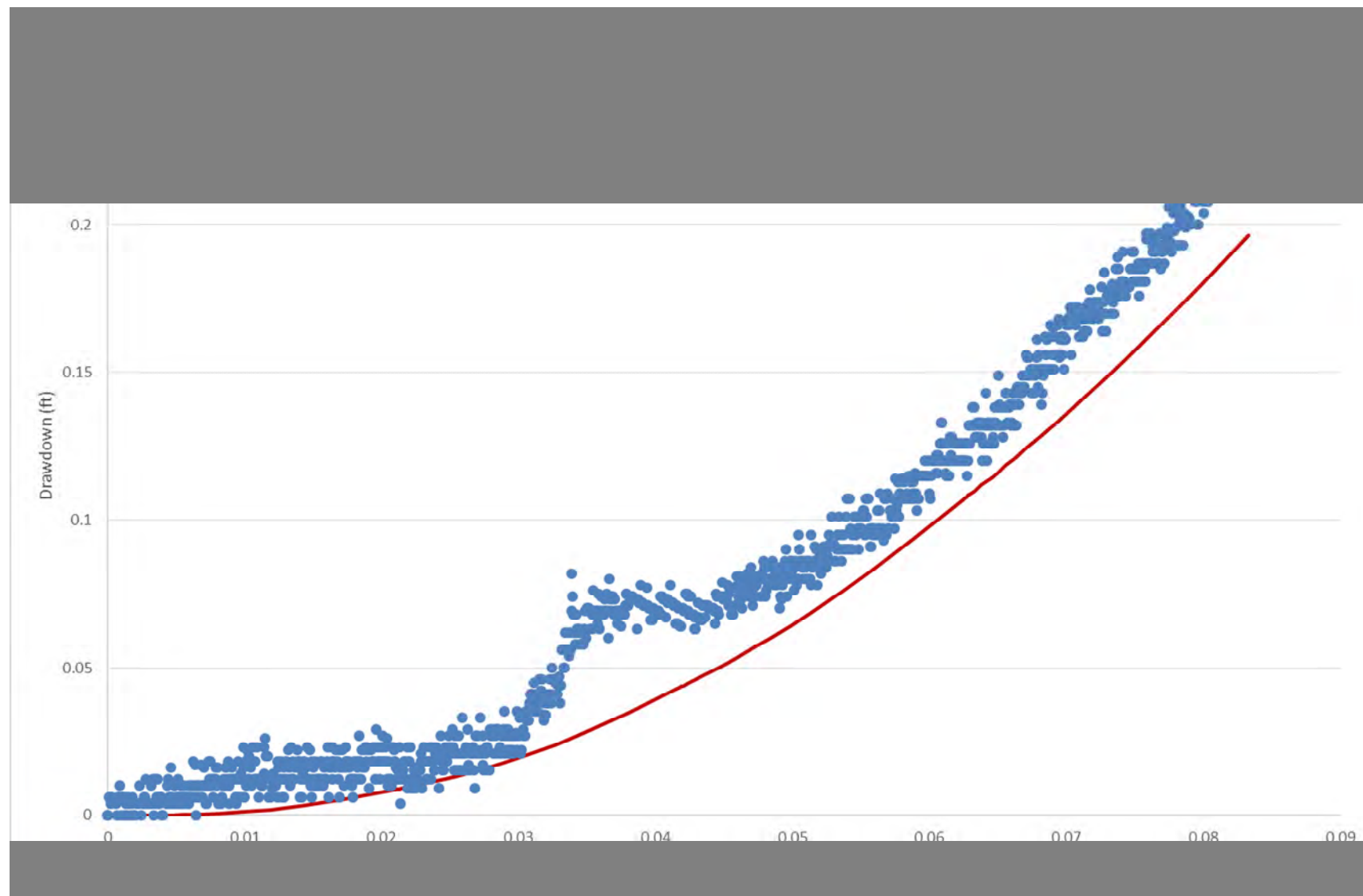


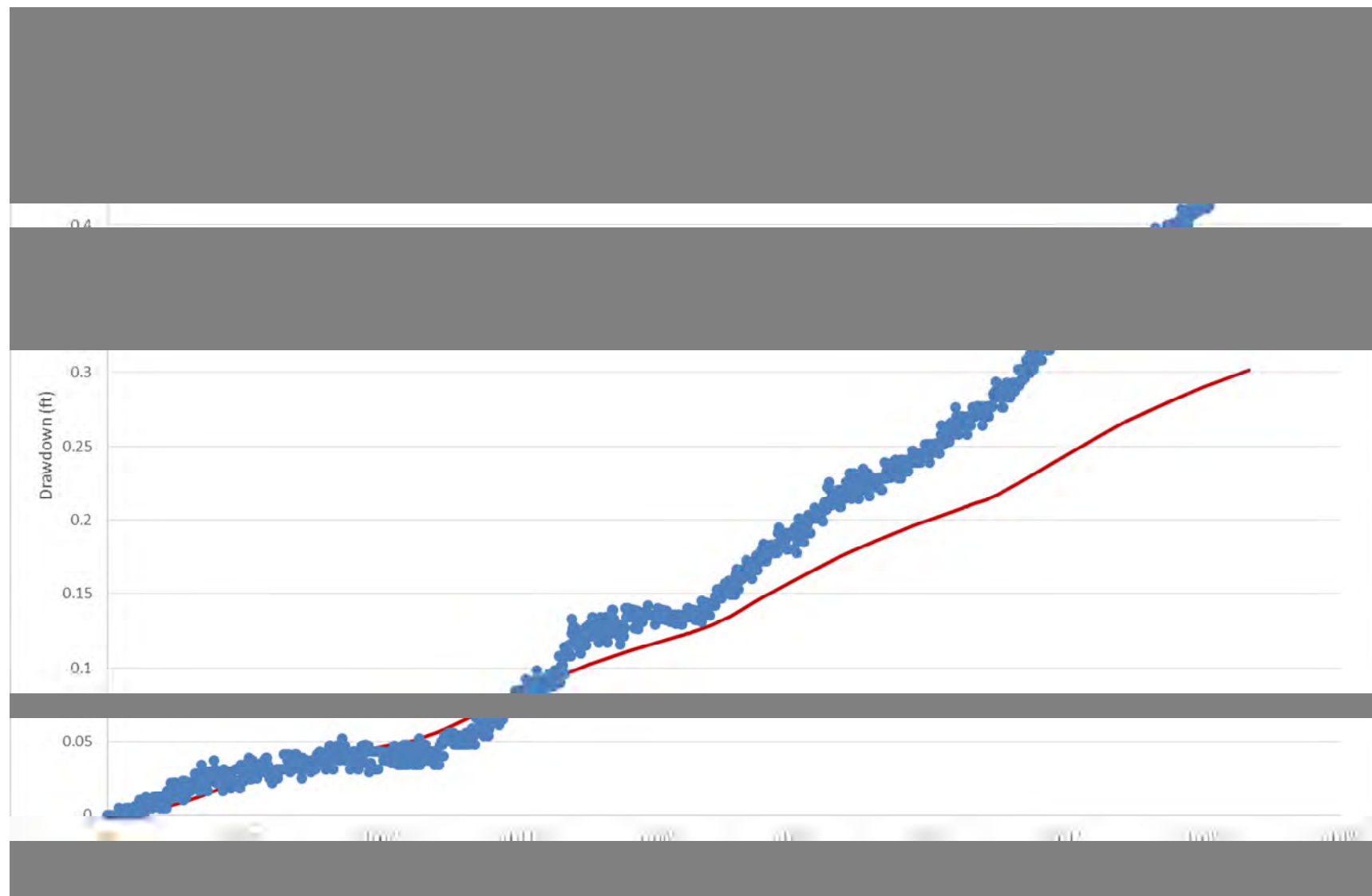








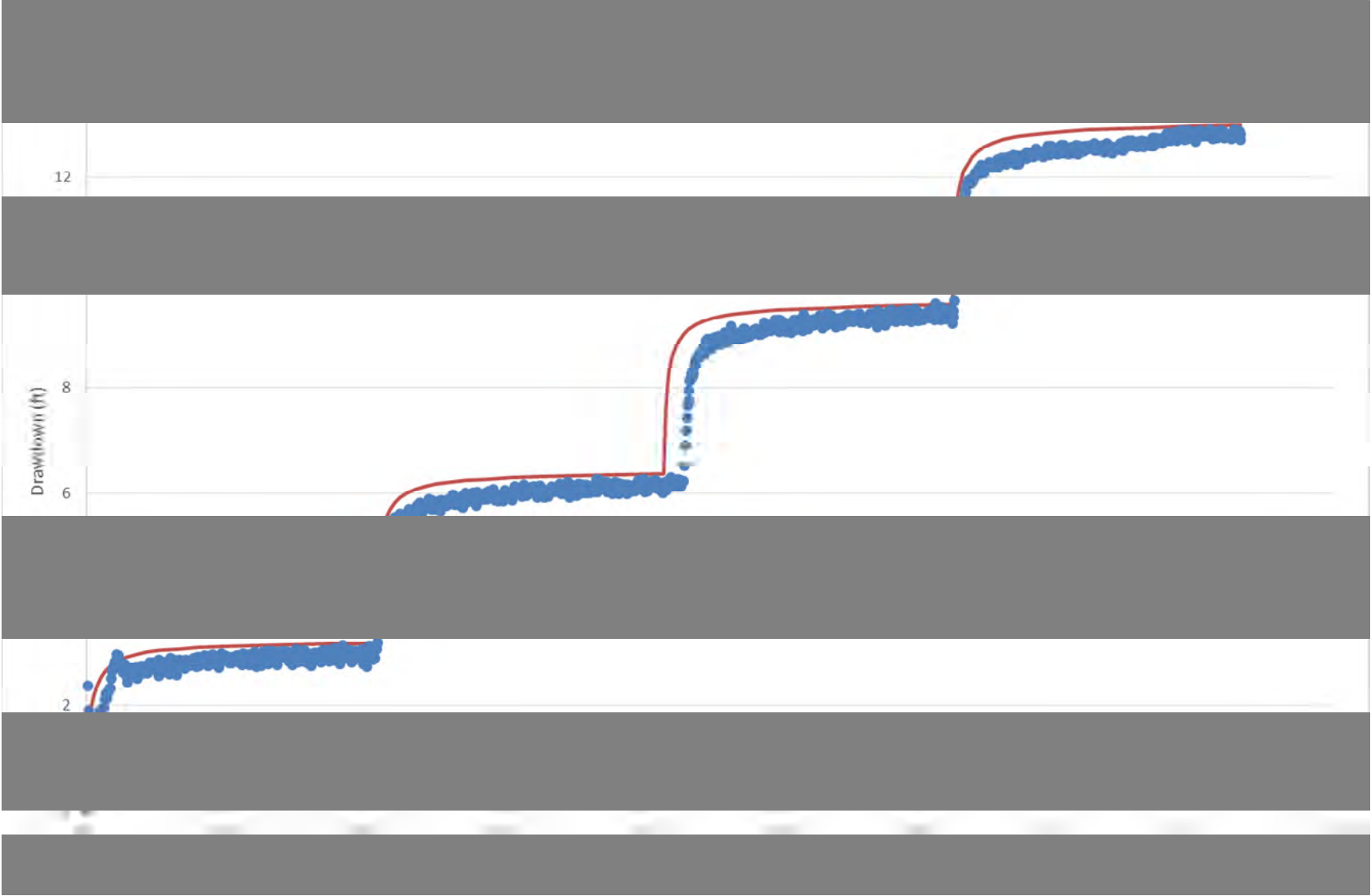


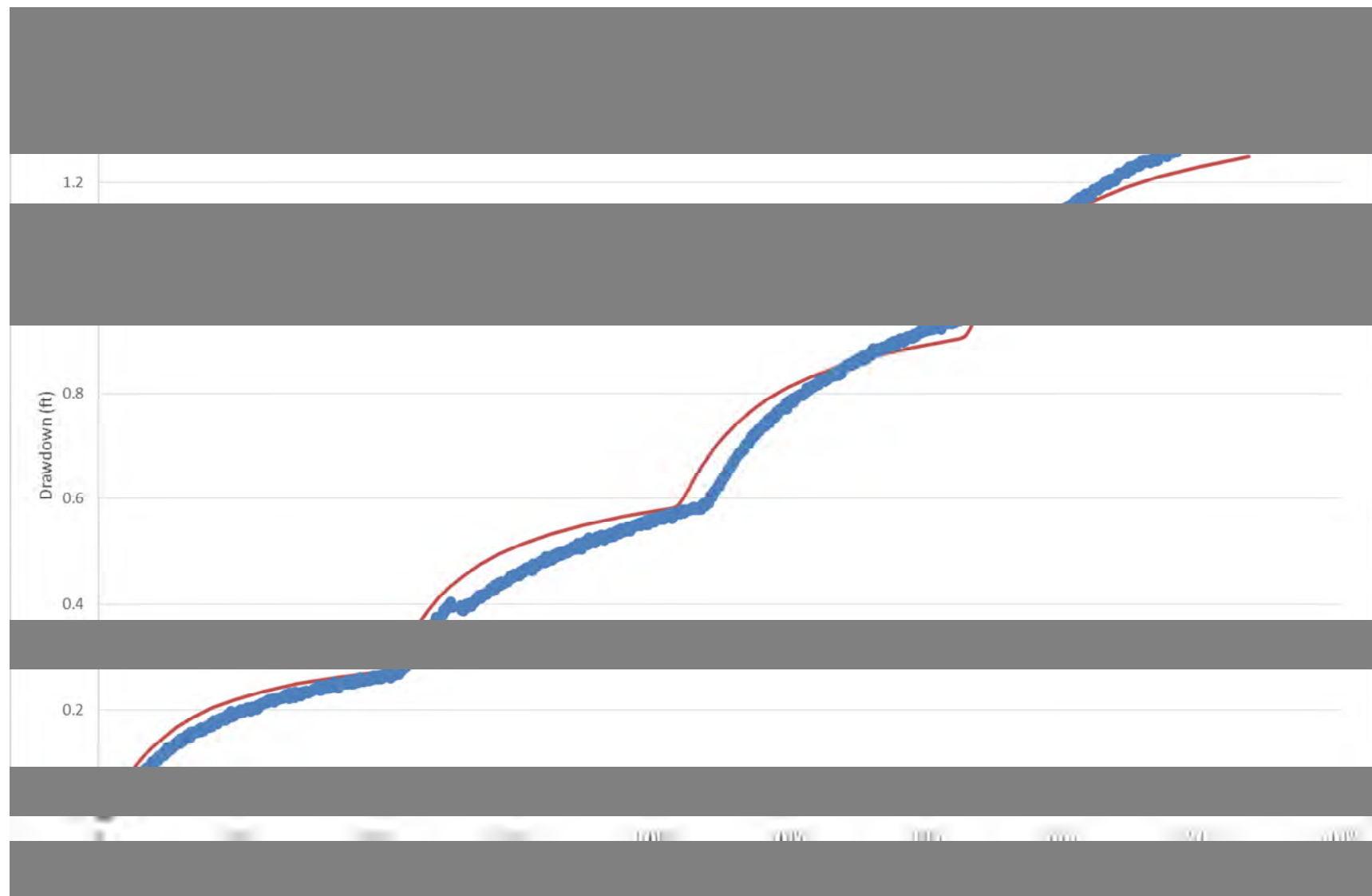


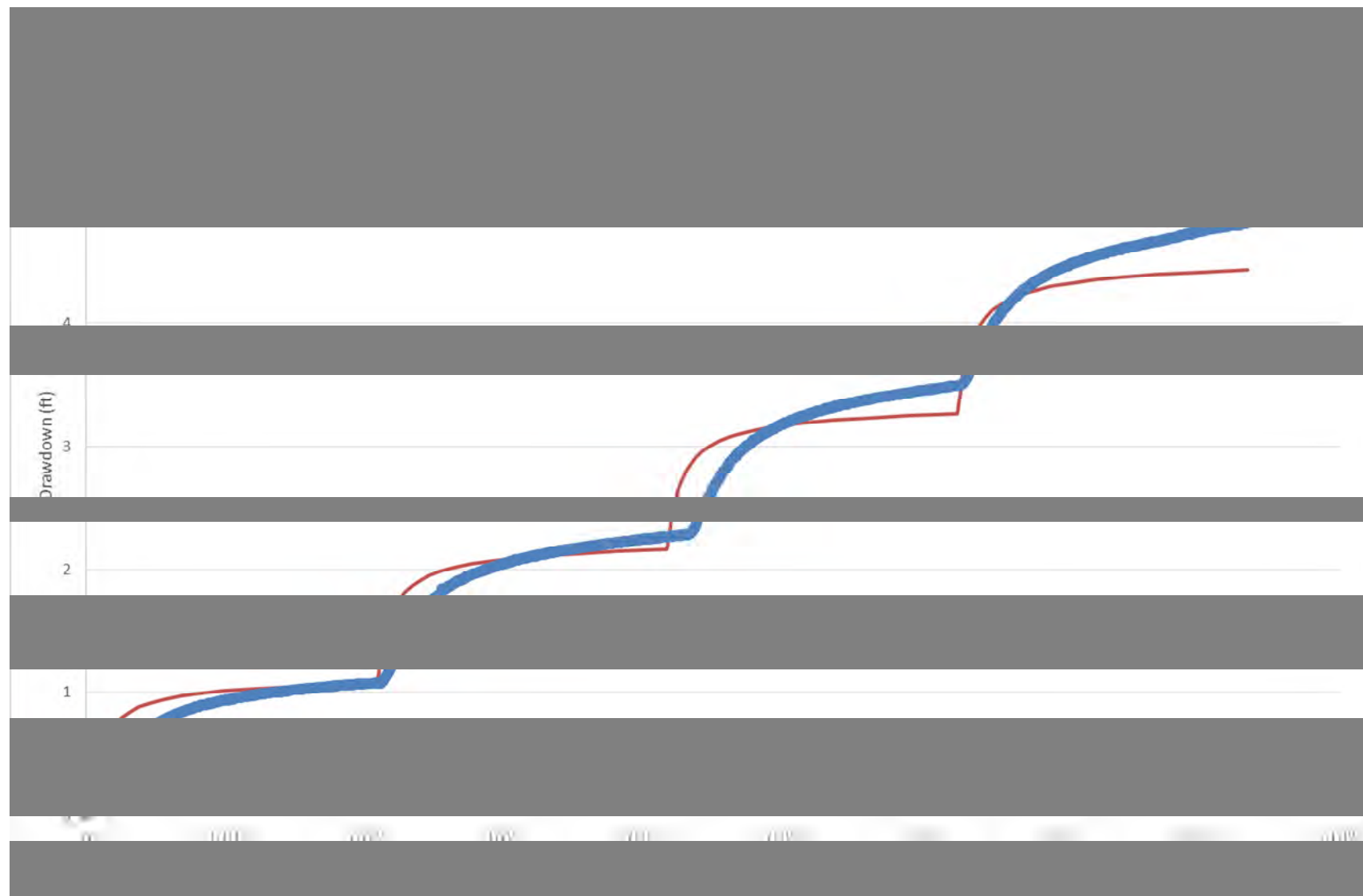


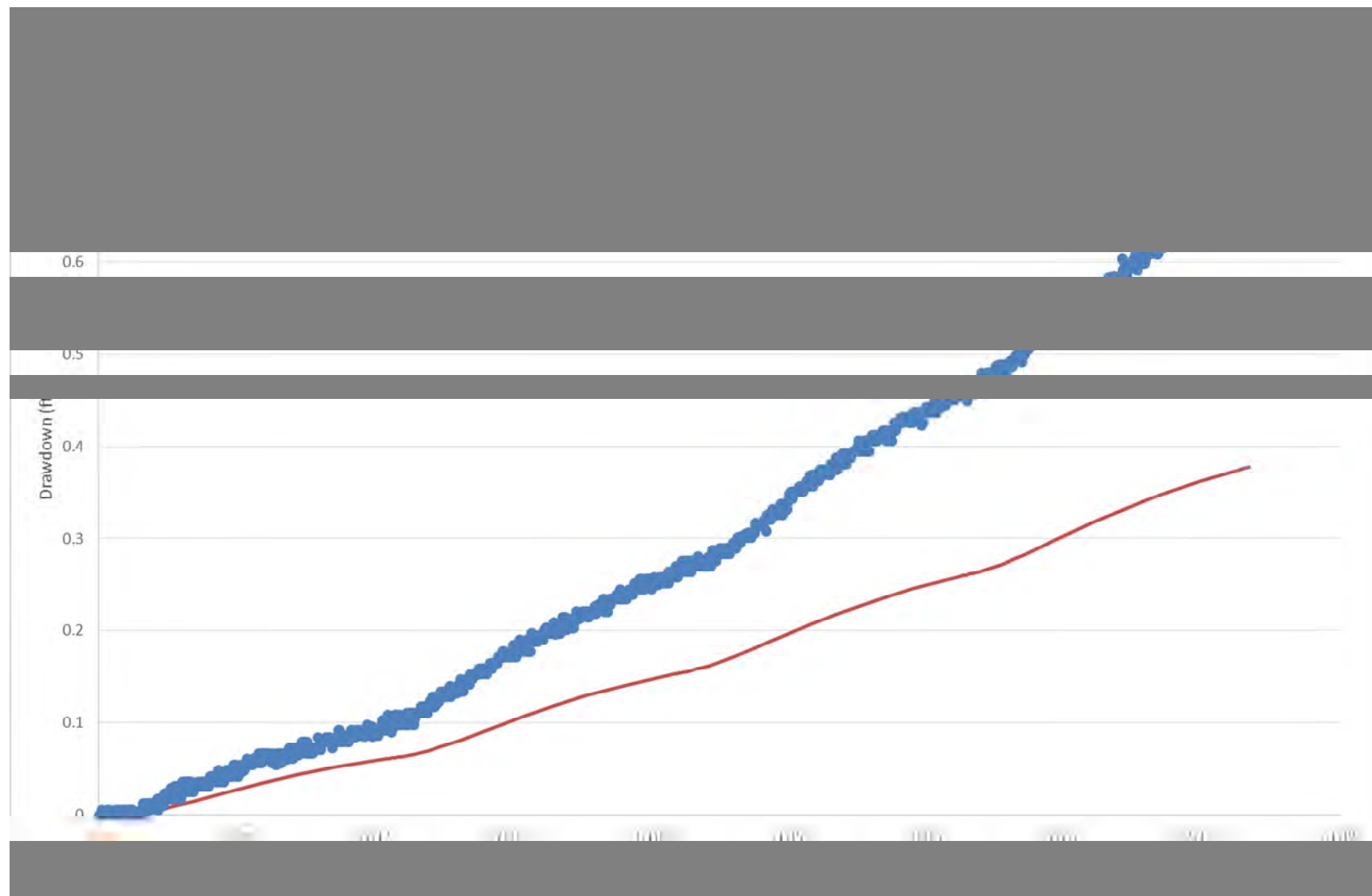
## Step-Drawdown Test M

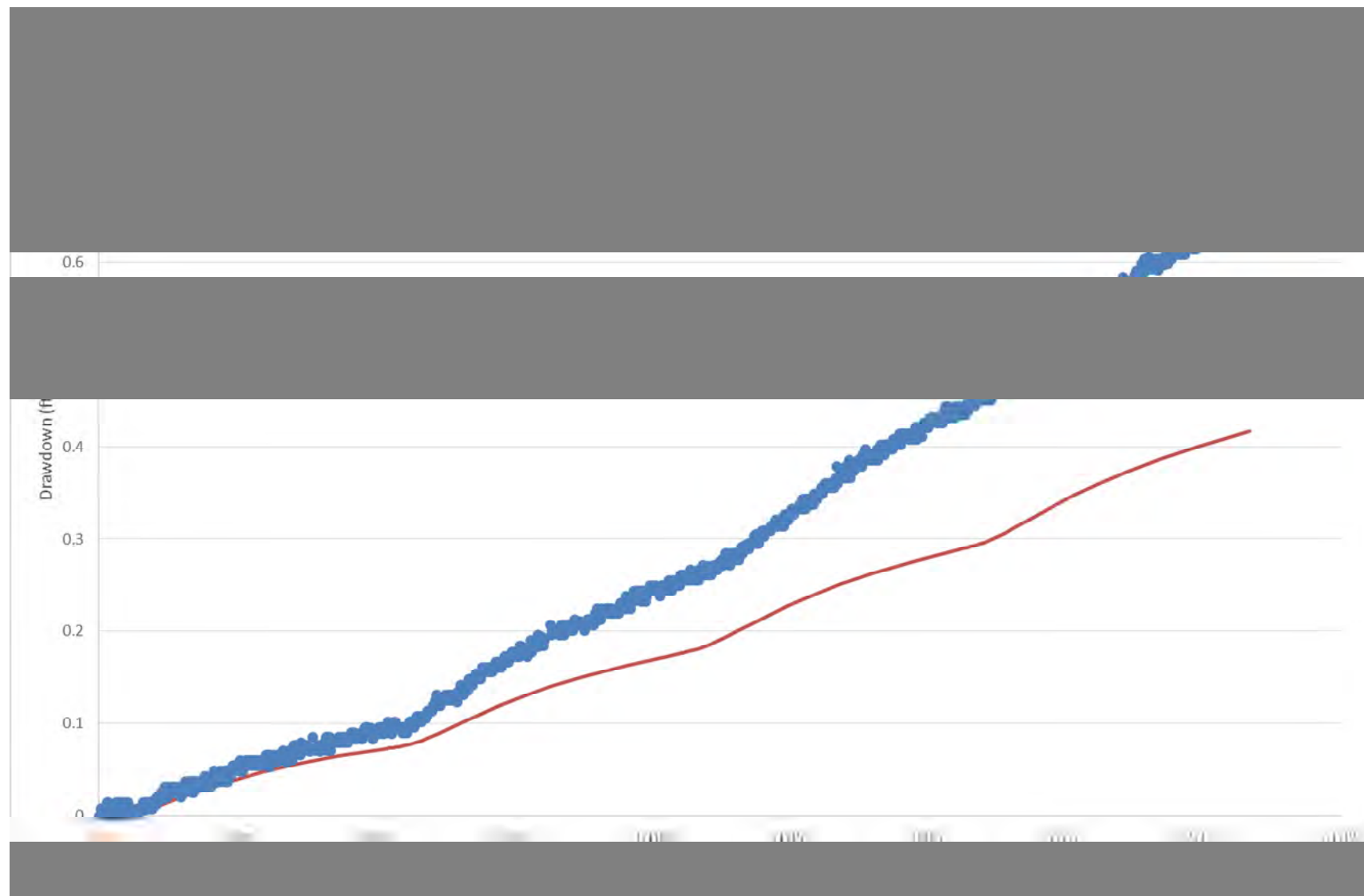
EW-04D Step Test	Average Rate (gpm)
Step 1	7.14
Step 2	14.27
Step 3	21.36
Step 4	28.85

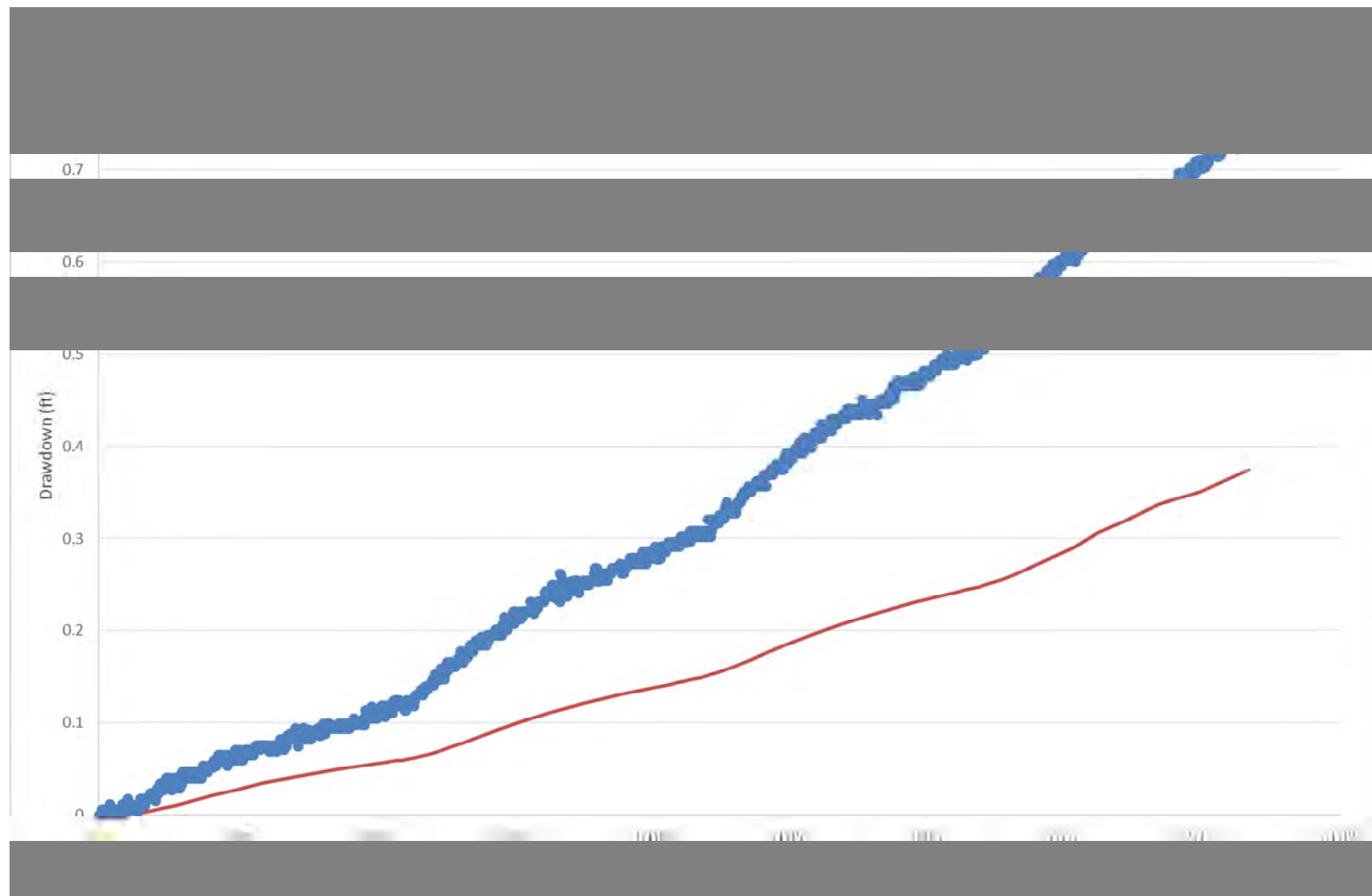


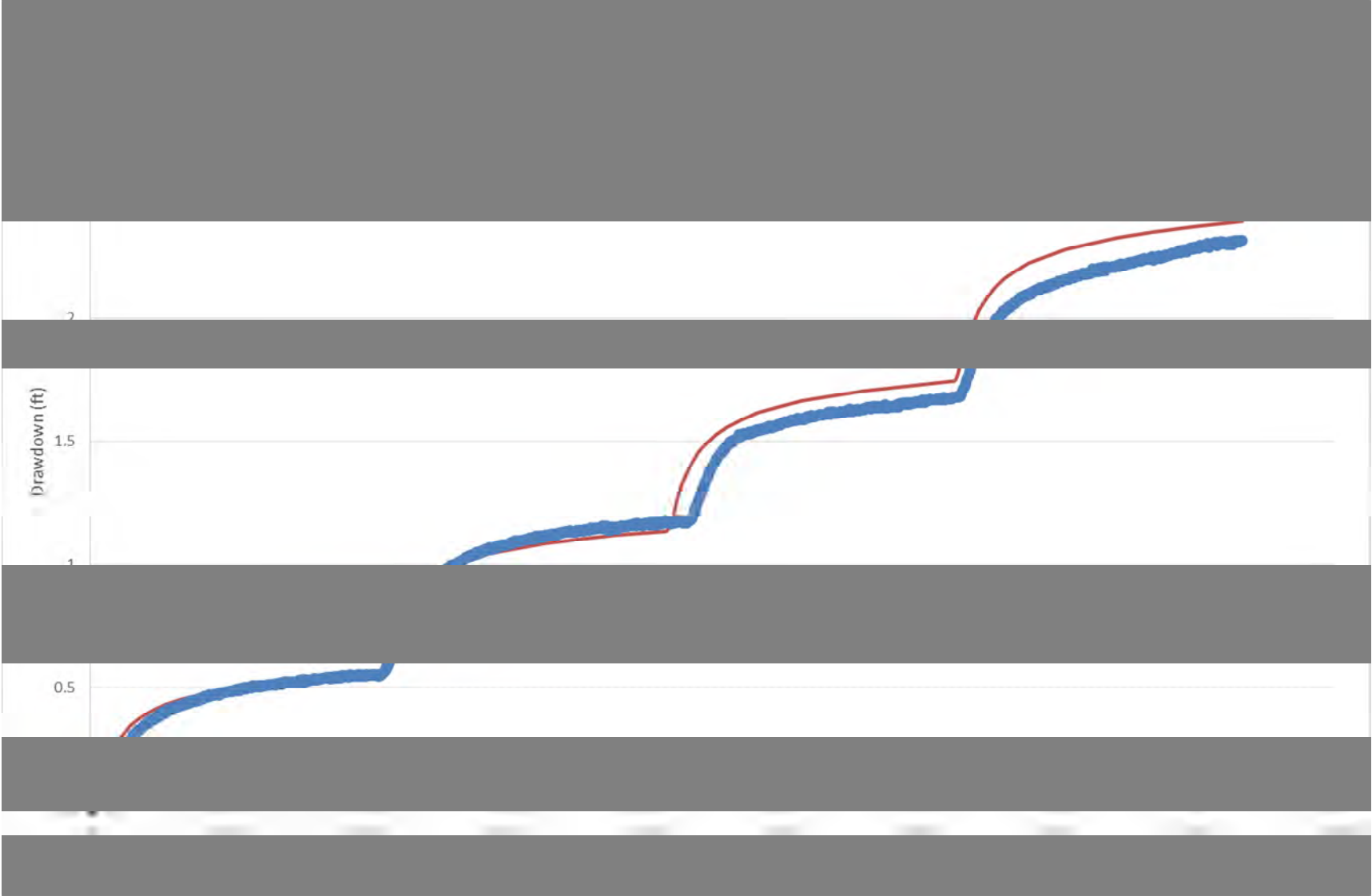




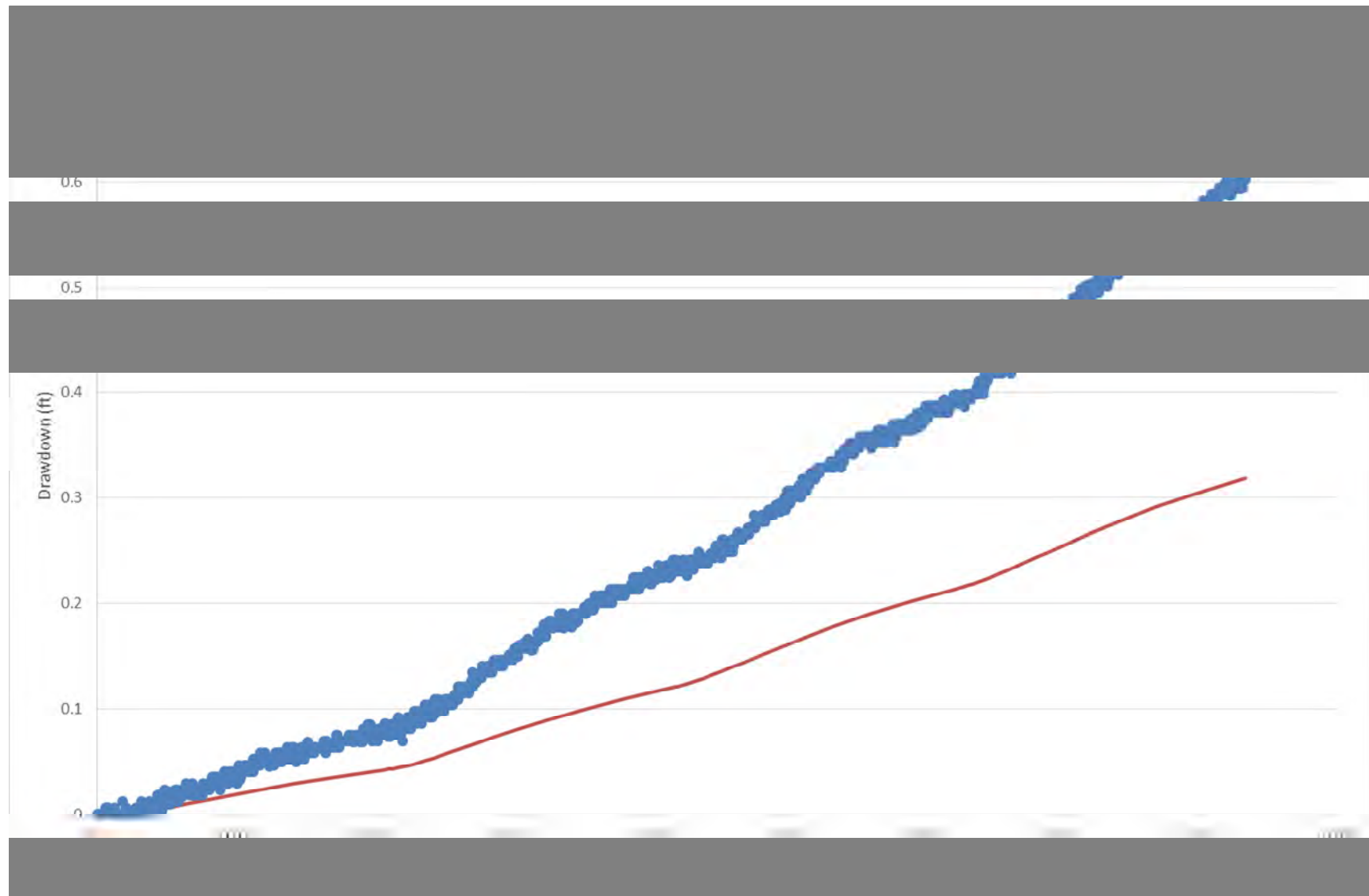












## Step-Drawdown Test O

EW-02I Step Test	Average Rate (gpm)
Step 1	7.30
Step 2	14.06
Step 3	21.30
Step 4	29.20

